APRIL 2016

REGIONAL SEA LEVEL SCENARIOS FOR COASTAL RISK MANAGEMENT:

MANAGING THE UNCERTAINTY OF FUTURE SEA LEVEL CHANGE AND EXTREME WATER LEVELS FOR DEPARTMENT OF DEFENSE COASTAL SITES WORLDWIDE

SERDP
DOD ▪ EPA ▪ DOE

NOAA
NATIONAL OCEANIC AND ATMOSPHERIC ADMINISTRATION
U.S. DEPARTMENT OF COMMERCE

OCEANOGRAPHER OF THE NAVY

COVER PHOTOS, FROM LEFT TO RIGHT:

- Overwash of the island of Roi-Namur on Kwajalein Atoll in the Republic of the Marshall Islands. A combination of unusually high tides and large swells contributed to the overwash on this Pacific atoll. (Photo – U.S. Geological Survey, Peter Swarzenski)

- Combined impacts of a migrating barrier island and several hurricanes in 2004 and 2005 (Ivan, Cindy, Dennis, Katrina, and Tropical Storm Arlene) on Fort Pickens Road, Santa Rosa Island, Florida. (Photo – Federal Highway Administration Resource Center, October 2000, The Environmental Quarterly)

- Flooding in portions of Fleet Parking at Naval Station Norfolk, Virginia, on September 18, 2003, caused by rain and heavy winds from Hurricane Isabel. (Photo – U.S. Navy, Photographer's Mate 1st Class Michael Pendergrass)

REGIONAL SEA LEVEL SCENARIOS FOR COASTAL RISK MANAGEMENT:

MANAGING THE UNCERTAINTY OF FUTURE SEA LEVEL CHANGE AND EXTREME WATER LEVELS FOR DEPARTMENT OF DEFENSE COASTAL SITES WORLDWIDE

April 2016

Prepared by:

John A. Hall, Stephen Gill, Jayantha Obeysekera, William Sweet, Kevin Knuuti, and John Marburger

Recommended Citation:

Hall, J.A., S. Gill, J. Obeysekera, W. Sweet, K. Knuuti, and J. Marburger. 2016. Regional Sea Level Scenarios for Coastal Risk Management: Managing the Uncertainty of Future Sea Level Change and Extreme Water Levels for Department of Defense Coastal Sites Worldwide. U.S. Department of Defense, Strategic Environmental Research and Development Program. 224 pp.

SERDP
DOD ▪ EPA ▪ DOE

4800 Mark Center Drive, Suite 17D08
Alexandria, VA 22350

The mention of a commercial or federal product does not constitute an endorsement by the Strategic Environmental Research and Development Program or any of the report authors' Agencies. Any opinions, findings, and conclusions or recommendations expressed in this report are those of the authors and do not necessarily reflect the view of the authors' Agencies.

Authors/Working Group Members

John Hall, Lead, Strategic Environmental Research and Development Program
Stephen Gill, National Oceanic and Atmospheric Administration (NOAA)
Kevin Knuuti, United States Army Corps of Engineers (USACE)
John Marburger, Office of the Oceanographer of the Navy
Jayantha Obeysekera, South Florida Water Management District
William Sweet, National Oceanic and Atmospheric Administration

Additional Working Group Members

Virginia Burkett, United States Geological Survey (USGS)
Ninette Sadusky, Office of the Oceanographer of the Navy

Technical Contributors

Alison Carisio, NOAA (Geographical Information System [GIS] support)
Carolyn Currin, NOAA (Figure 4.18 development)
Charles DeMets, University of Wisconsin (Vertical land movement rates from global positioning system stations)
Dean Gesch, USGS (Inundation mapping case study consultation)
Robert Kopp, Rutgers University (Ice-melt source contribution data)
Doug Marcy, NOAA (NOAA Sea Level Rise Viewer tool description)
Andrea O'Neill, USGS (USGS Coastal Storm Modeling System [CoSMoS] tool description)
Tim Pangburn, USACE (Low elevation methodology and data)
Mahe Perrette, Potsdam Institute for Climate Impact Research (Dynamical sea-level pattern scaling and ice-melt fingerprint data)
Michael Smith, USACE (Low elevation methodology and data)
Robert Theiler, USGS (USGS Coastal Vulnerability Index tool description)
Weibing Wang, NOAA (GIS support)
Kathleen White, USACE (USACE Sea Level Rise Calculator tool description)
Jianjun Yin, University of Arizona (Dynamical sea-level data)

Technical Support

Erik Tucker, Leidos (Project manager; author, inundation mapping case study)
Kim Gotwals, Leidos (Lead editor)
Ivan Limansky, Noblis (Scenario database and graphical user interface development)
David Bilinski, Noblis (Scenario database development)
Lizanne Carlos, Leidos (GIS database support; GIS, inundation mapping case study)
Ayesha Genz, University of Hawaii (Extreme value and regional frequency analyses)
Christina Hudson, Leidos (Program manager)
Jeffrey Marqusee, Noblis (Scenario database support)
Robert Wassmann, Noblis (Scenario database support)

Peer Reviewers*

John Church, Commonwealth Scientific and Industrial Research Organisation (CSIRO)
Ivan Haigh, Ocean and Earth Science, National Oceanography Centre, University of Southampton
Dan Sarewitz, Consortium for Science, Policy, and Outcomes, Arizona State University
Claudia Tebaldi, National Center for Atmospheric Research

Subject Matter Expert Reviewers

Dean Gesch, USGS
Chris Weaver, U.S. Global Change Research Program, National Coordination Office
Kathleen White, USACE

*The identification of the peer reviewers does not imply that they agreed with all of the content of this report. We list them here primarily to acknowledge that their comments significantly enhanced the final version of this report.

Acknowledgements

The Coastal Assessment Regional Scenario Working Group wishes to acknowledge many others who contributed to the development of the sea level and extreme water level scenarios, the final report, and the accompanying database: the more than 60 Military Service representatives who conducted Beta testing of the database and its associated graphical user interface, the behind-the-scenes support staff from Leidos and Noblis, and to the various audiences to which progress in our development of the scenarios was presented and from whom we received useful feedback.

TABLE OF CONTENTS

LIST OF FIGURES

LIST OF TABLES

ACRONYMS

ACE	Annual Chance Event
AMO	Atlantic Multidecadal Oscillation
AMOC	Atlantic Meridional Overturning Circulation
AOGCM	Atmosphere Ocean General Circulation Model
AR5	Fifth Assessment Report of the Intergovernmental Panel on Climate Change
CARSWG	Coastal Assessment Regional Scenario Working Group
CCAWG	Climate Change Adaptation Working Group
CMIP5	Coupled Model Intercomparison Project Phase 5
CGPS	Continuously operating Geographic Information System
CONUS	Continental United States
CoSMoS	Coastal Storm Modeling System
CVI	Coastal Vulnerability Index
DEM	Digital Elevation Model
DISDI	Defense Installation Spatial Data Infrastructure
DSL	Dynamical Sea Level
ENSO	El Niño Southern Oscillation
ER	Engineer Regulation
ETL	Engineer Technical Letter
EVA	Extreme Value Analysis
EWL	Extreme Water Level
GCM	General Circulation Model or Global Climate Model
GEV	Generalized Extreme Value
GIA	Glacial Isostatic Adjustment
GIS	Geographic Information System
GPD	Generalized Pareto Distribution
GPS	Global Positioning System
GUI	Graphical User Interface
HAT	Highest Astronomical Tide
InSAR	Interferometric Synthetic Aperture Radar
IPCC	Intergovernmental Panel on Climate Change
JPL	Jet Propulsion Laboratory
JPM	Joint Probability Method
LE	Linear Error
LIDAR	Light Detecting and Ranging
MHHW	Mean Higher High Water
MHW	Mean High Water
MIRTA	Military Installations, Ranges, and Training Areas
MLLW	Mean Lower Low Water
MLW	Mean Low Water
MSL	Mean Sea Level

NAO	North Atlantic Oscillation
NAVD88	North American Vertical Datum
NCA	National Climate Assessment
NCEI	National Centers for Environmental Information
NED	National Elevation Dataset
NGDC	National Geophysical Data Center
NGS	National Geodetic Survey
NOAA	National Oceanic and Atmospheric Administration
NPCC	New York City Panel on Climate Change
NRC	National Research Council
NTDE	National Tidal Datum Epoch
NTR	Nontidal Residual
OPUS	Online Positioning User Service
OSD	Office of the Secretary of Defense
PDI	Power Dissipation Index
PDO	Pacific Decadal Oscillation
RCP	Representative Concentration Pathway
RMSE	Root Mean Square Error
RFA	Regional Frequency Analysis
RPAD	Real Property Assets Database
SERDP	Strategic Environmental Research and Development Program
SLC	Sea-Level Change
SLR	Sea-Level Rise
SRES	Special Report on Emissions Scenarios
SRTM	Shuttle Radar Topography Mission
SWL	Still Water Level
TWL	Total Water Level
USACE	United States Army Corps of Engineers
USGCRP	United States Global Change Research Program
USGS	United States Geological Survey
VLM	Vertical Land Movement

Executive Summary

Global change, including climate change, poses unique challenges to the Department of Defense (DoD). In particular, coastal military sites, and their associated natural and built infrastructure, operations, and readiness capabilities, are vulnerable to the impacts of rising global sea level and local extreme water level (EWL) events. One way to assess vulnerabilities and impacts is to pose plausible and scientifically credible future conditions, or scenarios, with regard to sea level and EWLs. A multi-agency group conducted a literature synthesis and applied research effort to develop such scenarios. ***This report and its accompanying scenario database provide regionalized sea level and EWL scenarios for three future time horizons (2035, 2065, and 2100) for 1,774 DoD sites worldwide.*** The global nature of DoD's presence required a broad and comprehensive approach that to this point has been lacking in similar efforts.

These regionalized scenarios were based on five global sea-level rise (SLR) scenarios. The site-specific results reflect the fact that SLR is not uniform across the globe. The set of five global SLR scenarios (starting from 1992 and ranging from 0.2 meters to 2.0 meters by 2100) was developed consistent with other efforts of a similar nature that attempt to frame the plausible range of risk of concern to coastal managers. The suite of global scenarios and their associated storylines enable decision-makers to tailor their use of the scenarios to the decision under consideration and other factors. Although the scenarios extend only to the year 2100, for all global scenarios considered, sea levels will continue to rise past 2100. Decision-makers and planners with time horizons that go beyond 2100 should take this into account.

Adjustments to these global scenarios were developed on a site-specific basis that accounted for local vertical land movement (VLM), dynamical sea level (DSL), and ice melt from glaciers and ice sheets for the three future time horizons. The site-specific results reflect that one or more of the three adjustments can add significantly to the amount of sea-level change at a particular site (especially for the later time horizons), and that the various adjustments do not necessarily trend in the same direction (further increases or decreases in sea level from the global mean) at a particular site.

Extreme still water level estimates are provided for different annual chance events whose probabilities are contingent on the underlying SLR scenario assumptions. The EWLs include the effects of tides and storm surge, occurring on top of rising seas as specified in the five SLR scenarios. They do not include the effects of waves. A range of annual chance events was calculated to emphasize that not only the rare event is important to consider, but also the more frequent, low magnitude event that results in recurrent flooding issues.

The decision-making paradigm must shift from a predict-then-act approach to a scenario-based approach. As a decision-maker, the fallacy and danger of accepting a single answer to the question "What future scenario should I use to plan for sea-level change?" cannot be stressed enough. Those used to making decisions based on a "most likely" future may have trouble relating to this reality; however, a variety of uncertainties, including the uncertainties associated with human behaviors (i.e., emissions futures), limit the predictive capabilities of climate-related sciences. Therefore, although climate change is inevitable and in some instances highly directional, no single answer regarding the *magnitude* of future change predominates. Traditional "predict then act" approaches are inadequate to meet this challenge. The scenario information provided in this report and the accompanying scenario database is not meant to provide *the answer*. Conversely, they are intended to support decision-makers and others in making robust choices to better manage risks amidst plausible future sea levels and EWLs. The appropriate application of the scenarios in a context-dependent manner is often more important than the quantitative scenario values themselves. To that end we provide case studies and other information to assist the user in the use of scenario information.

The primary purpose of this report and its associated scenario database is to enhance and increase the efficacy of screening-level vulnerability and impact assessment for DoD coastal sites worldwide containing permanent or enduring assets. "Screening," in the context of this report, entails a level of assessment that can be supported by scenario information of a relatively coarse nature. Given that scenarios are not deterministic or probabilistic—but rather attempt to bound scientific and human-influenced uncertainties about the future—one must be careful not to consider them predictions or visions of a likely future. Their application also relies on other non-scenario related data, such as topographic information, that also has its own inherent, site-dependent uncertainties. To differing degrees, *planning* activities may be supported through use of the scenario information provided by this effort. For example, the information in the scenario database could be used to support DoD floodplain planning (and subsequent management) activities as an initial approach under the "climate-informed science approach" in the new Federal Flood Risk Management Standard. Caution should be exercised, however, in using the scenario information to design specific responses to projected vulnerabilities for implementation at the site level. The scenarios enable managers and planners at different organizational levels within DoD to perform relative vulnerability or impact assessments within a site or across sites.

Although the scenarios are not intended to directly support engineering design decisions, the scenario information in this report still can be a useful *starting point* for siting decisions for infrastructure investments within an installation or at a new location, engineering design considerations associated with infrastructure planning, or a response to a vulnerability at an existing site. The complexity, risk consequences, and potential costs of a decision should be the primary information used to determine whether the scenarios in the database and their application provide sufficient information to proceed. Local data collection or detailed process modeling also may be needed to support an initial decision. In this case the decision-maker is balancing the cost of additional analyses against the cost of the decision and the risk of being wrong.

This report covers both coastal and otherwise tidally influenced sites. For the purposes of this report, coastal sites were defined as those sites that have potential inundation impacts from relative SLR and coastal storm surge over the next century within a 20-kilometer buffer zone from the shoreline. This also included sites that are not necessarily located along the coast, but that are still tidally influenced. All DoD installation point files (sites) and installation boundary files were obtained from already compiled DoD data sources (i.e., the Real Property Assets Database [RPAD] via the Defense Installation Spatial Data Infrastructure or DISDI) and converted to Geographic Information System (GIS) shape files for display in ArcGIS. The dataset contains information regarding location, site type, and parent (installation and Military Service) organization. Any sites shown in this report for purposes of illustration are a subset of those in RPAD for which DoD has made locational information publically available through the Military Installations, Ranges, and Training Areas (MIRTA) database. The scenario database accompanying this report includes 1,774 sites, including those not in the public domain.

Adjustments were made to global SLR scenarios to provide site-specific scenarios. Global SLR scenarios served as the starting point for this effort and were based—most importantly with respect to the range—on those developed to support the Third National Climate Assessment. The range of plausible scenarios was further assessed against the extant scientific literature and confirmed as appropriate for coastal risk management purposes. New intermediate scenarios were developed and aligned with emissions-based storylines and global model projections taken from the literature. To regionalize the SLR scenarios to site-specific conditions, three adjustments were made to account for recognized deviations from the global means attributable to VLM, DSL, and ice-melt effects. Vertical land movement used three different data sources—local tide gauge, local global positioning system, or a glacial isostatic adjustment model—to assign site values based on proximity and measurement error as to the most reliable source. Dynamical sea level and ice-melt adjustments relied on global climate model-derived data and, for ice melt, application of "fingerprint" patterns, attributable mostly to gravitational effects, that determined how ice-mass loss effects from glaciers and ice caps, Greenland, and Antarctica, were spatially distributed across the globe.

Tide gauge data were used to provide quantitative estimates for extreme water levels resulting from storms and tides. Changes in sea level, absent the contribution of a long-term directional trend such as SLR, are a complex combination of tide-driven (deterministic) and storm-driven (stochastic) components that also have strong seasonal patterns. In the absence of wave contributions, what remains is termed "still water level" (SWL) in which the interest is on EWLs. Extreme Water Levels can be estimated from tide gauge records. As a result, this report focused on providing quantitative estimates for EWLs at each location for the 1%, 2%, 5%, and 20% annual chance events. Most importantly, however, was the innovative use of the technique known as Regional Frequency Analysis (RFA) to estimate values for these events at sites lacking a representative tide gauge or having a tide gauge but with a short record length. By using the RFA method, we were able to expand the number of sites for which EWL values could be provided. In addition, application of RFA also in many cases improved the confidence in the estimates of rare events by bringing additional regional information to bear and thus smoothing the effects of outlier events on the estimates. Finally, by assessing the effect of the 5% and 20% annual chance

events in conjunction with SLR, we provided evidence that the less severe but more frequent events (that will themselves become more frequent in the future) are of consequence. They will exacerbate recurrent flooding events and need to be factored into decisions.

Estimates of scenario adjustments are complex, with many contributing factors that differ in space and time. The interplay of physical setting, local climatology, time horizon, data availability, and data quality affect the degree to which regional and local factors alter future global mean and extreme sea-level patterns, as well as the ability to depict them at particular sites. Importantly, the various adjustments to global mean sea level considered herein were not necessarily spatially concordant in their effect. For example, VLM operates independently of direct climate effects, the fingerprint pattern that results from ice melt depends on the location of ice-mass loss, and storm surge magnitude depends on both coastal bathymetry and configuration and whether a site experiences tropical storms of some type. These differential responses to forcing factors generally meant that sites experience a complex set of interactions in which some factors are more important than others in determining their exposure to future sea-level change and extreme water levels. In addition, the time horizon considered affects whether a particular factor is important and the extent to which it needs to be taken into account.

Case studies can highlight potential applications of scenarios under specific circumstances. The case study section of the report attempts to provide additional context for the use of the scenario information. For example, a sub-section illustrates the influence of wave environments on extreme total water level estimates and the potential nonlinear effects of storm surge when sea levels rise. These two additional factors were beyond the scope of this effort to address in a quantitative manner. Another sub-section details the importance of data availability and quality and provides a more in-depth illustration of the use of an RFA versus a single tide gauge analysis. This sub-section describes how to address situations in which a site lacks local tidal datum or geodetic elevation reference information and illustrates that the type and quality of topographic information available affects the ability to map and accurately interpret the extent of scenario-dependent inundation at a site. A final sub-section details scenario application and decision-making under uncertainty, with an emphasis on a risk-based framing approach. Three scenario application approaches are addressed: (1) emissions-scenario based, (2) accounting for decision type, operational timeframe, and tolerance for risk, and (3) adaptive risk management. The sub-section concludes with a special case study on scenario application in the zero to twenty-year timeframe.

Overview of the Applied Research Effort to Develop Regionalized SLR and EWL Scenarios

We assert that the applied research effort described here makes both scientific and practical contributions to the field of coastal risk management. *This effort was not conducted solely for the sake of advancing scientific knowledge. Rather our goal also was to provide workable approaches to screening level vulnerability assessments for coastal and tidally influenced military sites subject to the impacts of rising sea levels and extreme water levels. We suggest this effort "moves the bar" by providing plausible site-specific SLR rise and EWL scenarios useful for planning purposes within a risk-based management framework.*

Not surprisingly, we uncovered areas that warrant additional research. *A few examples are provided here; more are described in the report. Factors that contribute to nonlinear storm surge magnitudes associated with SLR are complex and deserve ongoing research. In addition, understanding how to quantify the site-specific effects of waves during EWL events is an area deserving further attention. The VLM data available for our use were point data; some stakeholders may want continuous VLM data, perhaps through a gridded product at a useful spatial scale. And research will continue on the applications of scenarios and the characterization of uncertainty to assist decision-makers in their risk management choices.*

We made significant findings. *The accompanying database with the SLR and EWL scenarios for specific sites is the chief product of this effort, but we also contributed significant findings:*

- *The regional or local adjustments to global mean sea level considered herein—VLM, DSL pattern scaling, and ice-melt fingerprinting—are not necessarily consistent in their directionality (i.e., increases or decreases in sea level) and magnitude at a particular site. In some cases, positive and negative adjustments to sea level may cancel each other. In some regions, the VLM rate can exceed that of regional SLR from the combination of DSL and ice melt effects by an order of magnitude in either direction.*
- *VLM rates are independent of climate factors. Given the scenario independence and assumed linearity of VLM rates, geographic location plays the critical role in an assessment of relative SLR contributions from VLM compared with other components of regionalized adjustments.*
- *DSL adjustments generally tend to increase sea level at DoD sites in the northern hemisphere and decrease sea level in the southern hemisphere.*
- *The more prominent influence of near-field effects (i.e., sea levels fall [negative adjustment] near the area of ice mass loss) further amplifies late century impacts for DoD sites in close proximity to one of the three contributing sources of ice melt. The sites that will experience the greatest positive SLR adjustments from ice mass loss from Antarctica are located in the Pacific Ocean.*
- *By employing the RFA method, we were able to expand the number of the original 1,774 sites for which EWL values could be provided from 53% to almost 86% of the sites.*
- *With regard to EWL, we did not de-emphasize importance of the 1% event, but rather equally emphasized the importance of considering higher frequency events that result in recurrent flooding in coastal risk management decisions.*
- *Location with respect to physical setting (e.g., shoreline configuration and local and regional bathymetry) plays a significant role in determining whether storm surge is a key component of EWLs at a particular site and how these levels may change under SLR.*

THIS PAGE LEFT INTENTIONALLY BLANK

Section 1.0
Purpose and Scope

Global change, including climate change, poses unique challenges to the Department of Defense (DoD). In particular, coastal military sites, and their associated natural and built infrastructure, operations, and readiness capabilities, are vulnerable to the impacts of a rising global sea level and local extreme water levels from storm events, tidal variations, and dynamic conditions including waves. One way to assess vulnerabilities and impacts, initially through a screening perspective and later with a more directed focus, is to pose plausible and scientifically credible future conditions, or scenarios, with regard to sea level and extreme water levels. A multi-agency literature synthesis and applied research effort resulted in the development of this report, and an accompanying scenario database, that provide site-specific sea level and extreme water level scenarios for three future timeframes. Scenario development with respect to regionalized sea-level change and extreme water level scenarios is an emerging area of societal concern that extends beyond DoD.

Decision-makers and others may use the scenario information to inform a variety of robust decision processes, subject to the:

- decision to be made,
- level of expected performance of the decision under different future conditions,
- time horizon over which it has an effect,
- decision-maker's tolerance for risk,
- available scenario-related data, and
- degree of accuracy and precision needed to inform the decision.

...the scenario information provided in this report and the accompanying scenario database is not meant to provide the answer; rather, the scenarios are intended to assist decision-makers and others in making robust choices to manage their risks in the context of plausible future sea level and extreme water levels.

A variety of uncertainties, including the uncertainties associated with human behaviors, limit the predictive capabilities of climate-related sciences. In a future under climate change, although change is inevitable and in some instances highly directional, no single answer regarding the *magnitude*, along with its timing, of future change predominates. Traditional "predict then act" approaches are inadequate to meet this challenge. As a result, the scenario information provided in this report and the accompanying scenario database is not meant to

provide *the answer*; rather, the scenarios are intended to assist decision-makers and others in making robust choices to manage their risks in the context of plausible future sea level and extreme water levels. How the scenarios are applied in a context-dependent manner can be more important than the quantitative scenario values themselves. (See the text box on page 1-3 for further discussion.)

This section begins by briefly outlining the primary motivations that led to the development of this report, the accompanying scenario database, and their intended uses. Next, it describes the scope of the overall effort, some of its innovations, and some of its limitations.

This report represents a significant step forward toward providing actionable science for decision-making under the uncertainty of climate change futures, with a focus on DoD needs, for coastal risk management. The term "actionable science" refers to science that provides a variety of products useful for decision-making. Results of this study are not meant to be the final answer—of necessity, we must continue to learn—and this report is not intended to address directly all needs for managing the future risk of rising sea levels, but it is offered as a necessary step for assisting decision-makers by providing credible scenarios of future change and the contexts in which to apply them. As climate-related science and climate models advance, as key observational data sets mature, and as understanding of, tolerance for, and capacity to manage risk in the coastal environment evolve over time, scientists, boundary organizations, decision-makers, and practitioners will need to re-visit the underlying bases and current utility of scenarios of sea-level change and extreme water levels and revise them accordingly. Scenarios development and their use for coastal risk management purposes ultimately is an iterative and ongoing process.

Scenarios development and their use for coastal risk management purposes ultimately is an iterative and ongoing process.

1.1 Why This Effort?

The DoD has military assets located in proximity to the coastline or otherwise located along tidally influenced areas that therefore may be currently exposed to potential flood risks from storm surge and waves. This worldwide distribution of sites presents unique challenges for understanding current vulnerabilities, let alone developing plausible scenarios of future conditions. Individual sites managed by DoD exhibit a cross-section of physical settings, exposure to a variety of climatic forcings (e.g., sub-tropical storms and extra-tropical storms), infrastructure and mission importance, and data quality conditions. These factors affect a site manager's ability to apply future scenario information (or even understand current vulnerabilities). Despite these challenges a unified, consistent but flexible methodology that recognizes data limitations and uncertainties would be beneficial in certain contexts. ***Such a methodology could assist a large, complex organization such as DoD manage its overall risk to mission by better understanding the distribution and aggregation of vulnerabilities across the entire enterprise.***

Although other efforts are underway—some further along than others—to provide coastal risk management information, even at times in the form of scenarios of future conditions, none have

Shifting Paradigms: Transitioning from "Predict then Act" to "Robust Decision-Making"

Risk is defined typically as the likelihood of occurrence of some condition or event multiplied by the consequence. Within this context, futures that can be described according to a probability distribution, especially if associated with a central tendency, lend themselves to a "predict-then-act" decision-analytic approach. This often comports to a decision-maker's desire to base decisions on a "most likely," essentially deterministic future.

Given the uncertainties inherent with climate change, however, such strictly probabilistic approaches are not feasible. The uncertainties associated with the natural variability of the climate system, climate model input and output differences, and different possible emissions futures effectively preclude assigning probabilities to possible resultant futures. Climate change therefore leads to a class of decisions characterized by deep uncertainty. Here, we take a broader view of risk that is not dependent on assigning likelihoods or probabilities and instead use a risk-based framing approach. Such an approach acknowledges that risk under conditions of uncertainty cannot be defined in a strictly probabilistic sense and instead is dependent on the type of decision involved, the desired operational life of the asset in question, and a decision-maker's tolerance for the adverse consequences of a failed decision. The overall goal here is to increase the robustness of decisions against plausible future conditions. Such robust decision-making processes are iterative and adaptive by nature (Hallegatte et al. 2012) and can be used effectively to support a risk-based framing approach. See Sections 2.2 and 5.3.1 for additional details that contrast these two decision-analytic frameworks.

the broad scope that reflects the unique needs of DoD and its worldwide presence. They are either limited geographically (often restricted to the continental United States or finer scales) or do not address key considerations affecting localized sea-level conditions and data availability issues. In addition, often when sea-level change scenarios are merged with extreme water level conditions, the focus has been on rare events, such as hurricanes. But evidence is growing that the less severe but more frequent events (that will become even more frequent in the future) are of consequence and need to be factored into decisions (Sweet and Park 2014).

The DoD already has recognized that it has current vulnerabilities and must prepare for future vulnerabilities in the coastal environment (DoD 2014). In 2013 its Climate Change Adaptation Working Group—an action officer-level policy advisory group initially established in response to Executive Order 13514, *Federal Leadership in Environmental, Energy and Economic Performance*—recognized the need to develop plausible and scientifically defensible scenarios for future sea levels and extreme water levels to inform vulnerability and impact assessments for its coastal and tidally influenced sites. They also recognized the value of accomplishing such an undertaking as a whole-of-government approach, in which

But evidence is growing that the less severe but more frequent events (that will become even more frequent in the future) are of consequence and need to be factored into decisions. (Sweet and Park 2014)

outside agency expertise in coastal processes and management could be accessed to develop credible scenarios of future change. This perspective resulted in the establishment of an inter-agency working group—informally known as the DoD Coastal Assessment Regional Scenario Working Group—led by the Strategic Environmental Research and Development Program (SERDP) within the Office of the Secretary of Defense. The authors of this report are members of that working group.

The primary purpose of this report and its associated scenario database is to support worldwide screening-level vulnerability and impact assessment for DoD coastal sites containing permanent assets. Site identification is addressed more specifically in Section 3.1.

1.2 Scope

"Screening" in the context of this report refers to assessments that can be supported by scenario information of a relatively "coarse" nature. Given that scenarios are not deterministic or probabilistic—but rather attempt to bound scientific and human-influenced (i.e., emission futures) uncertainties about the future—one must be careful not to consider them predictions or visions of a likely future. Their application also relies on other non-scenario related data, such as topographic information, that also has its own inherent, site-dependent uncertainties. To some degree planning activities may be supported through use of the scenario information provided by this effort. For example, the information in the scenario database could be used to support DoD floodplain planning (and subsequent management) activities as an initial approach under the climate-informed science approach under the new Federal Flood Risk Management Standard (FEMA 2015); however, see limitations in Section 1.3. Caution should be exercised in using the scenario information to design specific responses to projected vulnerabilities for implementation at the site level.

Given that scenarios are not deterministic or probabilistic—but rather attempt to bound scientific and human-influenced (i.e., emission futures) uncertainties about the future—one must be careful not to consider them predictions or visions of a likely future.

Screening enables sites that are clearly not vulnerable to future sea-level rise and extreme water levels to be ruled out from further evaluation, which enables resources to be focused on potentially vulnerable sites for the next phase of assessment, planning, or management, as the case may be. Therefore, although the scenario information in this report can be a useful starting point for engineering design considerations associated with future infrastructure planning or a response to a vulnerability, depending on the complexity, risk consequences, and potential costs of a decision, the user must decide whether the scenarios in the database and their application provide sufficient information or whether additional local data collection or detailed process modeling may be needed first to support a decision. In this case the decision-maker is balancing the cost of additional analyses against the cost of the decision and the risk of being wrong. As described in subsequent sections, and in particular related to the use of global mean sea-level rise scenarios, this effort builds on previous SERDP efforts in coastal assessment (SERDP 2013) and efforts by the

National Climate Assessment to advance scenario development and risk management (see Parris et al. 2012).

Those efforts recognized both the need to regionalize global scenarios to the scale at which decisions are made and to incorporate other considerations such as storm surge under changing sea-level conditions. These efforts also recognized, as have other authors (see Hinkel et al. 2015), that scenarios are needed from the perspective of coastal risk management. As a result, though the report authors have tried to show correspondence (Section 3.3) to the global sea-level rise scenarios provided by the Fifth Assessment Report of the Intergovernmental Panel on Climate Change (IPCC; Church et al. 2013a), this scenario development approach is one of *managing* uncertainty versus what Hinkel et al. (2015) contend is the IPCC's aim to *understand* and *reduce* uncertainty. In addition, as previously described, the uniqueness of this effort is that it addresses needs in a worldwide context and uses some innovative approaches (Section 1.3).

Although the scenario information in this report can be a useful starting point for engineering design considerations…the user must decide whether the scenarios in the database and their application provide sufficient information or whether additional local data collection or detailed process modeling may be needed first to support a decision.

Although developed specifically for DoD sites and purposes, the methodological framework and approaches developed and applied in this report are generally applicable to other coastal sites, especially if sites are in proximity to representative tide gauge(s) of adequate record length. Although other sources of data are used herein to regionalize the scenarios (see Section 3.0), useful information of a local nature can be generated if tide gauge information is available, though particular attention should be paid to issues of proximity, representativeness, and record length.

1.3 Innovations and Limitations

To provide useful and credible information in a worldwide context, this effort had to be forward-leaning. First, the scientific literature has discussed that long-term changes in ocean circulation patterns and ice melt from glaciers, Greenland, and Antarctica due to climate change result in the differential distribution of water across the globe. We think this is the first effort to formally incorporate these effects on regional sea levels in the context of a broad range of global SLR scenarios to inform coastal risk management. Previous efforts have attempted regionalization, but generally only in association with tide gauges and for specific greenhouse gas scenarios, such as those from the IPCC. Second, the authors used multiple sources of information to estimate the effects of vertical land movement (VLM). Data on VLM is the most commonly applied adjustment to global SLR scenarios; however, typically one source of data is relied on for the adjustment. The approach here was to use the most locally robust data source (Section 3.4.2). Third, a significant portion of DoD sites are not located in proximity to a representative tide gauge of sufficient record length. This creates a significant challenge for estimating extreme water levels. We applied an approach emerging in the literature, Regional Frequency Analysis, to extend the use of tide gauge

information to provide reasonable information on extreme water levels for contexts in which such information may not typically be available (Section 3.5). Fourth, we have tried to identify practical considerations (e.g., how the quality of local topographic information affects scenario application) and used case studies to illustrate the appropriate use of scenario information. These last efforts are an attempt to move beyond merely providing numbers and expecting users to mostly fend for themselves in interpreting what they mean. Assisting in this enterprise, but without making the decision for the decision-maker, is likely just as important as providing credible and useful scenario values.

Despite the innovations above, the scenarios developed herein do not address some significant issues. First, as described in more detail in subsequent sections, extreme water levels do not include the effects of waves, which may be a significant impact for some military sites. In some locations around the world, waves can be the dominant component in damage from extreme events. The inability to include wave effects results from the fact that our data are extracted from tide gauges, which typically are located in protected areas that do not experience breaking waves. Short of more detailed hydrodynamic modeling, wave effects estimations were not possible in this study. This is an area of active research to determine if such information can be determined without detailed hydrodynamic modeling. Second, storm surge response conditioned on changes in near-shore water depth due to sea-level change is not necessarily linear. Response may be highly dependent on local shoreline configurations and bathymetry. Third, the authors do not account for the physical or biological response of shoreline features (e.g., erosion or migration of barrier islands, marshes, and so on) or the presence of built infrastructure (e.g., dikes and jetties) and how these may affect the flood risk mapping of the sea-level change and extreme water level scenarios. Finally, this report assumes stationarity in future storm statistics and therefore does not account for potential non-stationarity in future storminess (see text box). The preceding and other considerations are described in Section 3.6, accompanied by limited guidance on how to ensure these considerations are factored in, at least qualitatively.

Important Caveats:

The sea-level change and extreme water level scenarios discussed in this report and provided in the accompanying database do not account for ALL factors that may affect water levels.

Notably, the scenarios do not account for:

- *Wave run-up,*
- *Potential for nonlinear response of storm surge due to changes in near-shore water depth as sea levels rise,*
- *Geomorphological or biological responses to rising sea levels,*
- *Presence of built structures that may affect exposure to changes in water levels, and*
- *Potential non-stationarity of future storminess.*

1.4 Relationship of This Report to the Companion On-Line Scenario Database

This report represents the documentation of the datasets and methodologies supporting the development of the sea-level change and extreme water level scenarios provided in the database accompanying this report. The report also provides more detailed considerations and associated case studies to illustrate the application of the scenario information. The database's Graphical User Interface provides users access to the scenario information on a site-specific basis and also includes a tutorial that provides links to case study information in this report. The full database contains potentially sensitive site information and so is not publically available. A subset of site and scenario data is intended to be cleared for public release and will be available for community partners to use in coordination with their local DoD installations as appropriate.

THIS PAGE LEFT INTENTIONALLY BLANK

Section 2.0
Background

This report builds on important foundations. After a brief overview of the extent to which climate change poses significant challenges for coastal military installations worldwide—to both infrastructure and military readiness—a number of topics are introduced that set the stage for Section 3.0 Approach. Most importantly, the relationship to and utility of previously developed global sea-level rise (SLR) scenarios is discussed, along with an overview of this report's approach to the concept of decision framing relative to the use of scenarios and other information provided here. This section provides a brief background on the types of contributions to regional and local SLR adjustments and extreme water levels (EWL) and the three time horizons used in framing scenario information. The section concludes with an overview of the relationship of the work reported herein to other similar efforts. More detailed information relative to the last item is provided in the appendices.

2.1 Coastal Military Installations and Climate Change

A key finding of the third National Climate Assessment (Melillo et al. 2014) is that SLR, storm surge, and heavy downpours, in combination with the pattern of continued development in coastal areas, pose significant risks to United States (U.S.) assets, including ports and coastal military installations. The ability of these installations to meet their missions can be further compromised by the potential for increased damage, especially during extreme weather events, to surrounding infrastructure that serves installation needs, such as roads and utilities. Such needs can be as simple as providing access to an installation for those personnel who live off-site.

The concerns are not limited to U.S. installations, as the Department of Defense (DoD) maintains enduring and permanent installations and sites in the coastal environment

A Note about the Use of "Sea-Level Rise" *and "Sea-Level* Change"

Although sea levels are rising globally and are anticipated to continue to rise past 2100 under all anticipated emission scenarios (Meehl et al. 2012), when we talk generally about future sea levels, the term "sea-level change" is used to capture regions such as Alaska where, because of patterns of tectonic uplift, sea levels may fall under certain scenarios and time horizons.

Whereas many people are familiar with the use of the SLR acronym, this report will sometimes refer to SLC for sea-level change.

worldwide. "Sites" as used here refers to often smaller areas with permanent infrastructure that are administratively assigned to a parent, or primary, installation, regardless of whether the site is located in proximity to that parent installation. In addition, state-owned National Guard sites and DoD Washington Headquarters Services sites not necessarily assigned administratively to an installation are addressed as well. Finally, the term "coastal" also includes tidally influenced areas whose water levels will be affected by sea-level change (SLC) and storm surge.

Worldwide 1,774 individual sites are considered here for assignment of numerical values of SLC adjustments and extreme water levels; see Section 3.1 for additional details on site identification. See Figures 2.1 and 2.2 for a breakdown of site types. Given the worldwide distribution of sites, and the variety of hydrologic and climatologic settings in which they occur, this poses unique challenges for providing regionalized and local SLC and EWL scenarios in a generally consistent manner. Data availability and quality differ between U.S. and international sites. Even the inability to work robustly with consistent reference datums poses a challenge. Data availability and quality and consistent reference datums are issues addressed frequently in the remainder of the report. Their importance cannot be overstated with regard to their effect on the application and interpretation of scenario information.

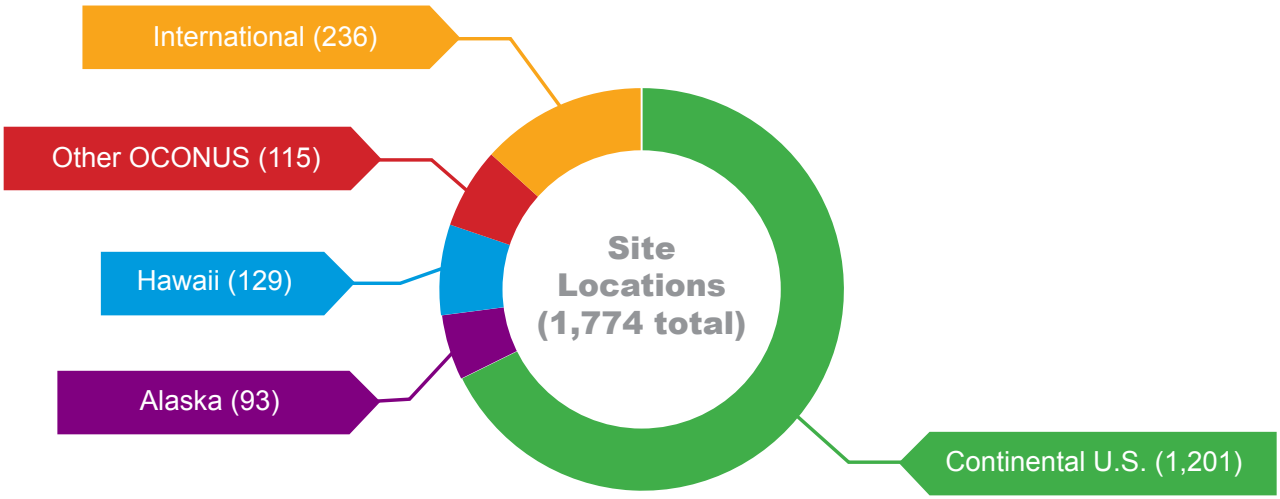

Figure 2.1 Geographic Locations of Sites Included in this Report

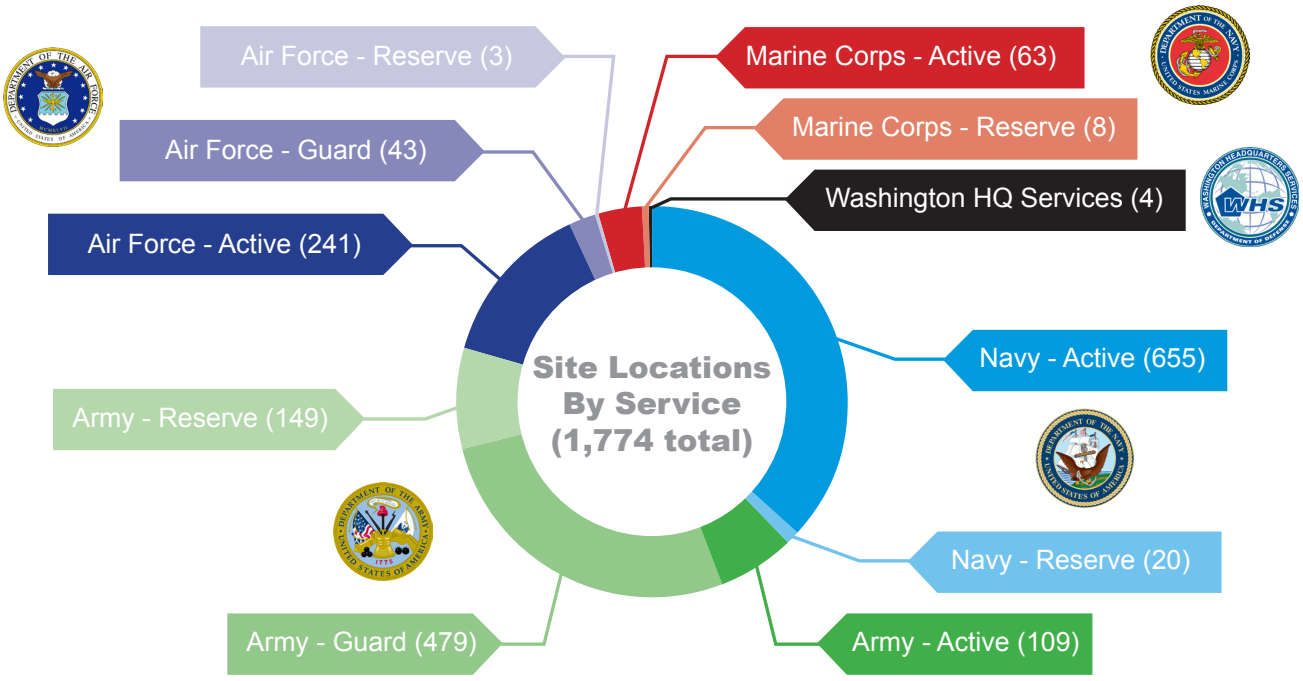

Figure 2.2 Sites Included in this Report by Military Service and DoD Component

A variety of military sites—in which each Military Service has some amount of equity—occur along the coast. The ability of any of these sites to fulfill their mission requirements could be disrupted in the future by climate change. A few studies have provided overviews of the implications of climate change for coastal military infrastructure and readiness (e.g., National Research Council [NRC] 2011, Russo and Hall 2012), which can be consulted for additional details.

A variety of military sites—in which each Military Service has some amount of equity—occur along the coast. The ability of any of these sites to fulfill their mission requirements could be disrupted in the future by climate change.

With respect to the focus of this report on sites with permanent infrastructure, the associated impacts of concern include direct impacts to natural and built infrastructure and the resultant indirect impacts to military readiness, as well as the direct impacts to installation-related operations and readiness that may occur during extreme events. For infrastructure in particular, the time horizon to be considered is critical to assessing the severity of an impact, as well as recognizing that each site—to the extent that it differs in geologic and climatologic setting from other sites—needs to be examined individually (NRC 2011).

The DoD's Strategic Environmental Research and Development Program (SERDP) funded research that evaluated data, models, and approaches that could be used to assess the impacts of climate change on coastal military installations. Based on this research, SERDP developed a report that outlined the policy implications associated with assessing impacts of climate change on coastal installations (SERDP 2013). The SERDP report

identified a number of technical and institutional considerations to inform policy development in this area. Several of these, including accounting for regional variation, selecting and applying future condition scenarios, ensuring data quality, and addressing uncertainty, are explicitly addressed in this report as they relate to SLR and EWL scenarios.

2.2 Global Sea-Level Rise Scenarios and Their Application within a Risk Tolerance-Based Decision Framework

The following discussion first provides a brief historical overview of the development of global SLR projections (Section 2.2.1) and then a description of their application in a decision-making context, including a discussion of the five global scenarios advanced in this study (Section 2.2.2).

2.2.1 Historic perspective on global SLR projections

The provisioning of global SLR projections through the use of climate models (e.g., Church et al. 2013a, Little et al. 2015b), semi-empirical approaches (e.g., Rahmstorf 2007), or physical-based processes that attempt to determine the maximum possible contribution from ice-sheet loss and glacial melting (e.g., Pfeffer et al. 2008) is an ongoing effort of the scientific community, with the goals of narrowing the uncertainty associated with such projections and refining our understanding of plausible bounding conditions. Starting in 1990, the Intergovernmental Panel on Climate Change (IPCC) reports have provided estimated ranges for global SLR based on different emission scenario assumptions. (See the text box on the following page.) The ranges provided have differed significantly across the five reports to date, reflecting the different emission scenarios considered, use of different reference periods, and components of the sea-level budget included (Jevrejeva et al. 2014). For example, the potential contributions from the ice-sheet dynamics associated with both Greenland and Antarctica have not always been included and often led to the IPCC estimates being viewed as overly conservative, though in some cases they also have been erroneously interpreted as depicting potential worst-case conditions (Church et al. 2013c).

The goal of the scientific community is to better understand the physical processes associated with climate forcing and SLR to more accurately project future changes in sea level and to narrow the uncertainty associated with such projections. The concepts of likelihood and confidence associated with projections, however, are not so easily translated into actionable science useful for decision-making. One addition to Jevrejeva et al.'s (2014) list above that also significantly affects the resultant range of potential global SLR values is the *likelihood* assigned to the range that is considered. For example, the latest IPCC range for the highest radiative forcing (emissions) scenario considered, Representative Concentration Pathway (RCP) 8.5, was reported as 0.52 to 0.98 meters by 2100 with a probability of 67% (i.e., a 33% probability exists that sea-level rise by 2100 may fall outside this range; Church et al. 2013b). By choosing other *likelihood* values (e.g., 95%, 99.5%, and so on), often as a way to better address a reasonable, but worst-case estimate for the upper bound of SLR by 2100, other investigators have significantly extended the upper limit of plausible SLR this century (e.g., see Jevrejeva et al. 2014, Kopp et al. 2014). Given the continuing questions about the physical basis for SLR, especially regarding ice-sheet dynamics, these higher estimates often rely on expert judgment rather than direct output of a process model (e.g., see Bamber and Aspinall 2013, Horton et al. 2014, Kopp et al. 2014).

Emissions Scenarios or Futures

Emissions scenarios are descriptions of potential future releases to the atmosphere of gases and aerosols (solid particles or liquid droplets) that affect the Earth's radiation balance. Along with other information such as land cover, they are the key inputs to climate models. As scenarios they are not predictions and are not assigned probabilities; instead, they reflect expert judgment. For the Third and Fourth Assessment Reports, the Intergovernmental Panel on Climate Change used different families of greenhouse gas (GHG) emissions scenarios that captured different socioeconomic, environmental, and technological assumptions to drive the climate models. The assumptions are described in the Special Report on Emissions Scenarios or SRES (Nakićenović et al. 2000). Of note, the SRES scenarios did not incorporate any policy measures that would limit emissions production and the emissions themselves were reported as atmospheric concentrations of carbon dioxide (the dominant greenhouse gas contributor) equivalents.

For the Fifth Assessment, however, the scenario development process and the climate forcing scenarios themselves were modified (Moss et al. 2010). Rather than starting with detailed socioeconomic storylines to generate emissions that then led to climate scenarios, the new process identified different levels of radiative forcings—expressed as watts per square meter—that were decoupled from specific socioeconomic or emissions scenarios. This time some of the scenarios required mitigation efforts to reduce GHG emissions. To force the climate models, however, a plausible emissions pathway still was needed to reach each target radiative forcing trajectory. These were labeled as "representative concentration pathways" (RCP) to reflect that they were one of many possible emissions pathways to reach a particular radiative forcing. When not necessary to specifically refer to the SRES versus the RCP scenarios, for simplicity we refer to "emissions scenarios" or "emissions futures."

Because of the way SLR interacts with other ocean-meteorological processes (e.g., tides and storms), as well as with the bathymetric characteristics of the shoreline, the increase in flood risk associated with SLR does not necessarily scale linearly. Moreover, infrastructure and environmental planners and decision-makers who, either by policy dictum or through prudent planning, must address issues within the coastal and tidal zone, often are concerned with chance events: for example, the 1% annual chance event or 100-year storm (see text box on next page) is an important consideration for the new Federal flood risk management standard (FEMA 2015). Beyond strict and often deterministic policy adherence, the need to factor hard-to-quantify rare events and other types of uncertainty into decisions is based on the tolerance for risk associated with the decision: that is, ultimately, the trade-off involved in the cost (monetary and otherwise) of taking an action to guard against the consequences of a plausible event versus the cost of inaction. Sea-level rise accompanied by EWLs under the non-

Sea-level rise, accompanied by EWLs,…poses unique challenges for risk management that encompass not only the uncertainty associated with future SLR but also its nonlinear interactions. The frequency and intensity of these events are themselves difficult to predict today, let alone how they may change in the future.

stationary conditions imposed by climate change poses unique challenges for risk management. These challenges encompass not only the uncertainty associated with future SLR but also its non-linear interactions associated with EWL events. The frequency and intensity of these events are themselves difficult to predict today, let alone how they may change in the future. More will be said about the preceding in subsequent report sections as the issue relates to scenarios selection and their application within a risk tolerance-based decision framework; however, for now it will suffice as an introduction to the rationale behind the selection of the bounding global SLR scenarios used in this report.

What is the difference between a 100-year storm and a 1% annual chance event?

Nothing. These are two different ways to reference the same event.

Statistical analyses are used to estimate the probability of the occurrence of a given precipitation event. It may be preferable to refer to a "1% annual chance event" when talking about a particular magnitude of storm that, based on historic data, has a 1 in a 100 chance of occurring in a particular year, but many people often use the shortcut terminology of "100-year storm" or "100-year event." One danger in that usage is that people may conclude that a location cannot have, for example, two 50-year storms in the same year. Not true. The designation of a storm is a purely statistical one; nature does not perform according to statistics. In this report, we use "return period" and "annual chance event" interchangeably. Many people are accustomed to "return period" or "return interval," though a recent trend is towards usage of terms that frame events around annual chance or probability (i.e., 1% storm rather than 100-year storm) as a more appropriate way to convey the frequency of event occurrence.

In addition, hydrologists often use the term Annual Exceedance Probability (AEP) to refer to the likelihood of exceeding a specified target in any year. The number is a fraction of one. A storm with a 0.20 AEP has a 20% chance of occurring in any given year.

The table below provides values relevant to the return periods used in this report.

Return Period (x-year event)	Probability of Occurrence in Any Given Year	Annual Chance Event (percent chance of being equaled or exceeded in any given year)	Annual Exceedance Probability (AEP)
100-	1 in 100	1%	0.01
50-	1 in 50	2%	0.02
20-	1 in 20	5%	0.05
5-	1 in 5	20%	0.20

2.2.2 Use of global SLR scenarios in decision-making

The transition from scientific prediction of global SLR futures to their explicit use in decision-making has been slow but gaining momentum. The first hurdle to overcome was allowing ourselves to reconsider how to address uncertainty, not only with respect to the limitations of our current scientific understanding of climate forcings and physical system responses, but with the realization that over longer time horizons (i.e., roughly mid-century and beyond) it is the behaviors that humans exhibit that will determine future emissions, which will significantly influence future SLC (Section 2.5 addresses this issue in more depth). This changes the role of climate models and other methodological approaches to estimate future sea levels from prediction machines within "predict-then-act" frameworks to scenario generators that provide insight into complex system behavior and aid critical thinking within robust decision frameworks (Weaver et al. 2013). Here, consistent with its usage in Parris et al. (2012), a "scenario" is defined as a description of future potential conditions in a manner that supports decision-making under conditions of uncertainty. By this definition, scenarios are explicitly not predictions about the future and as such are not assigned likelihoods or probabilities; rather, they represent plausible futures that can still be bounded by observations and physical constraints.

Here a "scenario" is defined as a description of future potential conditions in a manner that supports decision-making under conditions of uncertainty.

The U.S. Army Corps of Engineers (USACE) has proactively considered SLR scenarios in its Civil Works programs for over 20 years, with a more recent progressive increase in the degree to which the use of such scenarios has been mandated and implementation guidance provided (USACE 2009, 2011, 2013, 2014). Use of a multiple-scenario approach has been emphasized in these documents mandating an explicit upper global SLR scenario of 1.5 meters by 2100 for planning purposes but acknowledging that 2.0 meters is a credible upper bound (USACE 2011, 2014). Such an approach acknowledges the use of scenarios as a mechanism for addressing uncertainty and managing risk. Similarly, for the Third National Climate Assessment (NCA), Parris et al. (2012) recommended following a decision-framing approach that, based on a survey of the literature to date, established bounding scenarios for global SLR scenarios of 0.2 to 2.0 meters by 2100 (using 1992 as the reference period to reflect the latest tidal epoch information). In an international context, Lowe et al. (2009) developed multiple SLR scenarios for the United Kingdom, including what they called a "High-Plus-Plus" scenario (up to 1.9 meters) that they considered beyond the "likely" range but within physical plausibility.

Previous to this effort no coordinated, interagency effort in the United States had developed agreed upon global mean SLR estimates to support coastal vulnerability assessment, planning, policy development, and adaptive management. The Parris et al. (2012) authors ascribed very high confidence (a greater than 9 in 10 chance) that future global mean sea-level increases would not occur outside this range (definition of very high confidence is in accordance with Moss and Yohe [2011] and reflects a combination of strong evidence and high consensus). Within this range,

however, they did not assign any likelihood to any particular portion of the range though they acknowledged different realizations of the future (e.g., accelerated ice-sheet loss) would need to occur to attain higher ends of the range. Two intermediate scenarios also were developed in an attempt to show some correspondence to the climate change emission scenarios being considered by the Third NCA (Intermediate-Low scenario) and a limited ice-sheet loss scenario using semi-empirical projections (Intermediate-High scenario). Similar to the USACE documents, Parris et al. (2012) emphasized the use of multiple scenarios in assessing risk and basing the choice of which futures to consider largely on the tolerance for risk associated with a decision. Figure 2.3 shows the four SLR scenarios used to support the Third NCA.

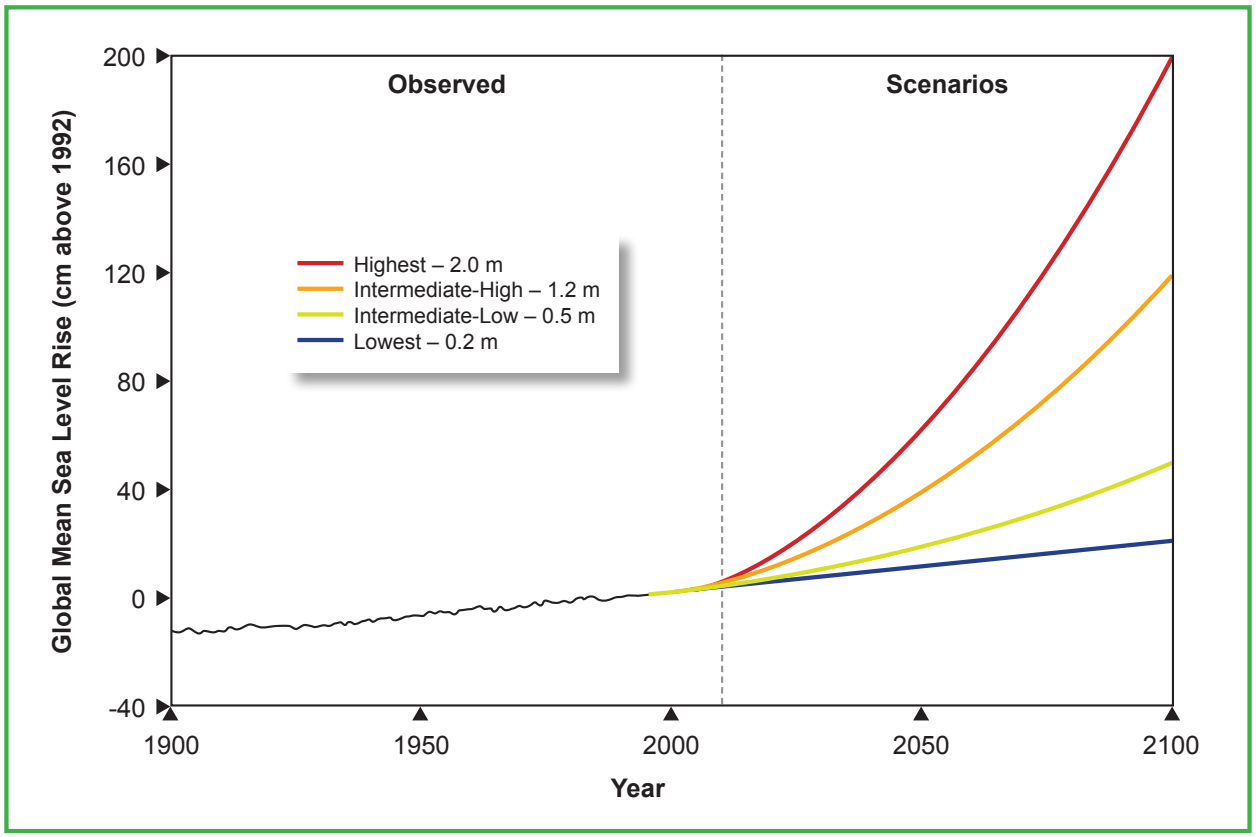

Figure 2.3 Four Scenarios Developed by Parris et al. (2012) to Support the Third NCA

This report starts with the bounding scenarios of Parris et al. (2012) as a foundation for identifying local and regional SLC scenarios (again using 1992 as the initial reference point). Intermediate scenarios, however, differ from Parris et al. (2012). Given that likelihoods are not assigned to any part of the range considered, and to avoid implying any specific accuracy of the intermediate scenarios, the intermediates are simply 0.5-meter subdivisions of the 2.0-meter bounding upper scenario. This results in the consideration of five global mean SLR scenarios for which regional or local adjustments will be provided, namely: 0.2, 0.5, 1.0, 1.5, and 2.0 meters (see Figure 2.4). Although we present five scenarios, we strongly discourage defaulting to the middle scenario (1.0 meter) as an appropriate choice for decision-making. Indeed traditional scenario development typically uses an even number of scenarios to preclude that situation. Given the way we chose increments, that option was not available.

Scientific findings published since the release of Parris et al. (2012) provide additional evidence for the selection of the 0.2- to 2.0-meter range. Discussion of these lines of evidence is in Section 3.3 as part of the overall storyline descriptions provided for the specific global SLR scenarios considered in this report. As a result, to provide additional context for those users of scenario information who may want to constrain their tolerance for risk based on their view of society's decisions regarding future emissions, Section 3.3.5 also provides storylines for the scenarios that relate to the RCPs used by the IPCC in its latest reporting.

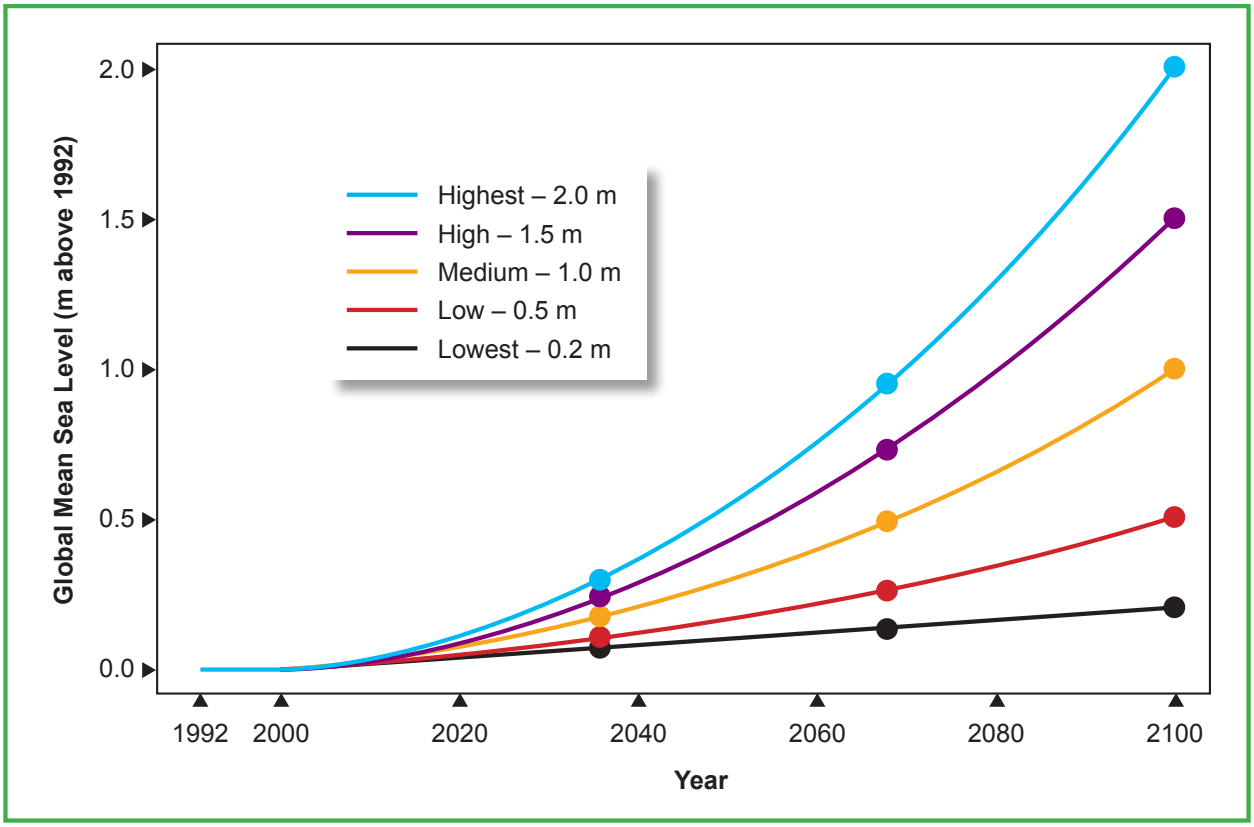

Figure 2.4 Five Global Sea-Level Rise Scenarios Advanced in Support of this Report

2.3 Regional and Local Adjustments to Global Mean SLR: Systemic Trends and Cyclical Patterns and Extreme Events

Global SLR scenarios, though a vital initial starting point, are themselves insufficient for decision-making at regional and local scales. Changes in sea level under climate change will not be expressed uniformly across the globe. In addition, the factors that contribute to derivations from the global mean do not behave in the same way. Finally, for risk management purposes, extreme water levels and their interaction with SLR also must be considered. The need for such adjustments is similarly recognized by the NCA and USACE approaches to scenario usage (Parris et al. 2012, USACE 2014). The adjustments considered in this report fall into two broad types: (1) those associated with systemic trends that are assumed to have a consistent directionality for a given location and (2) those associated with cyclical or sometimes infrequent events that have a significant locational dependency.

2.3.1 Systemic trends

Systemic trends expressed as specific numeric adjustments to the global SLR scenarios on a regional or local basis include vertical land movement, dynamical sea-level change, and changes in the shape of the surface of the oceans (or geoid), earth's crust, and earth rotation that result when the land-based ice sheets associated with Greenland and Antarctica melt (or calve) and redistribute mass across the oceans. Figure 2.5 illustrates the two primary causes of global sea-level rise: steric effects (green flag) and mass addition (red flag). Mass addition is also referred to as barystatic changes in sea level.

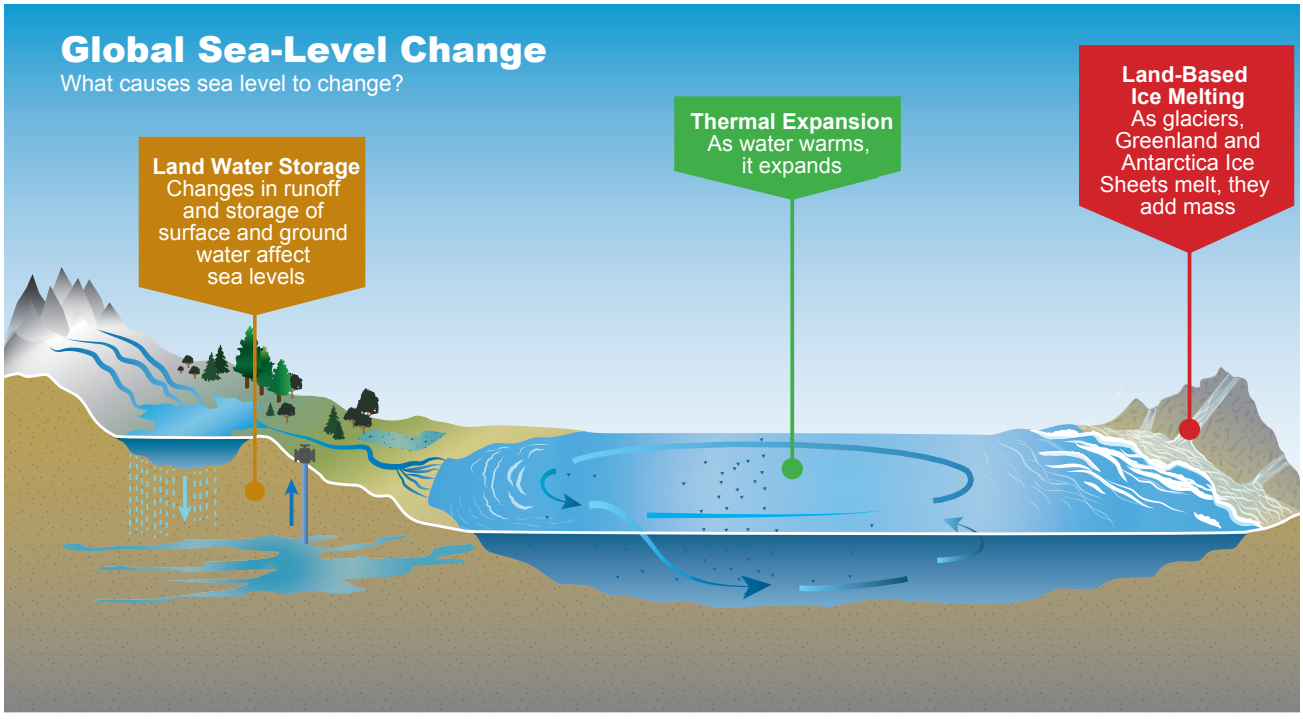

Figure 2.5 Two Primary Causes of Global Sea-Level Change – Thermal Expansion and Land-Based Ice Melting

Steric effects, or density changes, are primarily due to thermal expansion, but also could be attributed to salinity changes. (adapted from IPCC 2001)

In addition, land water storage (gold flag) may add or remove mass depending on global water management practices; however, this is a much smaller amount than the other two factors. Recent research (Reager et al. 2016) using satellite measurements indicates that climate-driven changes in land water storage and their contributions to sea-level rise may be important if considering decadal timescales. Given our focus here on longer timescales, however, we did not further consider the influence of land water storage on sea-level values. Figure 2.6 illustrates local or regional factors that affect sea level. (See the text box on the following page for additional details.)

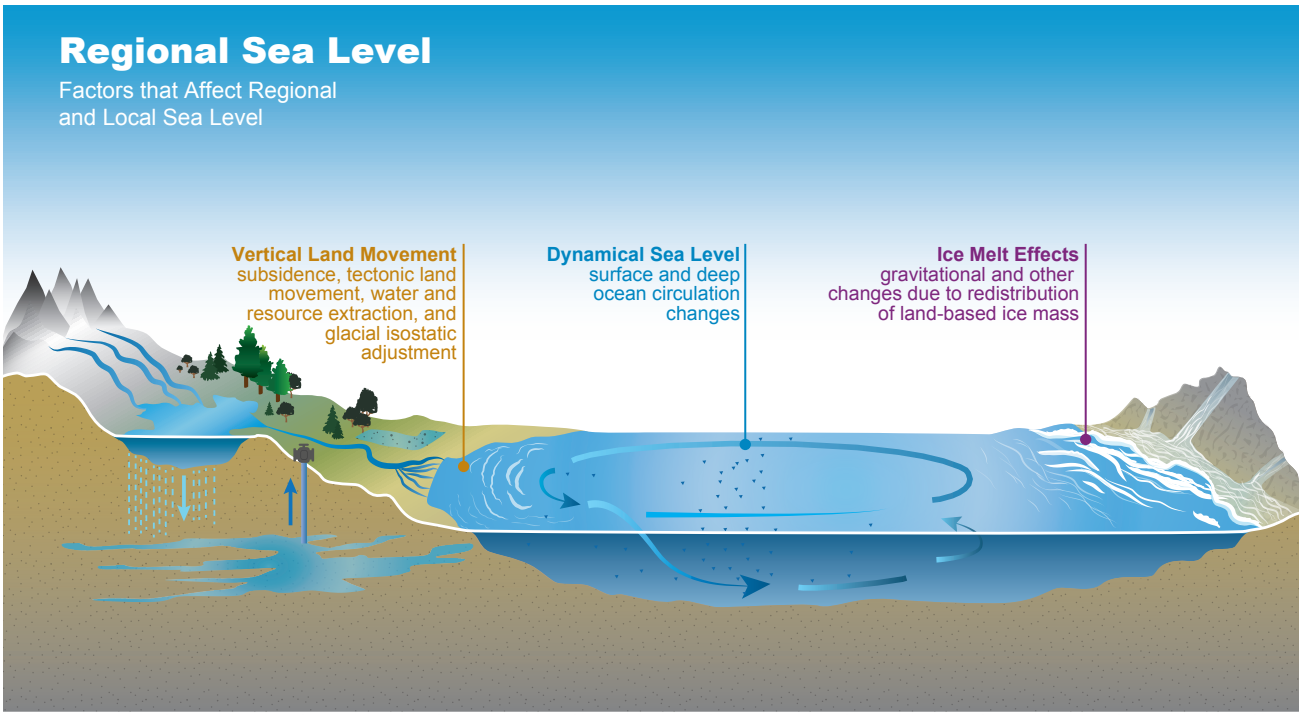

Figure 2.6 Regional and Local Adjustments to Sea Level
(adapted from IPCC 2001)

Vertical land movement (VLM) is a local process that can be attributed to phenomena such as glacial isostatic adjustment (GIA; the response of the land surface to the retreat of the Pleistocene glaciers), consolidation of loose, unconfined sediment layers, and groundwater withdrawal. Either local subsidence or uplift can occur as a result of GIA as the earth's surface accommodates to the loss of mass over the long term; however, the other contributions to VLM (excepting tectonics) will result in subsidence and an additional local contribution to SLR. Coastal geology, whether dominated by bedrock or coastal plain sediments, will control the degree to which local subsidence occurs (Miller et al. 2013). No matter the source, for the time period considered here (i.e., to 2100) it is assumed that the rate of VLM at a particular location will be linear over time. Section 3.4.2 provides the specific methodological approach for determining VLM on a site-by-site basis.

Current science enables *dynamical sea-level change* and *ice-sheet loss effects* to be expressed only coarsely (i.e., regionally) and for specific time horizons. Although this report assigns values for each site, they should not be interpreted to reflect any known granularity associated with their assignment. Indeed, the methodology used here identifies when the adjustments resulting from these phenomena are significant enough to warrant consideration at particular sites. The calculation of the regional adjustments to the global mean SLR that arise from dynamical sea-level change and ice-sheet loss are expressed as global "pattern-scaling" and as "fingerprints," respectively, and rely primarily on use of General Circulation Models (GCM) to determine their contributions as separate from steric contributions (attributable to changes in the density of water primarily due to thermal expansion). Although the effects of land water storage also may be associated with a fingerprint, as mentioned

Three Types of Regional or Local Adjustments to Sea-Level Rise

Sea-level rise does not occur consistently around the globe; the ocean is not a big bathtub. Locally and regionally, several factors influence sea-level changes.

***Vertical Land Movement**, either up or down, is due to:*

- *tectonic uplift,*
- *compaction of sediments,*
- *pumping groundwater or oil,*
- *post-glacial response (up or down) after the glaciers of the last ice age retreated (also called Glacial Isostatic Adjustment).*

Melting Land-Based Ice:

- *the mass of ice sheets exert a gravitational "pull" on the water around them; as the ice mass melts, the "pull" on the water decreases, and the water migrates away from the area of melting ice, making the counterintuitive impact of lowering sea level nearby,*

- *redistribution of mass around the globe also affects its rotation, which changes the "flattening" of the spinning globe, in turn affecting sea-level rise in specific areas,*

- *the earth's crust rebounds elastically in response to mass loss.*

Dynamical Sea Level (Ocean Circulation):

- *ocean currents, winds, temperature differences and salinity contours affect sea levels*

previously the overall contribution to sea level from land water storage is relatively small. As a result, we do not further consider this contribution to regionalized sea-level change.

Although seemingly counterintuitive, sea levels *fall* close to where the ice sheets are deteriorating and *rise* much farther away; this is due to changes in gravitational attraction (Mitrovica et al. 2011). The available information for both phenomena permits adjustments to the global mean only at specific time periods (see Section 2.4). As a result, only when their contributions are both negligible can extrapolations between time periods be made based strictly on VLM adjustments. Sections 3.4.3 and 3.4.4 provide the specific methodological approaches for determining dynamical sea-level changes and ice-sheet loss contributions to regional mean SLR. (See the text box on the previous page for descriptions of the three types of adjustments to global SLR.)

2.3.2 Cyclical patterns and extreme events

Changes in water level, even without the contribution of a long-term directional trend such as SLR, occur in response to several forcings acting over many time scales, from seasonal to decadal. Though much emphasis has been placed on assessing past and possible future changes in global mean sea level, it is high water events that are actually impacting locations at a site-specific scale. Extreme events result from a complex combination of tide-driven (deterministic) and storm-driven (stochastic) components. Many of the components have strong seasonal patterns (Haigh et al. 2010) and are affected by low-frequency meteorological phenomena such as the El Niño Southern Oscillation (ENSO) and Pacific Decadal Oscillation (PDO). This report focuses on providing a contemporary (and future) assessment of high water extreme probabilities in a spatial context (DoD sites) from a global network of tide gauges.

When considering the total water level that may be reached at a particular location, wave run-up (set-up plus swash) can be an important contribution though it is generally not measured directly by tide gauges. For the most part, tide gauges are located in sheltered, urbanized environments and do not experience breaking waves. In the absence of wave contributions, what remains is termed "still water level" (SWL) in which the interest is on extreme still water levels. See Figure 2.7 for a graphic depiction of these terms.

Extreme Water Level and many of its component contributions (e.g., instantaneous tide height, storm surge magnitude, etc.) can be estimated from tide gauge measurements. Tide gauges are the best platform to measure extreme water levels important for impact delineation because they are located along the ocean-land interface. Due to their maritime importance throughout history, they offer long and reliable measurements key to providing historic probabilities of extreme events. As a result, this report will focus on providing quantitative estimates for EWLs at each location for the 1%, 2%, 5%, and 20% annual chance events (see Section 3.5 for methodological details), which spans a range of events deserving consideration, from the rare destructive event (1%) to the less-extreme and more recurrent event (20%) now becoming problematic in many coastal communities due to local sea-level rise. Wave contributions are discussed in qualitative terms (see Section 3.6.2 for details).

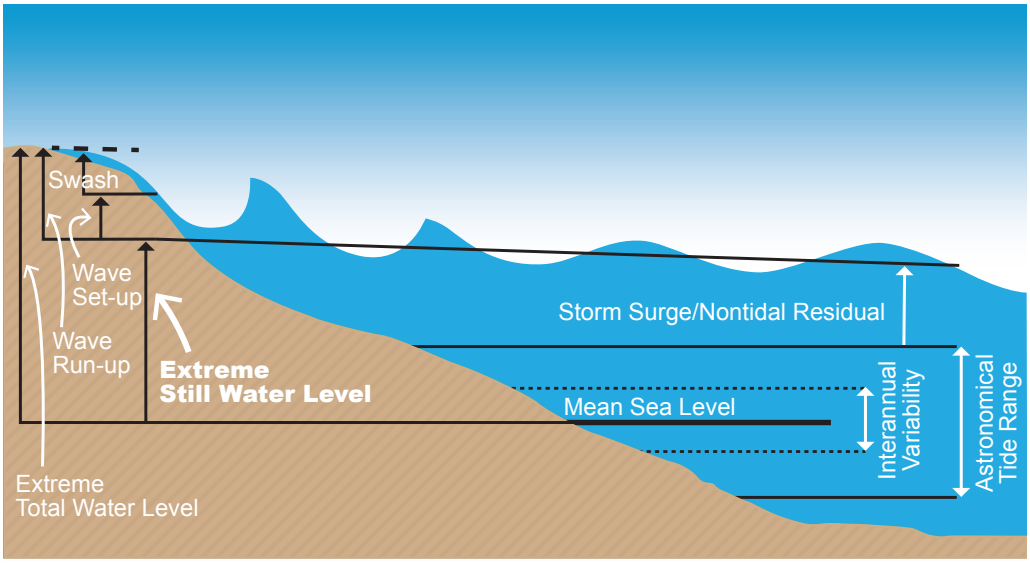

Figure 2.7 Components of Extreme Total Water and Extreme Still Water Level Measurements
This study focuses on Extreme Still Water Levels. (adapted from Moritz et al. 2015)

2.4 Time Horizons Considered

Decision-makers require information about future local SLR and EWLs over a variety of timeframes. This report considers the following time horizons: 2035, 2065, and 2100. The three time horizons are discrete. They were chosen to reflect different planning horizons associated with infrastructure planning. For example, 50 years (2015 to 2065) is generally used when considering the design life of built infrastructure. The above time horizons are similar to those considered by the USACE in its guidance on considering the effects of future sea-level change on its projects, with the exception that in lieu of stopping at 2100 (an 85-year time horizon) USACE uses a 100-year epoch as its longest-term analysis horizon (USACE 2014). Moreover, the 50-year time horizon is viewed as a typical economic analysis period (USACE 2014). Although our focus here is on time horizons out to 2100, we note that under all scenarios considered, sea levels will continue to rise beyond 2100 (see Section 3.3.3 for further details).

Section 5.3.5 includes a discussion to address situations for which sea-level rise scenario information is desired for the zero to 20-year timeframe. This reflects an attempt to provide relevant information in a continuous temporal manner for decision-making that is independent of the uncertainties associated with future emission scenarios. For this timeframe it is safe to assume that climate-related projections that result from using different emission futures do not diverge significantly and are swamped by internal (natural) variability in the climate system and model uncertainty (Hawkins and Sutton 2009, 2011).

Uncertainty is not a reason for inaction, because taking no action is a decision in itself.

2.5 Decision Framing: A Brief Discussion

Climate change is a catalyst not only as a driver of global environmental change but also as a force that will transition the way society makes decisions. Decision paradigms that rely on a view of the future that is "most likely" will undoubtedly be replaced by a view of the future that though highly uncertain can still be bounded. The previous guide, however, on bounding future conditions—the past—is no longer always the best option (Milly et al. 2008), especially as the time horizon for the utility of a decision extends past a couple of decades. As a result, decisions under uncertainty will need to be framed in a manner that is robust to different, but plausible future conditions, manages risks and costs in a balanced manner that is sensitive to the tolerance of a decision being wrong, and preserves future options (see Davis [2012] for a similar discussion of decision-making under uncertainty from a national security perspective). Preserving future options can serve to avoid overcommitting resources prematurely or making a maladaptive decision; a flexible approach will enable a phased response to climate change that can be adjusted over time as the actual climate is realized or understanding of plausible climate futures improves.

It is an erroneous assumption that systematic reduction of uncertainty in climate projections is required before information derived from such projections can be used by decision-makers (Lemos and Rood 2010). Uncertainty is not a reason for inaction, because taking no action is a decision in itself. Instead, in conjunction with an understanding of the decision to be made, the tolerance for risk associated with the decision, the expected performance under different future conditions, and the time horizon encompassed by the decision, selected scenario(s) (as defined in section 2.2) and other information can be used by decision-makers to identify strategies that are robust to an appropriate range of uncertainty that should be considered (Lemos and Rood 2010). As a result, the scenarios considered may differ as the factors above change or as the other non-climate-related information that bears on the decision changes.

This report attempts to follow the above philosophy as it conveys the use of scenario information. First, it is worth reminding the reader that the main purpose of the scenarios and other information presented here (and in the associated scenario database) is for guiding vulnerability and impact assessments at individual DoD sites worldwide. Decisions meant to support specific engineering design needs may require more granular information—not necessarily with respect to the scenarios but more so with respect to the available topographic or bathymetric data needed to visualize the results of scenario application—or complex hydrodynamic modeling. Second, in addition to providing some general recommendations on the application of scenarios, case studies are used to help illustrate scenario selection and application. These case studies use different examples showing that the appropriate choice of scenarios can accommodate different situations. It should be noted, however, that the case studies are not meant to be prescriptive as the ultimate choice of scenarios is either policy-based or left to the discretion of the decision-maker within certain

As a general rule this report recommends that a minimum of two scenarios be considered, though the spread in those scenarios will differ by decision and the time horizon considered.

guidelines. Third, planning for an uncertain future requires more than one number to plan to. As a general rule this report recommends that a minimum of two scenarios be considered, though the spread in those scenarios will differ by decision and the time horizon considered.

2.6 Relationship to Related Efforts

This section attempts to place this report's approach, findings, and recommendations into context with other efforts that attempt to develop regionalized SLR or flood hazard information. Section 3.3 provides an extensive discussion on the global scenarios used in this report and their rationale. This section will focus on other efforts that have attempted a regional focus to the development and use of SLR scenarios and in some cases the addition of extreme water levels.

The different types of approaches used to develop such information involve different assumptions and concerns. Some approaches attempt a given understanding of potential future SLR with no associated probabilities, others take a more probabilistic path, and the remainder rely on the use of a range of plausible future conditions or scenarios that are bounded by current scientific understanding of climate-related processes affecting coastal water levels. Figure 2.8 illustrates the differences of these three approaches—deterministic projections, ranges of projections with probabilities, and plausible scenarios. Hinkel et al. (2015) noted a specific dichotomy between viewpoints, such as those of Working Group 1 of the IPCC, whose aim Hinkel et al. contended was to understand and reduce uncertainty and those of coastal managers who desire to reduce risk (or to manage uncertainty). This difference in perspective is often the basis for the different approaches described below.

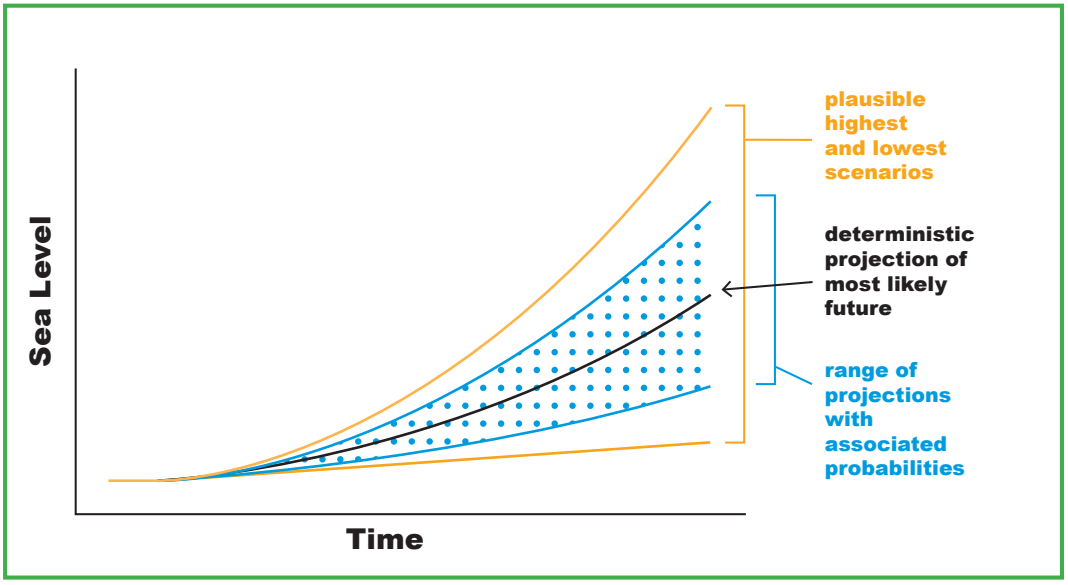

Figure 2.8 Conceptual Depiction of Differences Between Deterministic, Probabilistic, and Scenario-Based Approaches

2.6.1 National Research Council West Coast study

The National Research Council (NRC 2012) summarized published research results on the processes that contribute to sea-level change for the coasts of California, Oregon, and Washington, as well as adding its own analyses of relevant data and model results. The NRC initially updated the global SLR projections from the IPCC's Fourth Assessment Report (AR4; Bindoff et al. 2007). This resulted in a range of SLR projections for different time periods to 2100 (relative to 2000) that reflected uncertainties related to data fit, level of different GHG emissions (Special Report on Emissions Scenarios [SRES] B1 through A1FI), and future changes in the rate of ice flow from glaciers and the Antarctic and Greenland ice sheets (including possible dynamic contributions). Within the preceding ranges the NRC also provided "projections" (for three different time periods) based on a mid-range emissions scenario (A1B) for the steric component and an extrapolation of observations to estimate the ice loss contribution. The NRC then applied adjustments to reflect regional conditions along the West Coast of the United States that included differences in dynamical sea level (steric variations and wind-driven differences in ocean heights), VLM, and ice-melt fingerprinting. The summary presentation of SLR data (NRC 2012: Figure S.1, Figure 5.6, and Table 5.2) depicts the "projection" and the range for each time period and by region that also accounts for the regional adjustments. The VLM adjustments, which contributed significantly to regional differences, were based on Global Positioning System (GPS) measurements that reflected two tectonically distinct areas: Cascadia, the generally rising coastline north of Cape Mendocino, California, and San Andreas, the generally subsiding coastline south of Cape Mendocino.

The NRC (2012) "projections" represent a deterministic view of future SLR for the region because they are based in large part on an assumption of a mid-range emissions future and extrapolation of an observational record. The uncertainty bounds of these projections were determined by using other emissions scenarios, data, and statistical assumptions. This is certainly a reasonable approach for characterizing uncertainty, but it does not represent a strictly probabilistic approach. The ranges involved do not necessarily differ dramatically from those developed in this report; however, the efforts differ dramatically in placing emphasis on a "mid-range" projection. The authors of this report have emphasized that no ***one answer*** exists to address risk under future potential SLR. Moreover, we recommend an approach in which multiple plausible scenarios of the future are considered within a risk-based framing context. The NRC (2012) study, therefore, is also an example of the different perspectives between conveying scientific uncertainty versus addressing coastal risk management needs articulated by Hinkel et al. (2015).

Of note is that both efforts (NRC 2012 and herein) attempted to include several factors affecting the regionalization of SLR scenarios though the approaches differed. This report used multiple sources of VLM data and then applied them in a site-specific manner. For dynamical sea-level changes and ice-melt fingerprinting, in addition to using the more recent Coupled Model Intercomparison Project Phase 5 (CMIP5) results based on different RCPs versus the SRES-based projections, the effort herein used the model-based information to adjust individual global SLR scenarios and not just to create an uncertainty boundary for a mid-range emissions scenario. This required estimating ice-loss contributions for each global scenario prior to determining the regional fingerprint adjustment. Specific details on this report's approaches are provided in Section 3.0.

2.6.2 Other country, federal-, state-, and city-level approaches

Netherlands

Royal Netherlands Meteorological Institute (KNMI) developed a comprehensive set of climate scenarios (Klein Tank et al. 2015) by translating the global findings of the IPCC (Church et al. 2013a) to the situation in the Netherlands. Four scenarios, denoted as G_L, G_H, W_L, and W_H, were defined based on projected temperature rises for Year 2085 relative to the 1981–2010 mean. In the "G" or Moderate scenario (equal to the RCP 4.5 scenario) the temperature rise was assumed to be 1.5 degrees C. In the "W" or Warm scenario (equal to the RCP 8.5) the temperature rise was assumed to be 3.5 degrees C. The subscripts L (Low) and H (High) represent different influences of atmospheric circulation. Estimation of future sea levels along the Dutch coast included thermal expansion and mass loss from glaciers and the Greenland and Antarctica ice sheets. Although the gravitational changes due to ice mass loss were accounted for in the methodology, the land subsidence due to compaction of peat was not included in the scenarios because of the lack of reliable estimates (Klein Tank et al. 2015).

United States Army Corps of Engineers (USACE)

As mentioned in Section 2.2, the USACE has proactively and progressively considered SLR scenarios in its Civil Works programs for over 20 years (USACE 2009, 2011, 2013, 2014). The global scenarios considered are similar to those considered here. Current USACE regulations (USACE 2013) and guidance (USACE 2014) that address sea-level change requirements for Civil Works-related projects require a consideration of local VLM, but do not address regional adjustments associated with dynamical sea level and ice-melt fingerprinting.

Florida

The Southeast Florida Climate Compact organization produced what is known as "unified sea-level rise" projections for use as the basis for planning and impact assessment in the four-county region from the Florida Keys to Palm Beach County (SF Compact 2015). The projections included three scenarios, in descending order: the Parris et al. (2012) Highest Curve, the USACE High Curve (USACE 2013), and a curve corresponding to the median of the IPCC RCP 8.5 scenario (Church et al. 2013a). Specific guidance also was provided on when and how they should be used. All curves were referenced to 1992 but a methodology was provided to convert the projections to any other reference year. The curves were developed using the regional rate of SLR at Key West, and the global projections corresponded to an end-date of 2100.

Maryland

The state of Maryland issued its updated SLR projections in 2013 (Boesch et al. 2013). The Maryland study is of note here as it first assessed the global SLR scenarios from the NRC West Coast Study (NRC 2012), the Third National Climate Assessment (Parris et al. 2012), and USACE (2011) among other sources. The Maryland study ultimately relied heavily on the NRC (2012) study as the methodological basis for its recommendations. Curiously, in describing the NRC's (2012) mid-range emissions-based "projections" the Maryland study used the term "best projection" that unfortunately implies a connotation of "most likely" and deterministic (Boesch et al. 2013). Based

on the NRC (2012) study, the Maryland study also discounted the lowest (0.2 meters by 2100) and highest (2.0 meters by 2100) scenarios of Parris et al. (2012), but more recent research is supportive of these two extremes to appropriately bound risk (see discussion in Section 3.3).

Seemingly based on the extant literature at the time, the Maryland study adjusted the NRC's (2012) "mid-range" values and the uncertainty range by assigning "best projection" values (with associated low and high values applied to the ends of the range) for dynamical sea-level regional changes and ice-melt fingerprint contributions for 2050 and 2100 (Boesch et al. 2013). Finally, a best estimate for VLM for the state was suggested (also accompanied by a low and high estimate), though the potential for local differences was acknowledged (Boesch et al. 2013).

Massachusetts

The state of Massachusetts study (Massachusetts CZM 2013) is interesting not because it addresses explicitly all appropriate regional adjustments to global SLR (it does not); instead, it is unique in that it modifies the Parris et al. (2012) global scenarios directly by accounting for "local" VLM (uses one value for the state based on a Boston-area tide gauge station), adjusts the scenario starting date to 2003 using the method of Flick et al. (2012) to adjust the midpoint of the tidal epoch from 1992, and adjusts the mean sea-level tidal datum to the local geodetic datum (NAVD88). These adjustments are possible in part because the study does not explicitly address dynamical sea level and ice-melt fingerprinting, though it acknowledges them. Of note is that the adjusted scenarios force an increase in the assumed rates of sea-level rise acceleration for the upper three Parris et al. (2012) scenarios given the end date (2100) and end points (adjusted for VLM) are the same but the initiation point (2003 versus 1992) differs. Finally, the Massachusetts study also places the use of the scenarios into a risk-based decision-framing context.

New York City

The New York City Panel on Climate Change produced a set of climate projections specifically for New York City (NPCC 2013). The report included SLR projections for the 2020s and 2050s relative to 2000–2004. The projections were based on a process-based method that aggregated both global and local components. The projections included thermal expansion, ice mass losses from glaciers, Greenland, and Antarctica that accounted for the regional influence of gravitational fingerprints, land water storage contribution, and vertical land movement including glacial isostatic adjustment (GIA). For the 2020s the projections ranged from 2 inches (10^{th} percentile) to 4 to 8 inches (25^{th} to 75^{th} percentiles) to 11 inches (90^{th} percentile). The corresponding ranges for the 2050s were 7 inches, 11 to 24 inches, and 31 inches. The ranges were based on the model spread from the output of 24 General Circulation Models (NPCC 2013). The New York City Panel also produced several flood risk maps to illustrate the trends of future flooding under projected scenarios of SLR. The New York City effort is one of the more comprehensive studies incorporating global and local implications of sea-level rise contribution to a local region.

2.6.3 Probabilistic approaches

Probabilistic approaches to global (Grinsted et al. 2015, Jevrejeva et al. 2014, Kopp et al. 2014, Rohling et al. 2013) and regional (Grinsted et al. 2015, Kopp et al. 2014) SLR projections have recently been published. Such projections, most of which are more accurately viewed as providing

contingent probabilities given their dependence on non-probabilistic emissions futures, have extended the ranges of projected sea levels considered by the IPCC Fifth Assessment Report (AR5; Church et al. 2013a):

- through the use of geological evidence to incorporate the delayed responses to GHG emissions in a probabilistic framework (Rohling et al. 2013);
- through a combination of expert community assessment and elicitation and process modeling (Kopp et al. 2014);
- extending the probability range of Church et al. (2013a) for RCP 8.5, summing the highest estimates of individual SLR components simulated by process models for RCP 8.5, and using a semi-empirical model approach to estimate an upper bound (Jevrejeva et al. 2014); and,
- using a probabilistic projection of the major components of the global sea-level budget for RCP 8.5 (Grinsted et al. 2015).

The first three studies above referenced the expert elicitation of Bamber and Aspinall (2013) to adjust the tails of the distribution for ice-sheet loss, Grinsted et al. (2015) and Jevrejeva et al. (2014) used the expert elicitation as it was, and Kopp et al. (2014) reduced the contribution to match the AR5 median projection. Grinsted et al. (2015) estimated a higher high-end SLR by 0.6 meters (to 1.8 meters; upper end of the 5 to 95% probability range) than Kopp et al. (2014) for RCP 8.5 and 2100. Further discussion of the preceding studies in defining the upper bound of the global SLR scenarios considered herein is provided in Section 3.3.

Kopp et al. (2014) also accounted for regional adjustments to their global projections by considering dynamical sea level, ice-melt fingerprinting, and local VLM. They did this for 11 locations worldwide. Some of their underlying assumptions, data sources, and models for each of these components differed from those used here (for example, they used Mitrovica et al. [2011] for their ice-melt fingerprints; however, this report used the fingerprints of Perrette et al. [2013] that relied on Bamber and Riva's [2010] approach), but this report also relied significantly on Kopp et al.'s (2014) probability distributions for determining contributions from glaciers and ice caps and the Greenland and Antarctic ice sheets for the different global scenarios). See Section 3.4.4 for details.

Using only RCP 8.5 as a basis, Grinsted et al. (2015) first adjusted the probability distribution of the global RCP 8.5 SLR scenario of Church et al. (2013a) and then adjusted it for dynamical sea level, ice-melt fingerprinting, and VLM using a glacial isostatic adjustment (GIA) model for northern Europe. They found, not unexpectedly, that the dominant uncertainty was about the fate of Antarctica. Finally, they also attempted to consider uncertainty covariance between components, which broadens the probability distribution and increases the high-end SLR projections (Grinsted et al. 2015).

Rohling et al. (2013) used geological evidence and the fact that anthropogenic climate forcing is more than an order of magnitude larger compared to the past to develop a probabilistic framework for predicting future SLR. They compiled geological observations of past rates of ice volume/sea-level adjustment to formulate a logistic function to reflect mass loss from ice sheets gradually leading later to a rapid acceleration due to temperature feedbacks. The geological

data were used to constrain the parameters of this function. Using this model and probability distributions of some of its parameters, Rohling et al. (2013) conducted a Monte Carlo study to produce probabilistic estimates of future SLR. They concluded that the modern sea-level change is rapid by past interglacial standards but SLR around the 95% level of the probability distribution would require conditions beyond interglacial precedents such as catastrophic ice-sheet collapse. Little et al. (2015b) shed further doubt on a strictly probabilistic approach for determining future sea-level conditions. They assessed the uncertainty in a large ensemble of CMIP5 atmosphere-ocean general circulation model (AOGCM)-based projections of sea level at global and local scales (New York City; which includes a dynamic sea-level response) by partitioning uncertainty into model, scenario (RCP) uncertainty, and internal (natural) variability. Model uncertainty was important through most of the century globally and dominant locally through 2100. The choice of AOGCMs greatly affected the model-spread results, especially for RCP 8.5. Little et al. (2015b) concluded that the selection of AOGCMs with regard to performance against observations and number of individual model realizations strongly affects quantification of model-spread behavior and has important implications for local risk management.

Additional work extended the probabilistic approaches associated with SLR to also include storm surge (Kopp et al. 2014, Little et al. 2015a, Tebaldi et al. 2012). Generally unless detailed hydrodynamic modeling is used, this involves the use of local tide gauge information (Kopp et al. 2014, Tebaldi et al. 2012) that is not always available (see Section 3.5); however, Little et al. (2015a) develop their joint SLR-storm surge projections using changes in the power dissipation index (PDI; an integrated measure of tropical cyclone intensity, frequency, and duration) driven by RCP-dependent AOGCM simulations. Results were sensitive to the AOGCMs considered and the correlated relationship between model-derived SLR and PDI (Little et al. 2015a).

2.6.4 Federal agency coastal assessment tools

A variety of agency and private sector decision-support tools have been developed to assist the end-user community in the various aspects of coastal risk management. These tools may enable users to apply "what-if" scenarios, provide local adjustments to global sea-level change scenarios, view potential inundation levels that may result from a particular scenario application, and otherwise enable a description of a particular site's vulnerability to sea-level rise and storm surge. In general, the scenarios and applications developed herein extend the domain of any of these extant tools into a worldwide framework in which regionalization information (such as dynamical sea level and ice-melt fingerprinting) previously only applied to specific regions is now provided to sites worldwide, multiple sources of information are used to inform local vertical land movement, and innovative techniques are applied to derive extreme water level statistics for sites lacking representative tide gauges. As detailed in Appendix B, each of the tools described has its own unique applications, advantages, and disadvantages. We provide descriptions of some commonly used federal tools that agencies are currently using or developing to enable the reader to understand the utility of each tool and how they relate to the information developed in this study.

THIS PAGE LEFT INTENTIONALLY BLANK

Section 3.0
Approach

This section details the methodological approaches, sources of data, and rationale underlying the choices made in this research effort. It begins by describing the process for identifying those military sites that are the subject of this report (Section 3.1) and key considerations associated with tidal epochs, datums, and location (domestic versus international) that may affect the proper use of report information (Section 3.2). The next sub-section describes the basis for global sea-level rise scenarios (Section 3.3). The next two sub-sections focus on the methodologies associated with determining systemic trend adjustments to global sea-level rise (SLR) scenarios and determining the non-trend contributions to extreme water levels (EWL; Sections 3.4 and 3.5, respectively). The final sub-section focuses on other considerations that may affect sea-level trends or total water levels (e.g., EWL plus wave run-up for which the report and associated database do not provide specific numeric values (Section 3.6).

3.1 Identification of Department of Defense (DoD) Coastal Sites

Coastal sites are defined as those sites that have potential inundation impacts from relative sea-level change and coastal storm surge over the next century. This includes sites that are not necessarily located along the coast, but that are still tidally influenced. The steps to identify candidate sites are outlined below.

3.1.1 Datasets considered

All DoD installation point files (sites) and installation boundary files were obtained from already compiled DoD data sources (the Real Property Assets Database [RPAD] via the Defense Installation Spatial Data Infrastructure or DISDI) and converted to Geographic Information System (GIS) shape files for display in ArcGIS. The data set contains information regarding location, site type, and parent (installation and Military Service) organization. Any sites shown in this report for purposes of illustration are a subset of those in RPAD for which DoD has made locational information publicly available through the Military Installations, Ranges, and Training Areas (MIRTA) database. The scenarios database accompanying this report includes all 1,774 sites, including those not in the public domain. Although this database cannot be shared publicly as it contains For Official Use Only Information, a database that is a subset of the sites and information that can be made public is being considered.

3.1.2 Method for determining a coastal or tidally influenced site

Coastal sites were identified initially by determining the distance of a military site from the nearby shoreline. A GIS filter was designed to identify only those sites within 20 kilometers (km) of the shoreline. The 20-km buffer was selected based on professional judgment and knowledge of coastal topography and potential maximum limits of SLR estimates. The full resolution world shoreline from the National Centers for Environmental Information (NCEI; formerly the National Geophysical Data Center); http://www.ngdc.noaa.gov/mgg/shorelines, accessed January 2015), which is in the WGS1984 coordinate system, was converted from a polygon shape file to a line shape file. This converts the shoreline into line segments for application of the "Select by location" tool using 20-km distances. In some upper portions of tidal rivers, the GIS algorithm did not select all affected locations and additional locations were added manually in a second iteration of the coastal list. Multiple quality control checks were conducted to ensure the most complete list was developed and that no applicable locations were left out. We considered the approach above conservative in terms of capturing sites potentially vulnerable to sea-level rise and extreme water levels both today and in the future out to 2100.

3.2 General Considerations

The following sections describe the role of tidal epochs and datums, use of mean sea level (MSL), and determination of vertical elevation. This information is also placed in the context of differences between continental U.S. locations and other geographic areas in the availability and use of the underlying data.

3.2.1 Tidal epochs

Tidal epochs are specific 19-year periods of time used in tidal work to capture the 18.6-year lunar cycle called the "regression of the moon's nodes." The range of tide observed globally undergoes a slow cyclic modification resulting from a slowly changing lunar declination effect. The United States presently uses observations from the 1983 to 2001 National Tidal Datum Epoch (NTDE) for referencing all tidal datums and local mean sea level (MSL). The nodal cycle results in slowly varying amplitudes for the tidal constituents whose magnitudes differ globally depending on the type of tide. These variations influence high tidal levels (Haigh et al. 2011).

3.2.2 Datums and use of MSL

Two specific tidal datums generally are used in the estimation of coastal impacts from changing sea levels. First, local MSL is determined from tide gauge measurements relative to a NTDE. The center year of the NTDE period is the baseline year from which inundation estimates from SLR are initiated. For the 1983 to 2001 NTDE, 1992 is the center reference year. Second, depending on tide type, Mean High Water (MHW) and Mean Higher High Water (MHHW) are tidal datum elevations often used as baselines above which inundation is depicted on digital elevation models (DEM) and inundation maps. These datums represent the upper level of the normal daily vertical excursion of the tide. For this report, the elevation of *MHHW relative to MSL* and *MHHW relative to the North American Vertical Datum* (NAVD88) are used as baseline datum adjustments for assessing flood risk. Any inundation above the normal daily tidal inundation is considered to have

potential negative impacts from flooding. The schematic diagram in Figure 3.1 illustrates the relationships of the different tidal and geodetic datums mentioned above. Other tidal datums typically used in coastal mapping and tidal work (but not in this report) are Mean Low Water (MLW) and Mean Lower Low Water (MLLW).

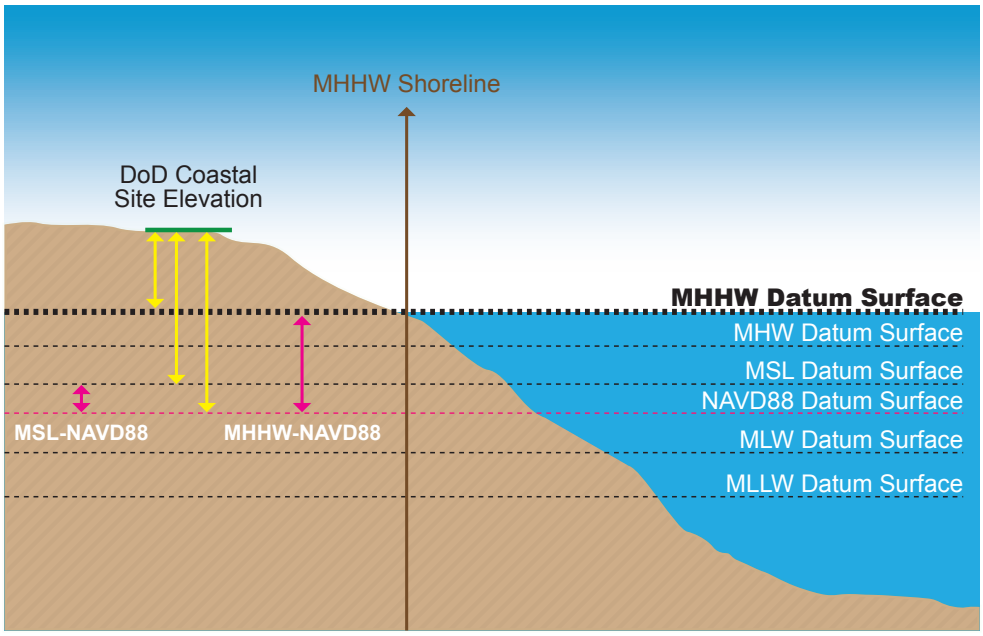

Figure 3.1 Concept Diagram of Tidal and Geodetic Elevation Relationships for a Coastal Site
Note that NAVD88 may be above or below Mean Sea Level. Mean Higher High Water is always above NAVD88. The example DoD site is for illustrative purposes.

3.2.3 Vertical land elevation (topography)

One type of important datum relates to vertical land elevation. Vertical land elevations in the U.S. lower 48 states are determined and referenced to the North American Vertical Datum (NAVD88) (see schematic in Figure 3.1 above). Elevation relationships between NAVD88 and tidal datums are determined through local surveys between tidal and geodetic bench marks at tide stations or by using static Global Positioning System (GPS) surveys on tidal benchmarks. In the lower 48 states the National Oceanic and Atmospheric Administration's (NOAA) VDatum tool (NOAA 2012) can be used to estimate datum relationships away from tide gauge locations. Topographic elevations (relative to NAVD88 from the U.S. Geological Survey (USGS) or relative to MHW [from NCEI]) can be obtained from various high resolution DEMs for the United States. Topographic Light Detecting and Ranging (LIDAR) data can be used if available for specific locations where DEMs do not exist. In the United States, VDatum interpolation from NAVD88 to MSL and MHHW can also be obtained.

The NAVD88 system does not extend to U.S. ocean island states and possessions. The reference datum used in Puerto Rico and U.S. Virgin Islands is PRVD02. For the Pacific Islands, the reference datum of Local Mean Sea Level (LMSL) is used for topographic elevations.

3.2.4 Domestic versus international considerations

The majority of the coastal sites being considered are in the continental United States (CONUS), Alaska, Hawaii, Puerto Rico, Virgin Islands, and other U.S. ocean island possessions. Many foreign sites, however, do not have known elevations of local MSL, MHW, or MHHW and the geodetic reference datum may be unknown. Land elevation reference systems and sea-level reference systems will have to be determined and reconciled for analysis depending on location.

In some international cases, range of tide information can be obtained from international tide table sources and global tide models to estimate relationships of MHHW to local MSL. Available topographic elevation data sources can then be used to estimate the relationship of the inundation above estimated MHHW or MSL relative to the land. These estimates will have significantly higher uncertainty than those with direct measurement data. For those sites that do not have geodetic or tidal datums, Section 5.2 contains guidance on how to proceed in these instances.

3.2.5 Estimation of elevations of coastal sites

Estimation of vertical land elevation of DoD coastal sites is required to complete the analysis of potential impacts of future SLR. Once the reference datum for land elevation data is determined, it can be overlaid with elevation information for MHHW and MSL obtained from other sources. This information is used in conjunction with the incremental estimation of SLR for each site to determine if the DoD site elevation is above or below the potential total SLR for each scenario. The database has been configured with MHHW-to-Reference Datum and MSL-to-Reference Datum Offsets for each coastal site.

Data Sources

Land elevation information for the United States can be obtained through the U.S. Interagency Elevation Inventory including the USGS National Elevation Dataset (NED) (Gesch et al. 2002) (http://viewer.nationalmap.gov/viewer, accessed April 2015 and http://coast.noaa.gov/dataregistry/#/search/dataset/info/inventory, accessed April 2015), and LIDAR data from NOAA, the U.S. Army Corps of Engineers (USACE), and other sources. The primary reference datum for topographic elevation data is NAVD88. NAVD88 is not used as the geodetic datum for U.S. ocean island territories and possessions, and the National Geodetic Service (NGS) has defined specific geodetic datums for each island based on long-term tide gauge measurements and local benchmarks. As described above for islands, in Puerto Rico the geodetic datum of PRVD02 is used. In Hawaii, the geodetic datum of LMSL is used. In any case, the topographic source data are in various spatial resolutions and accuracies which must be taken into account in assessing risk and assessing the impacts of SLR using topographic data (Gesch 2012).

Elevation data for foreign coasts must be obtained from alternate local and global datasets, usually with less accuracy and spatial resolution than the United States. Foreign elevation data were not obtained for this report. Countries with developed infrastructure, such as Japan and South Korea, have their own sophisticated geodetic datum reference systems and local elevation points and elevations may be obtained from those systems. Online databases such as the USGS NED may also be available. In many cases, local topographic and engineering survey data from individual

site surveys will have to be used, perhaps supplemented by a tide gauge or satellite data to obtain mean sea level and tidal datums relative to the topography.

The definition of the shoreline by NOAA is the intersection of MHW (or MHHW in areas of diurnal tides) with the land at the coast. Traditionally determined and mapped using photogrammetric technology ground-truthed by tide gauge data, LIDAR data can also be used after the elevation differences between NAVD88 and MHW are determined. LIDAR data are collected relative to the ellipsoid, but then converted to NAVD88 using GPS measurements taken during the LIDAR collection. Elevation differences between NAVD88 and MHW, MHHW, and MSL can be determined precisely at surveyed-in tide gauge locations, and then can be estimated for all other point locations and the shoreline contoured using the NOAA VDatum interpolation tool (White 2007).

Coastal Site Elevation Relationships for MHHW, MSL, and NAVD88

For DoD coastal sites that are within three km of a long-term tide gauge (93 U.S. DoD sites), the elevation relationships are established directly by the observed values and geodetic surveys from the tide gauge location. Three km is a reasonable distance within which the trends and elevation relationships are relatively constant. An additional 245 DoD coastal sites not located within three km of tide gauges are still found in the U.S. VDatum grid, meaning that they are near the shoreline and within the VDatum model grid thus have modeled MSL-MHHW-NAVD88 elevation relationship values.

Most DoD coastal sites are not located right at the shoreline and are generally located upland from the shore. For this study, MHHW and MSL elevation relationships to NAVD88 are estimated at these inland sites using VDatum with the convention shown in Figure 3.2. The elevation relationships between NAVD88 and MSL and MHHW are determined and fixed at the shoreline, and those fixed relationships are extended upland such that MSL and MHHW elevation relationships to NAVD88 can be estimated at upland installation points as well.

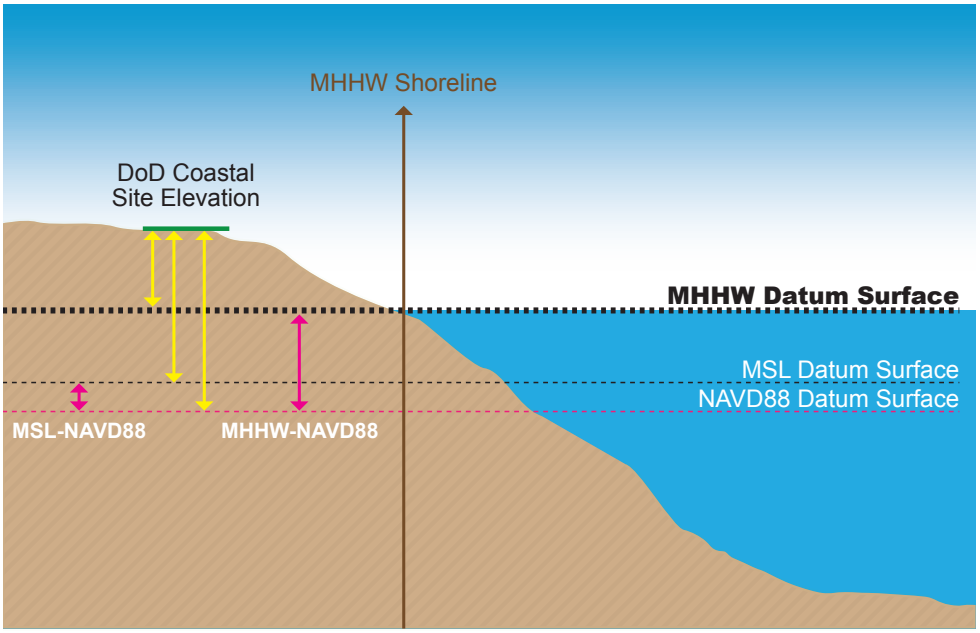

Figure 3.2 Convention Used to Estimate Inland Site Elevation Points Relative to Mean Higher High Water (MHHW) and Mean Sea Level (MSL)

Elevation relationships established at the shoreline are held fixed moving inland.

The following two pages provide an illustrative example of datum relationships for a site in Maryland.

Illustrative Example for Establishing NAVD88 Elevations, and NAVD88-MSL, and NAVD88-MHHW Elevation Relationships

DoD site locations associated in the vicinity of Annapolis, Maryland, serve to illustrate estimation of datum relationships (see map below). Sites depicted below correspond to sites in the RPAD and are assigned random numbers here for illustrative purposes.

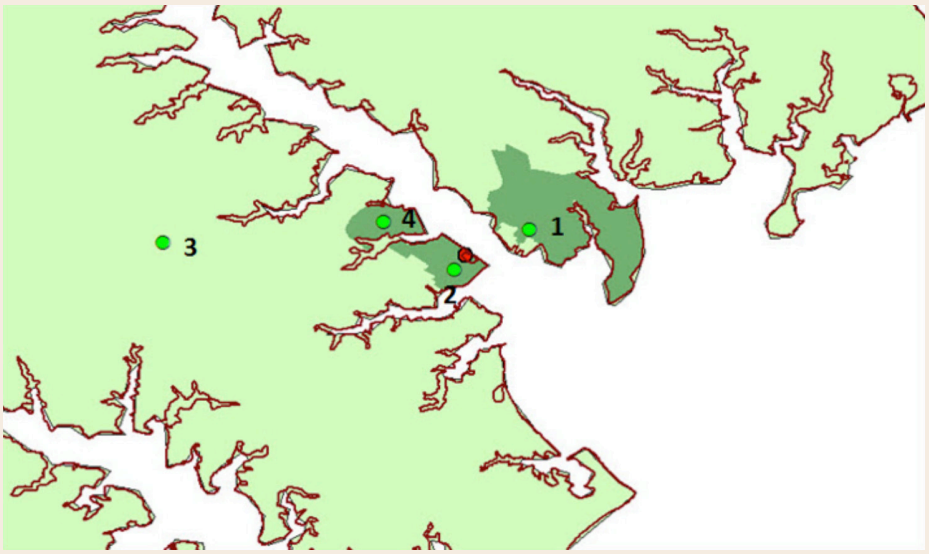

DoD Site Locations in the Vicinity of Annapolis, Maryland
Location of Annapolis tide gauge shown in red.

The latitude and longitude coordinates for each location are obtained from the DoD sites spreadsheet and transferred and formatted to a text file for loading into the USGS NED Bulk Point Query online utility. The query returns NAVD88 elevations in meters and feet (see below).

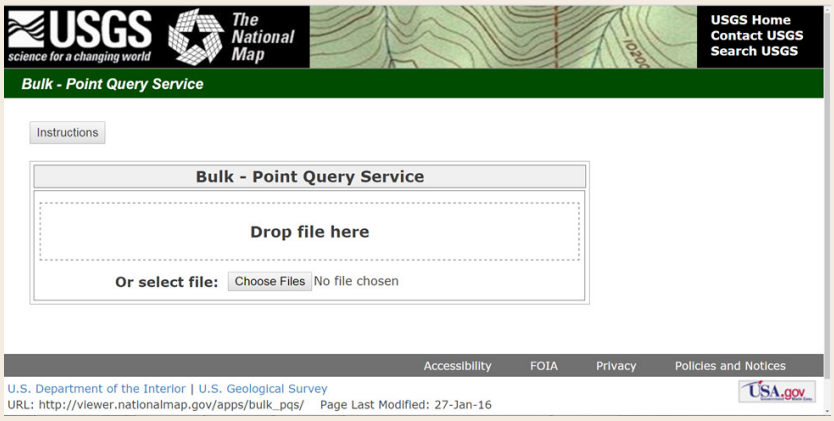

Screen Shot of USGS NED Bulk Point Query Tool Used for DoD Site Locations

(http://viewer.nationalmap.gov/beta/bulk_pqs/index.html, accessed June 2015)

The elevation relationships between NAVD88 and MSL and MHW are determined directly from a tide gauge location or are estimated using the NOAA VDatum tool, in which files on latitude and longitude coordinates can be input online to obtain elevation relationships for each location. The image below illustrates the VDatum output for an example DoD location site at Point Lookout, Maryland. The table below provides land elevations and elevation relationships for Annapolis sites.

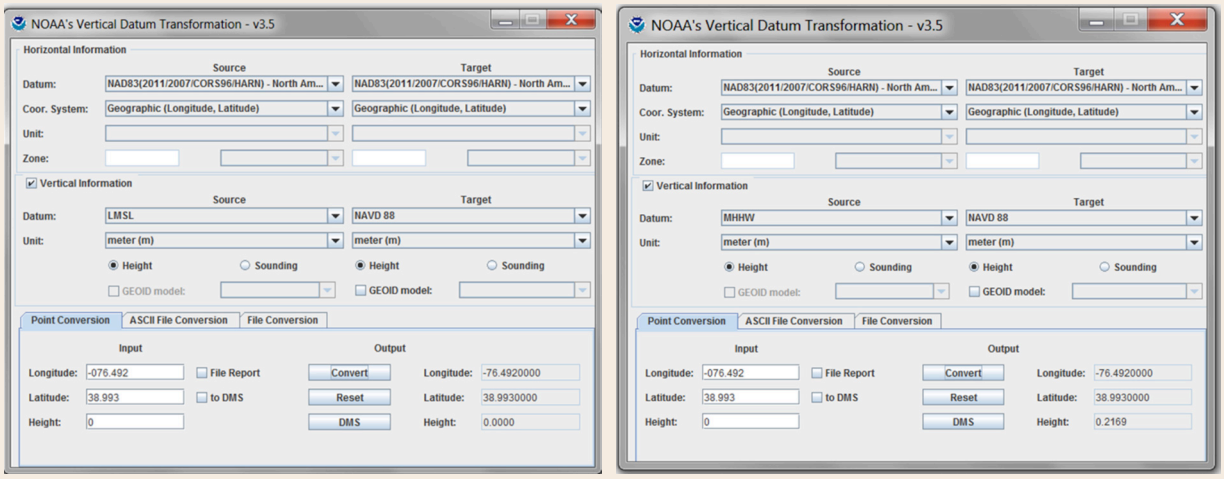

VDatum Elevation Relationship Output for Example DoD Sites at Upper Yard Annapolis, Maryland

Land Elevations and Elevation Relationships for Vicinity of Annapolis, MD

(all elevations are in meters)

Site Designation	Name	LONG	LAT	Elevation (NAVD88)	LMSL-NAVD88	MHW-NAVD88	MHHW-NAVD88
1	NSA Annapolis	-76.4687	38.9875	21.35	-0.01	0.12	0.18
2	Naval Academy North Severn	-76.4819	38.9805	1.25	0.00	0.14	0.20
3	NG LTC (MD) E. Leslie Medford	-76.5329	38.9853	20.37	0.00	0.15	0.22
4	Upper Yard Annapolis	-76.4943	38.9890	9.89	0.00	0.14	0.22

The estimated uncertainty in the datum elevation relationships is +/-0.15 m (one standard deviation).

Estimating Lowest Elevation Points for Sites Defined by Shape Files (Polygons) in the DoD Real Property Assets Database

Elevation plays a key role in determining whether a coastal site is actually exposed to sea-level change and extreme water levels. In some cases, sites within the 20-km buffer used to identify candidate sites for this study may occur entirely at elevations that are not vulnerable currently or under the future scenarios considered herein. The resolution and errors associated with available topographic information, however, affect the degree to which confidence can be placed in these determinations. Still, it is beneficial for users to consider initial screens based on topographic information and other factors that can confidently eliminate particular sites from the need for further assessment.

Sites within the DoD RPAD are associated with a mix of geospatial data, including both point information and polygons. Each site is assigned a coordinate location in the database, which for polygons is the centroid of the polygon. In the context of this study, for each polygon it is also helpful to know the lowest elevation point of the polygon. Of the 1,774 sites considered in this study, a total of 1,086 sites are associated with polygon information.

To determine lowest elevation points, we accessed generally available datasets of coarse elevation resolution and error. For sites located in the Continental United States (CONUS), Hawaii, and portions of Alaska and Puerto Rico (a total of 844 sites), we used digital elevation models (DEMs) available from the National Elevation Dataset (NED). The NED is a seamless raster product produced by the USGS. The NED data accessed for this project have a resolution of 1/3 arc-second (approximately 10 meters). The root mean square error for the NED is 1.55 meters (Gesch et al., 2014) These data are distributed in geographic coordinates by decimal degrees, and they conform to the North American Datum of 1983 (NAD83). All CONUS elevation values are in meters referenced to NAVD88. For the remaining Outside Continental United States (OCONUS) sites, elevation data available from the Shuttle Radar Topography Mission (SRTM) dataset (version 4) were accessed (http://vterrain.org/Elevation/SRTM/, accessed November 2015). The SRTM data accessed have a resolution of 1 arc-second (30-meter resolution dataset). The root mean square error for the SRTM dataset is approximately 5 meters.

The DEMs were retrieved and used to create a virtual raster of all combined DEM tiles. For each site projected to be affected by changing sea levels, its associated polygon was applied to the virtual raster as a layer mask. Elevation data for the masked installation area were extracted and analyzed to determine the minimum, maximum, and average elevation per cell. For each polygon, a minimum elevation, maximum elevation, and mean elevation were added to the site data in the accompanying scenario database for the 1,086 sites with polygon information.

Screening Sites against a Threshold Elevation

To conduct an initial coarse screening of sites defined by polygons that exceed a particular threshold elevation value, we combined the NED topographic information with a globally applied (worst case) scenario and other information to define an overall threshold value against which to screen. Given the larger errors associated with the SRTM dataset, we did not perform a similar

analysis using those data. Section 4.1 provides the details of threshold determination and the results of the initial screen. Sites located completely above the threshold value are flagged in the scenario database. Personnel responsible for site assessment may want to consider additional screens of this nature when higher resolution topographic data are available for specific sites and site-specific scenario information can be applied. Please note that the installation polygon boundary data and points obtained from the Real Property Assets Database are for planning purposes only and are not necessarily legal or surveyed land parcel boundaries. As a result, if portions of sites occur outside the polygons, these additional sites need to be separately assessed.

3.2.6 Use of digital elevation models (DEMs)

In addition to geographic point source elevation information in the database, the database also contains geographic boundary information. The topography within these boundaries is usually complex and not necessarily captured by the point locations alone. High resolution digital elevation models can be used to estimate elevations in a gridded depiction. This is what essentially is done in creating the NOAA National Centers for Environmental Information DEMs and NOAA Sea Level Rise Viewer inundation maps with topobathy related to DEM MHW and MHHW surfaces. Marcy et al. (2011) provide a brief history of previous sea-level change visualization pilot projects, a detailed discussion of new methods, and future plans for expanding the NOAA Sea Level Rise Viewer to the rest of the United States. The NOAA NCEI has produced several DEMs for coastal areas and supports a data portal (Carignan et al. 2011).

The NOAA VDatum tool (NOAA 2012) can be used to interpolate the relationships along the shoreline. Integration of the VDatum tool with DEMs allows for selection of point elevation relationships between tidal and geodetic datums and for delineating areas below (above) datum thresholds. An example of using a DEM for the military base at Camp Lejeune, North Carolina, is shown in Figure 3.3 and Table 3.1 whereby various site locations can be assigned elevation relationships for further analysis.

Table 3.1 NAVD88 Elevations and Tidal Datum Relationships for Camp Lejeune, North Carolina
(Elevations in meters)

Site Designation	Name	LONG	LAT	LMSL-NAVD88	MHW-NAVD88	MHHW-NAVD88
1	MCB Camp Lejeune	-77.3433	34.6626	-0.02	0.07	0.09
2	MCB Camp Lejeune West Site	-77.4424	34.7097	-0.01	0.07	0.09

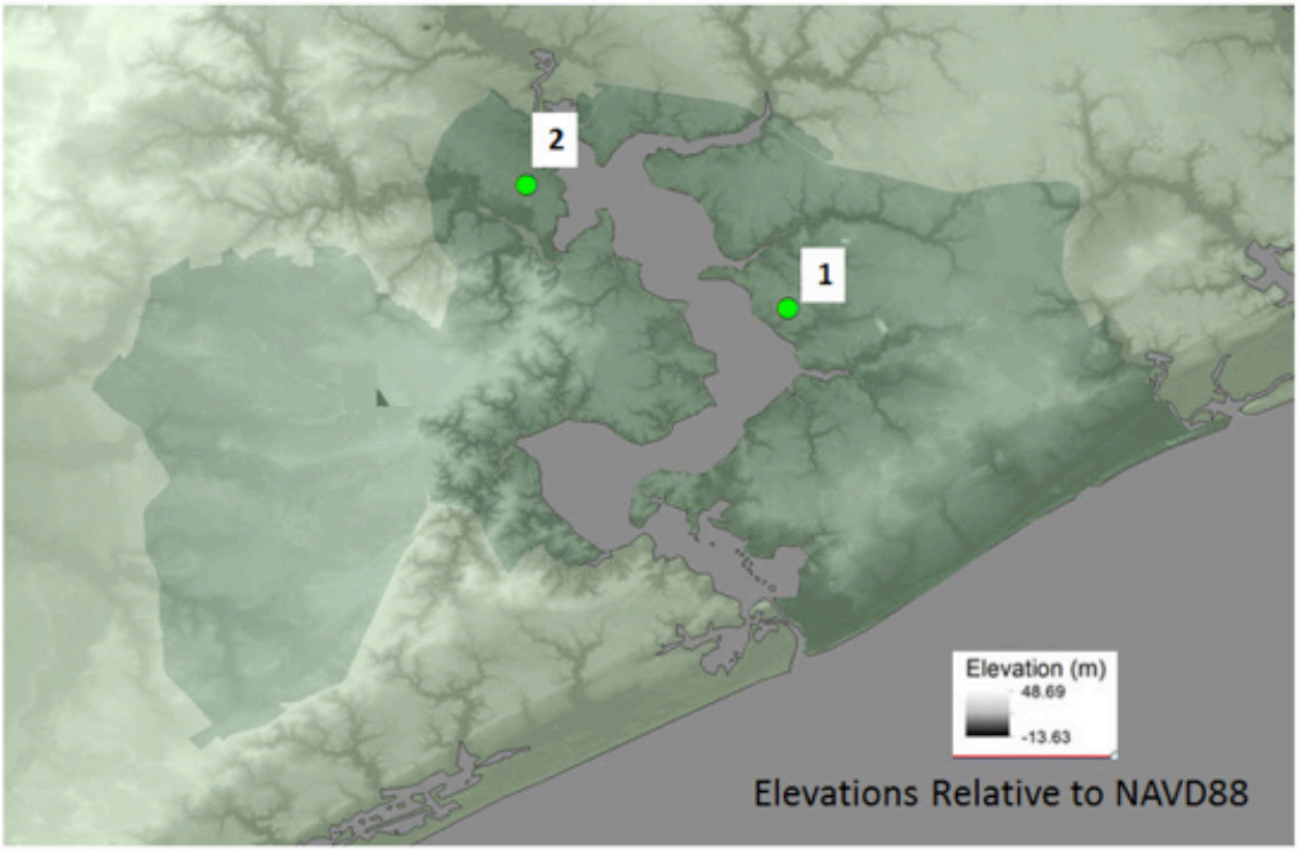

Figure 3.3 Use of a Digital Elevation Model (DEM) for Camp Lejeune, North Carolina
Sites depicted correspond to sites in the RPAD and are assigned random numbers here for illustrative purposes.

3.3 Global Scenarios

Predicting tomorrow's weather and projecting the state of the climate 50 years from now are quite different propositions. With respect to projecting future sea-level change the situation is similar. The approaches and tools differ depending on the time horizon to be considered. In this section the global SLR scenarios to be used as a basis for local or regional adjustment will be described, accompanied by a discussion of how time horizons of interest may affect scenario application. Scenarios were developed specifically for the discrete time periods of 2035, 2065, and 2100. For the time period 2015 up through 2035, this report offers some recommendations for decision-makers in adjusting their use of the scenarios to meet short- to medium-term planning and operational needs (see Section 5.3.5).

Scenarios, given that they are not probabilistic but rather plausible depictions of the future that can still be reasonably bounded, can facilitate decision-making under conditions of uncertainty when likelihoods are difficult to assign or potentially misleading when not placed into an appropriate context. Decision-makers and practitioners, however, although capable of considering uncertainty as part of their decision-making still desire to narrow as much as possible the range of choices

they must consider. Although decisions should be robust across a range of plausible futures, which would favor a multi-scenario approach, it is recommended here that a minimum of two global SLR scenarios and their local or regional adjustments should be considered. The key point is to avoid an assumption or a prediction of a "most-likely" future and instead consider a range of appropriate, plausible futures that bound the decision space and enable potential vulnerabilities and eventually response options and trade-offs to be assessed. The choice of bounding scenarios can be conditioned based on the decision type, the period of time for which the consequences of the decision need to be considered, and the tolerance for risk associated with the decision. Tolerance for risk may hinge on the monetary value of an asset at stake, its criticality with regard to mission, or its overall value in the context of other nearby military assets and functions. An alternative approach that may be favored by some decision-makers—though it does involve an element of subjective likelihood—is to condition their choice of bounding conditions on a selection of a potential emissions future that they view as credible and then use that selection to create bounding conditions. Several examples of scenario application are illustrated in case studies (see Section 5.3).

The key point is to avoid an assumption or a prediction of a "most-likely" future and instead consider a range of appropriate, plausible futures that bound the decision space and enable potential vulnerabilities and eventually response options and trade-offs to be assessed.

This report uses the bounding scenarios (i.e., 0.2 meters [0.7 feet] and 2.0 meters [6.6. feet]) prepared for the Third NCA (Parris et al. 2012) as its initial set of global SLR scenarios. The authors of that report expressed a very high confidence (greater than 9 in 10 chance) that future global mean sea levels would not fall outside that range, but did not assign specific probabilities or likelihoods to any of the individual scenarios addressed in their report (Parris et al. 2012). Findings since the publication of those scenarios have supported the use of these bounding conditions for vulnerability and impact assessment and associated risk management. (See the following sections for details.)

3.3.1 Findings in support of the lower bound

No current evidence points toward mean global sea level decreasing or even remaining stationary through the end of the century (Church et al. 2013a, Meehl et al. 2012).The challenge is to define a plausible lower amount of increase that current evidence would support. As a result, the choice of a lower bound generally comes down to a choice between the trend depicted by long-term tide gauge records and more recent (and shorter time series) data derived from satellite altimetry. For constructing a reliable long-range projection of sea level through the end of the twenty-first century, whether from the standpoint of evaluating accelerations or linear rates, the use of only a few decades of data (up to 60 years) can be problematic because of the presence of multi-decadal natural variability in sea-level records (on the order of tenths of meters; Scafetta 2014). For estimates of local trends in mean sea level, USACE (2014) advises against using records shorter than 40 years with time series of 50 to 60 years preferred. As a result, this report follows Parris et al. (2012) and uses the linear trend estimates from Church and White (2011), using long-

term tide gauge records (1.7 millimeters [mm]/year from 1900 to 2009) to set the rationale for the lowest bounding scenario of 0.2 meters by 2100 (scenario starts in 1992). The rate derived from satellite altimetry (3.2 mm/year based on less than 20 years of data; Church and White [2011]) rely on a record insufficient in duration for projecting century-scale global SLR (Parris et al. 2012); indeed, even this rate recently has been revised downward (Watson et al. 2015).This approach is also consistent with USACE's (2014) approach for establishing the low rate of SLR to be considered. We acknowledge, however, that setting the long-term (since 1900) and near-term (last 20 years or so) global SLR rates remains an area of active research and discussion (Hay et al. 2015) that calls for an ongoing assessment of the most appropriate rate to use. Decision-makers must also determine whether to assume a linear trend or a modicum of acceleration to set the lowest bounding scenario for coastal risk management purposes.

Most importantly, setting the lower bound based on a long-term observational record that also can be used to estimate other components of local flood risk provides confidence in the associated projection as a true minimum value for risk management purposes.

Most importantly, setting the lower bound based on a long-term observational record that also can be used to estimate other components of local flood risk provides confidence in the associated projection as a true *minimum* value for risk management purposes. The contemporary rate observed by satellite altimetry also was observed between 1920 and 1950 (Church et al. 2013a) and without a longer period of observation, could indicate a rate also confounded by natural variability. By *not* using a short-term trend to predict the potential amount of deviation from the long-term historical trend, the decision of what constitutes a plausible lower bound is left mostly in the hands of decision-makers to decide based on their tolerance for risk. (See the following sections for details.)

3.3.2 Findings in support of the upper bound

Parris et al. (2012) based their upper 2.0-meter bound principally on Pfeffer et al.'s (2008) finding of constrained, but physically possible, glaciological conditions (i.e., maximum possible glacier and ice-sheet loss by the end of the century) and estimated ocean warming. Upper bound projections are primarily limited by our understanding of ice-sheet dynamics (Jevrejeva et al. 2014, Lowe et al. 2009). Although modeling of land-ice contributions to SLR continue to improve, compared to the more constrained contributions from thermal expansion, human-induced land water storage, and Greenland surface mass balance (difference between snowfall and melt), challenges remain in accurately quantifying contributions from glacier mass loss, Antarctic surface mass balance, and dynamical responses of Greenland and Antarctic ice sheets (Church et al. 2013a).

The highest projection for SLR in the latest IPPC report (Assessment Report [AR] 5) was for a rise in global mean sea level by 2100 (compared to 1986–2005) of 0.52 to 0.98 meters (5 to 95% range of projections from process-based models, with a two-thirds probability and medium confidence) under the RCP 8.5 scenario (Church et al. 2013a). Church et al. (2013a) did allow for the possibility of additional global mean SLR attributable to the collapse of marine-based sectors of the Antarctic

ice sheet on the order of several tenths of a meter during the twenty-first century. They could not quantify this contribution precisely and assigned only medium confidence in the value. Semi-empirical approaches (e.g., Rahmstorf et al. 2007) that often projected higher values were deemed insufficiently reliable (i.e., low confidence) to be used for projections (Church et al. 2013a). In the highly calibrated uncertainty language of the IPCC, this means that a one-third probability existed that SLR by 2100 may lie outside the 0.52- to 0.98-meter range; however, insufficient evidence existed to evaluate probabilities of levels of SLR outside this upper bound (Church et al. 2013c). It is of note that Church et al. (2013c) advised against considering the 0.98-meter value as a worst-case upper limit and suggested that for policy and planning purposes other values may be appropriate as an upper limit, though these authors felt constrained by the current state of scientific knowledge to offer any guidance. Hinkel et al. (2015) clearly contended that the IPCC global mean SLR scenarios did not provide the right information for coastal risk management and decision-making.

Recent work has attempted to provide a plausible upper bound for global sea-level projections by 2100 to provide information more useful for decision-making. Given the uncertainties mentioned above regarding ice-sheet dynamics and overall contributions, the focus has been on providing estimates that, though of lower probability, cannot be ruled out. Techniques have included expert elicitations (Bamber and Aspinall 2013, Horton et al. 2014), surveys of semi-empirical approaches (Jevrejeva et al. 2014), process modeling alone (Jevrejeva et al. 2014), and combination approaches that use the preceding techniques to create and extend the use of probability distributions (Jevrejeva et al. 2014, Kopp et al. 2014). Expert elicitation generally extends the ranges of what are considered plausible extreme values by 2100 beyond the AR5 values, with Bamber and Aspinall (2013) estimating a 0.3- to 1.3-meter range at a 90% probability for RCP 4.5 and Horton et al. (2014) estimating a 0.5- to 1.5-meter range at a 90% probability for RCP 8.5. Using a combination of expert community assessment and elicitation and process modeling, Kopp et al. (2014) developed probability distributions across SLR components and RCPs. They used Bamber and Aspinall's (2013) results to calibrate the shape of the probability distribution of the tails for the contribution of the ice sheets. For RCP 8.5 their range for SLR by 2100 (note they used a 2000 baseline) was 0.5 meters to 1.2 meters at a 90% probability and 0.4 to 1.8 meters at a 99% probability. Similarly, Jevrejeva et al. (2014), for RCP 8.5 and again the timeframe 2000 to 2100, estimated an upper limit of 1.8 meters at a probability of 5% (1.8 meters represented the 95th percentile in their uncertainty distribution) and 1.9 meters based on assembling the highest estimates of individual SLR components simulated by process-based models. Their survey of semi-empirical model approaches resulted in an upper bound of 1.6 meters, which they determined provided good agreement with the other approaches (Jevrejeva et al. 2014).

Bounds higher than 2.0 meters recently have been suggested. Miller et al. (2013) have suggested a plausible upper bound of 2.7 meters based on modifications to the Pfeffer et al. (2008) 2.0-meter estimate that include a higher physically plausible upper bound due to thermal expansion (Sriver et al. 2012), a higher contribution from Antarctic melt based on Bamber and Aspinall (2013), and water storage contributions not considered by Pfeffer et al. (2008). Kopp et al. (2014) used their 99.9th percentile estimate for 2100 under RCP 8.5 of 2.5 meters as an estimate of a maximum physically possible limit. Despite these more recent estimates, authors of this report find that

overall the 2.0-meter value is supported by the scientific literature as a reasonable plausible upper bound for global SLR by 2100 for vulnerability assessment and risk management purposes. It should be noted that relatively small deviations from the Jevrejeva et al. (2014) and Kopp et al. (2014) upper bound estimates can be accounted for in part by the use of 2000 as a baseline by these studies versus the use of 1992 in this report.

Recently, other investigators have contended that those estimates associated with mass loss from Antarctica (and that are a major contributor to the upper-end scenarios used in this report) should be more constrained (see Clark et al. 2015, Ritz et al. 2015). We recognize the significance and scientific value of these recent findings and viewpoints, but still argue that a risk-based framing approach needs to account for all plausible future SLR scenarios even if the scientific community is not yet prepared to quantify a reasonable likelihood (from its perspective) of their occurrence with confidence.

Despite these more recent estimates, authors of this report find that overall the 2.0-meter value is supported by the scientific literature as a reasonable plausible upper bound for global SLR by 2100 for vulnerability assessment and risk management purposes.

3.3.3 Commitment to future SLR beyond 2100

Although this report addresses plausible SLR scenarios only through 2100, it is important to understand that sea levels will continue to rise past 2100. Indeed, even when considering aggressive mitigation scenarios (such as exemplified by RCP 2.6) sea levels will continue to rise (Church et al. 2013a, Meehl et al. 2012). For the higher RCP scenarios (e.g., RCP 8.5) the commitment to future SLR can be substantial with a low estimate of 2.5 meters using process models and a high estimate using the semi-empirical method of 9.6 meters by 2300 (Meehl et al. 2012). Although Meehl et al. (2012) did not explicitly provide a semi-empirical estimate for 2200 for RCP 8.5, inspection of their Figure 3 indicates an approximate value of 6 meters, which compares roughly to Rohling et al.'s (2013) 95% probability estimate of 5 meters by 2200 based on a natural precedent of SLR based on the geological evidence. Church et al. (2013a) also provide information on global SLR scenarios that extend past 2100.They provide a range of values by RCP and century out to 2500, but caution that some of these multi-century estimates are likely to be underestimates because of the limitations in ice-sheet models representing such changes. The point here is not to recommend specific scenario values beyond 2100, but to alert decision-makers interested in long-term decisions that the commitment to long-term SLR is present even under aggressive mitigation scenarios and can be quite substantial and plausible under scenarios that do not involve substantial mitigation.

The point here is not to recommend specific scenario values beyond 2100, but to alert decision-makers interested in long-term decisions that the commitment to long-term SLR is present even under aggressive mitigation scenarios and can be quite substantial and plausible under scenarios that do not involve substantial mitigation.

3.3.4 Modifications to and use of intermediate scenarios

Parris et al. (2012) identified two intermediate scenarios in addition to the bounding scenarios: an Intermediate-High scenario of 1.2 meters (3.9 ft) by 2100 based on an average of the high end of semi-empirical approaches and an Intermediate-Low scenario of 0.5 meters (1.6 ft) by 2100 based on the upper end of IPCC AR4 global SLR projections using the B1 emissions scenarios (see the Special Report on Emissions Scenarios [SRES] for a description of the SRES scenario families; Nakićenović et al. 2000). This report deviates from the use of these intermediate scenarios in two fundamental ways. First, we contend that because probabilities or likelihoods cannot be assigned to individual scenarios, *it is problematic to imply any particular accuracy in the values chosen for the intermediate scenarios*. Given the imprecise nature of estimating future SLR and associated uncertainties, as well as the vulnerability and impact assessment and risk management purposes that are the context for the information contained herein, this report uses equally proportional 0.5 meter-increment subdivisions of the upper bound 2.0-meter scenario to create intermediates: 0.5 meter, 1.0 meter, and 1.5 meter. Second, we acknowledge that some decision-makers will still want to see some correspondence with the IPCC AR5 SLR scenarios (Church et al. 2013a). For AR5 the use of RCPs to drive earth system climate models replaced the use of emission scenarios previously considered for AR3 and AR4. As a result, for purposes of aligning the intermediate scenarios used here to current scientific findings, RCP-based information from the literature is used to identify scenario correspondences, when feasible (see below).

3.3.5 Scenario rationales and/or correspondences

The development of RCPs by the research community reflected not only a need to update the earlier SRES emissions scenarios based on new science but also a different approach to their development and use (Moss et al. 2010). Rather than the previous sequential approach in which socio-economic scenarios led to emissions scenarios that led to radiative forcing scenarios that led to climate model scenarios, the new, parallel approach identified RCPs based on the literature that could be used to drive the climate models while new socio-economic and emissions scenarios both consistent with the RCPs and independent were developed. The RCPs are in essence "benchmark emissions scenarios" that are "compatible with the full range of stabilization, mitigation and baseline emissions scenarios available in the current scientific literature" (Moss et al. 2008). The previous SRES scenarios assumed no policy actions to mitigate climate change (Moss et al. 2010). The word "representative" indicates that each RCP relates to only one of many possible scenarios that would lead to the specific radiative forcing denoted by the RCP; however, to enable the climate modeling community to move forward on climate model experiments and produce new climate scenarios, the research community needed to identify a specific emission scenario—including the time series of emissions and concentrations and land use and land cover assumptions—from the peer-reviewed literature as a plausible pathway towards meeting each RCP's trajectory (Moss et al. 2008, 2010). Four RCPs were produced; however, for purposes of this report only three are relevant. They are described in Table 3.2. The RCP 6.0—another stabilization without overshoot pathway—was not considered a priority for modeling (Moss et al. 2008) and SLR projections based on this pathway are nearly identical to those using RCP 4.5 (Kopp et al. 2014, Little et al. 2015b), though the specific pathways of the SLR curves differ slightly before and after 2100 for each RCP (Church et al. 2013a).

Table 3.2 Types of Representative Concentration Pathways Considered in this Report[1]

Name	Radiative Forcing (Watts/Square Meter)	Concentration (ppm)	Pathway[2]
RCP 2.6[3]	Peak at about 3 W/m^2 before 2100 and then declines	Peak at about 490 CO^2-equivalent before 2100 and then declines	Peak and decline (low)
RCP 4.5	About 4.5 W/m^2 at stabilization after 2100	About 650 CO^2-equivalent (at stabilization after 2100)	Stabilization without overshoot
RCP 8.5	About 8.5 W/m^2 at stabilization after 2100	>1,370 CO^2-equivalent in 2100	Rising (high)

[1]From Moss et al. (2010).

[2]RCP 2.6 and RCP 8.5 also were viewed as the low and high emission pathways, respectively (Moss et al. 2008)

[3]This pathway was original identified as RCP 3-PD, with PD referring to peak and decline (Moss et al. 2008). Eventually an emissions scenario that resulted in a radiative forcing of 2.6 W/m^2 at 2100 was chosen to represent the pathway (Moss et al. 2010, Weyant et al. 2009).

In addition to the long-term tide gauge record (Church and White 2011), the 0.2-meter scenario also shows reasonable agreement to low-end estimates based on RCP 2.6 (Table 3.2). The Meehl (2012) estimate of 0.25 meters is dependent on the climate sensitivity of the climate model used. For example, Meehl et al. (2012) calculated a 0.142-meters contribution due to thermal expansion alone, whereas Yin (2012), using an ensemble of models, calculated a value of 0.13 +/- 0.03 meters. If decision-makers desire to associate individual SLR scenarios to specific RCPs, Table 3.2 shows scenario correspondence to three different RCPs: 2.6, 4.5, and 8.5. To the extent that decision-makers opt to assume a single potential set of emissions futures (single RCP) but still desire to bound their risk, they can use the range of projections associated with RCP 8.5 that encompasses both model spread and probability levels.

Table 3.3 summarizes the five global scenarios and their associated rationale. The rationale for the bounding scenarios of 0.2 meters and 2.0 meters was provided previously. Here, correspondences associated with each of the scenarios and RCP-based simulations of SLR are described.

Table 3.3 Rationale and/or Correspondences for the Five Global SLR Scenarios

Global SLR Scenario by 2100	Rationale/Correspondences to RCP-Based SLR Simulations
0.2 m (0.7 ft)	▪ Linear extrapolation of the long-term (since 1900) global tide gauge record (Church and White 2011) ▪ Within the 99% probability range of Kopp et al. (2014) for RCP 2.6 (relative to 2000) ▪ Meehl et al. (2012) derived an ensemble mean value of 0.25 m for RCP 2.6 using one coupled atmosphere-ocean global climate model in the middle of the range of climate sensitivities (relative to 1986 to 2005) ▪ Church et al. (2013a) identified 0.26 m as the 5th percentile of the range of projections from process-based models for RCP 2.6 considered "likely" (2/3 probability)
0.5 m (1.6 ft)	▪ Approximate upper bound (95th percentile) for the RCP 2.6 likely range of Church et al. (2013a) ▪ Approximate median value for the RCP 4.5 likely range of Church et al. (2013a) ▪ Approximate lower bound (5th percentile) for the RCP 8.5 likely range of Church et al. (2013a)
1.0 m (3.3 ft)	▪ Approximate upper bound (95th percentile) for the RCP 8.5 likely range of Church et al. (2013a)
1.5 m (4.9 ft)	▪ Approximate value using semi-empirical approaches (Jevrejeva et al. [2014], Meehl et al. [2012]), with the latter estimate explicitly tied to RCP 8.5)
2.0 m (6.6 ft)	▪ Physically plausible glacier and ice-sheet loss by the end of the century and estimated ocean warming (Pfeffer et al. 2008) ▪ Approximately equal to low probability but plausible estimates of Jevrejeva et al. (2014) and Kopp et al. (2014) associated with RCP 8.5

3.3.6 Characteristics of the five global SLR scenarios

The five global scenarios provided herein are assumed to have a baseline of 1992 (the last tidal epoch for which MSL data are available from NOAA and end in 2100). Figure 3.4 depicts the five scenarios. The 0.2-meter scenario extends linearly from 1992 to 2100, whereas the other four scenarios are assumed to have a quadratic form. The quadratic form indicates scenarios in which the rate of SLR is projected to accelerate over time. This parallels the behavior of emissions scenario-dependent projected temperature changes. The specific quadratic equation used to generate the latter four scenarios is provided below as Equation 3–1.

The equation for deriving global SLR scenarios "curves" in Figure 3.4:

$$SLR = a * (t - 1992) + b * (t - 1992)^2 \qquad [3–1]$$

in which *SLR* is the sea-level rise in meters (relative to 1992) and *t* is the Year (e.g., 2100). The coefficient *a* and *b* values are shown in Table 3.4 below.

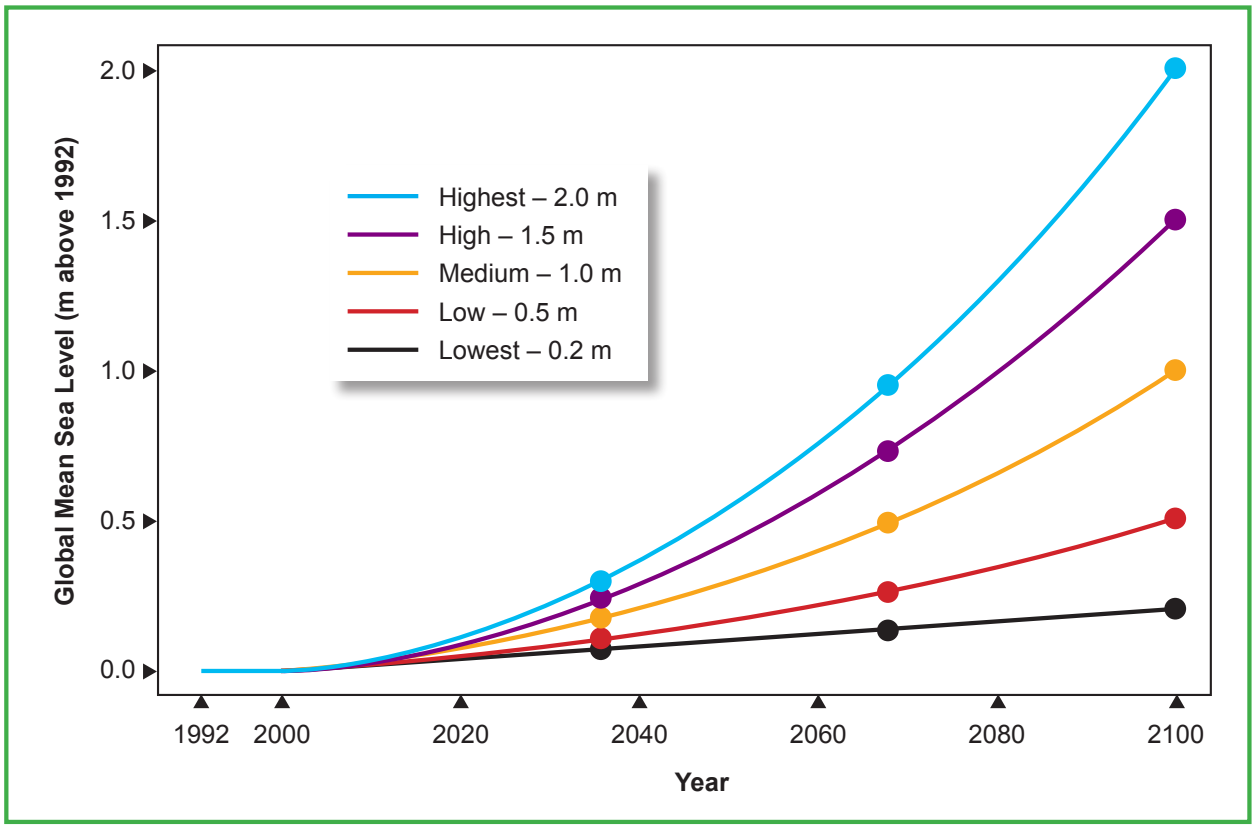

Figure 3.4 Five Global Scenarios Advanced in this Report

Note that sea levels will exhibit natural variability at any point in time, so the specific scenario value at a particular point in time will have additional associated uncertainty due to this natural variability (see Figure 5.11 for an illustration of natural variability around the 2.0-meter scenario.). As a result, it would be inappropriate to ascribe a particular accuracy to the global scenarios at any particular point in time. In addition, the 0.2-meter scenario is not quite an extension of the historic rate (assumed to be 1.7 mm/year); it was rounded to 0.2 meters.

Table 3.4 Values for a and b Coefficients in Equation 3–1

Scenario (m)	*a* (m/yr)	*b* (m/yr^2)
0.5	1.7×10^{-3}	2.7126200×10^{-5}
1.0	1.7×10^{-3}	6.9993141×10^{-5}
1.5	1.7×10^{-3}	$1.12860082 \times 10^{-4}$
2.0	1.7×10^{-3}	$1.55727023 \times 10^{-4}$

3.4 Systemic Trend Adjustments

Systemic trends as used herein are those components of sea-level change that are anticipated to exhibit a persistent directional trend in their behavior over the period 2015 to 2100. Before addressing the underlying science and methods associated with each component, a short descriptive overview is provided.

3.4.1 Overview

Three components are considered to contribute to regional- or local-scale adjustment to the global SLR scenarios. These are *vertical land movement* (VLM), *dynamical sea-level change* (due to local steric effects and ocean dynamics such as changes in circulation patterns), and gravitational (in the main) adjustments associated with the redistribution of mass from glaciers, ice caps, and land-based ice sheets. We note that other literature refers to the glaciers and ice caps component simply as "glaciers" (Church et al. 2013a). The effect on water levels from dynamical sea levels (DSL) and mass redistribution is expressed as patterns referred to herein as "pattern scaling" or "fingerprints" unique to each process. For the site-specific approach considered herein the adjustments due to dynamical sea-level pattern scaling and ice-melt fingerprints can be expressed only coarsely at a regional scale and for specific time horizons, whereas trends in VLM, especially when local processes dominate, often may be expressed as a fairly local phenomenon and in a temporally continuous manner.

Because trends in vertical land movement are based on measurements (though the source can differ based on data available at a particular location; see Section 3.4.2), a direct estimate of measurement error or confidence level is calculated. Confidence in pattern scaling and fingerprint values, calculated as deviations from the global mean water levels derived by climate models, is calculated based on model spread. The calculation of overall confidence level is additive and follows the procedure of Church et al. (2013b). Other types of uncertainty, such as the uncertainty associated with emissions futures, internal (natural) variability, and differences in climate model output for the same conditions (*sensu stricto* Hawkins and Sutton 2009, 2011) are addressed through the risk-tolerance decision-framing approach discussed elsewhere in the report (Sections 2.5 and 5.3).

Just because an adjustment to a global SLR scenario from one of the three components can be calculated does not mean it represents a significant deviation that should be considered in decision-making. Scenarios and their adjustments are provided to the nearest 0.1 meter; as a result, for an individual contribution to be considered, it must contribute at least 0.05 meter.

3.4.2 Vertical land movement adjustment

Rationale for Considering

Vertical land movement is an important factor when considering future vulnerability to inundation from SLR and coastal storms. Coastal areas with high rates of vertical land subsidence are at above-normal increased risk in the future as sea level rises. Vertical land movement can be due to a variety of factors, including response of the earth's surface to the last ice age (modeled by Glacial Isostatic Adjustment [GIA] models), local uplift from isostatic rebound in glacial fjords, post-

earthquake deformation, and slow tectonic movement. Locally, land subsidence also can be due to withdrawal of hydrocarbons (oil and gas) and groundwater and local sediment compaction. Rates of local subsidence can change over relatively short time periods (a decade) if a local pumping withdrawal activity stops or mitigation by fluid replacement occurs; however, *for purposes of this report a simplifying assumption is that VLM has a constant linear trend through 2100 for any given site*. Subsequent iterations of the effort reported here are anticipated to update site-specific rate assumptions on a periodic basis but still rely on a constant linear trend for scenario projections for each update.

Rates of VLM can be quite significant and can be greater than the rates from regional and global SLR alone. This is the case for Houston, Texas, where VLM subsidence can exceed 10 mm/year or in Southeast Alaska where local VLM uplift can exceed 15 mm/year. The areas of subsidence can be particularly vulnerable to future inundation even if the assumption of future global SLR is a small increase. The areas of uplift have significant and continued mitigation of vulnerability to inundation.

Rates of VLM can be quite significant and can be greater than the rates from regional and global SLR alone.

Tide gauges measure sea-level change relative to the land and do not distinguish between VLM and oceanographic sea-level variations; however, it is possible to back out VLM from long-term tide gauge records by decomposing the record into long-term global trend input and regional oceanographic variability (Zervas et al. 2013). A growing network of continuously operating GPS systems (CGPS) is now being used to estimate VLM and an international effort exists to co-locate long-term tide gauges and CGPS. Use of CGPS is relatively new and requires, in general, longer time series to narrow the measurement uncertainties.

Datasets Considered

Multiple types of VLM data were considered.

1. Estimated rates of VLM were obtained from long-term tide gauge records (Zervas et al. 2013). Uncertainty estimates are correlated with length of record and estimates are not possible for location with land motion discontinuities (strong earthquakes).
2. Direct measurements of VLM were obtained from continuously operating GPS stations (Snay et al. 2007). Global estimates are available from sources such as the Jet Propulsion Laboratory (JPL 2013).
3. A source of nationwide GPS analysis was obtained from the University of Wisconsin (C. DeMets, personal communication 2014). Uncertainty estimates for GPS-derived VLM are highly correlated with length of GPS measurement (Snay 2007).
4. Glacial Isostatic Adjustment model output was used to estimate vertical land movement; however, these are large global scale models with low spatial resolution (Peltier 1998, 2004). Model output is VLM rates reported by latitude and longitude for each Permanent Service for Mean Sea Level PSMSL global tide gauge location.
5. Local geological study sources and use of interferometric synthetic aperture radar (InSAR) technology (Galloway et al. 2000) can be considered as a supplement to the preceding, but were not used for this report.

Priority of Usage

The following lists the priority applied in this report for determining the VLM rate to use for a specific site.

1. Co-location of a site point with a tide gauge: site is located 3 km or less from a tide gauge. The VLM rate is derived directly from the rate at the tide gauge: Tide Gauge Direct (TGD).
2. Co-location of a site point with a GPS station: site is located 3 km or less from the GPS station. The VLM is derived directly from the nearby continuous GPS site: GPS Direct (GPSD).
3. Extrapolation of a rate of VLM from a nearby (greater than 3 km) tide gauge when no co-located tide gauge or GPS location is available to derive the VLM rate. Here the rate derived from a nearby tide gauge is used to extrapolate to the site point: Tide Gauge Extrapolated (TGE).
4. Extrapolation of a rate of VLM from a nearby (greater than 3 km) GPS station when no co-located tide gauge or continuous GPS site is available and the extrapolation from a tide gauge is not adequate: GPS Extrapolated (GPSE).
5. Glacial Isostatic Adjustment model estimates when neither defensible tide gauge nor GPS estimates exist. The Peltier GIA global model (Peltier 1998, 2004) provides VLM rates over large regions due to post-glacial isostatic adjustments only. Similar to proximity assumptions for GPS and tide gauge, we consider GIA model adjustments direct (GIAD) when the site is 3 km or less from the GIA model latitude and longitude output and extrapolated (GIAE) when greater than 3 km away.
6. Other local studies and reports: Other local studies may take precedence if they include robust measurements or models with uncertainty estimates. Otherwise, these studies can be used as verification of estimates from above sources. In some instances satellite-based InSAR data may be available. This technology offers local VLM information with relatively high spatial resolution, but with less accuracy than an individual long-term continuous GPS dataset. This dataset will be useful for analyzing VLM gradients for sites with large geospatial footprints.

Justification of Priority Setting for VLM Estimates and Source Validation

All VLM data sources in the vicinity of a military site were evaluated for regional consistency, spatial trends and changes, and outliers. The regional comparison of VLM rates from all sources, including from other special reports and studies, validates the information eventually used as the primary source. In general, VLM rate estimates from tide gauges (TGD and TGE) were of higher priority than those estimated from continuous GPS stations (GPSD and GPSE) for locations at which tide gauge and GPS data could be used. So for direct co-locations, tide gauges received priority and for extrapolations, the closest tide gauge (if located nearby) received priority. The GPS sources outnumbered tide gauge sources. But confidence intervals of VLM rates from long-term tide gauges generally show less uncertainty than from GPS counterparts, mainly due to the relatively short record lengths of continuous GPS data (often less than 10 years). Confidence intervals from continuous GPS records are expected to improve significantly with time and will eventually outperform rates derived from tide gauges.

The GPS VLM rates from two separate data analysis sources (i.e., C. DeMets, personal communication 2014, JPL [2013]) were available for most of the GPS locations used in this analysis. These were inter-compared regionally and the source with the lowest 95% confidence interval was

used for individual locations. The two analyses often used different time periods for the same GPS data source and were a source of validation.

Uncertainty Characterization, Error Budgets, and Data Quality Issues

Data sources generally were not used and shown unless they were accompanied by uncertainty estimates. Uncertainty estimates were used to determine which data sources took precedence for estimating VLM at each location when several sources were available. Conflicting rates were often seen in GPS stations at the same location and sources with the narrowest 95% confidence interval prevailed. Although the two investigators (C. DeMets, personal communication 2014, JPL [2013]) used the same GPS data sources, they performed independent analyses and often used different time periods of data for the same location. In general, the time period used for GPS analysis was less than 15 years. Uncertainty in the application of these rates to a specific site location also will depend on the distance away; in general, uncertainty will increase with increasing distance between the VLM source and the site of interest. No algorithm or statistical method is available to estimate this uncertainty component due to the nature of VLM. In many cases, large geographic areas may have the same VLM rate, whereas in others, VLM rates can differ significantly over smaller distances. VLM rates were determined looking at all of the nearby VLM sources, their uncertainties, and their distances away. When sources were similar distances away from a particular site, the closest source with the lowest uncertainty bounds was used. The TGD and GPSD VLM sources are considered the most accurate because they are essentially co-located (3 km or less). The 3-km threshold for designation between a direct and extrapolated VLM value is not based on an exhaustive analysis; however, it is a reasonable expression of co-location of a site location with a measurement source.

In many cases, large geographic areas may have the same VLM rate, whereas in others, VLM rates can vary significantly over smaller distances.

Other considerations for use of the VLM estimates used in this study should be noted. The first is the assumption of a constant VLM rate to 2100. This assumption should be valid in most instances; however, some locations may experience dynamic changes in VLM over the study timeframe due to human interference (for instance, increased or decreased local water or hydrocarbon fluid withdrawal) and some locations may experience abrupt change in VLM rates due to earthquakes. The second assumption is that for the longer distances to the VLM sources, the VLM rates are the same at the site as at the VLM source. This may not be the case if the underlying surface geology differs significantly over relatively short distances. This may the case, for instance, if the site along the coast is located on a sandy spit formation, but the closest GPS VLM source is located several kilometers away on a bedrock formation.

Because of these complex factors surrounding the spatial variability of VLM, the quantification of uncertainty due to distance from a site to the VLM source is difficult to estimate. Each site must be looked at individually for these considerations before finalizing the total sea-level adjustment. Uncertainties for the VLM source data are provided in the database but do not include quantification of uncertainty due to distance and are largely dependent on length of observation. The average uncertainty of the computed VLM trends at the 95% confidence interval for the tide

gauge sources (TGD and TGE) is 0.16 mm/year. The average uncertainty of the computed trends (95% confidence interval) for the GPS sources (GPSD and GPSE) is 1.29 mm/year. The TGE and GPS VLM estimates will have added uncertainty depending on distance between the VLM source and the site location and what (if any) actual differences in VLM may be present between them. The modeled GIAE and GIAD sources do not have uncertainties assigned but are thought to have larger uncertainties because they rely on a global model with coarse spatial resolution.

3.4.3 Dynamical sea-level adjustment

Rationale for Considering

Regional sea levels may differ substantially from a global average due to a variety of factors that may be associated with natural and anthropogenic modes of the climate system and other factors such as ocean dynamics and vertical land movement (Church et al. 2013a). The dynamical redistribution of ocean water masses discussed in this section is caused by both episodic and long-term changes in winds, air pressure, air-sea heat and freshwater fluxes, and ocean currents. Over timescales from about a year to several decades, natural climate variations alter surface winds, ocean currents, temperature, and salinity, all of which result in sea-level variations both in time and space. Because such variations also can be affected by natural variability and are typically episodic, their prediction into the future is difficult. The modes of variability include coupled ocean-atmospheric systems such as El Niño Southern Oscillation (ENSO), North Atlantic Oscillation (NAO), Atlantic Multi-decadal Oscillation (AMO), and Pacific Decadal Oscillation (PDO).

Persistent patterns of sea-level variations, however, may result from long-term changes in the wind fields, changes in the regional and global ocean heat and freshwater content and the associated redistribution of ocean properties (Church et al. 2013a, Yin et al. 2010). For instance, Yin et al. (2009, 2010) identified persistent robust features of the DSL pattern, such as the relatively faster and larger changes in sea-level rise north of the Gulf Stream and along the northeast coast of North America compared with other regions, as well as a belt-like pattern in the Southern Ocean that becomes more pronounced with increased amounts of warming. It is important to account for such DSL variations in predictions of regional and local sea levels for planning purposes. The global climate models of the twenty-first century provide sea-level patterns that can be expected in the future under various climate change scenarios.

The causes of changes to the sea-level pattern due to ocean dynamics are well known. Thermal expansion lifts the elevation of the sea surface non-uniformly. To balance the resulting pressure gradient, water masses will flow from areas of large water depths into shallower continental shelf areas (Richter et al. 2013, Yin et al. 2010). The resulting changes to sea level may be induced by changes to the ocean circulation patterns (Yin et al. 2009, 2010). The change in the distribution of mass in the oceans also will modify the Earth's gravitational field, and this will cause further readjustment of mass distribution. The combination of the latter processes is known as Self Attraction and Loading (SAL), a phenomenon that must be accounted for in future projections of regional sea level (Grinsted et al. 2015, Tamisiea et al. 2010, Vinogradova et al. 2011). The concept of SAL may also be used to describe redistribution of mass from sources other than ocean dynamics. This will be discussed subsequently with respect to mass loss from glaciers and ice sheets in section 3.3.5.

Data

The estimation of regional DSL adjustment for each location and specified global scenario is somewhat challenging. Consistent data sets needed to obtain such adjustments are not available readily. For the present development of regional SLR scenarios at locations around the globe that accounts for DSL, the pattern-scaling approach used in Perrette et al. (2013) and the underlying data were used. Perrette et al. (2013) used 22 Coupled Model Intercomparison Project Phase 5 (CMIP5) global models that were available at the time of their study (Table S1, Supplemental Material reproduced below as Table 3.5). In support of the present study, M. Perrette (personal communication 2014) made specific runs for the years 2035, 2065, and 2100 and provided global means and gridded data on a one-degree global mesh of relevant components contributing to regional sea-level change. The Monte Carlo approach he used allowed for uncertainty characterization. The corresponding methods are documented in Perrette et al. (2013). In the ensuing sections, any key deviations from the methodology of Perrette et al. (2013) are noted. Based on the availability of data, only 20 out the 22 models listed in Table 3.5 were used for computing DSL; HadGEM2-CC and INM-CM4 were not used. The Supplementary Datasets available from the IPCC AR5 report (Church et al. 2013b) and the other published research on future sea-level variations (Yin 2012) were used for validation.

TABLE 3.5 Summary Table of the 22 CMIP5 Models Used in Perrette et al. 2013

The Thermal and Dynamic columns indicate whether the models were used to compute global mean thermal expansion and dynamic sea-level change. The Institution column lists the institution providing model outputs.

Model Name	Thermal	Dynamic	Institution
BCC-CSM1.1	Yes	Yes	Beijing Climate Center, China Meteorological Administration
BCC-CSM1.1(m)	Yes	Yes	-
CanESM2	Yes	Yes	Canadian Centre for Climate Modelling and Analysis
CNRM-CM5	Yes	Yes	Centre National de Recherches Meteorologiques / Centre Europeen de Recherche et Formation Avancees en Calcul Scientifique
CSIRO-Mk3.6.0	Yes	Yes	Commonwealth Scientific and Industrial Research Organization in collaboration with Queensland Climate Change Centre of Excellence
FGOALS-s2	No	Yes	LASG, Institute of Atmospheric Physics, Chinese Academy of Sciences
GFDL-ESM2G	No	Yes	NOAA Geophysical Fluid Dynamics Laboratory
GFDL-ESM2M	No	Yes	-
GISS-E2-R	No	Yes	NASA Goddard Institute for Space Studies
HadGEM2-CC	Yes	No	Met Office Hadley Centre
HadGEM2-ES	Yes	Yes	-
INM-CM4	Yes	No	Institute for Numerical Mathematics
IPSL-CM5A-LR	Yes	Yes	Institut Pierre-Simon Laplace
IPSL-CM5A-MR	Yes	Yes	-
MIROC-ESM	Yes	Yes	Japan Agency for Marine-Earth Science and Technology, Atmosphere and Ocean Research Institute (The University of Tokyo), and National Institute for Environmental Studies
MIROC-ESM-CHEM	Yes	Yes	-
MIROC5	Yes	Yes	Atmosphere and Ocean Research Institute (The University of Tokyo), National Institute for Environmental Studies, and Japan Agency for Marine-Earth Science and Technology
MPI-ESM-LR	Yes	Yes	Max Planck Institute for Meteorology
MPI-ESM-MR	Yes	Yes	-
MRI-CGCM3	Yes	Yes	Meteorological Research Institute
NorESM1-M	Yes	Yes	Norwegian Climate Centre
NorESM1-ME	Yes	Yes	-

Method

The following provides the methodology used to determine the DSL adjustment at a particular location around the globe for a particular global SLR scenario (that ranges from 0.2 to 2.0 meters) and for time horizons 2035, 2065, and 2100.This method is based on a scaled representation of the global pattern of steric sea-level rise data following the methodology of Perrette et al. (2013). The phrase "pattern scaling" used here is defined as the deviation of dynamical sea level from the mean steric sea-level rise (mean thermal expansion) scaled by the global mean surface temperature. This phrase, as opposed to "fingerprints," was used to avoid any confusion between the spatial patterns from that defined for the regional signature associated with redistribution of melting land ice (Section 3.3.5). Specifically, the pattern scaling is computed using the following equation:

The phrase "pattern scaling" used here is defined as the deviation of dynamical sea level from the mean steric sea-level rise (mean thermal expansion) scaled by the global mean surface temperature. This phrase, as opposed to "fingerprints," was used to avoid any confusion between the spatial patterns from that defined for the regional signature associated with redistribution of melting land ice.

$$Dyn\_slr(x,t) = global\_steric\_mean(t) + scale\ factor(x) * global\_mean\_air\_temp(t) \quad [3–2]$$

in which *Dyn_slr* is the regional steric sea level, *x* denotes a particular location, and *t* is the time. The scale factor denotes a normalized value at a particular location that represents the pattern scaling. The quantities, *global_steric_mean(t),* and *global_mean_air_temp(t)* are the global averages of steric sea level and temperature at time *t*. Perrette et al. (2013) also used ocean heat content to determine global mean thermal expansion (i.e., values for global steric mean; see also Bilbao et al. [2015]). Perrette et al. (2013) also developed scaled factors using the results of 20 General Circulation Models (GCMs; see Table 3.5 under Dynamic) and a regression approach to normalize the DSL changes as a function of mean air temperature, which also enables accounting for atmospheric effects such as wind. The use of temperature in this manner in the scaling coefficient made the use of this method more convenient for our purposes here in which dynamical changes must be computed for multiple scenarios. It is noted that Grinsted et al. (2015) use a slightly different approach in which the spatial pattern ("fingerprint" in their nomenclature) that is attributed to the thermal expansion and dynamical ocean response and the global mean temperature is not considered directly.

Perrette et al. (2013) showed that this pattern-scaling approach is a convenient means for normalizing DSL patterns and provided the magnitude of the associated errors (Figures 3, S3, and S4 of Perrette et al. 2013). An example of the DSL pattern scaling computed using Equation 3–2 for the RCP 8.5 scenario and Year 2100 is shown in Figure 3.5. The pattern scaling shows primary characteristics of DSL distribution reported by Yin et al. (2010). In the North Atlantic, sea level is higher north of the Gulf Stream but is lower to the south. This dipole pattern has been attributed

to the weakening of the Atlantic meridional overturning circulation (AMOC). In the North Pacific, an opposite dipole effect may be observed, which has been attributed to the strong steric effect and a poleward expansion of the subtropical gyre. Finally, a belt-like pattern is present in the Southern Ocean.

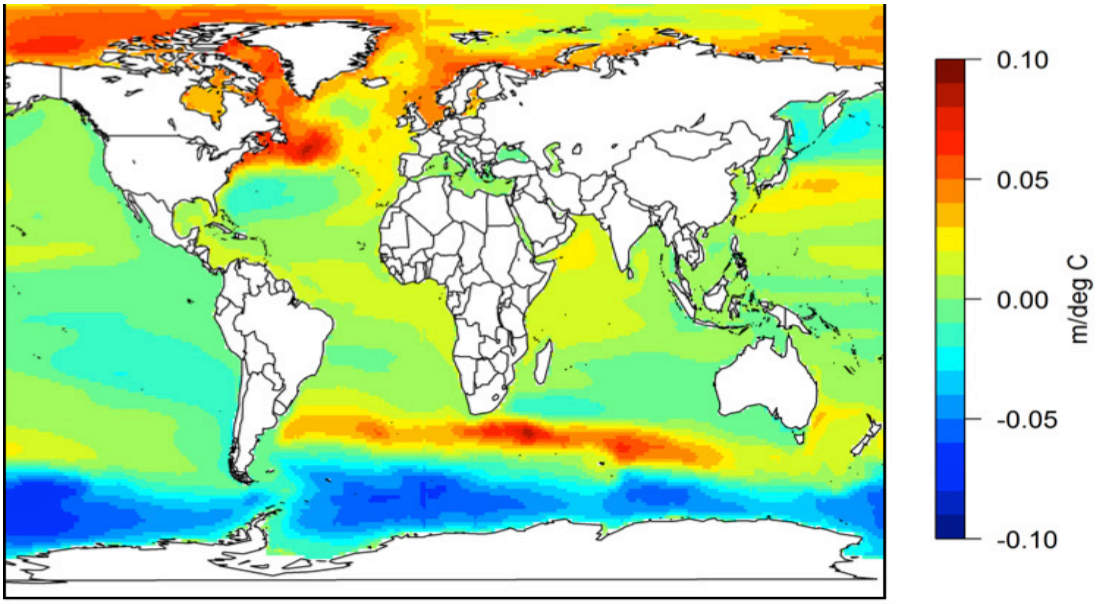

Figure 3.5 Pattern Scaling of Median Steric Data Corresponding to RCP 8.5 Scenario for Year 2100
(using data provided by M. Perrette, personal communication 2014)

Perrette et al. (2013) also provided 5th and 95th percentiles of the steric data from their Monte Carlo analysis of the GCMs. Their estimates are expected to provide a larger range of uncertainty relative to Church et al. (2013a) model results because of the bootstrapping (resampling) of GCMs from the CMIP5 suite. The snapshots produced by Perrette et al. (2013) are useful for providing estimates of uncertainty associated with model spread.

The pattern-scaling approach assumes that the DSL distribution scaled by global mean steric SLR and the temperature is sufficient to compute the dynamical adjustment for any time epoch and future climate scenario. We assume that the pattern-scaling multiplied (scale factor in Equation 3-2) by the global air temperature for a particular timeframe and SLR scenario provides the necessary adjustment to the global mean sea level to account for sea-level variations in the spatial dimension. Because of the multiple global SLR scenarios that are considered here, the pattern-scaling of the closest RCP scenario provided by Perrette et al. (2013) was used (Table 3.6). For the higher scenarios that are outside the projections of the IPCC (Church et al. 2013a), such as 1.5 meters and 2.0 meters, the semi-empirical (Perrette et al. 2013) scaling factors available for RCP 8.5 were used. The selection of global mean temperature, however, for each global SLR scenario was computed as described below.

As an initial validation exercise, the median values of steric sea-level rise and the temperature estimates produced by Perrette et al. (2013) using a Monte Carlo analysis were compared to those from Church et al. 2013a (Figure 3.6). It is noted that Perrette et al. (2013) used the IPCC AR5 model results and therefore this is not an independent comparison but rather a quality control exercise. This comparison shows that the data of Perrette et al. (2013) reproduce mean values reasonably well but result in a broader range of uncertainty (error bars in Figure 3.6) as expected. The Monte Carlo method produces a range of values that cover a broader range than those produced from a limited number of physical process models.

The consistency of the global SLR scenarios and the data obtained from Perrette et al. (2013) were verified by plotting global temperature against the global scenarios (Figure 3.7). For the 1.5-meter and 2.0-meter scenarios, the estimates from the semi-empirical method (See Table 3.6) corresponding to RCP 8.5 scenario (Perrette et al. 2013) were used. The global temperature required for computing the dynamical adjustments from the fingerprints were determined from the linear regression fitted to data shown in Figure 3.7. Based on the approach, Table 3.6 was prepared to identify the source that would be used to compute the DSL adjustment at a particular location.

Table 3.6 Datasets (following Perrette et al. [2013] as modified by Perrette [personal communication 2014]) for Computing Scaling Factors

Shown are AR5 process-based model versions (in terms of RCPs) used for 0.2-meter, 0.5-meter, and 1.0-meter scenarios [50% value] and the semi-empirical method results for the 1.5-meter [50% value] and 2.0-meter [50% value] Scenarios). For computing scale factors, Eq. (3–2) is applied using the median (50%) values of the parameters, global mean steric sea level, and global mean surface temperature.

Parameters in Equation 3–2			
Global SLR Scenario (m)	**Steric sea level rise from:**	**Global mean steric SL**	**Global mean surface temp.**
0.2	RCP 2.6* (50%)	RCP 2.6 (50%)	RCP 2.6 (50%)
0.5	RCP 4.5 (50%)	RCP 4.5 (50%)	RCP 4.5 (50%)
1.0	RCP 8.5 (50%)	RCP 8.5 (50%)	RCP 8.5 (50%)
1.5	RCP 8.5, Semi-Empirical (50%)	RCP 8.5, Semi-Empirical (50%)	RCP 8.5, Semi-Empirical (50%)
2.0	RCP 8.5, Semi-Empirical (50%)	RCP 8.5, Semi-Empirical (50%)	RCP 8.5, Semi-Empirical (50%)

*This pathway was originally identified as RCP3-PD (see Section 3.3.5 for details).

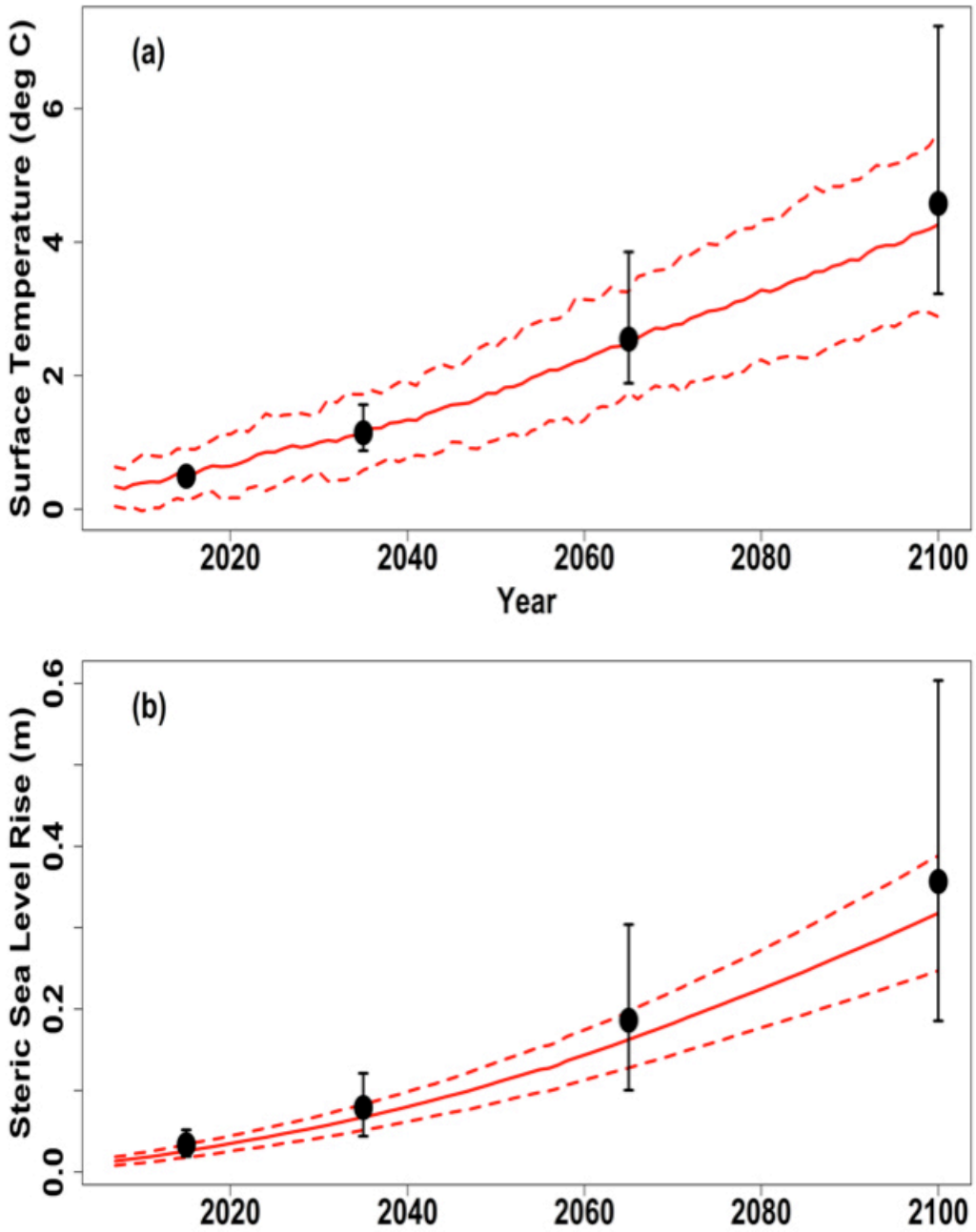

Figure 3.6 Comparison of Global Mean Values of (a) Temperature and (b) Steric Sea Level of Two Data Sources

Data are from M. Perrette (personal communication 2014; black dots and error bars) and IPCC AR5 results (median and error bounds) from Church et al. (2013b; red continuous lines). Both sets of error estimates have been computed from model spreads (5th and 95th percentiles).

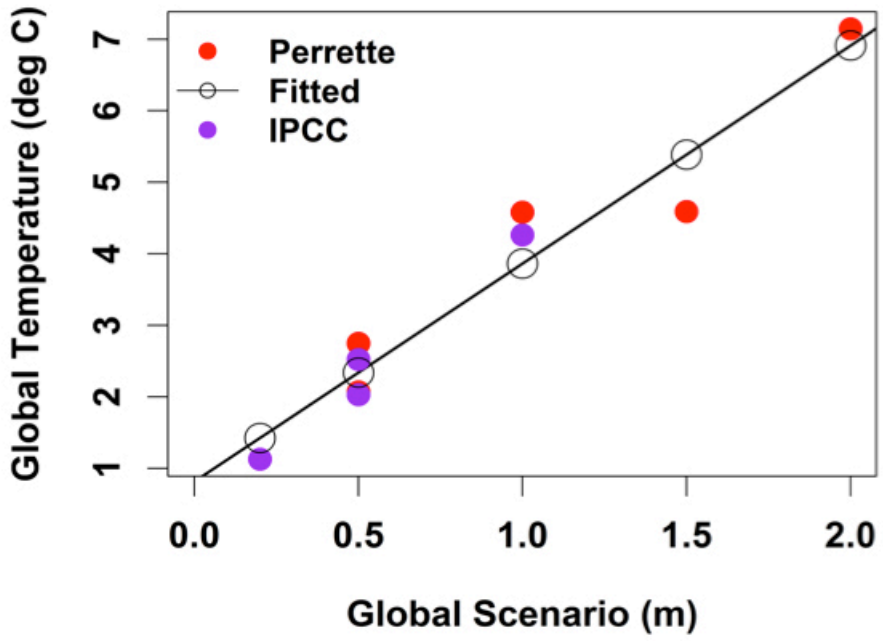

Figure 3.7 Relationship between the Global Average Temperature Anomaly Versus Global SLR Scenarios Developed in this Study

Analysis used data provided by M. Perrette (personal communication 2014; red circles). The solid line and the open circles represent the linear regression fitted to that data. Also shown are the IPCC AR5 (Church et al. 2013b) estimates for comparison (purple circles).

Comparison with other Approaches from the Literature

Because the DSL values corresponding to the exact scenarios of this study are not available directly, an order of magnitude comparison of DSL for the 1.0-meter scenario used herein was made using the results reported by Yin (2012) for the RCP 8.5 scenario. As shown in Table 3.6, the 1.0-meter scenario was assumed to be aligned with the process-based model results of the RCP 8.5 scenario. This comparison serves to ensure that the methodology used herein produces estimates of DSL similar to those already published in the literature for similar conditions. The spatial patterns of the two datasets are shown in Figure 3.8. Both are similar in terms of spatial pattern and magnitude, demonstrating that the DSL adjustments computed using the method applied herein is consistent with those of Yin (2012).

(a) DSL adjustment (in meters) for the 1.0-meter scenario developed in this study.

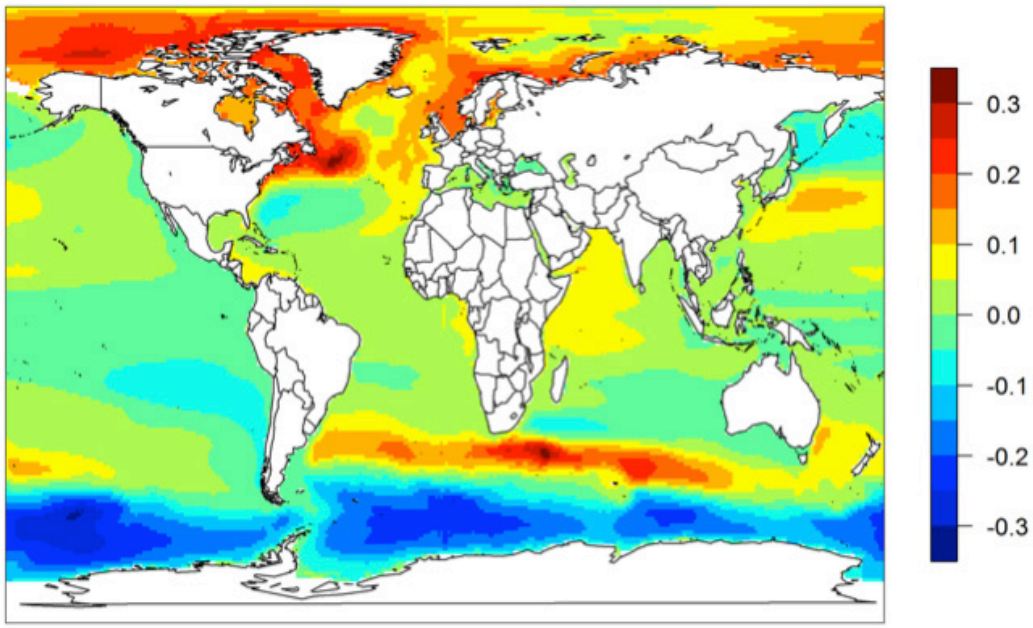

(b) Multi-model mean projection of the DSL change (in meters) for RCP 8.5 Scenario from Yin (2012)

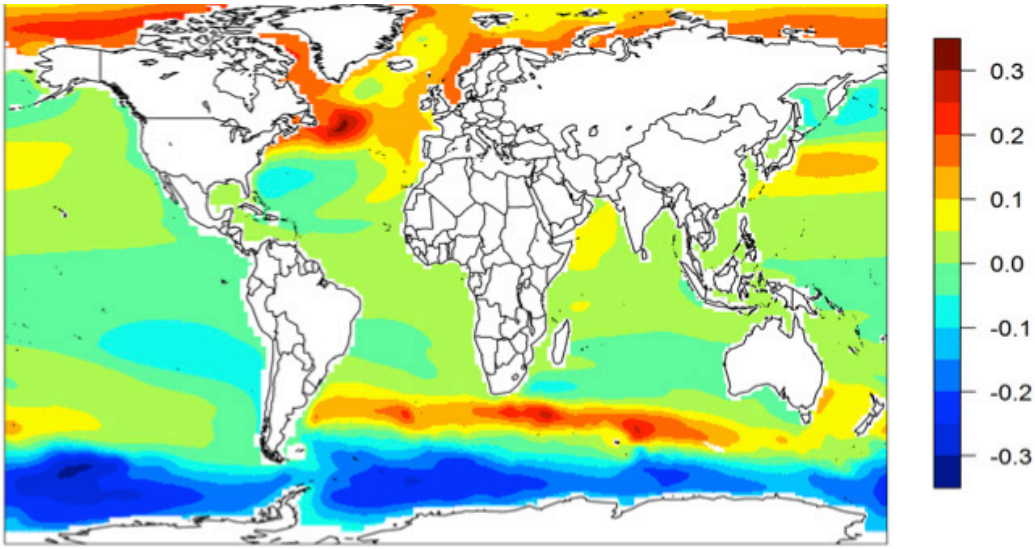

Figure 3.8 Comparison of the DSL Adjustments Computed in this Report to Results from Yin (2012)

Shown are results for the 1.0-meter global scenario and the multi-model mean projection of the same for RCP 8.5 as reported by Yin (2012).

(a) DSL adjustment for the 1.0-meter scenario developed in this study and (b) Multi-model mean projection of the DSL change for RCP 8.5 Scenario from Yin (2012). The estimates are in meters.

Uncertainty Estimation

It is assumed that the spatial pattern is robust and that the uncertainty in DSL esimates arises from the accuracy in the global mean temperature projected for each scenario. The methodology used for uncertainty computation is basically identical to the approach used to calculate the median DSL adjustments as illustrated in the previous sections except that the uncertainty bounds of global mean temperature (5^{th} and 95^{th}) were obtained from the Monte Carlo analysis results reported by Perrette et al. (2013). They were estimated for each SLR scenario identified in this study by using linear regression fits, as demonstrated in Figure 3.7, except that the global mean temperature corresponding to the 5^{th} and 95^{th} percentiles were used as the dependent variable.

3.4.4 Regional sea-level adjustments associated with ice-mass loss

Rationale for Considering

When the terrestrial ice (i.e., glaciers and ice caps, ice sheets) melt due to warming, the corresponding effect on regional sea level due to mass redistribution is far from uniform and the spatial signature of the melt water is complex and quite variable in space (Church et al. 2013a, Grinsted et al. 2015). This non-uniform pattern may be attributed to multiple causes that manifest themselves in a complex and interactive manner. When ice sheets melt, the gravitational attraction of the area undergoing mass loss on the ocean nearby weakens and, as a result, the regional sea level falls in the vicinity of mass loss. The falling of sea level could span up to a radius of about 2000 to 2200 km away from the melt location (Mitrovica et al. 2011, Slangen et al. 2012). In the far field, the migration of water leads to a rise in sea level in excess of the global mean level (Mitrovica et al. 2011). The change in the surface loading (in both land and ocean) due to ice melt causes a deformation of the Earth's surface that in turn also affects the Earth's gravity field (i.e., geoid) and this leads to an additional redistribution of water (Slangen et al. 2012). In many studies (e.g., Grinsted et al. 2015, Tamisiea et al. 2010) the Earth's response to the change in surface loading is assumed to be instantaneous (i.e., elastic). Furthermore, the ice melt and the deformation of the Earth surface will lead to a change in Earth's rotation and its rotation axis that in turn affect the redistribution further. Finally, shoreline change due to melt water and the changes in continental water storages also affect the regional sea-level pattern (Mitrovica et al. 2011, Tamisiea et al. 2010).

Woodward (1888) was the first to recognize that rapid melting would lead to geographically varying sea-level change. Its modeling was initially attempted by Farrell and Clark (1976) who considered the case of a deformable, non-rotating earth with fixed shoreline geometry (Mitrovica et al. 2011). Computing regional sea-level patterns typically requires the solution to what is known as the "Sea Level Equation" (Hay et al. 2013, Mitrovica et al. 2011) and over the years, many attempts have been made to improve this equation to account for the variety of causes associated with redistribution patterns.

Mass change in each ice sheet (i.e., Greenland or Antarctica) or a continental glacier and ice cap produces a distinct spatial signature of the redistributed water, and the resulting geometric patterns are generally known as sea-level "fingerprints" (Mitrovica et al. 2011, Spada et al. 2013). The fingerprint is typically expressed as a ratio of regional change and the volume of mass loss associated with a given source that can be expressed as a change in sea surface elevation. The result of accounting for the regional distribution in the form of ice-melt adjustments to a given

global scenario at a particular location can be significant. The ensuing sections describe the methodology used for adjusting global SLR scenarios developed as part of this study at various military sites worldwide.

Datasets and Approaches Considered

Published literature contains multiple versions of the regional sea-level patterns computed from solving various forms of the Sea Level Equation (Grinsted et al. 2015, Hay et al. 2013, Mitrovica et al. 2001, 2011, Perrette et al. 2013, Plag and Juttner 2001). Depending on assumptions used, such regional patterns may show significant differences in spatial patterns but the normalized fingerprints generally look similar. Mitrovica et al. (2011) analyzed the discrepancy between two fingerprints and suggested that even relatively small differences in fingerprints can be explained through a careful analysis of the physics that underlie the predictions. Grinsted et al. (2015) accounted for uncertainties in fingerprints through Monte Carlo simulations. For the effort here, the fingerprints available from M. Perrette (personal communication 2014) were used and were found to be fairly complete and comprehensive. The fingerprints were derived from the solution to the Sea Level Equation using the same model as in Bamber and Riva (2010), which accounts for the gravitational effect, changes in Earth rotation, shoreline migration, and elastic crustal uplift (Perrette et al. 2013). As in the case of DSL, the resolution of the global fingerprints is 1 degree by 1 degree and the same models that were used for DSL were used (Table 3.5).

To compute the regional adjustments by ice melt source (glaciers, Greenland and Antarctica ice sheets), time epoch (2035, 2065, and 2100), and scenario (0.2 meter to 2.0 meter), the magnitude of the global sea-level contribution attributable to each source is needed. It is used, along with the fingerprints, to compute specific adjustments at installation sites. In view of the large number of estimates needed for a variety of configurations (scenario, source, and time), a decision was made to use probability distributions when determining ice-melt contributions by source made available from the work of Kopp et al. (2014). They used a combination of up to 29 process models from the CMIP5 suite (Table S2, Kopp et al. 2014) as used in AR5 and expert elicitation in a Monte Carlo framework to derive the probability distributions. The next section elaborates on the specific use of results from Kopp et al. (2014) and Perrette et al. (2013) for computing regional adjustments at military sites worldwide.

Methods

Fingerprints

The fingerprint associated with a given component, *c*, of ice melt is computed in general as:

$$Fingerprint^{c}(x) = Contribution\ to\ Regional\ Sea\ Level^{c}(x) / global\ mass\ addition^{c} \quad [3–3]$$

in which *x* is the location and *Contribution to Regional Sea Level*^{c} (in meters) is the spatial pattern of regional sea-level adjustments (location dependent) generated by the model (here the model of Bamber and Riva [2010] as used by Perrette et al. [2013]), and *global mass addition*^{c} (equivalent depth in meters based on the amount of mass addition) is the global contribution, both attributable to component, *c*. The components are ice melts from glaciers and ice caps

(GIC), Greenland ice sheet (GrIS), and Antarctica ice sheet (AIS). Note that the ice-melt fingerprints combine both the pattern-scaling and magnitude-scaling aspects that for dynamical sea level could be more easily distinguished; here, they are interrelated. Once the global mass addition from a particular source is known, the adjustments for any location can be computed using the fingerprint in Equation 3–3.

As in the case of DSL, the fingerprints were computed from the data made available by M. Perrette (personal communication 2014, Perrette et al. 2013). Correspondence of each global mean sea-level rise (GMSLR) scenario to a corresponding RCP used to drive IPCC AR5 process models is shown in Table 3.7. Because the 1.5-meter and 2.0-meter scenarios used here exceed the highest global mean sea level projected for all RCPs for 2100 by Church et al. (2013a) using process-based model approaches, the spatial patterns and global mass additions corresponding to the semi-empirical method (Perrette et al. 2013) were used for those fingerprint calculations. In addition, semi-empirical datasets were used for AIS in the case of all GMSLR scenarios as the process-based datasets were not available for AIS from Perrette et al (2013). Because the fingerprints are generally assumed to be scenario independent, the exception adopted for the AIS fingerprint is deemed reasonable. Figure 3.9 shows the fingerprints computed using the above methodology.

Table 3.7 Sources of Fingerprints for Each Global Mean Sea-Level Rise Scenario

Global Scenario (m)	Dataset used for computing fingerprint*
0.2	RCP 2.6 (Process-based)**
0.5	RCP 4.5 (Process-based)
1.0	RCP 8.5 (Process-based)
1.5	RCP 8.5 (Semi-Empirical)
2.0	RCP 8.5 (Semi-Empirical)

*In the case of AIS, all scenarios used semi-empirical datasets.

**This pathway was originally identified as RCP 3-PD (see Section 3.3.5 for details).

(a) Glaciers and Ice Caps (GIC)

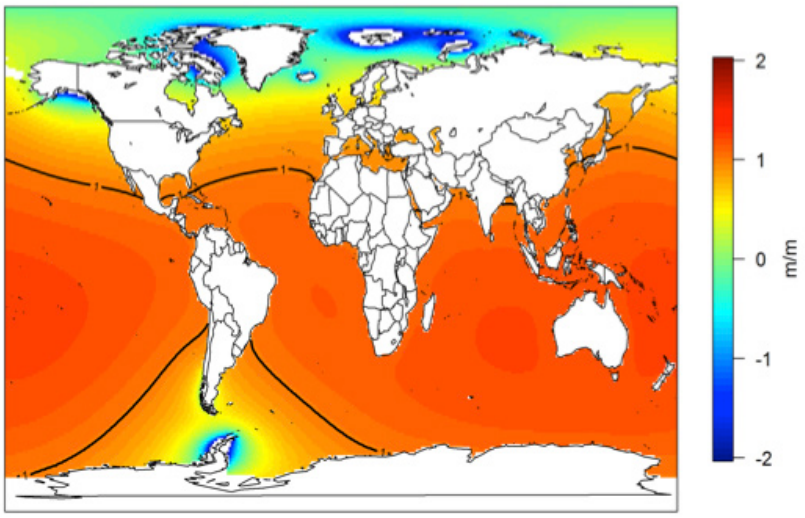

(b) Greenland (GIS)

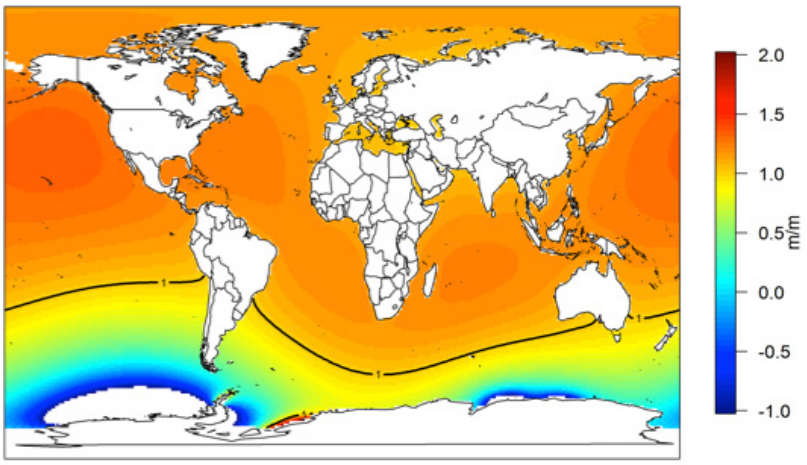

(c) Antarctica (AIS)

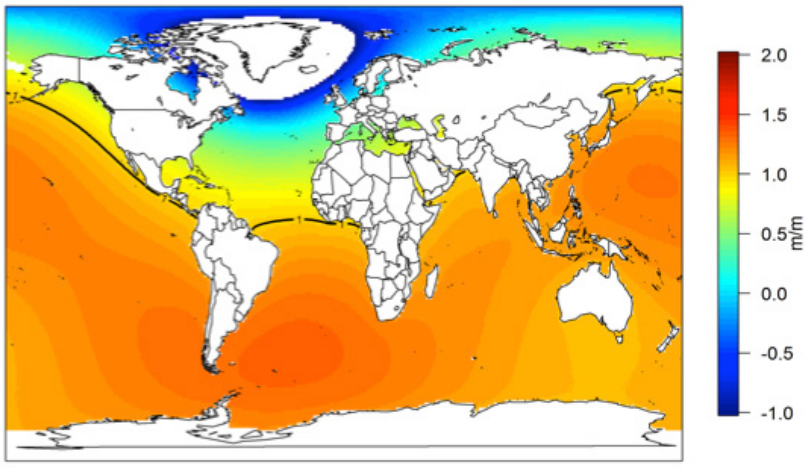

Figure 3.9 Fingerprints of (a) Glaciers and Ice Caps, (b) Greenland Ice Sheet, and (c) Antarctica Ice Sheet

The scale bar represents the ratio of SLR at a particular location to the melt volume (in meters) associated with each of the source components. The solid contour line (ratio equals 1) represents locations where the sea-level increase associated with ice melt from a particular component is equivalent to the global mean value of sea-level increase due to the associated increased mass addition from ice melt from that component.

Ice-Melt Contributions of the Scenarios

Unlike many previous studies that address the spatial signature of ice-melt contributions associated with a specific IPCC AR5 scenario (e.g., Grinsted et al. [2015] addressed only an RCP 8.5 end-of-century scenario), the approach here requires regional adjustments for all three components (GIS, GrIS, and AIS), each scenario (0.2 meter, 0.5 meter, 1.0 meter, 1.5 meter, 2.0 meter), and a given time epoch (2035, 2065, and 2100). Constraining the regional signature of each ice-melt contribution to a specified global scenario is a challenging exercise. The probability distributions available from Kopp et al. (2014) were employed for estimating the contribution of each ice-melt source subject to a global total sea-level rise scenario. The following steps were used to achieve that purpose:

Step 1: Fit analytical distribution to ice-melt contributions

Using the percentiles of various ice-melt contributions available for each applicable RCP scenario (2.6, 4.5, and 8.5) and a given time epoch from the data made available by R. Kopp (personal communication 2014, Kopp et al. 2014), analytical distributions (lognormal distribution unless otherwise stated) were fitted to each component of the GMSLR. It is assumed that the global SLR is given by the sum of thermal expansion, land-based water addition to the ocean, ice melt from glaciers and ice caps, and the two ice sheets, Greenland and Antarctica. Kopp's data were available for 2030, 2060, and 2100, and the first two time periods were assumed to closely represent the 2035 and 2065 time horizons for the scenario adjustments developed here, respectively. All contributions, except for AIS, were found to fit a lognormal distribution reasonably well. In the case of Antarctica, a lognormal fit to the percentiles was found to be inadequate for simulating potential contributions in cases of the higher-end scenarios (i.e., 1.5 meter and 2.0 meter). Consequently for AIS, the probabilistic percentiles available from the data provided by R. Kopp (personal communication 2014, Kopp et al. 2014) were used directly to form an empirical distribution. The fitted lognormal distributions for the other four components, the empirical distribution for the RCP 8.5 scenario corresponding to Year 2100, and the total distribution are shown in Figure 3.10. Similar distributions were determined for the other RCP scenarios used and each time epoch.

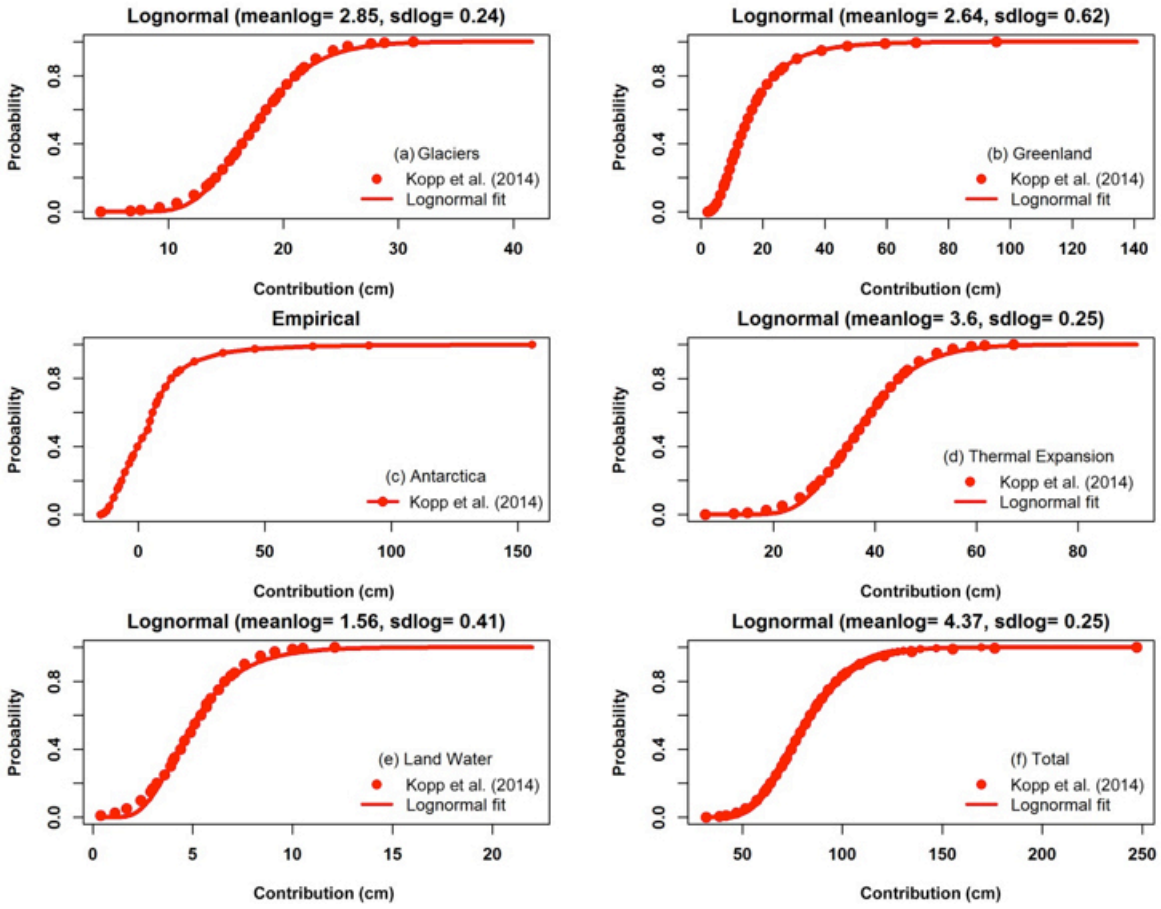

Figure 3.10 Lognormal Fits and the Empirical Distribution (only for Antarctica) for RCP 8.5 and Year 2100
(derived from data provided by R. Kopp [personal communication 2014]). The estimated parameters of the fitted lognormal distributions are shown above each panel (as mean and standard deviation of lognormal, meanlog and sdlog respectively). Each panel depicts the magnitude (in centimeters) of the contribution from each source as noted inside the panel.

Step 2. Monte Carlo simulation of contributions to GMSL scenarios

The total GMSLR was assumed to be the sum given by the following equation:

$$Total\ GMSLR = GIC + GrIS + AIS + T + LW \qquad [3–4]$$

in which *GIC* is the contribution from the glaciers and ice caps, *GrIS* and *AIS* are the contributions of the two ice sheets, Greenland and Antarctica, *T* is the thermal expansion, and *LW* is the contribution of land-based water. To simulate a large number of samples to select combinations of the five components that would sum to a given scenario value of GMSLR, a Monte Carlo approach was used by sampling from the distributions fitted to the components (shown in Figure 3.10). After some initial testing, it was found that 500,000 simulations were adequate to obtain a stable set of

results. For a given GMSLR scenario, say 1.0 meter, all combinations of the five components that sum to about that scenario value (within ± 20%) were selected and summarized. Using multiple samples enables the estimation of uncertainties associated with each GMSLR scenario. The resulting subsample for that scenario was bias-corrected to ensure that the total GMSLR amount coincides with the specified scenario. The subsamples selected for each GMSLR scenario were used to compute the uncertainty bounds (5^{th} and 95^{th} percentiles) corresponding to the global contribution of each component corresponding to a specified scenario. The final results are shown in Table 3.8.

Table 3.8 Median Ice-Melt Contributions in Meters to GMSLR and the Lower (5%) and Upper (95%) Bounds

Contributing components include Glaciers and Ice Cap (GIC), Greenland Ice Sheet (GrIS), Antarctica Ice Sheet (AIS), Thermal (T), and Land-based Water (LW). As an example, the highlighted cells in the Median results provide values for the five components totaling to 1.00 meters added to Global Mean Sea Level for 2100.

		5%					Median					95%				
Component	**Year**	**0.2**	**0.5**	**1.0**	**1.5**	**2.0**	**0.2**	**0.5**	**1.0**	**1.5**	**2.0**	**0.2**	**0.5**	**1.0**	**1.5**	**2.0**
GIC	2035	0.01	0.02	0.02	0.03	0.03	0.02	0.03	0.05	0.06	0.07	0.03	0.04	0.07	0.09	0.11
GrIS	2035	0.01	0.01	0.02	0.02	0.02	0.02	0.02	0.02	0.03	0.03	0.02	0.02	0.03	0.03	0.03
AIS	2035	0.00	0.00	0.00	-0.01	-0.02	0.00	0.01	0.01	0.02	0.03	0.01	0.01	0.03	0.05	0.08
T	2035	0.02	0.04	0.06	0.08	0.10	0.03	0.05	0.09	0.12	0.16	0.04	0.07	0.11	0.16	0.22
LW	2035	-0.01	-0.01	-0.01	-0.01	-0.01	-0.01	0.00	0.00	0.00	0.00	0.00	0.01	0.01	0.01	0.01
TOTAL	2035	0.06	0.09	0.14	0.20	0.27	0.07	0.10	0.17	0.23	0.29	0.07	0.12	0.19	0.25	0.31
GIC	2065	0.03	0.04	0.06	0.06	0.06	0.05	0.07	0.11	0.12	0.11	0.06	0.10	0.15	0.18	0.17
GrIS	2065	0.02	0.02	0.02	0.02	0.01	0.03	0.04	0.08	0.11	0.10	0.04	0.06	0.14	0.19	0.18
AIS	2065	-0.02	-0.03	-0.04	-0.04	0.19	-0.01	0.01	0.04	0.15	0.39	0.00	0.04	0.11	0.33	0.58
T	2065	0.04	0.08	0.13	0.14	0.12	0.06	0.12	0.21	0.25	0.23	0.07	0.16	0.28	0.36	0.34
LW	2065	0.00	0.00	0.00	0.00	0.00	0.01	0.01	0.01	0.01	0.01	0.01	0.01	0.02	0.02	0.02
TOTAL	2065	0.11	0.20	0.36	0.54	0.73	0.12	0.24	0.44	0.64	0.84	0.13	0.28	0.51	0.74	0.95
GIC	2100	0.06	0.07	0.12	0.12	0.12	0.09	0.13	0.20	0.21	0.20	0.12	0.19	0.28	0.29	0.28
GrIS	2100	0.01	0.00	0.02	-0.04	-0.21	0.04	0.09	0.23	0.37	0.38	0.07	0.17	0.43	0.79	0.98
AIS	2100	-0.10	-0.10	-0.11	-0.08	0.17	-0.06	0.02	0.11	0.42	0.95	-0.03	0.14	0.34	0.92	1.72
T	2100	0.07	0.14	0.27	0.26	0.25	0.12	0.25	0.44	0.48	0.45	0.16	0.35	0.62	0.71	0.66
LW	2100	0.01	0.01	0.01	0.01	0.01	0.01	0.02	0.02	0.02	0.02	0.02	0.02	0.02	0.02	0.02
TOTAL	2100	0.17	0.41	0.82	1.25	1.63	0.20	0.50	1.00	1.50	2.00	0.23	0.59	1.18	1.75	2.37

The Monte Carlo simulations assumed that the five components contributing to the GMSLR are independent. In reality, some dependence is present among the variables. For instance, if the temperature is higher, resulting in greater thermal expansion, the ice-melt components also will be higher with a positive correlation between them. The independence assumption should not affect the median values; instead, the uncertainty bounds around the medians are affected and they would tend to be broader because of covariance among variables. No widely accepted procedure is available to compute a reasonable covariance estimate and therefore no significant effort was made to incorporate it in the Monte Carlo simulation. Grinsted et al. (2015) attempted to incorporate some form of a covariance matrix, based on IPCC AR5 results but even in their case a couple of variables had to be dealt with separately from the ice-melt variables. Future efforts may attempt to incorporate covariance using such methods as copulas (i.e., multivariate probability distribution) to address the covariance among melt contributions.

Step 3. Computation of regional adjustments

The final step was to compute the regional sea-level adjustments for each ice-melt contribution for specified locations. This was accomplished by combining the fingerprints with the median contributions to global mean sea level shown in the middle columns of Table 3.8. The specific adjustment was computed using the following equation:

$$\textit{Regional adjustment}^{c}(x) = \textit{fingerprint}^{c}(x) * \textit{global mass addition}^{c} \qquad [3\text{–}5]$$

in which x denotes the location and the superscript c represents the particular contribution (GIC, GrIS, or AIS). Regional adjustments were computed for each of the time epochs: 2035, 2065, and 2100.

Comparison with other Approaches from the Literature

Fingerprints shown in Figure 3.9 are similar to the regional spatial distribution patterns that are available in the literature and therefore no particular effort was made to validate them. Because Perrette et al. (2013) used the fingerprint model of Bamber and Riva (2010), their published figure (Perrette et al. 2013: Fig. 2) generally mimics the patterns shown above in Figure 3.9. The melt contributions from the three primary sources (GIC, GrIS, and AIS) as computed using the Monte Carlo approach with data provided by R. Kopp (personal communication 2014) were compared against the available IPCC AR5 data (Church et al. 2013a). Comparison was made for two GMSLR scenarios: 0.5 meter and 1.0 meter. For the 0.5-meter scenario, RCP 4.5 median data available in Table 13.5 of Church et al. (2013a) was used. Because no equivalent set for the 1.0-meter scenario is available from Church et al. (as median values), the upper bound figures of RCP 8.5 values from the same table were used. Church et al.'s sum for total SLR is 0.48 meters for RCP 4.5 and 0.98 meters for the upper bound of RCP 8.5. They are assumed to represent the 0.5-meter and 1.0-meter scenario storylines used for the approach developed herein. The comparison is shown in Figure 3.11. As shown in this figure, the estimates of mass contributions from the three sources are quite comparable and for a screening analysis, the values computed from the Monte Carlo approach are deemed reasonable.

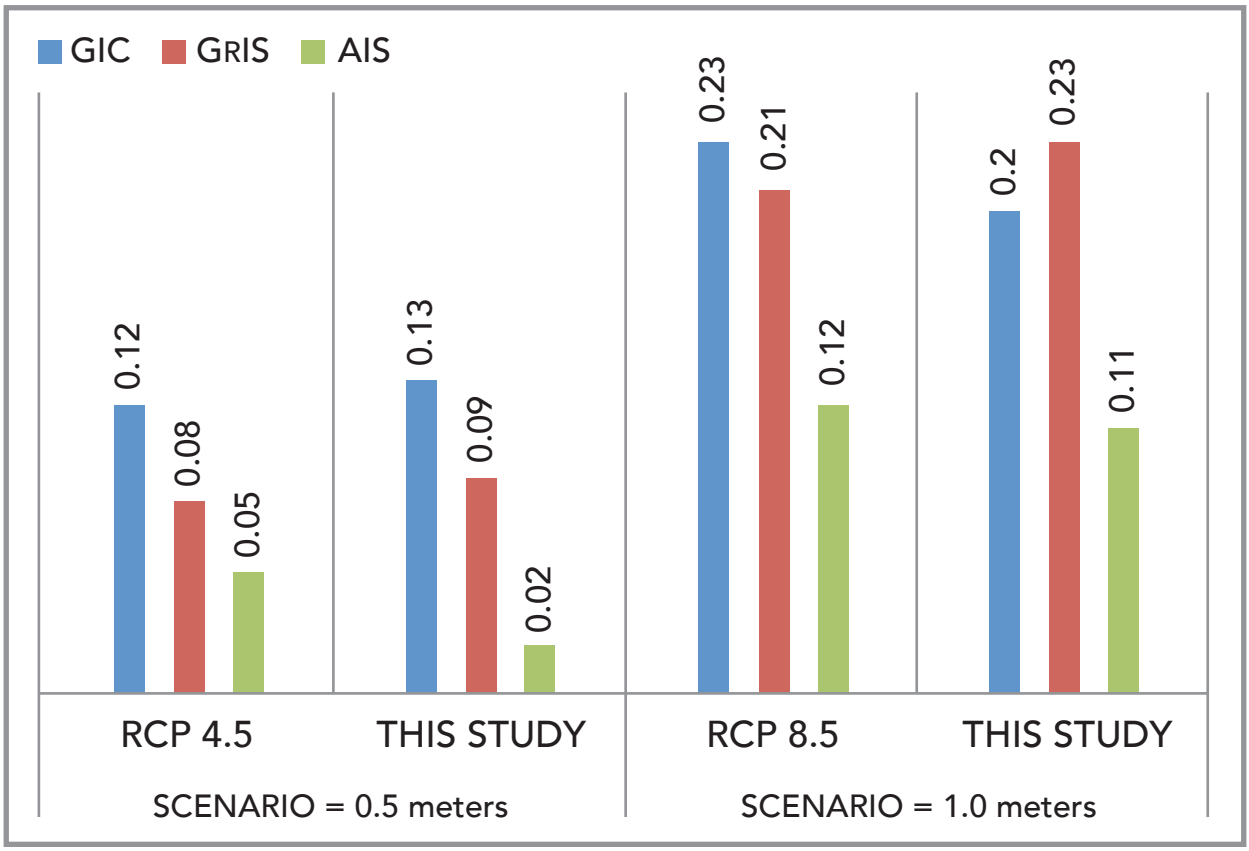

Figure 3.11 Comparison of IPCC-AR5 (Church et al. 2013a) Results (in meters) with Those Computed for the 0.5-Meter and 1.0-Meter Scenarios Used in this Study
For these scenarios the median values computed from the Monte Carlo approach were used.

Uncertainty Estimation

At least two sources of uncertainty are present in the regional adjustments computed from Equation (3–5). First, the uncertainty in the global mass addition for each component for a given global scenario was incorporated using the lower and upper bounds shown in Table 3.8. The second source of uncertainty is in the fingerprint. Grinsted et al. (2015) incorporated the uncertainty in the fingerprints by using alternative configurations presented by Bamber and Riva (2010) and Kopp et al. (2014); however, their projection was for one scenario, namely RCP 8.5. We considered the upper and lower bounds of the fingerprints provided by Perrette et al. (2013) but they yielded unrealistic results for uncertainty bounds and were not considered further. In view of the lack of uncertainty estimates for fingerprints in the current body of literature, particularly for all the scenarios considered in the current study, it was assumed that the median fingerprints provided by Perrette et al. (2013) are reasonably robust and meet the needs of a screening-level analysis of regional projections.

Another uncertainty in the regional adjustments is the lack of consideration for future effects of postglacial rebound (i.e., GIA) on both regional and global mean sea level. Grinsted et al. (2015) made an attempt to incorporate it into their regional adjustments. Bamber and Riva (2010) provided a detailed description of the potential impact of GIA on regional sea levels. The largest GIA signals are confined to land masses that have experienced the largest changes in ice loading, in particular North America (Figure S1 in Bamber and Riva 2010). The incomplete knowledge of the ice-load history has been recognized as a serious limitation. The GIA contribution to global mean SLR is considered to be small (Perrette et al. 2013, Tamisiea 2011). It is noted that the GIA due to historic deglaciation that occurs over millennia is different from the instantaneous elastic response due to current and future melting (Perrette et al. 2013). The consequence of not considering GIA in regional sea level is likely to be greatest in latitudes above about 40 degrees (Bamber and Riva 2010).

Another factor that may cause uncertainty in fingerprints is the incomplete knowledge of the geometry of melt. The model used by Perrette et al. (2013), attributed to Bamber and Riva (2010), assumed the present-day distribution of mass loss though the distribution is likely to change in the future. The exact distribution of mass loss is important only in the near-field of an ice sheet (less than 1000 km) (Perrette et al. 2013).

3.5 Extreme Water Level Adjustments

The following section describes the factors affecting extreme water levels and the calculations used to account for tidal and nontidal influences, such as storm surge, on sea levels. This section includes the methodology followed for Generalized Extreme Value (GEV) analyses to estimate extreme event probabilities over specific time periods. In addition, Regional Frequency Analyses (RFA) were performed for coastal military sites with sufficient tide gauges to support the analyses. The section concludes with a discussion of single gauge analyses and recommendations regarding sites with limited tide gauge data.

3.5.1 Background

Before discussing the methodology for determining site-specific extreme water levels, a brief overview of the components of EWL, historical changes in EWLs, and techniques for assigning probabilities to EWLs is provided below.

Extreme Water Levels

Coastal flooding, erosion, and damages from extreme water events are a constant concern along the coast. Knowledge of the probability of occurrence of extreme events is of importance to decision-makers charged with maintaining critical infrastructure, public works, and functionality of sector-specific systems. The demand for this type of information has only increased with recognition of the need to understand and anticipate how impacts from extreme events relating to both sudden and gradual changes in sea level have varied in the past or may change with a changing climate (e.g., Hunter 2010, Menéndez and Woodworth 2010, Salas and Obeysekera 2014, Sweet and Park 2014, Tebaldi et al. 2012).

Extreme water levels, referred to as extreme still water level (SWL) in this study because we are using tide gauge measurements, form from superposition of several components. Most notably are the astronomical tide and a storm surge in response to a local storm, both of which occur over a regional mean sea level (MSL) seasonal cycle and any less-noticed MSL anomaly that may exist. Equation 3–6 below defines extreme still water level as used in this report:

$$SWL = Tide\ (astronomical + MSL\ seasonal\ cycle) + Nontidal\ Residual\ (storm\ surge + sea\ level\ anomaly) \quad [3–6]$$

in which SWLs are measured by tide gauges (Moritz et al. 2015). Equation 3–6 is typically simplified into a predictable tidal (tide = astronomical tide + MSL seasonal cycle) and a nontidal residual (NTR = storm surge + anomaly) component. In the few instances where a tide gauge may be located in a breaking wave location (e.g., on an ocean pier), some degree of wave set-up may be included in the NTR; the contribution would be minor (Sweet et al. 2015). Water heights are reported relative to a tidal datum (e.g., MSL) estimated over a multi-year epoch, such as the current national tidal datum epoch of 1983 to 2001 (NOAA 2001) as illustrated in Figure 3.12 (repeated from Section 2). Extreme still water level, the focus of this report, does not include wave set-up and swash (which are collectively referred to as wave run-up).

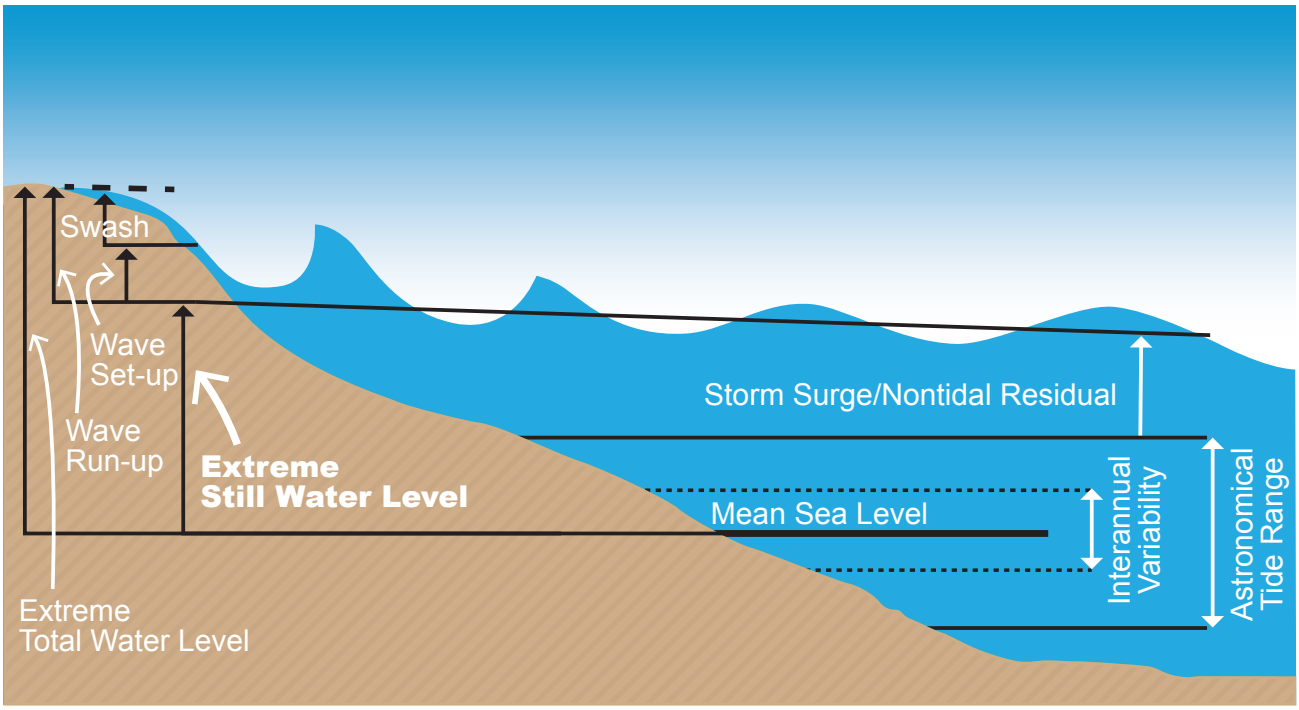

Figure 3.12 Profile View Schematic of the Components of Extreme Water Levels (adapted from Moritz et al. 2015)

Tide gauges offer long-term reliable measurements of water levels around the world (Figure 3.13). The benchmark network of tide gauges typically permits tidal datum and derived event probabilities to be locally tied to a geodetic datum and a framework to assess potential local land elevation impacts. Historic EWL events reflect the nature of the regional physical forcing regime such as whether or not intense extra-tropical or tropical cyclones have occurred. Local bathymetric characteristics also are a factor, such as the width of the adjacent continental shelf which modulates the degree of local set-up during an event, as shown in Figure 3.14(a).

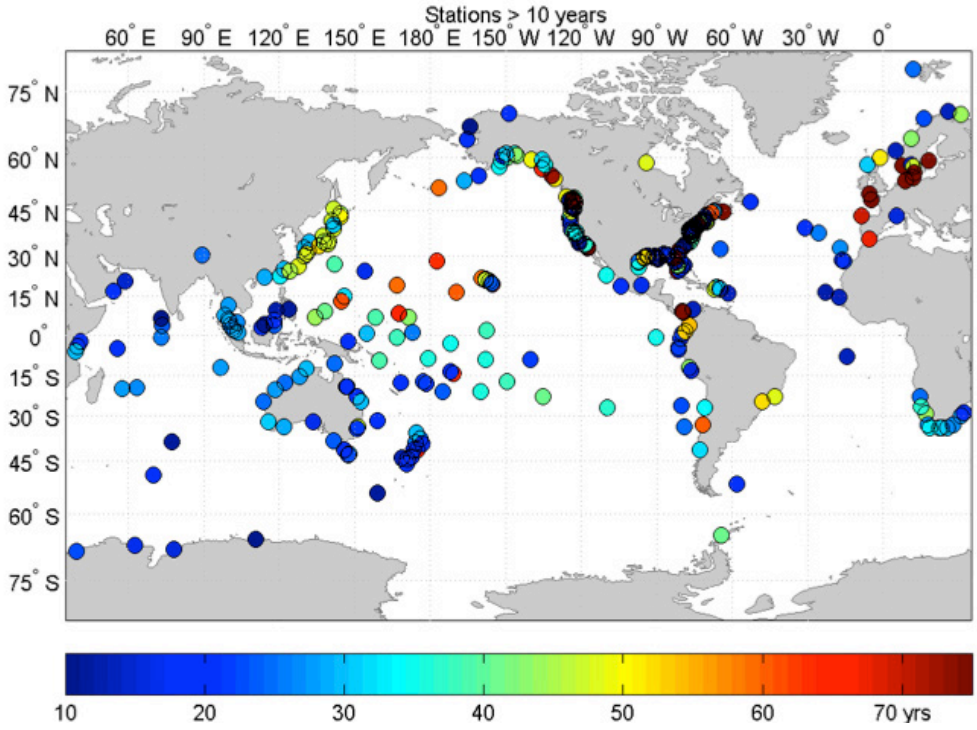

Figure 3.13 Global Tide Gauges with 10+ Years of Data Used in this Study
(color-coded record length shown in map legend; data obtained from University of Hawaii Sea Level Center and NOAA CO-OPS)

Strictly in terms of storm surge (or NTR values), highest values usually result from intense low-pressure storms or systems (inverse barometer effect) and wind-driven storm surge on a wide continental shelf, as shown in Figure 3.14(b). For example, though the tide range is fairly large along the U.S. West Coast, extreme events are relatively small in magnitude, usually occurring in response to high "king" tides (Sweet et al. 2014) riding atop prolonged elevated sea-level anomalies associated with El Niño conditions (Menéndez and Woodworth 2010). Along the U.S. Northeast Coast, strong winter storm systems (nor'easters) are the

Strictly in terms of storm surge (or NTR values), highest values usually result from intense low-pressure storms/systems (inverse barometer effect) and wind-driven storm surge on a wide continental shelf.

prevailing threat and can produce large storm surges, whereas along the U.S. Southeast (SE) and Gulf Coasts even larger storm surge occurs from hurricane strikes. Local bathymetric characteristics enhance or constrain the NTR response; Figure 3.14 (b) highlights the difference in tropical storm landfall responses along the U.S. Gulf and SE Coasts (wide continental shelf) and the Caribbean and Western Equatorial Pacific Island locations (narrow continental shelf).

Historical Changes

The regional storm impact-response patterns in Figure 3.14 are similar from year to year (e.g., Merrifield et al. 2015) though in any given year altered storm tracks may affect the intensity or frequency of storms impacting a location. The magnitude of typical high waters relative to a fixed-elevation threshold, however, has been changing over time due to local SLR, closely tracking trends in local MSL observed in both tide gauge (Menéndez and Woodworth 2010) and satellite altimeter data (Woodworth and Menéndez 2015). Where local MSL has been rising, not only does inundation from extreme events flood higher elevations but flood frequencies relative to fixed-elevation infrastructure also increase (Church et al. 2006, Hunter 2010, Sweet et al. 2013, Tebaldi et al. 2012). Recurrent flooding from SLR is apparent in the historic records most readily in terms of exceedances above a *lesser-extreme* threshold as illustrated in Figure 3.15. The magnitude shown in Figure 3.15(a) is the average of annual maximum water levels recorded over the 1983 to 2001 period, which has an approximate probability of recurring every two to three years (Merrifield et al. 2013). Because of local SLR, the event frequency has been rapidly increasing, as shown in Figure 3.15(b) in many locations (Church et al. 2006, Ezer and Atkinson 2014, Sweet and Park 2014, Sweet et al. 2014). The frequency increase is substantial along the U.S. East Coast and the Western and Central Equatorial Pacific regions where SLR rates have been quite high over the last couple of decades (Merrifield et al. 2012). On the other hand, the U.S. West Coast has not experienced a significant increase over this time because Pacific Decadal Oscillation (PDO) impacts have stagnated MSL over the last couple of decades (Bromirski et al. 2011). In some locations a decrease in event frequency is occurring where local MSL has been steadily decreasing from rebounding land rates (upward VLM) such as around the U.S. Alaskan coastline.

Where local MSL has been rising, not only does inundation from extreme events flood higher elevations but flood frequencies relative to fixed-elevation infrastructure also increase (Church et al. 2006, Hunter 2010, Sweet et al. 2013, Tebaldi et al. 2012).

(a)

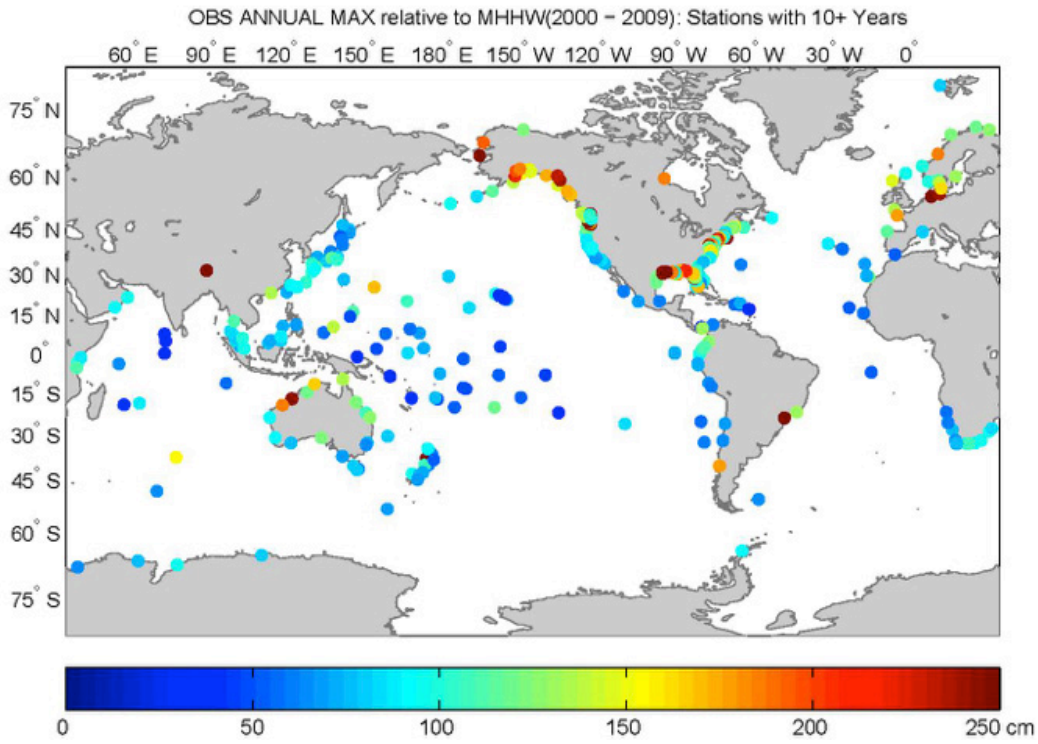

(b)

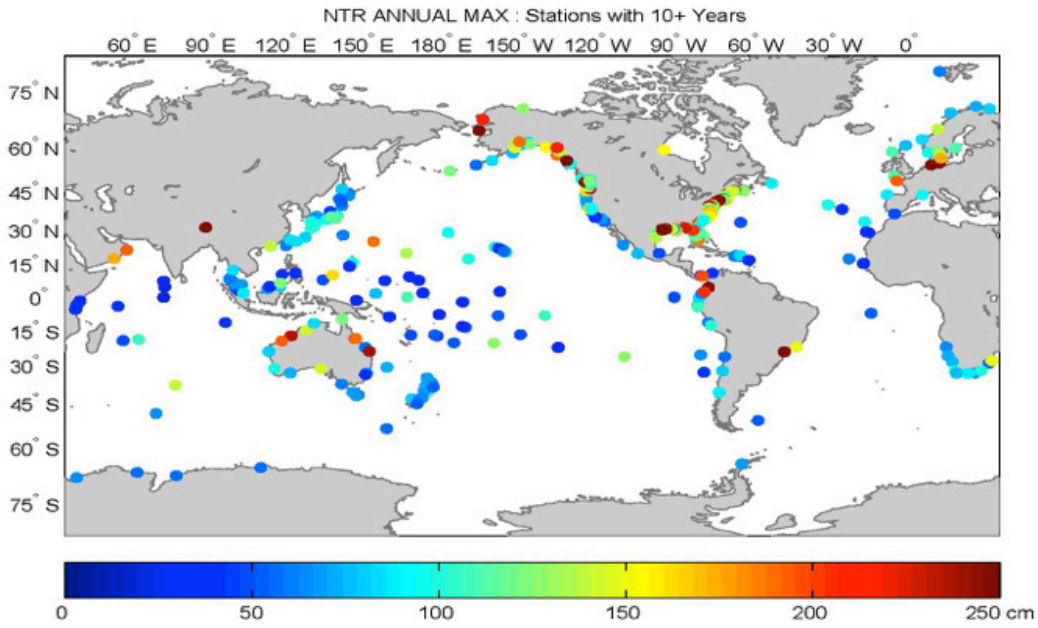

Figure 3.14 Highest (a) Observed Water Level above MHHW over Period of Record for each Tide Gauge and (b) Nontidal Residual (NTR) Event
(relative to a 2000-2009 Epoch)

(a)

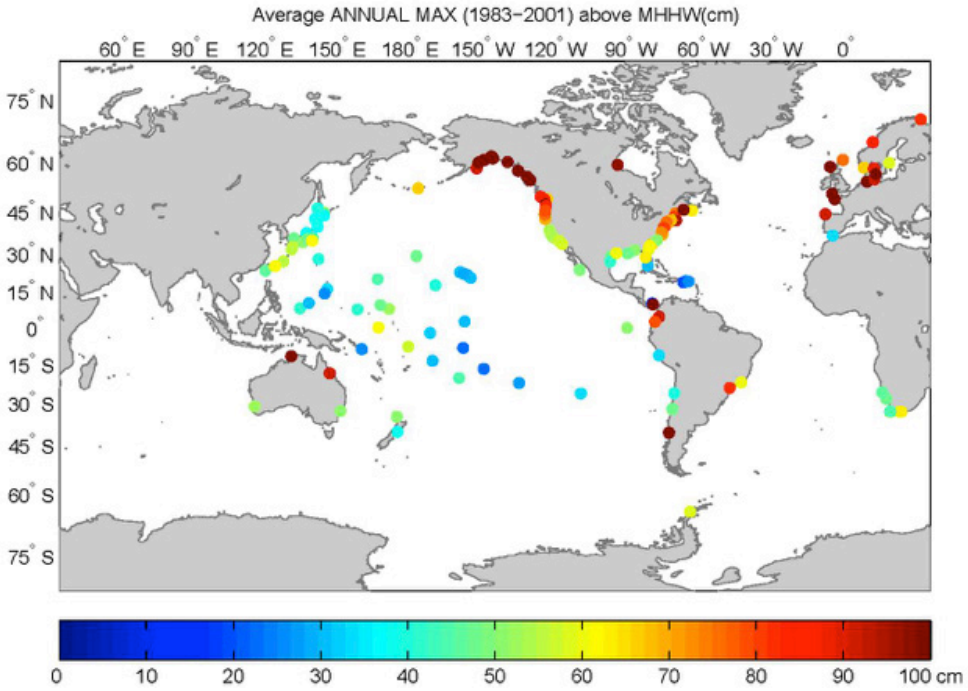

(b)

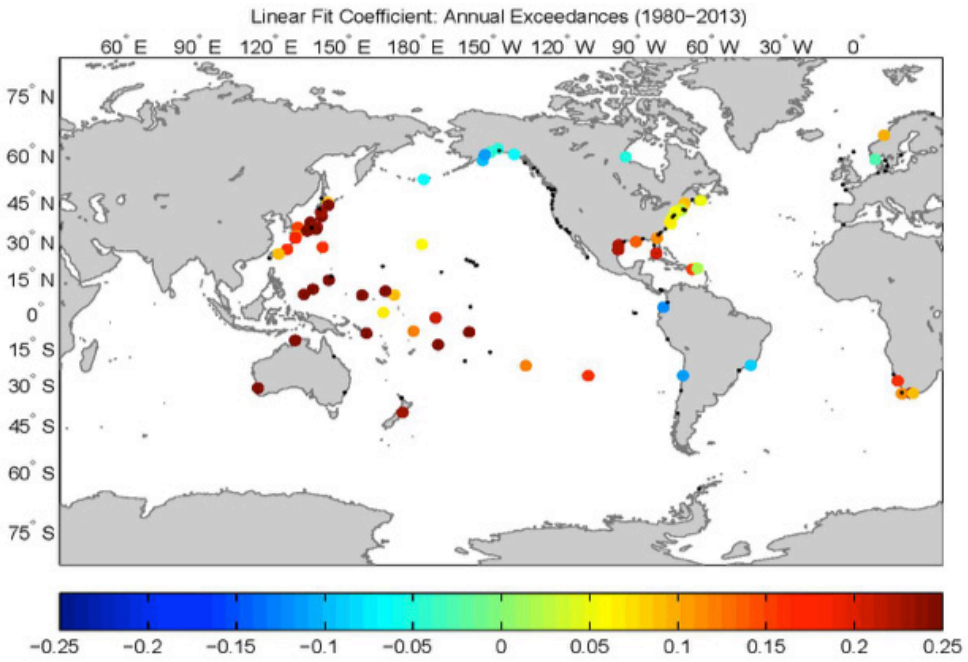

Figure 3.15 (a) The Average of the Annual Maximum Water Levels over 1983 to 2001 (Relative to MHHW); (b) Linear Regression Coefficients Significant Above the 90% level (p values < 0.1) for Yearly Exceedances Above the Levels Shown Based on Methods of Sweet and Park (2014) in (a) Over the 1980 to 2013 Period

A black dot is shown for stations with no significant linear fit.

Assigning Probabilities

To assess current and future risk exposure from EWLs, probability estimates of exceeding a certain extreme sea level are required (e.g., Marbaix and Nicholls 2007, Obeysekera and Park 2013). Extreme value analysis (EVA) techniques are used to establish a probability distribution when sufficient data records exist to describe historic flooding associated with the rare and often destructive event by characterizing the upper tail of a location's water level distribution (Coles 2001). Such models provide recurrence intervals (return periods), which are the inverse of the probability of exceeding particular elevation level (return level). Two types of EVA techniques—direct and indirect methods—are typically used. Direct methods estimate probabilities directly on the data (observed or modeled). One common method analyzes water level maxima over a block of time; typically, the Annual Maximum Method (AMM) is used and fit with the family of three Generalized Extreme Value (GEV) distributions to approximate the range of extremal behaviors (Coles 2001). Zervas (2013) applied the AMM fit with GEV distributions at NOAA tide gauges (http://tidesandcurrents.noaa.gov/est, accessed September 2015). A more data-inclusive method is the peak-over-threshold (POT)/Point Process approach (Coles 2001), which evaluates all exceedances above a high threshold using a Generalized Pareto Distribution (GPD). The GPD is also described by the three GEV distribution types. This method is used by Tebaldi et al. (2012) to produce estimates around the United States, which are in agreement with those of Zervas (2013). Generalized Pareto Distribution and GEV estimates for 100-year NTR events (Figure 3.16) are quite similar and follow patterns shown in Figure 3.15. As discussed later, however, neither method necessarily delivers robust probabilities of events outside the historical record (e.g., Hurricane Sandy).

(a)

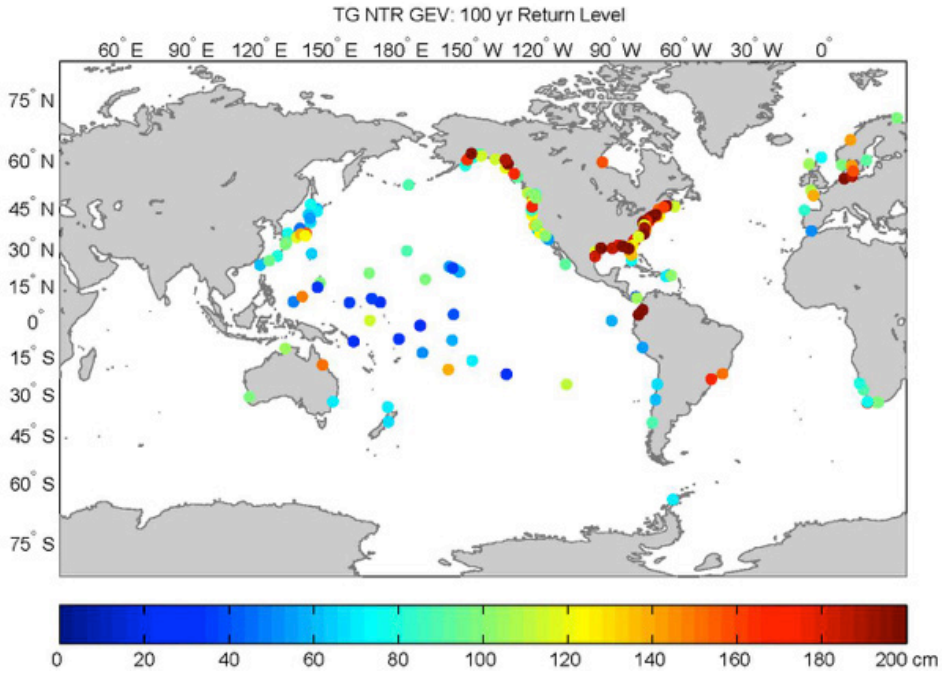

(b)

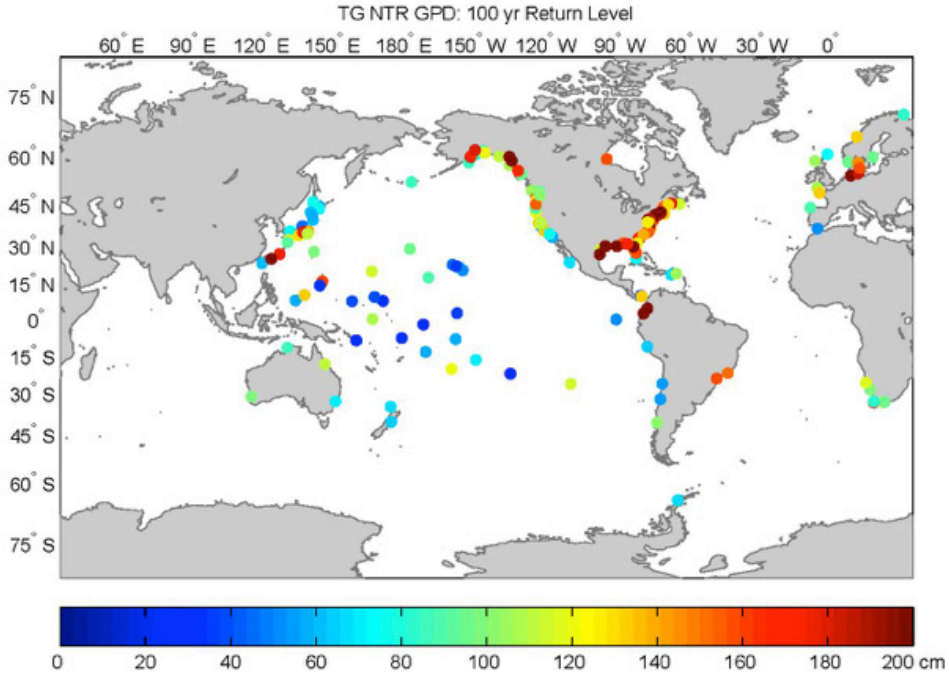

Figure 3.16 NTR (observed-tide) Heights Associated with the 100-Year Event Probability for Tide Gauges with > 30 Years of Data

(a) Generalized Extreme Value distribution fits of annual maximum values (method described below) and (b) a Generalized Pareto Distribution for exceedances above the 98th percentile of daily maximum with a 5-day event independence criterion longer than most synoptic-scale disturbances following procedures discussed by Sweet et al. (2014).

Indirect methods maximize usage of historical data and most approaches revolve around variations (e.g., Tawn 1992, Tawn and Vassie 1989) of the joint probability method (JPM) (Pugh and Vassie 1980) to obtain a summed probability distribution through convolution of astronomical tide and NTR probability densities. Indirect methods expand the range of possible probabilities over the observed record because all surge events are taken into account, not just those that lead to extreme levels. Robust return level estimates can be estimated by indirect methods from relatively short records (e.g., 10 years or more; Thompson et al. 2009) for environments with large tide ranges and not experiencing tropical storms (Nadal-Caraballo and Melby 2014). Indirect methods use various approaches to estimate the NTR, often simply by removing the tidal prediction from the observation series. It is known, however, that spurious NTR values may emerge due to tide phase changes during storm events as well as tide-surge interactions that constrain timing of highest surge levels (Horsburgh and Wilson 2007). To compensate for potential aliasing, NTR-skew surge can be examined, which acts to minimize discrepancies due to tide phasing and ensures characterizations of tides and surges occurring near high tides (Batstone et al. 2009; Mawdsley and Haigh, In Press). An example is shown for Bridgeport, Connecticut, when Hurricane Sandy hit, revealing a slight change in tidal phase that is not accounted for in a straightforward subtraction-based method to compute NTR, as shown in Figure 3.17(a). It can be seen in Figure 3.17(b) that NTR estimates as compared to those estimated using the skew-surge method are in general 30% higher based on linear regression.

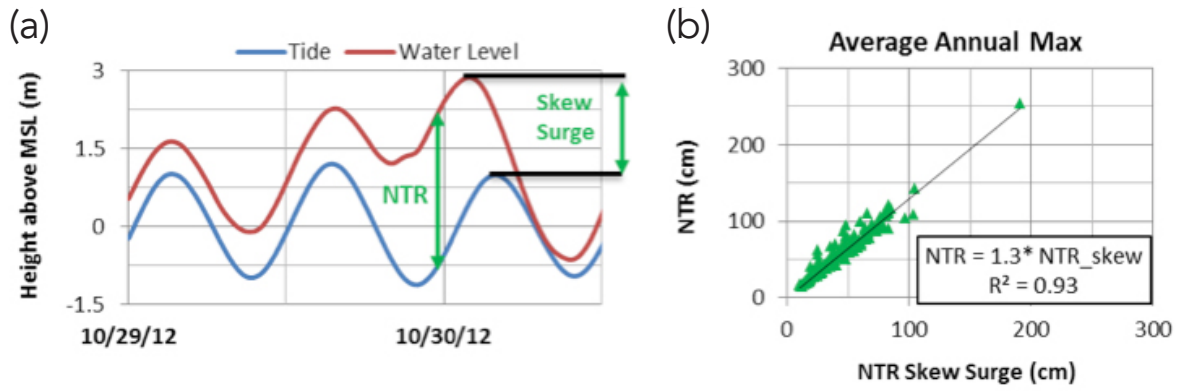

Figure 3.17 Nontidal Residual Skew

(a) Example of skew-surge estimated during Hurricane Sandy at Bridgeport, CT and (b) linear regression (significant above the 99% level, p value < 0.01) between average annual maximum NTR skew surge and NTR at global set of tide gauges with >30 years of data.

Both direct and indirect methods using only observational data may suffer when estimating return periods for low probability events such as locations exposed to tropical cyclone landfalls (Nadal-Caraballo et al. 2015). Not only are rare events often "outliers" and contribute to a large spread in model confidence intervals, but they typically are not homogeneously distributed in time or space, leading to difficulty in assessing their probability from a fixed point in space (i.e., tide gauge location) over a limited time (i.e., tide gauge record). To illustrate this, Figure 3.18 shows the

spread of the 90% confidence interval (difference between the 5% and 95% levels) of the 10-year event in Figure 3.18(a) and the 100-year event in Figure 3.18(b) as a function of shape parameter value, which represents the "skewness" of the GEV distribution. A location with a larger and more positive shape parameter has generally experienced one or more extreme events, which in contrast to past events, are outliers. It can be seen that as the shape parameter increases, a nonlinear increase in the spread of the 90% confidence interval is apparent. A similar finding is shown for the 10-year event; however, because these events occur more often, they are better represented in the model with less uncertainty associated with their impacts.

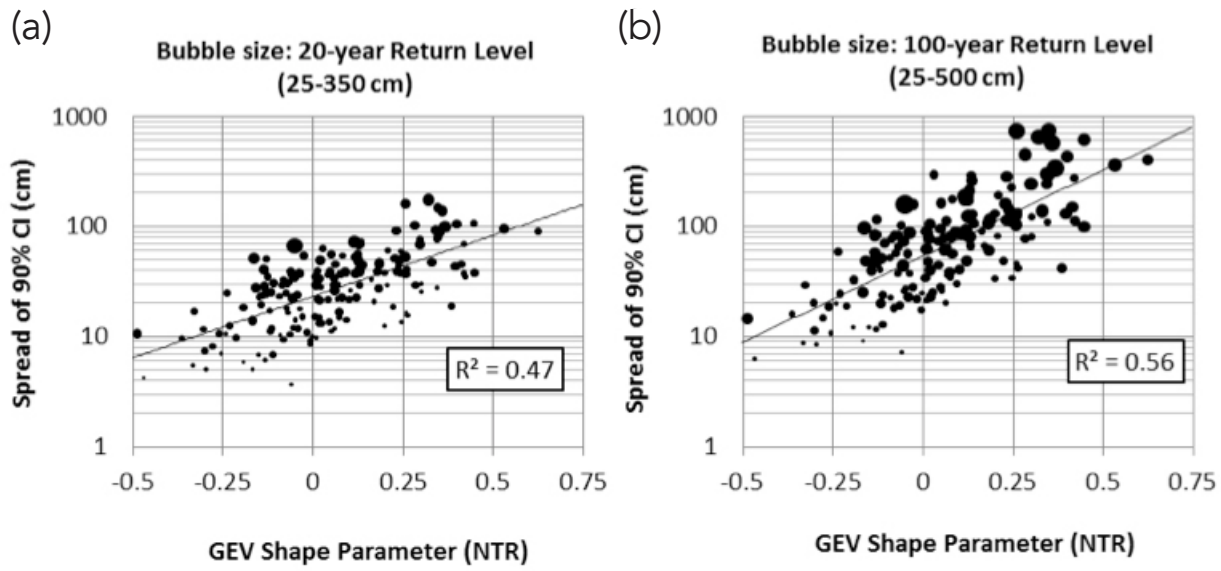

Figure 3.18 GEV Shape Parameter Fit (via method described in text) to Annual Maxima NTR Values Plotted Against the Spread of the 90% Confidence Interval (CI; 95% - 5%)
Bubble size represents return level for (a) the 20-year and (b) the 100-year event probabilities for global tide gauge set with >30 years of record. Exponential fits shown are significant above the 99% level (p value < 0.01).

Other measurements, empirical evidence, and statistical-bias issues should be considered when computing the rare-event probability. For instance, recovery of historic anecdotal high-water marks or archival data recovery (e.g., of tide-gauge data beyond the digitized period of record) can help determine historic impacts and distinguish secular trends in extreme water level (Talke et al. 2014). Depositional overwash evidence is another such method; along the Northeast U.S. in the regions impacted by Hurricane Sandy in 2012, overwash evidence has identified periods throughout history more prone to intense hurricane formation (Donnelly et al. 2015, Lin et al. 2014). Sweet et al. (2013) discuss this fact and those associated with data record length when presenting tide gauge probability estimates associated with Hurricane Sandy along the mid-Atlantic seaboard. When strictly based on an annual maximum fit by a GEV distribution of observed storm tide levels, a 1500+ year return period was computed for Hurricane Sandy at the Battery, New York, though compatible overwash deposits suggest several such impacts have occurred over the last several centuries (Scileppi and Donnelly 2007). In addition, Sweet et al. (2013) show that record length

biases return period estimates when comparing Battery, NY and Sandy Hook, NJ as shown in Figure 3.19. Tide gauges in both locations typically measure similar water levels during extreme events as was the case during Hurricane Sandy (and during other events historically). Data from each location, however, estimate a distinctly different return period for Sandy. Many studies recognize the limitations of tide-gauge estimates of the rare events and make the necessary disclaimers (Kopp et al. 2014, Tebaldi et al. 2012). To overcome such limitations, high-resolution hurricane models can be employed to increase the number of samples (extend the record length) used in the computations to provide more robust probability estimates with lower model uncertainty spread (Haigh et al. 2014a, McInnes et al. 2009, Nadal-Caraballo et al. 2015).

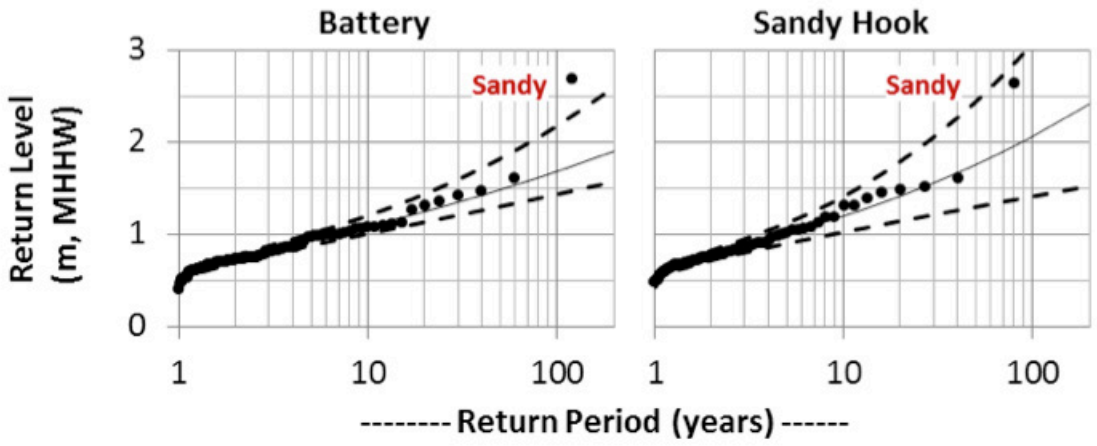

Figure 3.19 Return Level Interval Curves for the Battery, NY and Sandy Hook, NJ (black line) and Spread of 90% Confidence Intervals (dash) Fit to Annual Maximum Water Levels (dots) Return periods for Sandy levels based on GEV fit to annual maximum water levels are (a) 1570 and (b) 295 years, respectively. (from Sweet et al. 2013)

3.5.2 Study requirements and assumptions

Providing EWL probabilities for 1700+ global sites poses many challenges. Namely, a method was sought that utilizes readily available water level data (i.e., tide gauges) because developing hydrodynamic models for most of the globe was beyond the scope of this study. Specifically, a method was sought that: (1) improved the estimates (reduces prediction error) of low probability events (e.g., 100-year event) as compared to a single tide gauge-based analysis, (2) minimized record-length statistical biases (i.e., Figure 3.19), and most importantly, (3) permitted estimates for locations not co-located with a tide gauge. In this effort, several plausible assumptions were made. First, we assume the tide gauge measurements are representative of extreme still water levels (Moritz et al. 2015) and did not include breaking wave contributions. We note that wave effects are of considerable importance for regions with smaller storm-surge potential and a high wave environment, such as the Pacific Basin where wave impacts are often the major contribution to total water levels (TWL) during extreme events (Hoeke et al. 2013, Serafin and Ruggiero 2014). In sheltered harbors, however, where tide gauges are generally located, wave run-up (i.e., wave set-up and swash) are usually of lesser importance.

Second, we also assumed that the NTR probabilities are possible over the entire tide range, which permits usage of historical high NTR events that might not have manifested as an EWL event because they occurred during a low astronomical tide. In our analysis, we assumed that the tidal and NTR components are independent processes. But tide-surge interactions that govern the timing and magnitude of a storm relative to tidal phases have been shown to exist at locations around the world (Mawdsley and Haigh, In Press). Our assumption of tide-surge independence, however, could be viewed as a more cautious estimate (e.g., highest surge could occur during peak high tide); in some limited cases this may lead to an overestimate of a storm-surge event magnitude and resultant EWL probability.

Third, we assumed that the only factor that will cause future EWL (tide + NTR) probabilities to change will be changing MSL (i.e., SLR scenarios). This assumption has been the case historically at most tide gauges (Menéndez and Woodworth 2010) as well as when viewed globally by satellite altimeter data (Woodworth and Menéndez 2015). However, this assumption assumes trend-stationarity in future storm-surge statistics (i.e., NTR or skew-surge NTR), which has been found to be the case overall through historical investigation of tide-gauge records (Mawdsley and Haigh, In Press, Zhang et al. 2000). This assumption is further supported by several studies finding no strong evidence for increasing trends in tropical cyclone activity globally (Weinkle et al. 2012) or specifically within the Atlantic as summarized in Knutson et al. (2010). A notable exception is the slight decreasing tendency in U.S. landfalling hurricane frequency since the late 1800s (Vecchi and Knutson 2008), a time period not considered and thus potentially biasing the findings of Grinsted et al. (2012) who detected an upward trend in the frequency of large surge events using a proxy that roughly corresponded to tropical storms magnitude in tide-gauge records since the early 1920s. Thus, the evidence for long-term trends in storminess is inconclusive at this point.

Fourth, we do not attempt to prescribe any interannual variability in MSL (and thus EWL) with respect to the SLR scenarios, though MSL and storm surge frequencies do possess time-varying (e.g., climate patterns, cycles) characteristics (Marcos et al. 2015, Menéndez and Woodworth 2010, Sweet and Zervas 2011, Thompson et al. 2013, Wahl and Chambers 2015). Such time-varying characteristics can be important over short time horizons (i.e., less than 20 years). This concept is illustrated within the Pacific by Menéndez and Woodworth (2010) who show that in the Western Pacific, the level of the 100-year event is strongly modified by MSL variability during phases of the El Niño Southern Oscillation. Fifth, we also do not attempt to account for future changes in storm-surge magnitude or tidal range (e.g., Mawdsley et al. 2015) due to future SLR relative to today's bathymetric-controlling characteristics; that is, we do not account for non-stationarity in these processes.

3.5.3 Data

We used verified hourly water levels from a global set of 343 tide gauges with greater than 10 years of data available from the University of Hawaii Sea Level Center (UHSLC) and NOAA (Figure 3.13). Most water level series show a clear MSL trend (rise or fall) due to local VLM, global SLR, and regional variability; these trends in MSL affect high tide levels, storm tides, or a particular extreme event. For instance, an event that occurs earlier during a water level record will not reach a level as high as a similar-sized event that occurs later in the record. To account for local MSL

trends inherent in the water level data, each individual water level series is detrended by linear regression with zero-crossing at year 2005 because several gauges have only about 10 years of data (e.g., 2001–2010). In addition, because the water level data are measured relative to a unique "gauge datum," the data also are de-meaned relative to their 2000–2009 epoch to put the data onto a contemporary MSL datum to enable gauge-to-gauge comparisons. Both the detrending and de-meaning processes establish a modern reference level for extreme event characterization. The focus of this study concerns the NTR values (i.e., not associated with the astronomical tide); to obtain them, the tidal component was computed on an annual basis using a harmonic analysis program using 67 standard constituents (T-tide; Pawlowicz et al. 2002) and removed from the data. We stress that our choice of a 10-year threshold applies mostly to our regionalization approach (described below) and is applicable because we were not deriving historical sea-level rise estimates which typically require 30+ years of data (Zervas 2009). Roughly half of the 343 tide gauges used in our study have a record length of less than 30 years and are located internationally (Figure 3.13).

3.5.4 Regional frequency analysis

To reduce prediction error of low probability events, minimize record-length statistical biases, and provide probabilities for locations not co-located with a tide gauge, we used a regional frequency analysis (RFA) approach (Hosking and Wallis 1997). The RFA method estimates extreme event probabilities, making the assumption that coastal environments with similar forcing attributes will experience a similar flood frequency response and share a similar extreme water level probability density up to a localized scaling factor (flood index event, discussed below). The RFA method effectively enlarges the amount of data analyzed by combining tide gauge data from different locations over a region to provide a more robust rare event parameterization. Regionalization provides a more common context for events that may be identified as an outlier based solely on a single tide gauge. The RFA method benefits individual sites with shorter data records (e.g., less than 30 years) by supplementing them with longer-term measurements; this also helps to minimize record length biases inherent to subsequent statistical routines. Lastly, the RFA method provides an approach to assign an extreme probability at an ungauged location based on regionalized information. The RFA method has been successfully applied in numerous hydrological studies (Dalrymple 1960) and more recently for coastal storm surge applications (Arns et al. 2015, Bardet et al. 2011, Bernardara et al. 2011) and coastal wave heights (Weiss et al. 2014), as well as for impacts from tsunamis (Hosking 2012).

Regional Definition

As discussed by Weiss et al. (2014), to effectively use an RFA, regions need to be identified in terms of a statistical homogeneity from exposure to similar physical forcing regimes and event frequencies. In our usage of the RFA method, we did not attempt to identify and delineate the spatial extent of homogenous regions. Rather, the regions were bounded with a maximum distance of 400 km (about 250 miles) around a particular military site. The RFAs were conducted using water level records from up to five tide gauges. Our regional range was smaller than the approximately 1000-km synoptic scale of extratropical disturbances (i.e., storm footprint), approximated the diameter (twice the radius) of maximum winds associated with the largest of the 1000+ synthetic hurricanes recently modeled by the U.S. Army Corp of Engineers (Nadal-Caraballo et al. 2015), and was on the order of (Weiss et al. 2014) or smaller than (Hosking 2012) homogeneous regions

identified in related RFA-based studies. Sites were assigned to categories with an RFA criterion that three to five gauges must be within a 400-km radius of the site:

- Category 1: local gauge within 50 km and record length greater than 30 years
- Category 2: local gauge within 50 km with record length greater than 10 years but less than 30 years
- Category 3: closest gauge more than 50 km away (no local gauge) with a record length greater than 10 years
- Category 4: fewer than 3 gauges within 400 km

The next step in the RFA process was to test the homogeneity of the selected tide gauge records for each site through a heterogeneity "H" score (Table 3.9). Heterogeneity is a measure of the variation between sites of a location's summary distribution statistics relative to the amount of dispersion expected if the locations were indeed a homogeneous region. Statistical L moments are used to provide the summary statistics that quantify the distribution characteristics (Hosking and Wallis 1997).

Table 3.9 Percentage of 1,774 DoD Sites that Fit the Four RFA Regional Definitions
Category 1 has a local tide gauge with > 30 years record that is < 50 km away from the site; Category 2 has a local tide gauge with < 30 year record that is < 50 km away; Category 3 has no local gauge < 50 km away but may have regional tide gauges that are < 400 km away; Category 4 has no local or regional tide gauges within 400 km or L moments were not resolvable. To conduct an RFA for Categories 1, 2, and 3, three to five gauges (including a local gauge when present) must be located < 400 km away and have > 10 years record. The summary percentages of sites meeting these criteria are shown in the highlighted cells in the table.

Category	H < 1	1 ≤ H < 2	H ≥ 2	No 3-5 gauges	ALL
Category 1	40.9	4.9	2.1	4.7	52.6
Category 2	17.2	1.6	0.8	0.5	20.1
Category 3	13.0	1.0	1.7	5.1	20.9
Category 4	NA	NA	NA	6.0	6.5
SUM	71.1%	7.6%	4.6%	16.3%	100%

The estimation of H was used in an iterative fashion for selection of the final number of gauges ultimately included within a site's region (Figure 3.20). If H was less than 1, then the sites were considered "acceptably homogeneous" and an RFA could be performed. If H was less than or equal to 1 and less than 2, the sites were considered "possibly heterogeneous." We performed an RFA for these groups. If H was greater than or equal to 2, then the group of sites was "definitely heterogeneous" and RFA results would have been invalid.

Figure 3.20 illustrates the iterative process used to determine the inclusion of tide gauges in RFAs, based on H values. In the analysis we grouped the number of tide gauges (three, four, or five) for each site based on the H measure. If a local representative gauge was present (Category 1 in Table 3.9), it was included as one of the gauges considered in the RFA. If H was less than 1 for five gauges, all five gauges were used in the RFA. If H was greater than 1 for five gauges and H was less than 1 for either four or three gauges, the gauges that had H less than 1 were used. If both three and four gauges had H less than 1, we used four gauges. If all three groups had an H value greater than or equal to 1 and less than 2, we used five gauges. If H was greater than 2 for five gauges and H was greater than or equal to 1 and less than 2 for either four or three gauges, we used the number of gauges that had an H value greater than or equal to 1 and less than 2. If both three and four gauges have an H value greater than or equal to 1 and less than 2, we used four gauges. If all three groupings have an H value greater than or equal to 2, we kept all five gauges, but disregarded the results. Table 3.9 shows the percentage breakdown between various categories. A summary of Categories 1, 2, and 3 for H values less than 1 and H value greater than or equal to 1 and less than 2 indicates that an RFA analysis yielded useful results for estimating EWL at 78.7% of the 1,774 sites considered (see colored cells in Table 3.9). An additional 6.8 % of the sites can use a single gauge analysis to estimate EWLs in the absence of an RFA analysis.

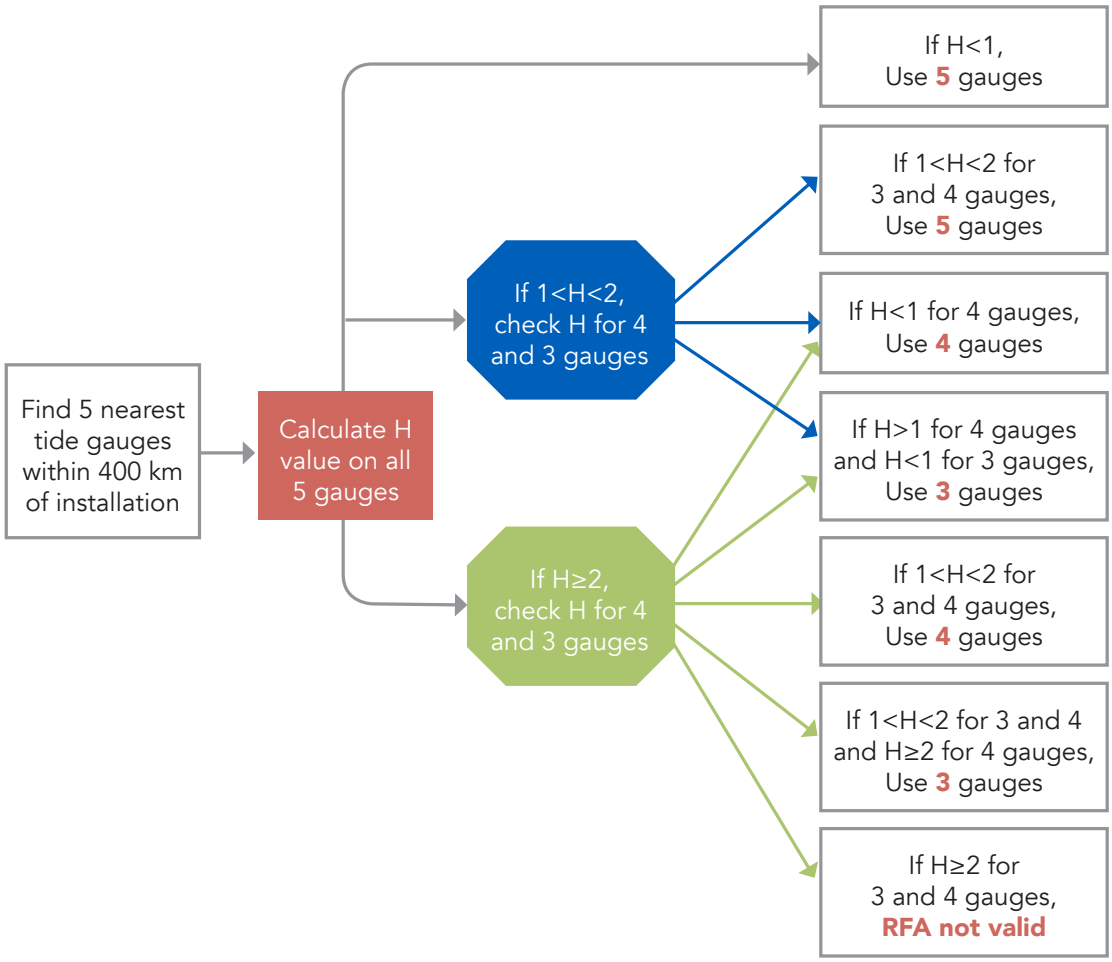

Figure 3.20 Iterative Process of H Estimation to Determine Inclusion of Gauges for a Site's Regional Frequency Analysis

3.5.5 Generalized extreme value (GEV) analysis

Once the number of tide gauges was established for each site region, the "index event" for each gauge was calculated as the mean of the annual maximum NTR values. The index event quantifies localized differences in response within the homogeneous region, for example, related to consistent location-specific storm surge responses due to differing topo-bathymetric characteristics. Each NTR time series was normalized (divided) by its index event so that all gauges were standardized and could be combined into one time series. We fit this new regional time series with the family of GEV distributions defined by Coles (2001):

$$G(z) = exp\left\{-\left[1 + \zeta\left(\frac{z - \mu}{\sigma}\right)\right]^{-1/\zeta}\right\} \quad [3–7]$$

in which $\{z: 1 + \zeta (z - \mu) / \sigma > 0\}$, $-\infty < \mu, \zeta < \infty$, and $\sigma > 0$. The parameters μ, σ, and ζ are the location, scale, and shape parameters, respectively, of the GEV family and were estimated using the L-moment method on the NTR time series (Hosking and Wallis 1997). (See the text box on the following page for more details on GEV parameters.)

The GEV *location* parameter represents the median magnitude of the annual maximum NTR, the *scale* parameter represents the spread in extreme NTR values, and the *shape* parameter represents the skew of the distribution from the occurrence (or lack of occurrence) of the very rare events. The return levels and associated 90% spread (5–95%) in confidence intervals are estimated using a Bayesian Markov Chain Monte Carlo (MCMC) algorithm composed of 5000 iterations and three chains of the MCMC algorithm (http://127.0.0.1:19757/library/nsRFA/html/BayesianMCMC, accessed June 2015).

For Category 1 and 2 sites, the regional return levels and uncertainties were scaled (multiplied) by the local index event of the closest tide gauge. For Category 3 sites, the mean of all index events was used to scale the regional return levels and their uncertainties. If at least three tide gauges did not occur within a 400-km radius of a site, then the RFA method was invalid and a single-gauge GEV analysis was applied if a tide gauge with greater than 30 years record was located within a 50-km radius of the site. Note that although a stationary analysis is applied, secular changes in local MSL were accounted for through the detrending and de-meaning process, which results in contemporary probabilistic estimates.

In addition to performing an RFA-based GEV analysis for the DoD sites, we also performed RFA analyses using each individual tide gauge as a "site" following the "regional definition" procedures (above) for method characterization purposes. Thus, in this circumstance, the local "index event" was the average of annual maximum NTR at the particular tide gauge. In all cases (unless otherwise noted), EWLs were presented with respect to mean higher high water (MHHW) tidal datum, which are shown in Section 4 to provide robust estimates when compared to other studies based on direct methods and synthetic storm modeling. Note that tsunami events were not removed if present within the hourly water level records; their occurrence is an important consideration in assessing a location's risk to extreme impacts.

We note that the RFA assumes independence between events within the regional data set. In our usage, spatial filtering of the annual highest NTR, if employed, might identify and remove all but the highest NTR value at the regional set of tide gauges affected by the same discrete event (e.g., specific wind storm). Such a spatial filter would reduce the regional sample size and likely inflate (broaden) the confidence interval estimates of the fitted GEV distribution. Difficulties in spatial filtering arise in properly determining the extent and any propagation of a physical process generating the extreme and its impact footprint (Weiss et al 2014). Temporal filters could be applied (e.g., Bernardara et al. 2011) to categorically filter out all but the maximum water level at the regional set of tide gauges over a certain period (e.g., 5-day filter). But such a systematic rejection of data would not distinguish any rapid succession or clustering of storms, which is known to occur (Mailier et al. 2006). Due to these considerations, the fact that there are 1700+ sites and corresponding "regions" and that each region has only a limited number of tide gauges (3-5 gauges) with varying record length (greater than 10 years minimum), we have chosen to include all regional data as some studies have done (e.g., Bardet et al. 2011). In Section 5, we provide a case study to assess effects of inter-site dependence.

Generalized Extreme Value

The generalized extreme value (GEV) distribution is a family of continuous probability distributions that combine the:

- *Gumbel (shape parameter = 0),*
- *Fréchet (shape parameter > 0), and*
- *Weibull (shape parameter < 0) families.*

These three distributions also are known as type I, II, and III extreme value distributions. Shown here for nontidal residual (NTR) annual maxima values at Norfolk and San Diego (top figure), the GEV distributions are a parametric fit (bottom figure) in which:

- *generally the location parameter represents the median magnitude of the annual maximum NTR,*
- *the scale parameter represents the spread in extreme NTR values, and*
- *the shape parameter represents the skew of the distribution from the occurrence (or lack of occurrence) of rare events.*

Note that these GEV fits are not based on regional frequency analysis; they are for single tide gauge locations (not installation sites). Compared to San Diego, Norfolk has a higher average storm surge value (based on the location parameter) and experiences higher storm activity (based on the scale parameter). Norfolk also is prone to impacts from the rare tropical storm, whereas San Diego does not (positive shape parameter value at Norfolk).

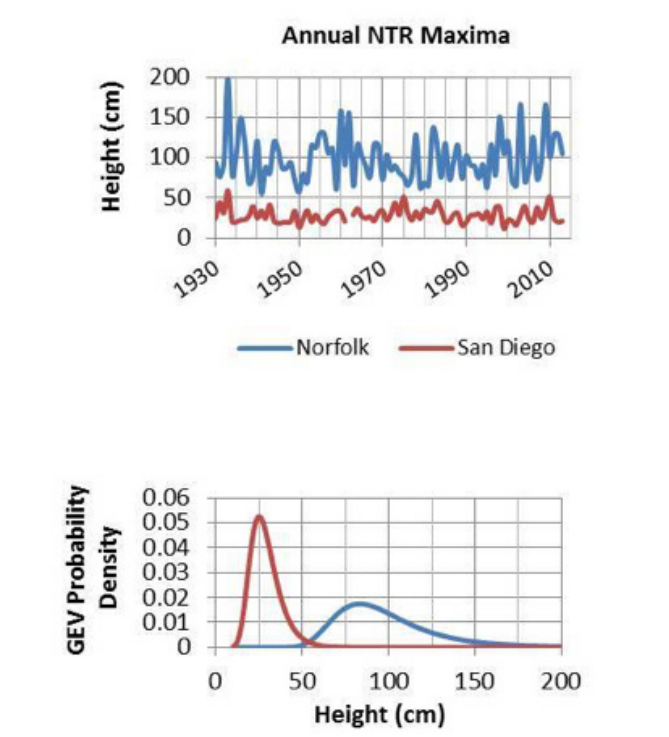

	Location (cm)	Scale (cm)	Shape
Norfolk	85	21	0.07
San Diego	25	7	-0.02

3.5.6 Single gauge

In several locations (21.3%), the RFA process could not be used to provide an EWL estimate at a particular site; however, 6.8% of these (i.e., Category 1 sites with H values greater than 2 or without three to five tide gauges within 400 km as shown in Table 3.9 above) could use results from a single-gauge analysis using a gauge within 50 km and with greater than 30 years of hourly data. In this case the annual maxima NTR component of the water levels is fitted with a GEV distribution, though without any scaling by an index event. The return levels and associated 90% spread (5–95%) in confidence intervals were estimated using the same methods as outlined above.

3.6 Considerations Not Included in This Study

Many factors affect the local expression of increases in global mean sea level and the associated changes in extreme water levels. This report, given its global and screening-level assessment focus, has attempted to develop a methodological approach that can be consistently applied but also is innovative in its ability to address an underappreciated aspect of the scenario development and application challenge: how to deal with data availability, representativeness, and quality issues. As such, a number of the advances in scenario development offered here—for example, choice and application of vertical land movement data sources and regional frequency analysis of tide gauge information—are in large measure a response to these data issues.

Still, Section 1.4 identified a number of limitations to the approaches taken in this report, and this section will expand on these to provide additional context related to their significance and in some instances offer potential paths forward to address the limitations. The first factor affects the local expression of global sea-level change; additional factors affect the estimates of EWL values.

3.6.1 Factors potentially affecting local sea-level change

Water levels in a semi-enclosed sea (bay or estuary) respond to changes in offshore sea levels based on the magnitude and frequency of the offshore forcing, depth and shoreline configuration of the bay or estuary, and the degree of bottom friction. In particular, bay or estuary response is dependent on the degree of match between the natural resonance frequency of the semi-enclosed water body and the forcing frequency at the offshore boundary, and for shallow systems, the frictional strength (Zhong et al. 2008). As sea levels rise, this may affect the resonance characteristics of a particular bay or estuary. It follows that this change in resonance may also change the tidal datum and geodetic datum relationships.

As sea levels rise, this may affect the resonance characteristics of a particular bay or estuary. It follows that this change in resonance may also change the tidal datum and geodetic datum relationships.

Water level variations and tidal characteristics of inland bays may also change as the result of geomorphological changes in tidal inlets and in creation of new inlets from coastal storms. In addition, large channel-deepening projects and dredging of some tidal streams may affect tidal characteristics. Finally, harbor seiche induced by

wave forcing also may be exacerbated under higher sea levels if seiche resonance amplitudes become enhanced. This is similar to the semi-enclosed sea issue but different in the type of tidal constituent that is being affected.

Mawdsley et al. (2015) recommend that changes in tidal levels (high water, low water, and tidal ranges) should be considered when predicting impacts of sea-level rise. They note, however, that the trends in tidal levels are not necessarily correlated to the trends in mean sea level and present a complicated picture in which the mechanisms and timescales are not well understood.

3.6.2 Factors potentially affecting extreme water levels

Wave Set-up and Swash

Total water levels include the effects of wave set-up and swash (in combination referred to as wave run-up), whereas *still* water levels do not. The extreme water level estimates provided in the scenarios database are extreme still water estimates. This is primarily the result of using data from tide gauges whose engineered design, generally sheltered locations, and long period-sampling rate usually do not provide such information because their primary purpose is harbor navigation. A recent study by Sweet et al. (2015), however, using high-frequency water level samples collected at NOAA tide gauges since the 1990s has shown that tide gauges still experience a high degree of water level variability whose amplitude is correlated with offshore deep-water wave heights but is generally substantially attenuated at the gauge itself. In regions where storm surge is generally low and wave heights and impacts are high (e.g., the West Coast and island regions), Sweet et al. (2015) show that high-frequency water level variability can be as large or larger than the NTR storm surge component measured at the gauge during events, typically a handful of times each year.

Wave set-up and swash up a sloping beach can be highly significant components of total water level contributions, especially in regions with a large wave environment and with narrow continental shelves with steep drop-offs in near-shore bathymetry (e.g., the Pacific Islands). Under these conditions, wave heights during storms can be much higher than the surge itself and their effects are the more damaging factor overall. Figure 3.21 (H. Moritz, personal communication 2015) shows the contributions of various components to total water level at different geographic locations to illustrate the relative effects of these components. Sites that experience significant wave heights would be well served to include quantitative estimates of such heights when available and qualitative when not, as part of their application of the combined sea-level change and extreme water level scenarios. See Section 5.1.2 for additional information on adding wave influences to extreme water levels.

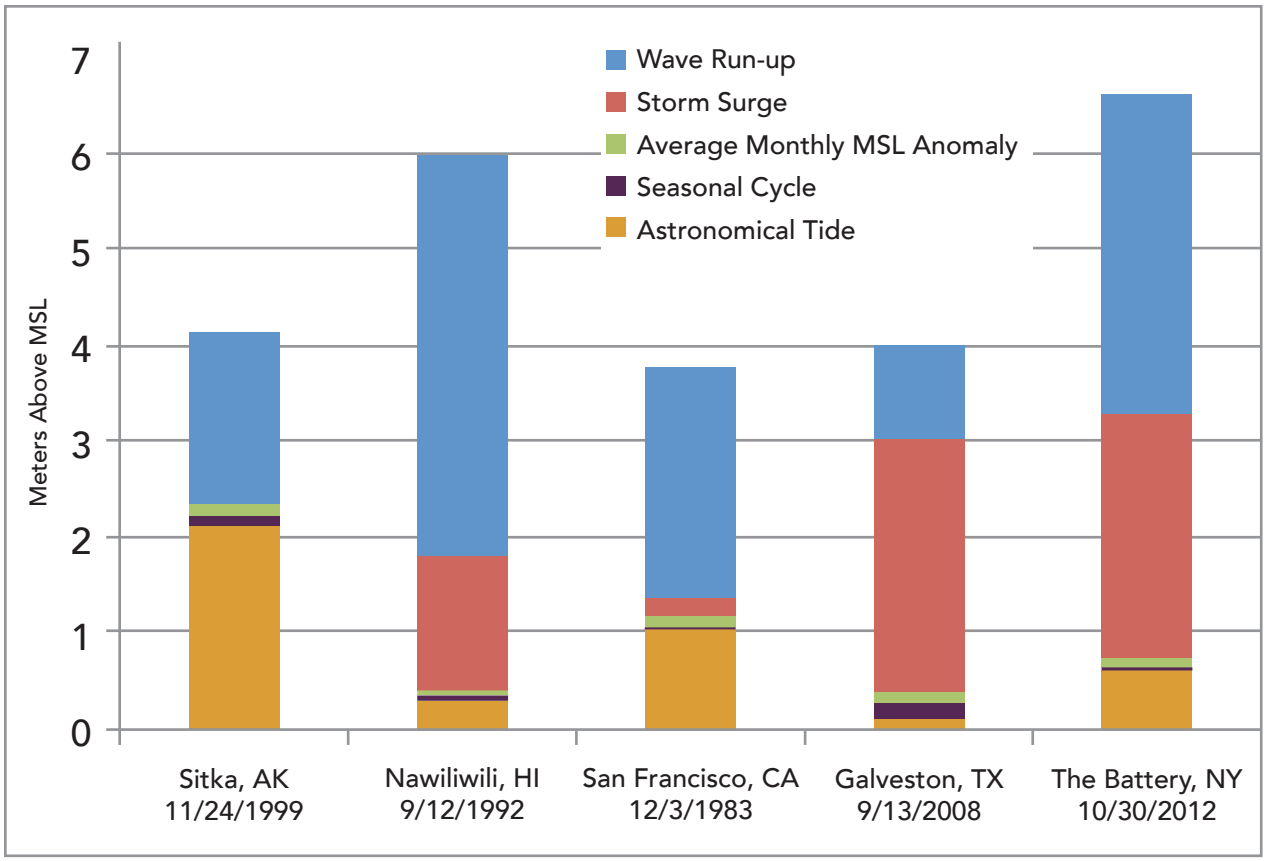

Figure 3.21 Total Water Levels for Selected Extreme Events
A representative event is shown for a location on each of five coastlines in the United States: Alaska, Hawaii, West Coast, Gulf Coast, and East Coast. The components of the total water level for each event are plotted in terms of absolute magnitude demonstrating the relative importance of different processes in different locations. Each event is in the top 10 most extreme water levels at its location in terms of water level above mean higher high water. (from H. Moritz, personal communication 2015)

Storm Surge Interaction with a Changing Bathymetry

Storm surge behavior during a storm event is in part dependent on the bathymetry and obstacles such as marshes in the near-shore environment that will determine how much frictional resistance the surge will encounter. In shallow bathymetry environments the increased depth of water will result in less frictional resistance and a potential concordant nonlinear increase in the total resultant surge heights. The assumption used in this report was that storm surge would behave in a linear fashion with increases in sea level. Depending on shoreline configuration and local bathymetry, this could be a non-conservative assumption. Surge responses under rising seas can be quite complex and quite localized in magnitude (e.g., see Arns et al. 2014). Detailed hydrodynamic modeling with intense quantification of local bathymetry would be necessary to develop quantitative estimates of the potential nonlinear relationship between sea-level rise and storm surge. "Rules of thumb"

that assess general shoreline configuration and bathymetry characteristics to generate at least qualitative estimates of the nonlinear response may be possible but are beyond the scope of this report.

Future Non-Stationarity of Extreme Events

The extreme water level statistics generated by this report's approach and provided in the scenario database assumed the stationarity of historic storm statistics. This affects the estimates of the different exceedance probabilities if future climate change results in either more frequent storm events from storm track changes (i.e., increases in the GEV "scale" parameter) or increases in the intensity of a given storm impacting an RFA-based region (i.e., increases in the GEV "shape" parameter). Given that the science is still emerging on how storm properties may change in the future, especially on a regional basis, we have concluded that for now assuming stationarity is a reasonable assumption. Moreover, the methodology chosen in this report to calculate EWL statistics is based on analyses of historic tide gauge records that implicitly assume stationarity. The use of historic tide gauge records in this manner is a pragmatic limitation that enables us to calculate EWL statistics for most of the 1,774 sites. See Section 3.5.2 for additional details.

Related to the above, but somewhat different as they relate to the effects on lessor extremes, are changes in climate modes, such as the El Niño Southern Oscillation and Pacific Decadal Oscillation, that operate on interannual and decadal timeframes, respectively. Although their effects over long timeframes, such as the 50- and 85-year time periods considered in this report, will likely average out relative to a particular scenario, over more moderate timeframes (e.g., 20 years) their oscillations and how they may change (or are changing) under climate change may be important to consider in terms of associated impacts. For example, in the western Pacific, sea levels over the last couple of decades are rising at rates of about 1 cm/year (Merrifield et al. 2012), which is five to ten times greater than the long-term (1950-2000) average rate estimated by Church et al. (2004). On shorter time scales, effects from phases of ENSO can significantly compound "nuisance" tidal flood frequencies (Sweet and Park 2014) and higher magnitude event probabilities (Menéndez and Woodworth 2010) on an interannual basis. As a result, the effects of climate modes may be important to factor into scenarios that are used over short to moderate time horizons. See Section 5.3.5 for a further discussion of the preceding and how scenario users may consider the preceding.

Riverine Flooding

Storms often are associated not just with ocean-derived surge but also inland precipitation that may contribute to swollen rivers and overland storm-water flow that interact with surge to exacerbate the water levels that are ultimately experienced. This report did not attempt to address these situations. Site-specific analyses would be needed to assess and develop scenarios that address the combined effects of changes in sea levels, surge, and riverine flooding occurring concurrently. Sites that may be subject to these conditions may consider adding an additional safety factor to their scenarios.

3.6.3 Other factors affecting water levels and vulnerabilities outside the scope of this report

Some additional factors that affect water levels are not tied to climate change. The most obvious example is a tsunami. Exposure zones for tsunamis are fairly well defined and sites so exposed must factor tsunamis into their coastal risk management planning. Certainly, the impacts of tsunamis of a certain magnitude will be exacerbated in the future under higher initial sea levels. A meteotsunami, or meteorological tsunami, is a tsunami-like wave of meteorological origin (atmosphere and air pressure related) that could be of concern locally.

Shorelines are dynamic environments, both in terms of physical and biological response. Barrier islands will respond to rising seas and storm events based on their geometry, underlying geology, and sand sources. Absent human interference, they may simply change their position landward. Similarly, marshes, depending on the rate of sea-level rise, will accrete sediments and potentially stay ahead of sea-level rise or if unable to accrete sediment fast enough simply drown. Rising seas and surge generally will result in erosional forces that, dependent on the sediment and geology exposed, will alter shoreline conditions in spatially and temporally variable ways. These natural responses also occur within a human-built environment that adds protective features, such as dikes and levees, or artificially alters sediment source conditions. To truly understand future flood risks, especially in a quantitative manner, the scenarios developed in this report and provided in the scenarios database must be combined with other sources of information that may affect ultimate inundation and flood levels.

Finally, the scenarios developed herein can be used directly, subject to the caveats above, to assess vulnerabilities and impacts to natural and built features that occur on the surface. Although additional modeling can be done for a site, the scenarios, when mapped, do not directly address such issues as saltwater intrusion that involves interactions with the sub-surface.

Section 4.0
Results and Application

This section details results of applied research and analysis efforts conducted as described in Section 3.0 Approach. When evident, we identify key regional, temporal, or scenario-based patterns in the results. After a brief overview section (Section 4.1), in which the results of an initial coarse screening against a threshold elevation are presented, results are described in terms of adjustments to global mean sea level for the 1,774 military sites included in this report. These include vertical land movement (VLM) in Section 4.2, dynamical sea level (DSL) in Section 4.3.1, and ice melt from glaciers, ice caps, Greenland, and Antarctica in Section 4.3.2. Results for extreme water levels (EWL) that take tidal influences and storm surge into account are provided in Section 4.4. Many of the results are provided here as illustrative maps. We show, however, spatially related information only for that subset of sites for which spatial information already is in the public domain via the Military Installations, Ranges, and Training Areas (MIRTA) database (https://catalog.data.gov/dataset/military-installations-ranges-and-training-areas).

The scenario database accompanying this report provides specific numerical scenario values on a site-specific basis for all sites considered. This section also includes a discussion of several considerations to take into account when selecting and using scenarios (Section 4.5) and concludes with a discussion of uncertainty characterization (Section 4.6). As the reader considers these results, it is important to keep in mind that the primary purpose of the scenario values developed and illustrated herein is to support *screening level* vulnerability and impact assessments for Department of Defense (DoD) sites worldwide.

4.1 Overview of Results

The interplay of physical setting, local climatology—regardless of whether non-stationarity is considered—time horizon, and data availability and quality affect the degree to which regional and local factors alter future global mean and extreme sea-level patterns and the ability to depict them at particular sites. Importantly, the three adjustments to global mean sea level considered herein are not necessarily spatially concordant in their effect. For example, VLM operates independently of direct climate effects, the fingerprint pattern that results from ice melt depends on the location of the melting ice, and the degree of storm surge depends on both coastal bathymetry and configuration and whether a site experiences tropical storms of some type. These differential responses to forcing factors generally mean that sites experience a complex set of interactions in which some factors are more important than others. This is vital for site managers trying to

determine their sites' exposure to future sea-level change (SLC) and extreme water levels. In addition, the time horizon considered affects whether a particular factor is important and the degree to which it needs to be taken into account. In the sections that follow, we use a mix of global sea-level rise (SLR) scenarios and time horizon examples to illustrate how these different assumptions affect the contributions of the individual components to regional differences. Text boxes and other devices are used to highlight regional differences and to provide additional explanatory material.

The individual sections provide information on the ranges of values that each component may contribute to the SLC or EWL scenario adjustments. Here, we briefly summarize the relative contributions for the various global scenarios and time horizons across all DoD sites evaluated (Table 4.1). Appendix C provides a breakdown by timeframe, scenario, and regional adjustment component to better visualize contributions to the minimum and maximum values. Note that the EWL annual chance event probability values are independent of scenario and time horizon; for purposes of this effort we considered their contributions stationary given our reliance on the use of tide gauge information to calculate EWL statistics. To the degree that climate non-stationarity will alter these statistics, this represents another type of uncertainty that end-users should acknowledge (see Section 4.6).

Table 4.1 Summary of Min-Max Values for Regional Adjustments to Global Sea-Level Change and Extreme Water Level Values for 1,774 DoD Sites Worldwide

Values depicted reflect the full range of site-specific median values for sea-level change adjustments and mean (or expected values) for annual chance events across all 1,774 sites.

<table>
<tr><th rowspan="2">Global Scenario</th><th colspan="3">Range of Sea-Level Change Adjustments by Scenario and Time Horizon (meters)</th><th colspan="4">Range of Annual Chance Event Values (ACE) (meters)</th></tr>
<tr><th>2035</th><th>2065</th><th>2100</th><th>20% ACE</th><th>5% ACE</th><th>2% ACE</th><th>1% ACE</th></tr>
<tr><td>0.2 meters</td><td rowspan="5">-0.9 to 0.5</td><td rowspan="4">-1.6 to 0.8</td><td rowspan="3">-2.3 to 1.2</td><td rowspan="5">0.2 to 3.0</td><td rowspan="5">0.3 to 3.6</td><td rowspan="5">0.3 to 4.0</td><td rowspan="5">0.3 to 4.3</td></tr>
<tr><td>0.5 meters</td></tr>
<tr><td>1.0 meters</td></tr>
<tr><td>1.5 meters</td><td>-2.3 to 1.3</td></tr>
<tr><td>2.0 meters</td><td>-1.6 to 0.9</td><td>-2.2 to 1.5</td></tr>
</table>

Regional SLR adjustments vary significantly depending on timeframe, scenario, and geographical location. High-level patterns emerge in response to each set of conditions. Each of the three component factors driving regional SLR adjustments can play the dominant role in shaping observed trends, depending on the respective set of conditions chosen. Taking all sites into consideration, the worldwide average adjustment ranges between 0.0 meters and 0.4 meters depending on scenario and timeframe, but the full set of individual site-specific adjustments spans almost ten times this range. This result indicates the site-specific nature of adjustments to the global SLR scenarios. Vertical land movement, DSL, and ice melt each influence this large variability in site-specific SLR adjustments.

4.1.1 Findings related to vertical land movement

Given the scenario independence and assumed linearity of VLM rates, geographical location plays the critical role in a broad assessment of relative SLR contributions from VLM compared with other components of regionalized adjustments. In some regions the VLM rate can exceed that of regional SLR from the combination of dynamical sea level and ice melt effects by an order of magnitude in either direction. For example, subsidence in Texas and Louisiana can cause over 80% of projected SLR for the region, inclusive of all timeframes and scenarios. In contrast, VLM uplift in southeastern Alaska dwarfs projected sea-level increases from dynamical and ice melt effects by a factor of twenty, resulting in regional sea level decreasing under all timeframes and scenarios. The influence of VLM linearity and scenario independence is especially apparent in the earliest future timeframe of 2035 in which, regardless of chosen scenario, only VLM adjustments exceed +/- 0.1 meters for any DoD site and they constitute the total range of adjustments for the 2035 period.

4.1.2 Findings related to dynamical sea level

Dynamical sea level and ice melt effects create more pronounced changes in sea level during the later time horizons (2065 and 2100 in Table 4.1), though VLM is still a significant contribution. Of note, DSL and ice melt do not ever contribute large co-directional adjustments to regional SLR in the same region: in terms of magnitude they do not generate large net compounding effects. Regardless of scenario and timeframe, no DoD site has component regional SLR contributions of DSL and ice melt that are both greater than 0.1 meters, nor are these contributions both less than -0.1 meters at any DoD site.

Pattern scaling indicates that sea-level change in response to DSL adjustments generally tends to *increase sea level in the northern hemisphere* and *decrease sea level in the southern hemisphere* (see Figure 3.5). Given that worldwide DoD sites are concentrated more heavily in the northern hemisphere, DSL adjustments tend to increase regional sea level rather than decrease regional sea level at military sites. Inclusive of all timeframes and emission scenarios, none will experience a negative DSL adjustment larger than -0.1 meters, and fewer than ten DoD sites worldwide are projected to experience a -0.1 meter

Pattern scaling indicates that sea-level change in response to DSL adjustments generally tends to increase sea level in the northern hemisphere and decrease sea level in the southern hemisphere.

DSL adjustment. Positive DSL adjustments resulting in greater regional SLR also remain muted to 0.1 meters or less for all DoD sites under the two lower scenarios regardless of timeframe and all scenarios for 2035. Under the 1.0-meter and higher scenarios, however, some DoD sites will experience projected adjustments of 0.2 to 0.5 meters in 2065 and 2100, with the majority located in the northeastern United States.

4.1.3 Findings related to ice melt

Analysis of ice melt contributions presents an additional layer of complexity due to the interplay of three separate factors: fresh water melting from Greenland, from Antarctica, and from glaciers and ice caps. In general, sites that will experience the greatest positive SLR adjustments from ice melt are located in the Pacific Ocean, and large negative adjustments occur in Europe and Greenland. Ice melt plays no role in DoD-wide adjustments under the two lower scenarios (0.2 meter and 0.5 meter) and no more than 0.1 meters of adjustment under the 1.0-meter scenario. Ice melt effects do play a large role in producing much of the additional global SLR beyond 1.0 meters in the high (1.5-meter) and highest (2.0-meter) scenarios; as a result, respective regional SLR adjustments are more pronounced for these scenarios. In addition, the more prominent influence of near-field effects (i.e., sea levels *fall* near the area of melting ice) further amplifies late century impacts for DoD sites in close proximity to one of the three contributing sources of ice melt. For example, under the two highest scenarios, sites nearest Greenland experience a further decrease in regional sea level of at least a full meter between 2065 and 2100.

…the more prominent influence of near-field effects (i.e., sea levels fall near the area of melting ice) further amplifies late century impacts for DoD sites in close proximity to one of the three contributing sources of ice melt. For example, under the two highest scenarios, sites nearest Greenland experience a further decrease in regional sea level of at least a full meter between 2065 and 2100.

4.1.4 Findings related to extreme water levels

Table 4.1 also shows the range of EWL values relative to mean higher high water (MHHW) for the different annual chance event probabilities considered in this study. Of note, across all four annual chance event probabilities, the maximum median EWL values exceed the maximum values for the SLR regional adjustments by at least a factor of two. The minimum EWL values do not differ significantly across event probabilities, however, the maximum values do increase significantly as the probability of an event decreases.

4.1.5 Issues related to data availability and quality

Given its global nature, this study was faced with a number of data availability and quality issues in determining scenario adjustment values. Any study of similar magnitude will be similarly challenged. We hope we have identified important issues and in some cases their resolution, as well as offered some innovative approaches to resolving data gap issues and improving confidence in the results (see Section 5.2 for specific examples). Of note was the use of various data sources

for estimating local VLM rates and the application of Regional Frequency Analysis (RFA) techniques to determine extreme values statistics, especially in situations for which local representative tide gauges of sufficient record length are lacking. By applying RFA we increased the percentage of sites for which EWL statistics could be provided from 53% to almost 86%. The remaining 14% or so of sites draw attention to the value of having basic information, such as a local representative tide gauge, and where lacking such information makes estimation of exposure to future SLR and EWLs difficult. Even the lack of a local geodetic datum is problematic when determining exposure to future scenarios. From a DoD perspective, this lack of datum information—in some cases combined with relatively poor topographic (and perhaps bathymetric as well) information—increases the uncertainty associated with assessing future vulnerabilities, in particular for those sites located outside the continental United States that have less complete datum information.

The limitations of currently available data sources and the manner in which the global models are used to provide information affected the manner in which scenario information could be provided spatially and temporally. The dynamic sea level and ice melt adjustments were gridded products at a resolution of 1 degree. Because they were dependent on process models operating at the global scale that produced data for discrete time slices and not in a temporally continuous manner, we were restricted to providing their contributions for specific time horizons. Although spatially coarse, the preceding data products had the advantage of providing a value for any site across the globe. Vertical land movement data differed in quality based on data source; the more accurate local data (i.e., tide gauge or global positioning system) were subject to measurement proximity (extrapolation) and length of record issues. To translate this type of information to a gridded product across an entire coastline in a continuous manner presents unique challenges based on the currently available datasets and techniques.

Finally, because we used a 20-kilometer (km) buffer to identify candidate sites potentially deserving of vulnerability or impact assessment to SLR and EWLs, we recognized that a potentially significant number of sites within that buffer might occur entirely at elevations that would not be exposed under any conceivable future scenario. Because our purpose here was not to conduct actual vulnerability or impact assessments, we conducted only an extremely coarse screen to rule out from further consideration these sites (note these sites and their associated information are still retained in the scenario database but are "flagged" accordingly). To accomplish this screen, we used "global" assumptions to construct a threshold elevation value against which to screen sites: that is, values that were maximum in a global sense and not site specific. Table 4.2 provides the components, their assigned values (rounded to the nearest 0.1 meter), and their sources contributing to the threshold value. To calculate a wave component we followed Federal Emergency Management Agency standards (FEMA 2013) and defined the wave run-up elevation as the value exceeded by 2% of the run-up events (or $R_{2\%}$). To determine a global, conservative value for $R_{2\%}$ we assessed a sample of the literature to estimate a value for run-up in high wave environments that we concluded would not be exceeded.

Table 4.2 Components, Values, and Sources Used to Establish a Threshold Elevation for Purposes of a Coarse Vulnerability Screen

Component	Value (meters)	Source
SLR Scenario	2.0	Highest scenario considered herein at 2100
Regional Adjustment	1.5	Maximum total median adjustment value from the scenario database
Mean Higher High Water	3.3	Global maximum MHHW value from the scenario database
1% Annual Chance Event (nontidal residual or storm surge)	4.3	Global maximum EWL value for the 1% annual chance event from the scenario database
Run-up ($R_{2\%}$)	< 15	Conservative estimate from a survey of the literature of potential run-up values in high wave environments
Topographic Error	4.8	1.96 times a root mean square error of 1.55 meters for the National Elevation Dataset (95% confidence value)
Total (threshold value)	**30**	**Rounded sum of contributing components**

The screen was applied against sites for which geospatial information in the form of polygons was available and for which we determined a minimum elevation value using 1/3 arc-second (about 10 meters) National Elevation Dataset (NED) digital elevation model information. Sites lacking polygon information or for which NED information was not available were not evaluated. For the sites identified only by point information (i.e., no polygons), we lacked confidence in the spatial footprint of these sites and the representativeness of the centroid elevation for assessing vulnerability. Table 4.3 provides the results of the coarse screen using the threshold value obtained from Table 4.2. Of the 1,077 (of 1,774) sites having polygon information, 839 of these had associated NED information that enabled screening against a threshold value. Of these 839 sites, 158 can be safely eliminated from the need for further vulnerability or impact assessment (Table 4.3). These sites are flagged accordingly in the accompanying scenario database. To provide some sense of how the choice of threshold value affects the number of sites eliminated (i.e., above the threshold value), a five-meter adjustment above and below the 30-meter threshold value resulted in a range of 135 to 181 sites being eliminated. In other words, the number of sites eliminated is not sensitive to the threshold value at this order of magnitude.

Table 4.3 Results of Coarse Elevation Threshold Screen for DoD Sites Having Associated Polygon Information, Including an Estimate of Minimum Elevation

Polygon Information Available?		NED Information Available (for sites with polygons)?		Above/Below Threshold (for sites with NED data)	
Yes (# sites)	No (# sites)	Yes (# sites)	No (# sites)	Above (# sites)	Below (# sites)
1,077	697	839	238	**158**	**681**

4.2 Vertical Land Movement

Vertical Land Movement is defined here as the rate of change in the elevation of the earth's surface at a specific site. Movement can be negative (land subsidence) or positive (land uplift) and was estimated at each site using the closest and most accurate measurement source available. Vertical land movement can be a significant contributor to the total adjustment for sea-level change over time and in some extreme instances can be the largest contributor.

Vertical land subsidence will be an exacerbating factor to the negative impacts of global SLR; as a result, locations with vertical land subsidence may have a greater exposure to SLR. In the opposite sense, where VLM rates are positive, the land is moving up and out of the sea. Upward movement of the earth's crust will help mitigate impacts of global SLR.

On global scales, VLM is mainly due to global isostatic adjustment (GIA) and the large-scale response to the last ice age. GIA can be positive (large scale rebound) or negative (forebulge collapse). Regionally, positive and negative rates can be due to tectonic plate movement and post-earthquake deformation, for example. The highest negative rates of VLM are found in local areas of subsidence from subsurface fluid withdrawal and sediment compaction. The highest positive rates of VLM are found in localized areas of coastal glacier melt and subsequent land rebound.

Location Matters: Areas with Significant Vertical Land Movement

Vertical land movement can prompt significant adjustments for sea-level change over time and in some extreme instances can be the largest contributor.

Areas with the largest negative rates (subsidence):

- *Region around Houston, Texas (-3.0 to -10 millimeters (mm)/yr),*
- *Eastern North Slope of Alaska (greater than -6.0 mm/yr),*
- *Coastal Louisiana (approximately -6.0 mm/yr), and*
- *San Joaquin River delta area near Stockton, California (approximately -3.6 mm/yr).*

Areas with the largest positive rates (uplift):

- *Coastal areas of northern Gulf of Alaska, Cook Inlet, Prince William Sound, eastern Aleutian Peninsula (+3.0 to +5 mm/yr),and*
- *Southeast Alaska (+10 to +21 mm/yr).*

The impacts of sea-level rise will be exacerbated in areas with significant subsidence rates. Conversely, significant uplift will mitigate the impacts of sea-level rise.

Figure 4.1 is a histogram of the VLM rates for the entire set of 1,774 sites that were evaluated. The statistical distribution is largely contained within -3.5 to +2.0 millimeters (mm)/year, is biased slightly towards negative VLM rates, and has the longer distribution tail found on the positive VLM rate side.

Figure 4.2 is a histogram of the distances away from each site location at which the VLM rates were estimated. Approximately 95% of the sites had the VLM source within 60 km. In a few instances, the closest source was greater than 300 km away.

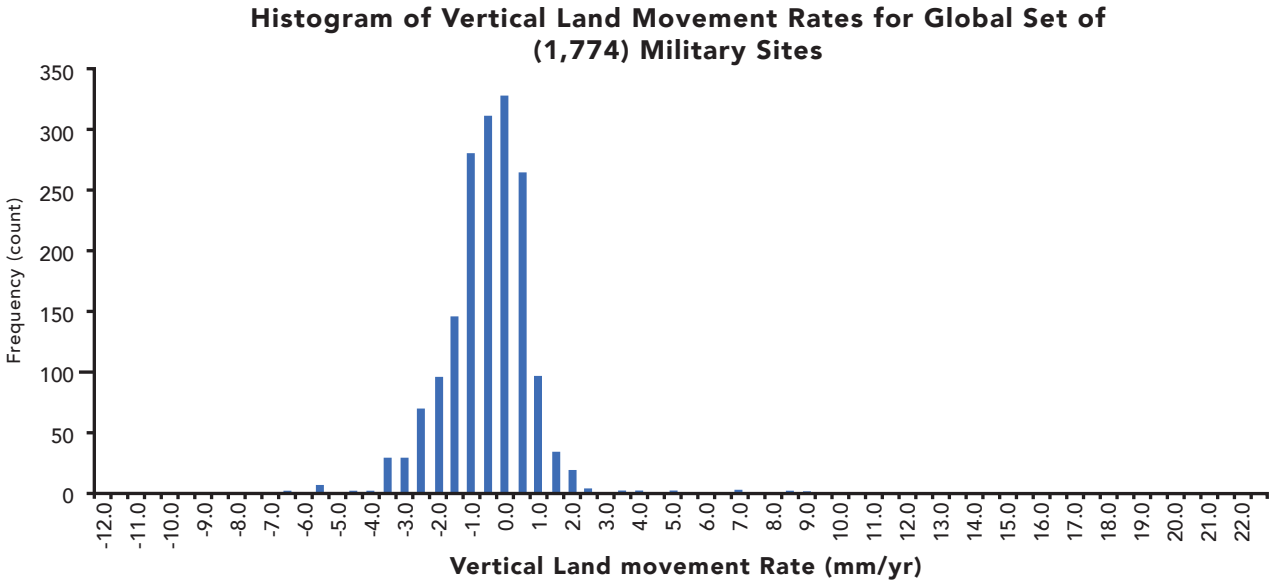

Figure 4.1 Histogram for Rates (in millimeters/year) of Vertical Land Movement (VLM) at 1,744 sites

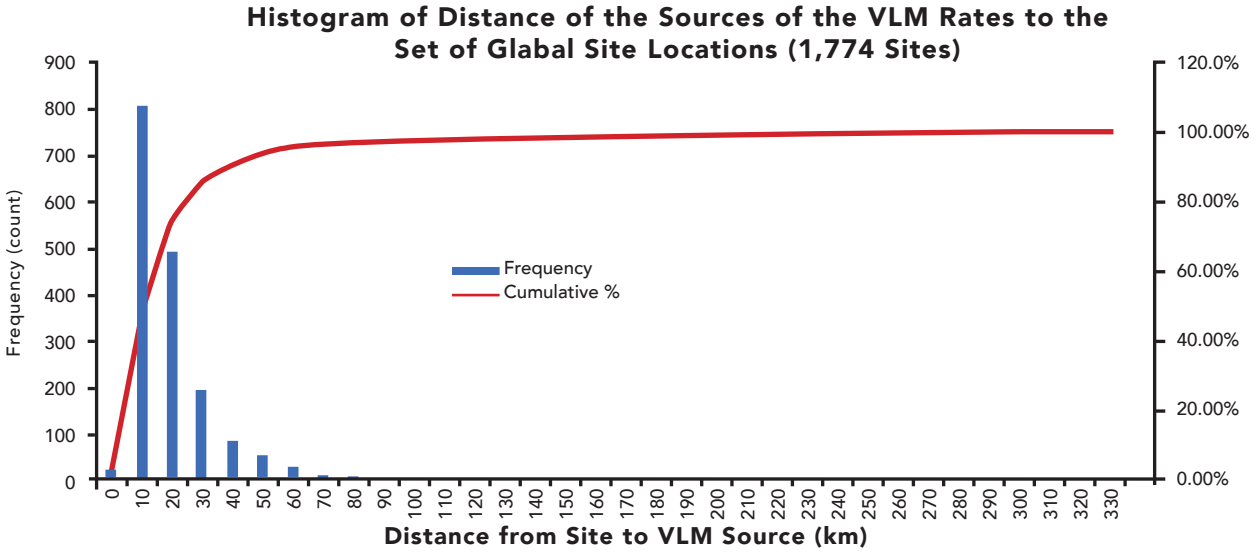

Figure 4.2 Histogram of Distances (in kilometers) from Each Site to the Location of the VLM Rate Source

The rate of VLM at each site location is estimated from either the closest tide gauge, the closest continuous GPS system, or from a GIA model. The VLM sources include estimates of uncertainty (95% confidence interval) in the rates. The accompanying database supporting the analysis in this report also provides the distance from the VLM source to the installation. VLM can be estimated indirectly from the long-term sea-level variations in the tide-gauge record; uncertainty in those derived VLM rates is dependent on tide-gauge series length. This is also the case for rates of VLM derived from continuous GPS systems.

Uncertainty in the application of these rates to a specific installation location also depends on the distance away; in general, uncertainty increases with increasing distance between the VLM source and the site of interest. No algorithm or statistical method is available to estimate this uncertainty component because of the nature of vertical land movement. In many cases, large geographic areas may have the same VLM rate, whereas in other areas, VLM rates can differ significantly over smaller distances. Variation in regional or local surficial geology may affect the representativeness of the VLM estimate at a specific site when using GPS or a tide gauge. VLM rates were determined by looking at all of the nearby VLM sources, their uncertainties, and their distances away. When sources were similar distances away from a particular site, the closest source with the lowest uncertainty bounds was used. Table 4.4 shows the number of times a particular type of VLM source was used for all sites. A GPS was used as the source the most number of times, followed by tide gauges, and then the GIA model. The GIA model was used primarily as the source for sites located in foreign countries.

Table 4.4 Distribution of the Number of Times a Particular Type of VLM Source Was Used

VLM Source	# of Sites Using Source Type	Site 3 km or Less Away	Site More Than 3 km Away
Glacial Isostatic Adjustment Model Direct (GIAD)	17	✓	
Glacial Isostatic Adjustment Extrapolated (GIAE)	69		✓
Continuous GPS System Direct (GPSD)	128	✓	
Continuous GPS System Extrapolated (GPSE)	919		✓
Tide Gauge Direct (TGD)	94	✓	
Tide Gauge Extrapolated (TGE)	546		✓

The Tide Gauge Direct (TGD) and Continuous Global Positioning System (CGPS) VLM sources are considered the most accurate because they are essentially co-located (less than 3 km). As discussed in section 3.4.2, the other considerations for use of the VLM estimates are:

- assumption of a constant VLM rate to 2100, and
- assumption that for the longer distances to the VLM source reported in Figure 4.2 above, the VLM rates are the same at the site as at the VLM source.

Each site must be looked at individually for these considerations before finalizing the total sea-level adjustment.

4.3 Regional Systemic Trends

Two types of regional climate change-related adjustments were considered. Section 4.3.1 provides the results for DSL and Section 4.3.2 provides the results for ice melt.

4.3.1 Dynamical sea level

Using the scaling factors as computed using information detailed in Section 3 (Table 3.6) and the global average temperature computed from the regression fits (Figure 3.7), the DSL adjustment for the nearest grid cell encompassing a site was estimated. Figure 4.3 shows the dynamical adjustments for each of the 1,774 DoD sites computed using the approach described in Section 3 for the 1.0-meter scenario in 2100.

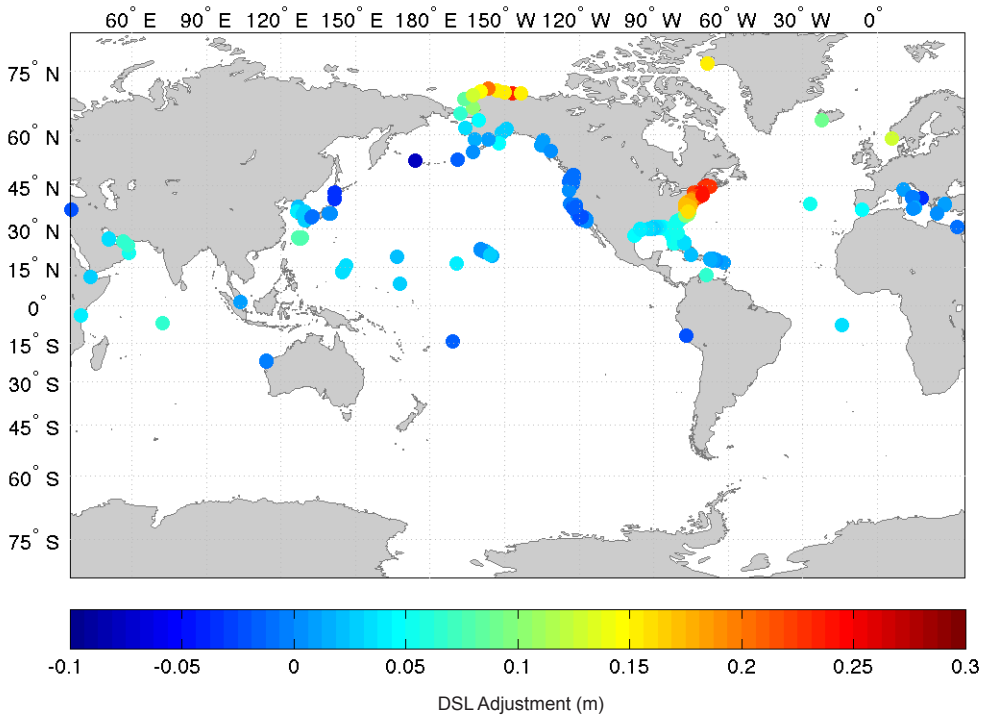

Figure 4.3 Dynamical Sea-Level Adjustment Corresponding to the 1.0-Meter Scenario for Year 2100

The dynamical sea-level effects for clusters of sites are consistent with the spatial signature shown in the pattern-scaling map (Figure 3.5). Two general regions stand out in terms of larger DSL effect. First, in the vicinity of sites along the northeastern United States, the DSL effect appears to be large, up to about 0.25 meters or more (for the 1.0-meter global scenario). As shown in Figure 4.4, the gradient actually increases from south to north in the magnitude of the DSL effect in this region. The DSL adjustments range from about 0.10 meters in the south to about 0.25 meters in the north (Figure 4.4). Numerous research papers have reported this region having a significant degree of ocean dynamics attributable to persistent changes in the Gulf Stream, North Atlantic Oscillation, and ENSO (Ezer 2013, 2015, Ezer and Atkinson 2014, Ezer et al. 2013, Kopp et al. 2015, Sweet and Zervas 2011).

A similar region is found north of Alaska, though the adjustments in general are somewhat lower, on the order of 0.1 to 0.2 meters. The DSL effect in the vicinity of most sites is on the order of 0.0 to 0.1 meters. In southeastern United States (off the coast of Florida) the magnitude of the DSL adjustment is about 0.1 meters. Recently, Park and Sweet (2015) attributed the acceleration of sea-level rise since about 2004 to the decline in the Florida Current, though it is not clear if it is a reflection of a persistent DSL effect projected in this current study.

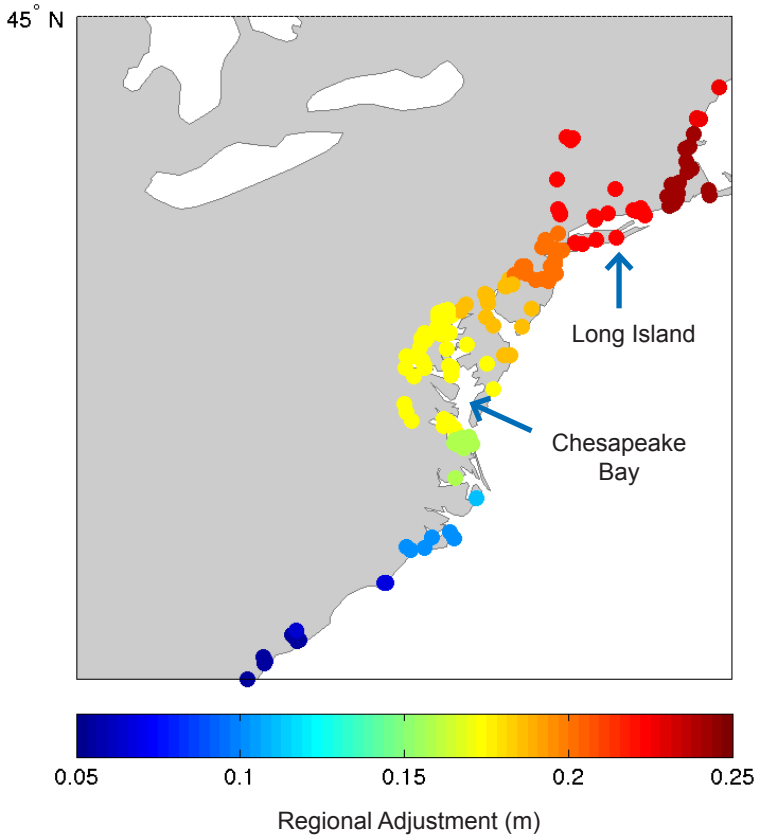

Figure 4.4 Dynamical Sea-Level Adjustment Near the Sites in the Vicinity of Northeastern United States for the 1.0-Meter Global Scenario for Year 2100

4.3.2 Ice melt

The adjustments computed for each melt contribution for all military sites are shown in Figures 4.5, 4.6, and 4.7. Once again, the pattern of site-specific effects of ice melt is consistent with the fingerprints shown in Figure 3.9(a), (b), and (c) for each source (glaciers, Greenland, and Antarctica) in Section 3.4.4. (Note that the color scale bars differ for the ice-melt maps.) As discussed previously, sea level falls in the vicinity of the location of melt and consequently the sites located near the source experience a negative (negative here meaning a decrease in sea level) effect of ice melt. In the case of glaciers (Figure 4.5), the largest effects are observed on the southern coast of Alaska and at the two sites near Greenland. At sites along the coast of United States, the adjustments due to glacier melt also are negative (i.e., sea level is lower than the global mean); see the associated fingerprint in Figure 3.9(a).

A similar effect is observed for ice melt from Greenland [Figure 4.6 and Figure 3.9(b)]. The effect is negative at most sites and the adjustment is the largest in the vicinity of two sites near Greenland. Most military sites are located north of the 1 meter/meter contour as shown in Figure 3.9(b). Figure 4.7 and Figure 3.9(c) show a positive effect due to ice melt from Antarctica. For the 1.0-meter scenario, however, the adjustment is only about 0.04 meters (see below).

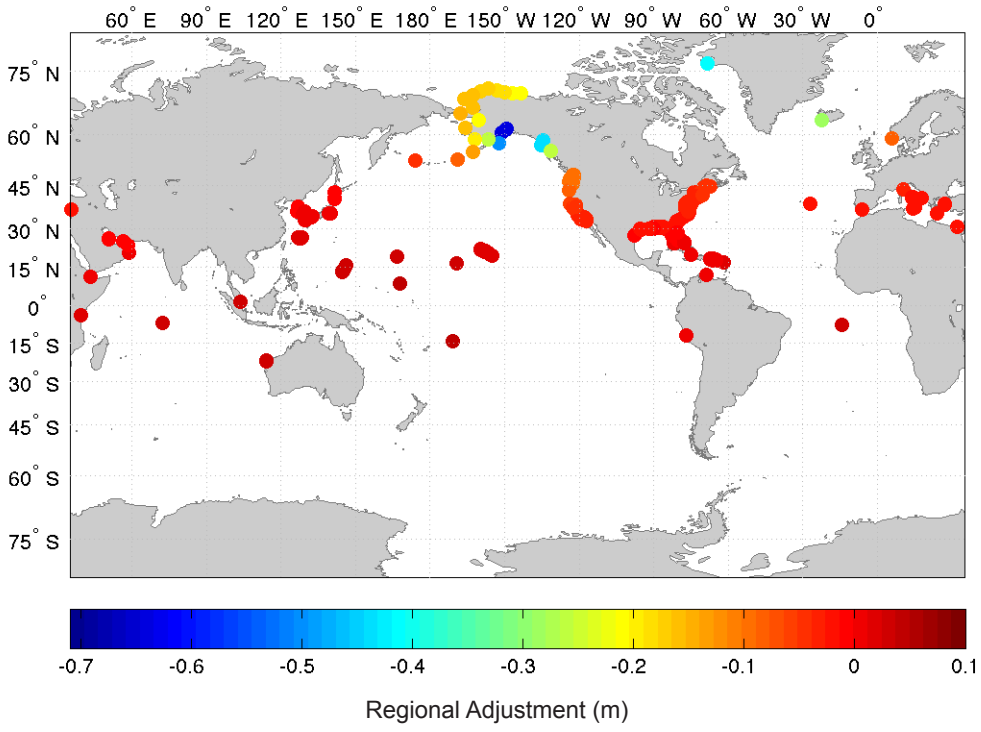

Figure 4.5 Regional Adjustments for Ice-Melt Contributions from Glaciers and Ice Caps for the 1.0-Meter Scenario in 2100
The scale bar reflects the adjustment in meters for the particular scenario (1.0-m scenario for this figure).

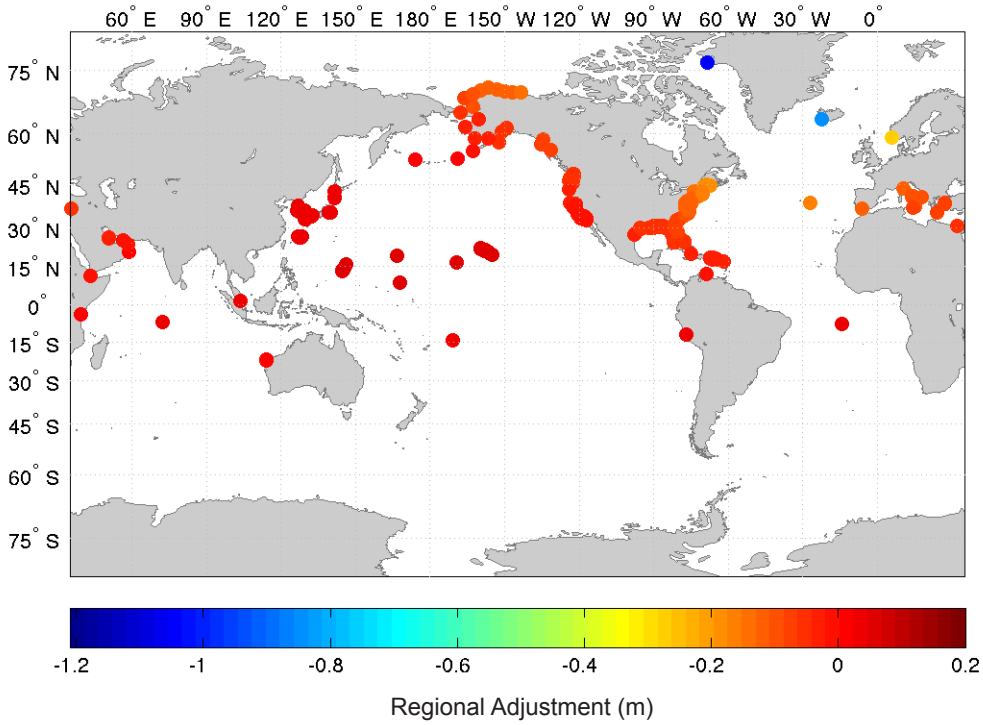

Figure 4.6 Regional Adjustments for Ice-Melt Contribution from Greenland for the 1.0-Meter Scenario in 2100
The scale bar reflects the adjustment in meters for the particular scenario (1.0-m scenario for this figure).

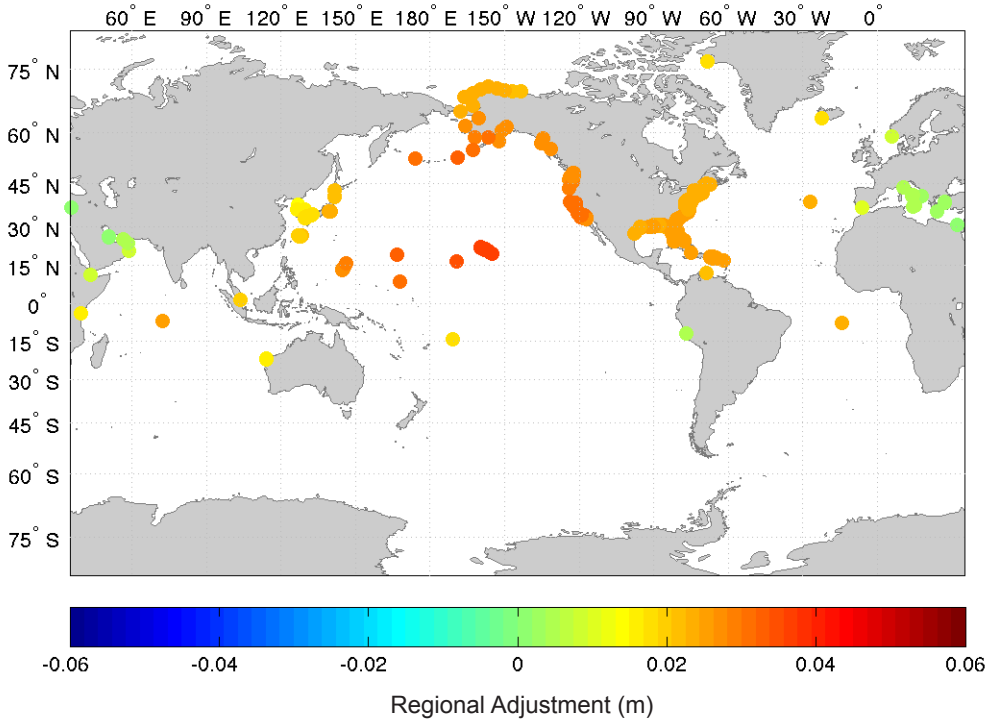

Figure 4.7 Regional Adjustments for Ice-Melt Contribution from Antarctica for the 1.0-Meter Scenario in 2100
The scale bar reflects the adjustment in meters for the particular scenario (1.0-m scenario for this figure).

For each site, what matters is the cumulative effect of ice melt attributable to all three sources. Figure 4.8 shows the cumulative adjustment for the 1.0-meter scenario. At most sites the cumulative adjustment is negative. Two regions in particular emerge as having the largest negative effect: the southern region of Alaska and the two sites on or near Greenland. At these sites the adjustment is large enough to compensate for the global sea-level rise due to thermal expansion and the volume addition due to ice melt. The net effect is positive primarily in the Pacific region (within the ellipse shown in Figure 4.8). Even in this region, however, the net effect is only on the order of 0.1 meters (see below).

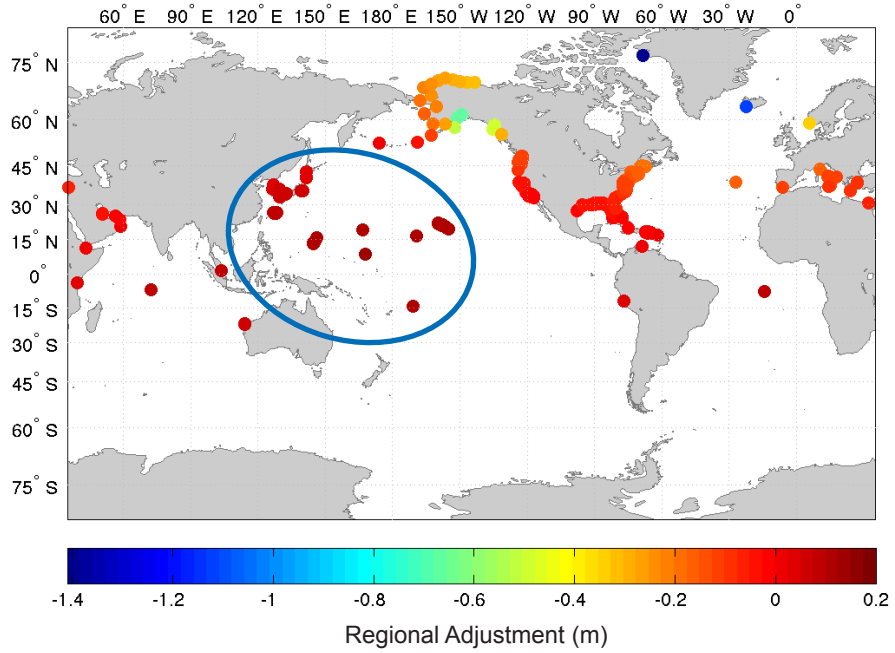

Figure 4.8 Cumulative Regional Adjustments for Ice-Melt Contributions from Glaciers and Ice Caps, Greenland, and Antarctica for the 1.0-Meter Scenario in 2100
The scale bar reflects the adjustment in meters for the particular scenario (1.0-m scenario for this figure).

Particular attention is drawn to the contribution of Antarctica ice melt in the high-end scenarios (1.5 meters and 2.0 meters). Figure 4.9 shows the regional adjustment due to Antarctica ice melt for the 2.0-meter scenario. Because most sites are away from the source of melt (i.e., Antarctica), the large negative effect that is characteristic of the locations near the source is not seen at any of the sites. The effect is positive at most sites (Figure 4.9) within the mid-Pacific region (near Hawaii).The adjustment in these locations is on the order of 0.3 meters. The global contribution of Antarctica for the 2.0-meter scenario is about 0.95 meters (Table 3.8, Section 3.4.4) and the highest regional adjustment in the Pacific is about 30% higher than the global Antarctica contribution. The results depicted in this figure are consistent with what is reported in the literature, which shows this region having the largest effect of Antarctica melt on the order of 25% to 30% above the global value (e.g., Ferrell and Clark 1976, Hay et al. 2014, Mitrovica et al. 2009).

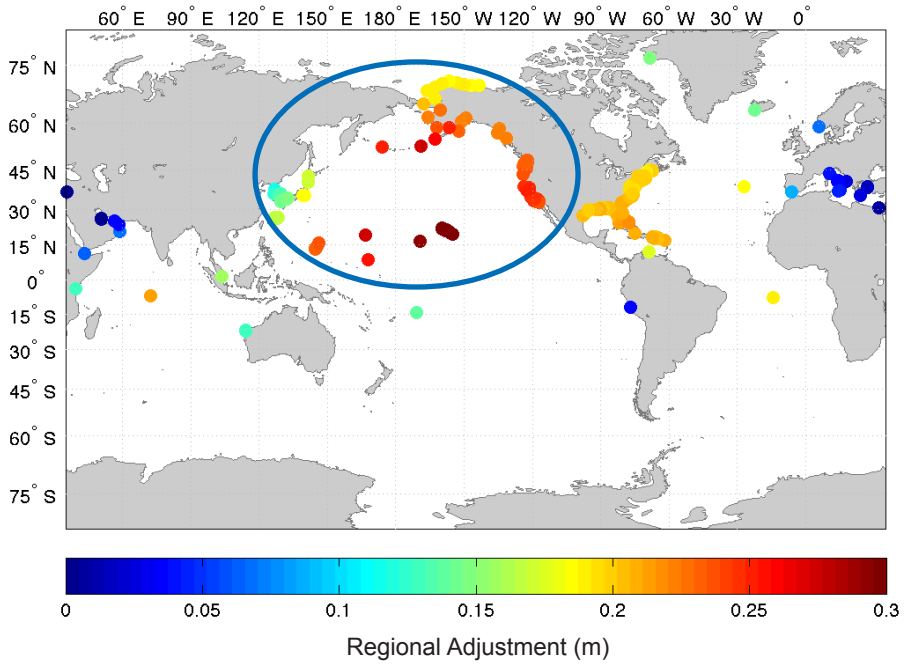

Figure 4.9 Regional Adjustment due to Antarctica Ice Melt for the 2.0-Meter Scenario

A similar effect, but with a large negative value, is projected for two sites near Greenland due to its ice melt in the 2.0-meter scenario (Figure 4.10). For this scenario, the adjustment at the Greenland site is about -1.8 meters and at the Iceland site about -1.4 meters. Because these two sites are extremely close to the source of ice melt (i.e., Greenland), such a large adjustment is expected. The adjustments effectively mitigate the global average sea-level rise, which in this case is 2.0 meters.

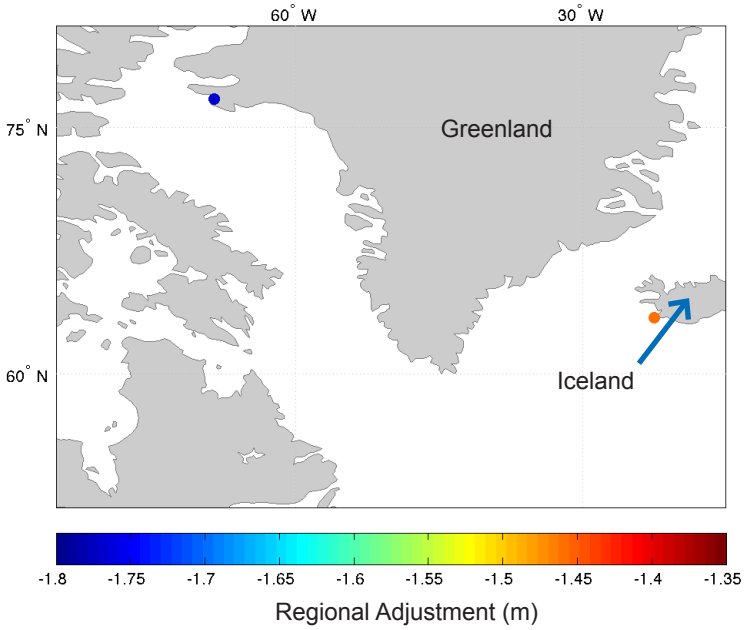

Figure 4.10 Adjustment near Greenland and Iceland due to Greenland Ice Melt for the 2.0-Meter Scenario

4.4 Regional Extreme Water Levels

The following sections describe the results of estimating extreme value statistics for the 1,774 DoD coastal sites considered in this study. When tied to the MHHW tidal datum, these statistics provide a method to estimate EWL scenario information for each site. Section 4.4.1 provides the results of regional frequency analyses (RFA) for those sites for which an RFA was possible. Section 4.4.2 briefly addresses situations in which either only a single tide gauge analysis was possible or insufficient tide gauge data was available to provide an estimate of extreme value statistics. Sections 4.4.3 and 4.4.4 provide comparisons of the RFA to other studies and to the single gauge analyses (where feasible), respectively.

4.4.1 Regional frequency analysis results

Figure 4.11 shows return levels for nontidal residual (NTR) values (i.e., storm surge) for the 20%, 5%, 2%, and 1% annual chance events (5-, 20-, 50-, and 100-year event return periods, respectively) based on RFA of annual maxima NTR values fit by Generalized Extreme Value (GEV) distributions at the DoD sites for which an RFA is feasible. The RFA return levels are similar to the spatial patterns using single-gauge GEV or Generalized Pareto Distribution (GPD) method (Figure 3.16 in Section 3.5.1). Highest RFA-derived NTR 100-year return levels in Figure 4.11(d) are found where tropical storms (e.g., U.S. Southeast and Gulf Coasts) and strong extratropical storms occur (e.g., U.S. Northeast Coast, southern Alaska, and northern European coast facing the North Sea) and especially so when such events make landfall with a wide adjacent continental shelf. On the other hand, relatively low NTR return levels are found along the U.S. southwestern Pacific mainland coasts and ocean islands due to bathymetric constraints on storm surge magnitudes occurring over narrow continental shelves found in these regions. Similar patterns are found and described by Tebaldi et al. (2012) and Zervas (2013). An example of such a spatial pattern is evident when comparing the 100-year probabilities at sites in the U.S. Virgin Islands and those along the Southeast Atlantic and Gulf Coasts. The Virgin Islands have experienced several land-falling hurricanes such as Hurricane Marilyn, which struck in 1995 as a strong category 2 storm. This event, however, registered only as less than a meter storm surge at the NOAA tide gauge located in Charlotte Amalie at Saint Thomas in the Virgin Islands, which is less than a third of values often experienced by similar magnitude storms impacting the Southeast Atlantic and Gulf Coasts.

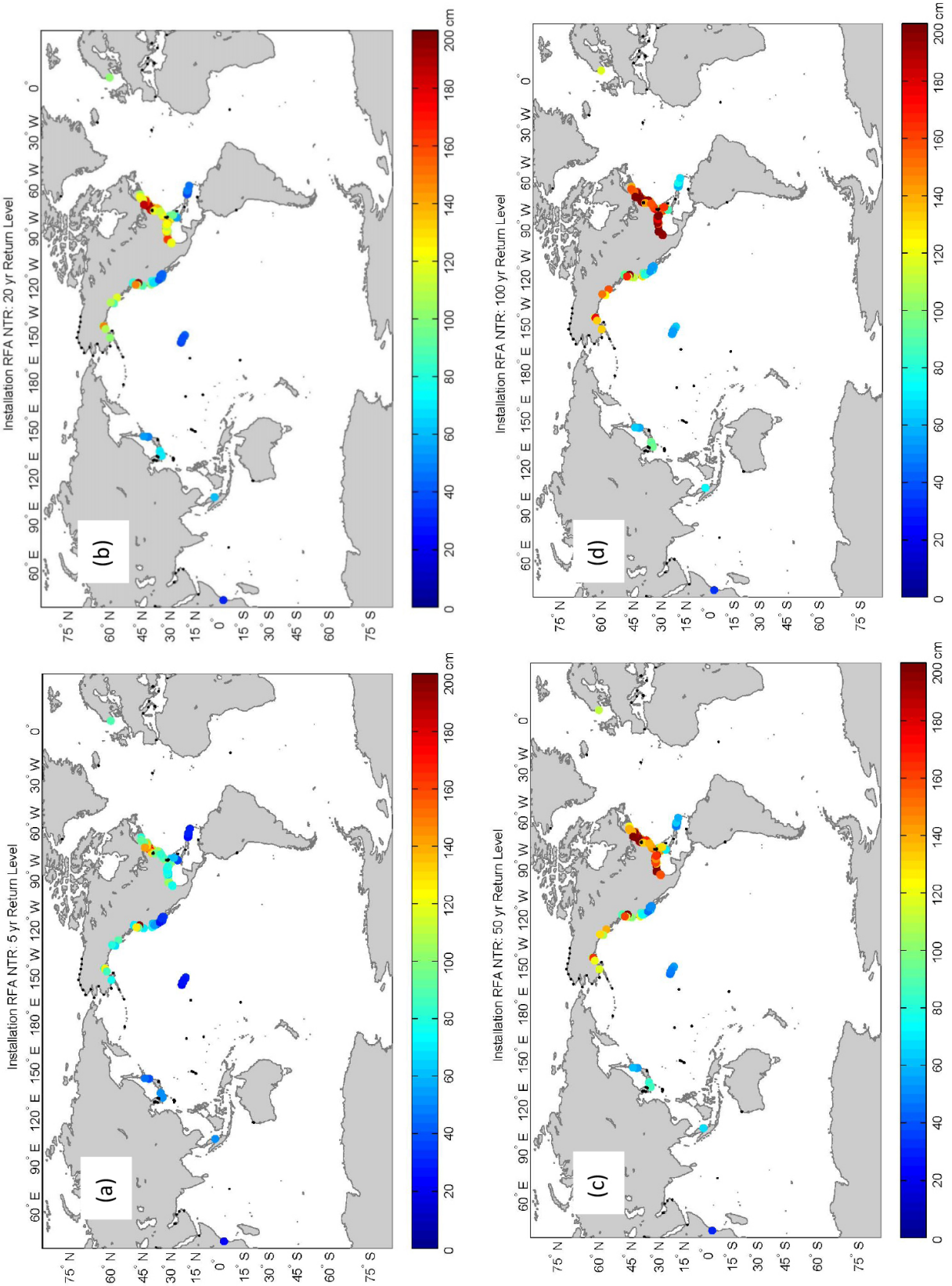

Figure 4.11 (a) 5-Year, (b) 20-Year, (c) 50-Year, and (d) 100-Year Return Levels (cm) for NTR Levels at DoD Sites

Anomalously high values due to fluvial effects occur in a few locations. The two most obvious examples occur upstream of the Delaware River along the mid-Atlantic Coast and Columbia River along the U.S. Pacific Coast (i.e., red dots in 100-year return level plots in Figure 4.12). The high water probabilities are elevated by fluvial influences during periods of high river discharge in spring, similar to findings of Sweet et al. (2014) who found highest "nuisance-level" flood frequencies during the spring at tide gauges with noticeable fluvial influences; these are in contrast to the prominent regional fall-winter time peak in response to cool-season, storm-related (i.e., nor'easter) forcing. Comparisons of mean and maxima water levels at tide gauges along the Columbia and Delaware Rivers (the basis for the high values at the sites) show a progressive decline in water levels downstream nearing the open coast (https://tidesandcurrents.noaa.gov/map/index.shtml?type=PreliminaryData, accessed October 2015). Overall, assignment of RFA-based extreme event probabilities was possible at 1,395 sites out of the 1,774 total (78.7%).

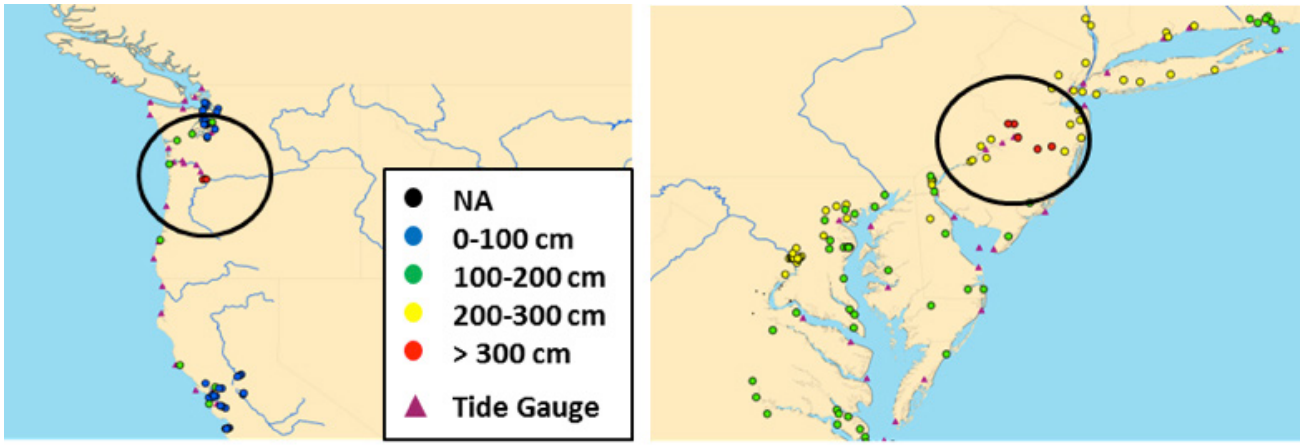

Figure 4.12 Close-Up of Figure 4.11 (above) Showing the 100-Year NTR Probabilities Where Alluvial Influences Create Regionally Anomalous High Values
Red dots within circled regions) upstream of the Columbia River (left) and the Delaware River (right).

4.4.2 Situations in which only a single gauge or no analysis was possible

For several locations (21.3%), the RFA process was not able to provide an extreme estimate at a particular site, though 6.8% of these (i.e., Category 1 sites with Heterogeneity, or H, greater than 2 or without at least three tide gauges within 400 km as shown in Table 3.9 in Section 3) can use results from a single-gauge analysis from a gauge within 50 km and with greater than 30 years of hourly data. Figure 4.13(a) shows the 100-year NTR probabilities for sites that have local tide gauge (less than 50 km) RFA-dependent H values greater than 2 (do not represent a homogeneous set of tide gauges); these sites primarily are in the region of the Georgia-Florida border and their values are comparable to those of the RFA-based analysis (above in Figure 4.11). Figure 4.13 (b) illustrates mostly island sites that do not have more than three tide gauges within a 400-km radius, but have a local tide gauge (less than 50 km). That leaves about 14.3% of the sites with no EWL information to guide their screening-level vulnerability or impact assessment. (See the text box on page 4-20 for tips on addressing this situation.)

(a)

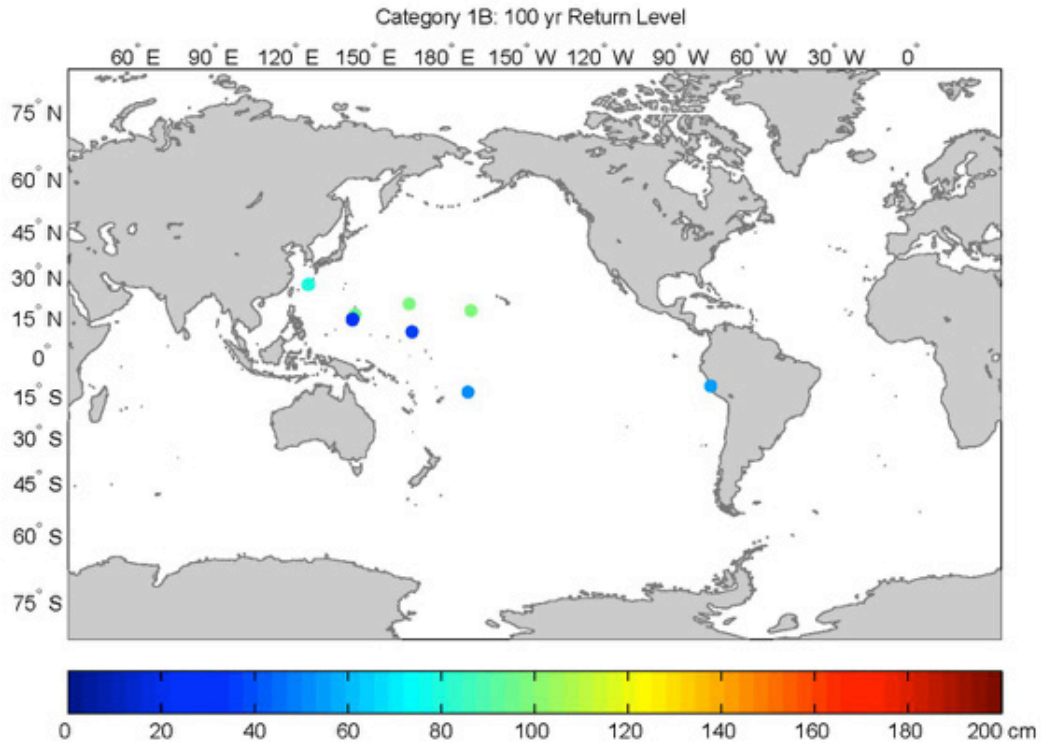

(b)

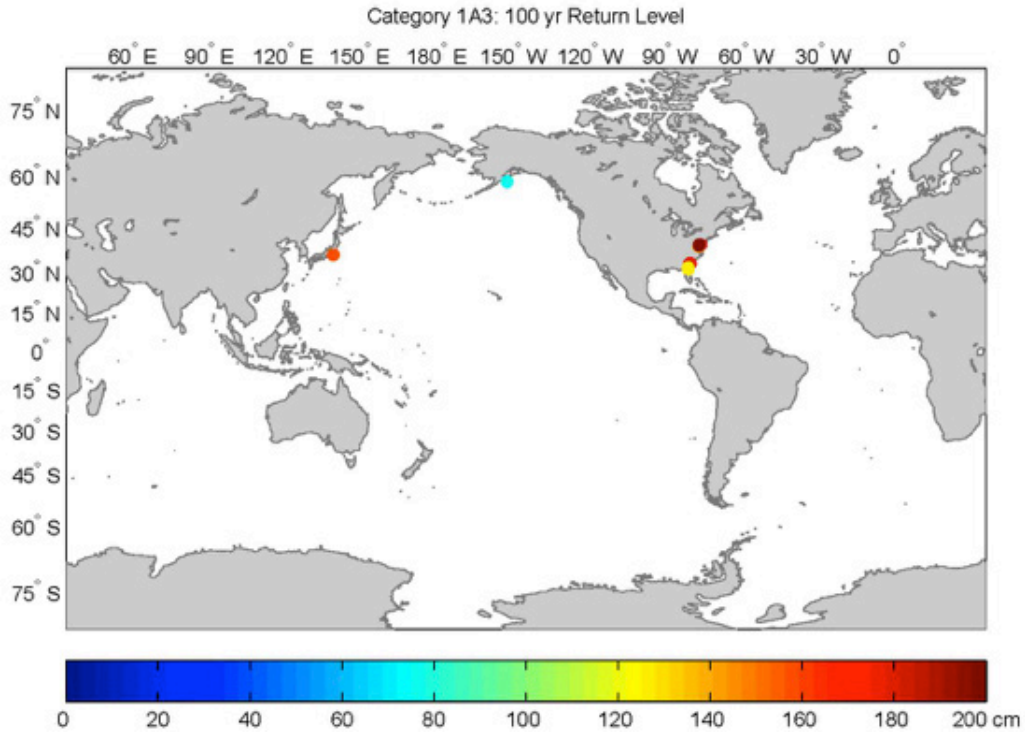

Figure 4.13 100-Year Return Levels (in centimeters) for NTR Levels at DoD Sites from Analysis of a Long-Term (> 30 years) Single Tide Gauge within 50 Kilometers
RFA-based estimates were not obtainable because of (a) lack of homogeneous set of tide gauges (H value > 2) within 400-km radius or (b) lack of ≥ 3 tide gauges within a 400-km radius.

4.4.3 Comparison of the regional analysis results with other studies

In addition to performing an RFA-based GEV analysis for the DoD sites that met the criteria for an RFA (Figure 4.11), a similar RFA analysis was conducted using only those individual tide gauges as "sites" that had a local tide gauge less than 50 km away with greater than 30 years' record (i.e., Category 1 sites) following the same procedures (described in Section 3.5.6) to enable method comparisons to other published results. Thus, in this circumstance, the local "index event" is the average of annual maximum NTR at the particular tide gauge. Results from this procedure also are compared to results using the same methods for a single gauge but that do not include the RFA process (see Section 4.4.4 below). Here, the results are compared to storm tides estimates (NTR + tide level) from: (1) Zervas (2013), which are the basis of NOAA's extreme water level probabilities (http://tidesandcurrents.noaa.gov/est, accessed August 2015), (2) Tebaldi et al. (2012) updated for entire record length, which support the Climate Central's Surging Seas analysis (http://sealevel.climatecentral.org, accessed August 2015), and (3) the synthetic-storm model results of Nadal-Caraballo et al. (2015) that support the U.S. Army Corps of Engineers North Atlantic Coast Comprehensive Study (https://chs.erdc.dren.mil, accessed September 2015). The comparisons were made over the mid-Atlantic region from Maine to Virginia, which is the domain of common overlap between all three data sets in Figure 4.14. In addition, comparisons to Zervas (2013) and Tebaldi et al. (2012) were made along the West Coast for tide gauge "sites" between southern California north to Anchorage, Alaska. In comparison to storm-tide estimates (tide + NTR), this study's NTR extreme estimates are shown relative to MSL datum with the MHHW offset applied.

Settings with Insufficient Tide Gauge Data

Some locations may have insufficient tide gauge information to support a statistically valid Regional Frequency Analysis. In these circumstances, it is recommended that:

- *water levels be collected to reach a sufficient record length for direct statistical estimates, or that*
- *indirect assessments be made through information obtained from local tide and storm surge models (with sufficient resolution to capture most impacting events – extratropical or tropical storms)*

These data will allow the user to numerically simulate a sufficient hindcast of water levels to estimate extreme water level probabilities (e.g., Haigh et al. 2014a,c).

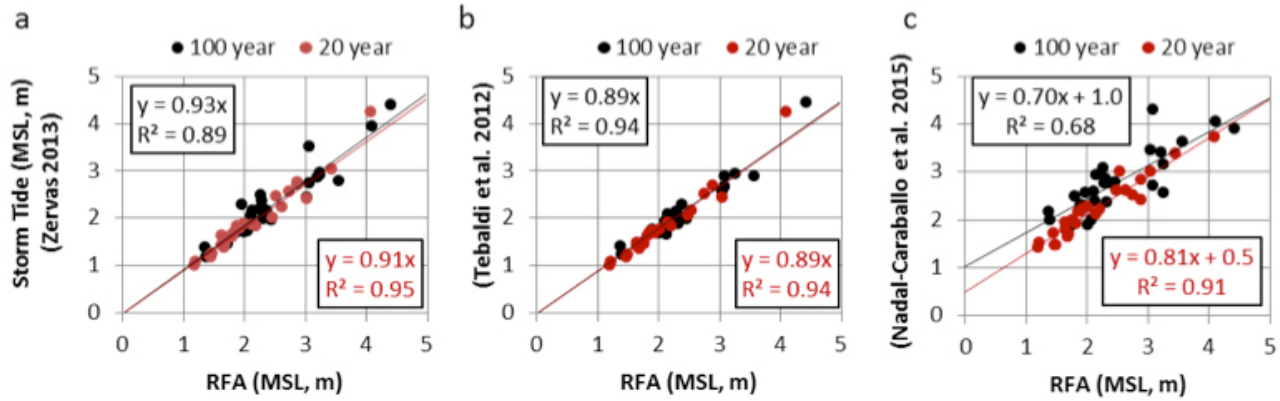

Figure 4.14 Comparison of RFA-based Probabilities from this Study (Using Individual U.S. East Coast Tide Gauges as a "Site") to Estimates from Other Studies

Shown are results for (a) Zervas (2013), (b) Tebaldi et al. (2012), and (c) Nadal-Caraballo et al. (2015). The RFA estimates are shown relative to MSL by applying the local tide gauge MSL-to-MHHW offset to the NTR probability estimate. Regression significant above the 99% level (P values <0.01).

Comparison to the results of Zervas (2013), who used GEV fits of maximum annual storm-tide levels, are in close agreement at the 20- and 100-year return levels along the mid-Atlantic Coast in Figure 4.14(a). Linear regression coefficients show that Zervas's (2013) estimates from a single gauge analysis are systematically 9 and 11% less than those by the RFA process for the 20- and 100-year levels, respectively. The largest difference is found at Bridgeport, Connecticut, where the RFA-based 100-year value is approximately 0.7 meters higher than that of Zervas (2013).

Generalized Pareto Distribution (GPD) fits of storm tide levels based on a peak-over-threshold approach of Tebaldi et al. (2012), whose results have been updated to include the entire hourly water level record (C. Tebaldi, personal communication 2015), also closely match the RFA results, though linear regression coefficients between results reveal that the GPD estimates are 11% less than those from the RFA analysis for the 20- and 100-year return levels in Figure 4.14(b). Comparison to estimates derived from synthetic storms generated by high-fidelity modeling of tropical and extratropical storms of Nadal-Caraballo et al. (2015) are quite close at the 20-year return level (r^2=0.91), though less so (r^2=0.68) when comparing the 100-year values as shown in Figure 4.14(c). Some notable differences in 100-year values between methods occur at Providence, Rhode Island (1.22 meters), Atlantic City, New Jersey (0.81 meters), and Sewells Point, Virginia (Norfolk; 0.77 meters), with larger values estimated using the model simulations. Higher model-based estimates are to be expected because a primary purpose of efforts such as those of Nadal-Caraballo et al. (2015) is to better assess the likely distribution of extreme storm response from rare phenomenon (e.g., direct hurricane strikes), which are generally lacking in the tide gauge records themselves. Some instances, however, occur along the Maine coastline in which the RFA-based 100-year estimates are larger than those of the model-based approach, such as at Eastport, Bar Harbor, and Portland (0.53, 0.68 and 0.38 meters, respectively).

Along the U.S. West Coast, 20- and 100-year estimates of Zervas (2013) and Tebaldi et al. (2012) in Figure 4.15(a) and (b) are similar or slightly higher than the RFA-based estimates (NTR probability + MHHW-MSL offset), respectively. For instance, linear regression coefficients suggest close agreement with Zervas's (2013) 20- and 100-year levels, whereas the Tebaldi et al. (2012) 20- and 100-year levels are systematically 8 and 14% larger than the RFA-derived levels. The fact that our RFA-based estimates are less when compared to West Coast levels of Tebaldi et al. (2012) is presumably due to the higher discrepancies between astronomic-forced tidal heights. Tidal amplitudes vary considerably throughout the year and over the approximately 19-year nodal cycle, which is characterized in Figure 4.15(c) in terms of the difference between the average of highest daily tide (MHHW) and the highest astronomical tide (HAT), and more so along the West Coast as compared to the East Coast as shown in Figure 4.15(c). As shown in Merrifield et al. (2013) on a global scale and in Sweet et al. (2014) specifically for the U.S. coasts, when extreme water level events occur along the West Coast, typically the ratio of the tide to the NTR contributions indicates a much higher dependence on the tidal amplitude because storm surge is typically much less than occurs along the East and Gulf Coasts. Thus results for storm-tide based extreme events on the West Coast (e.g., Tebaldi et al. 2012, Zervas 2013) are more sensitive regarding selection of the high-tide datum on which to add the RFA NTR extreme probability than along the East or Gulf Coasts. For purposes of this study, the weight of evidence across sites evaluated led to the selection of MHHW for this study as the high tide datum to serve as the base elevation upon which to add our NTR probabilities to obtain extreme SWL probabilities. This approach provides robust estimates compared to other study estimates for a variety of regions around the United States.

...specifically for the U.S. coasts, when extreme water level events occur along the West Coast, typically the ratio of the tide to the NTR contributions indicates a much higher dependence on the tidal amplitude because storm surge is typically much less than occurs along the East and Gulf Coasts.

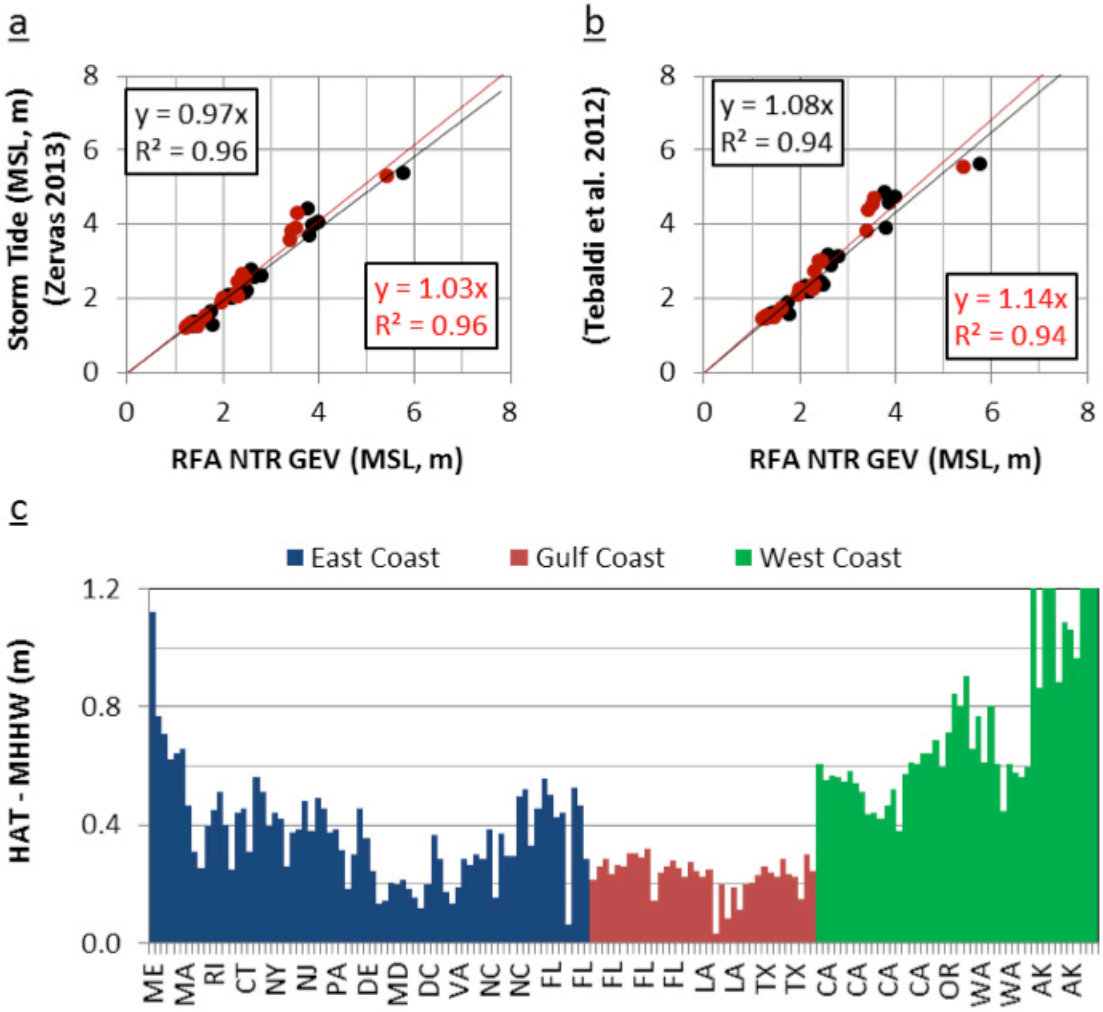

Figure 4.15 Comparison of RFA-Based Probabilities from this Study (Using Individual U.S. West Coast Tide Gauges as a "Site") to Other Studies
Compared to estimates from (a) Zervas (2013) and (b) Tebaldi et al. (2012). In (c) are the height differences by geographic region between the highest astronomical tide (HAT) and mean higher high water (MHHW) tidal datums for U.S. NOAA tide gauges.

4.4.4 Comparison of the regional frequency analysis results to single gauge analyses

Figure 4.16 compares the 20- and 100-year NTR return levels and spread of the 90th percentile confidence interval (difference between 5th and 95th percentiles) estimated by RFA and single-gauge GEV (not using the RFA procedure) for tide gauges in the global set with greater than 30 years' data and RFA H values less than 2. In Figure 4.16(a), the 20-year return levels (red dots) are similar and highly correlated (r^2=0.98) with a linear regression coefficient of approximately 1. Comparison between the 100-year return levels are slightly less correlated (r^2=0.89) with single-gauge estimates and are on average 5% larger than values from the RFA-based estimates. Differences between methods are more noticeable at larger values (e.g., greater than 2 meters) in 100-year return levels in which the RFA estimates are on occasion lower than those estimated

by the single-gauge method. Most notable (1 meter) differences between the single-gauge and the RFA-based results are found at the Washington, D.C., and Juneau, Alaska, tide gauges where in both cases the RFA analysis provides lower estimates. Close inspection of data at these two tide gauge locations reveal that at D.C., extremes are often during high river discharge when the tidal signal attenuates and contributes to an approximately 1-meter oscillatory NTR signal (due to difference from the assumed continuation of the astronomic tide) during times of highest waters. At Juneau the discrepancy may be an artifact of an apparent shift in hourly water levels occurring near the beginning of 1984 that creates a tidal phasing computational issue that influences the resultant NTR signal. In both cases the RFA-derived 100-year values more closely equate to estimates of Zervas (2013) and are considered the more robust estimate.

A noticeable difference between RFA and single-gauge estimates is the spread of the 90th percentile confidence intervals. This is most evident for those associated with the 100-year return levels shown in Figure 4.16(b) due to higher data inclusion of the RFA method. As described in Section 3, the RFA method typically assumes that all observations (i.e., annual maximum NTR) are event-independent within a region. Due to the complexities in assessing such independence at the extremely high number of "regions" formed about our DoD sites, there may be some inherent inter-gauge data (annual highest NTR) dependence, resulting in narrower (underestimated) probability confidence intervals. But as discussed in Hosking and Wallis (1988) and Weiss et al. (2014), the RFA method is still shown to be quite robust in the presence of regional inter-site dependences and is the preferred method over a single-record analysis when estimating extremely low probability events (i.e., 100-year return periods). In Section 5.2.1 (Regional frequency analysis versus a single tide gauge analysis), results are compared when applying an arbitrary 5-day filter on annual maximum NTR values from each tide gauge in a region. Such a filter helps ensure that only the highest regional value is retained in order to minimize possible event dependencies that might have resulted in response to a common storm.

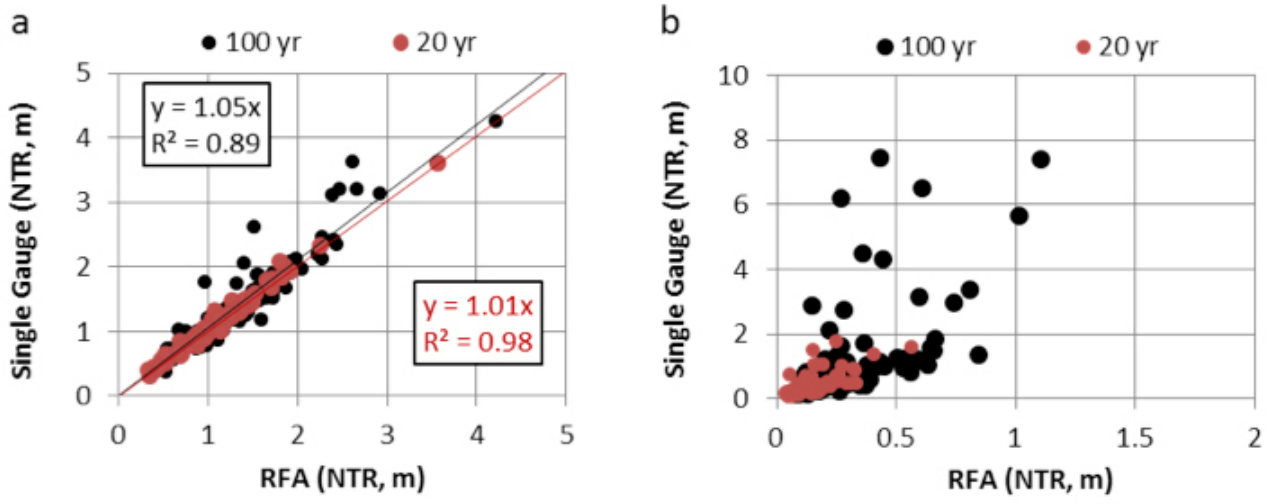

Figure 4.16 Comparison of Single-Gauge and RFA-Based GEV Analyses
Comparison of (a) return level estimates for the 20- and 100-year event between a single-gauge GEV and RFA-based GEV analysis of annual maximum NTR and (b) their spread of the 90th percentile confidence interval

In this report NTRs are expressed as different annual chance events or return periods (e.g., 5% and 1% events or 20- and 100-year events, respectively), which affect specific particular elevations above a reference datum. Because our SLR scenarios were not continuous functions, but rather time slices at three periods in the future, we did not quantify expected increases in the number of flood events at a particular annual chance event over a specified time horizon. The ability to express increases in flood events in this manner is often useful to assess future risk to pre-existing infrastructure from a threshold event that becomes more recurrent in the future (Hunter 2012). The text box below provides an example of how the probability of an annual chance event for a particular elevation for two different cities today will increase in time due to local SLR. In the curve for San Diego, an additional rise in sea level of approximately 25 centimeters will result in the storm surge normally associated now with a 100-year storm occurring at a much greater frequency (approximately becoming the 5-year storm).

Local Sea-Level Rise and Future Flood Probabilities Relative to Today's Infrastructure

As local sea levels rise, the likelihood for exceeding a given elevation threshold during a storm will increase more dramatically in some locations than in others. A first-order estimate is dependent on local MSL increases and inversely related to the range (related to the GEV scale parameter) of extremes experienced in the past, which is reflected by the height difference between high and low probability events (e.g., 5- and 100-year event probabilities). For instance, in the figure below, the flatter "return interval curve" at San Diego, compared to the curve for Norfolk, implies that under equal amounts of local SLR (e.g., 25 cm) the more "rare" water level event today will have a much higher probability of recurring in San Diego than in Norfolk (e.g., 100-year event at San Diego becomes approximately a 5-year event whereas a 100-year event becomes approximately a 50-year event in Norfolk).

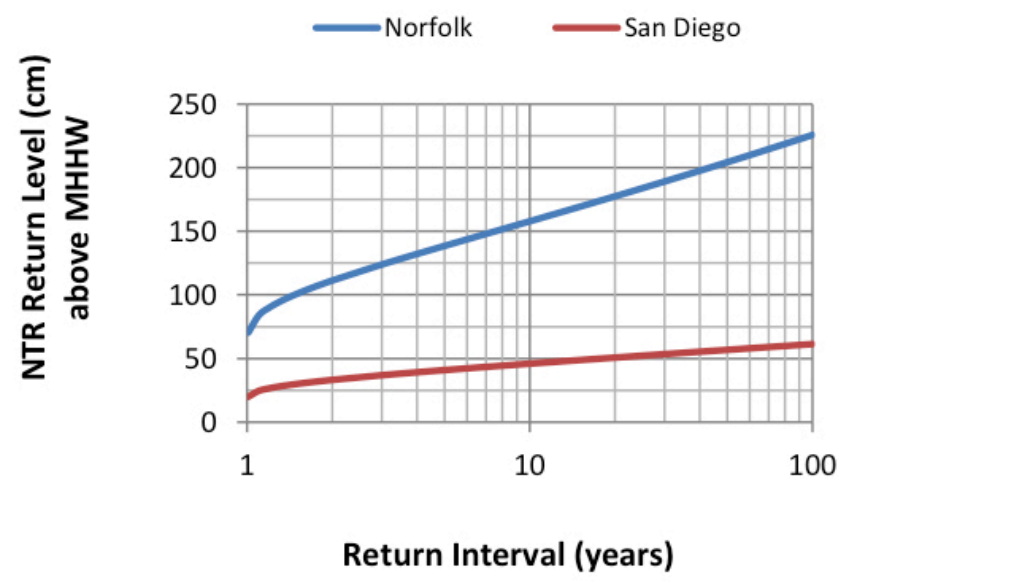

4.5 Scenario Application Considerations

The sea-level change and extreme water level scenario database that accompanies this report provides its information relative to a point location associated with sites contained in the DoD Real Property Assets Database (RPAD). Sites that may represent specific small-footprint facilities or assets could be spatially remote or within the confines of a traditional installation boundary. The latter situation gives rise to a separately identified site when a particular Military Service facility or asset is located within the installation boundary of another Service. For RPAD sites that correspond to an installation polygon, the point location is the centroid of the polygon. To assist DoD planners and managers in gaining an initial sense of a site's vulnerability, the scenario database also contains information on the lowest elevation point for a site polygon (see below for additional details). Still, a scenario applied to a centroid or lowest elevation location may not represent a site's potential vulnerability across its spatial extent. Stated in a different way, one data point for land elevation and mean high water offset may not be appropriate across an entire site, especially if that site is either complex topographically or in its shoreline configuration.

The task remains, therefore, of converting the point information in the database to a spatial area of interest: that is, an installation polygon or otherwise. When accomplishing this, a number of considerations come into play. To begin, three types of information are needed: an elevation reference, base surface elevation, and water surface elevation (NOAA 2010a). A datum is a base elevation used as a reference from which to reckon heights or depths. When available, the scenario database references information to a reference or more specifically a geodetic datum, which generally includes areas in North America that use the North American Vertical Datum 1988 (NAVD88) as the reference datum. Outside North America, availability of a geodetic reference datum may be more limited, but is included when known. A tidal datum, which is a standard elevation defined by a certain phase of the tide, also is important to know for scenario application. Tidal datum information enables determining local mean sea level (MSL) and associated tidal information such as MHHW; however, again, such information is not always available, especially if a location lacks a representative local tide gauge. Section 5.2 provides guidance on developing at least a rough estimate of tidal datum information for a site that currently lacks such information.

Base surface information includes both surface elevation (topography) and its underwater equivalent (bathymetry) information. We are concerned here only with surface elevation, though a site manager who wants to understand in more detail how storm surge may change non-linearly with sea-level rise will need to have accurate bathymetric information. See Section 5.1 for additional information on accounting for the nonlinear effects of storm surge with rising sea levels. Accurate topographic information is vital for effective mapping of scenario information. Section 4.5.1 below addresses applying point-based scenario information to a spatial area of interest and Section 5.2 addresses more directly the effect of resolution and vertical accuracy of the topographic data used for mapping on the ability to show the horizontal extent of permanent inundation and temporary flooding (and their associated uncertainty) that results from a particular scenario at a site.

Water surface elevation, from which tidal datum information is generated, is obtained from a tide gauge. Such information, however, can be highly localized and should not be arbitrarily

extended into areas with differing oceanographic characteristics (NOAA 2010a). Tidal datums along a coastline can differ locally for many reasons: for example, changes in bathymetry; presence of barrier islands, tidal flats, and river interactions; geographic and volumetric changes in the shoreline and associated embayments; and the presence of shoreline engineering structures (NOAA 2010a). If none of these factors affects a given area (e.g., a straight coastline or absence of the other factors mentioned above), extrapolation of the tidal datums can usually be made by assuming that a constant datum difference extends inland. The EWL scenarios developed by this report are provided relative to MHHW (NOAA 2012). Section 3.5 provides additional details on this choice. Section 4.5.2 addresses how to account for local tidal datum variability when applying scenario information by providing examples of the appropriate use of a constant MHHW value and situations when different values may need to be considered.

Finally, although not discussed further here, scenario users also should recognize the importance of addressing local hydrologic connectivity (NOAA 2012). In particular, engineered structures, such as dikes, levees, culverts, ditches, and canals may alter hydrologic flow paths and thus affect what ultimately is potentially inundated or flooded. In addition, lower-lying areas inland from the coast may or may not be flooded under specific scenarios, dependent on whether and when they are hydrologically connected to the shoreline. High quality topographic data may assist in resolving the latter issue; however, unless supplemented by addition information on the spatial location of linear infrastructure, the former situation may create additional errors in the mapping of scenarios (Poulter and Halpin 2008).

Sections 4.5.1 and 4.5.2 provide basic guidance on applying point-based scenario information to a spatial area of interest and accounting for local tidal datum variability, respectively. The latter is accomplished in Section 4.5.2 by using Marine Corps Base Camp Lejeune in North Carolina to illustrate this application. For this example, locations are provided for only those sites that already occur in publicly available databases. In lieu of specific site identifiers that are contained in the real property database, dummy location numbers are used. For additional detailed information on the issues addressed in this section, the reader is referred to NOAA (2010a, 2012).

4.5.1 Applying point-based scenario information to a spatial area of interest

This study focused on 1,774 DoD sites worldwide within 20 km of the shoreline or otherwise tidally influenced. Each of these sites is contained in the DoD real property database and is described by latitude and longitude coordinates. With the exception of sites embedded within other sites (i.e., within an installation polygon) and in some cases regardless of this relationship, sites occur within unique physical settings that may differ topographically or with respect to the local water surface elevation. Each site location, when information was available, was independently assessed for topographic elevation, estimated rate of vertical land motion, and tidal datum elevation relationships to a geodetic reference datum, as well as regionalized adjustments to global SLR and EWLs. The database and Graphical User Interface (GUI) that accompany this report provide this site-specific information.

This single point information does not necessarily provide what is required to properly assess the exposure component needed to conduct vulnerability and impact assessments at all sites.

Many of the 1,774 sites are unique buildings, structures, and facilities that can be pinpointed and fully assessed for vulnerability to SLR and EWLs using a unique latitude and longitude position. A significant number of these locations, however, are centroid coordinates for a larger installation footprint that may not necessarily be described by one coordinate because of spatially complex topography. Polygons for these installation "sites" are usually available as shapefiles in GIS; however, they differ greatly—both across and within sites—in the quality and extent of the associated topographic information available to describe them.

It is important that a site's surface elevations can be tied to a reference or geodetic datum and later to a tidal datum (see Section 4.5.2 below). For the site centroid elevation information contained in the accompanying scenario database, elevations were estimated using the U.S. Geological Survey NED website with respect to an NAVD88 elevation. Lowest point elevations, when applicable, were estimated using the best publically available dataset, also with respect to NAVD88 for North America sites (see Section 3.2 for details). Individual sites should use the best quality topographic data available to them and estimate elevations with respect to a geodetic datum across the entire area of interest. In some cases site-specific topographic data may represent an improvement in the vertical accuracy of the elevation information used in the database. For mapping the scenarios a site manager should account for the resolution and accuracy of the topographic data used (see Section 5.2) when determining the horizontal extent of inundation or flooding relative to a particular scenario. Accurate mapping of site topography with respect to a reference datum is the first step in applying the point-based scenario information in the scenario database. Additional details about reference datums, sources of topographic information, and the importance of these, as well as accounting for errors in their usage, can be found in NOAA (2010a).

4.5.2 Accounting for local tidal datum variability

Once the reference datum and topographic information referenced to the datum are spatially determined for an area of interest, the next step prior to actually mapping the scenarios involves accounting for any significant tidal variation in MHHW that may occur across a site. An example is provided below in which tidal variation is an important consideration.

The Marine Corps Base Camp Lejeune (MCBCL) is a good example showing complex variability of tidal datum elevations. Figure 4.17 shows two site locations associated with MCBCL and Table 4.2 provides the location-specific information. Locations 1 and 2 are sites defined by their latitude and longitude coordinates in the RPAD.

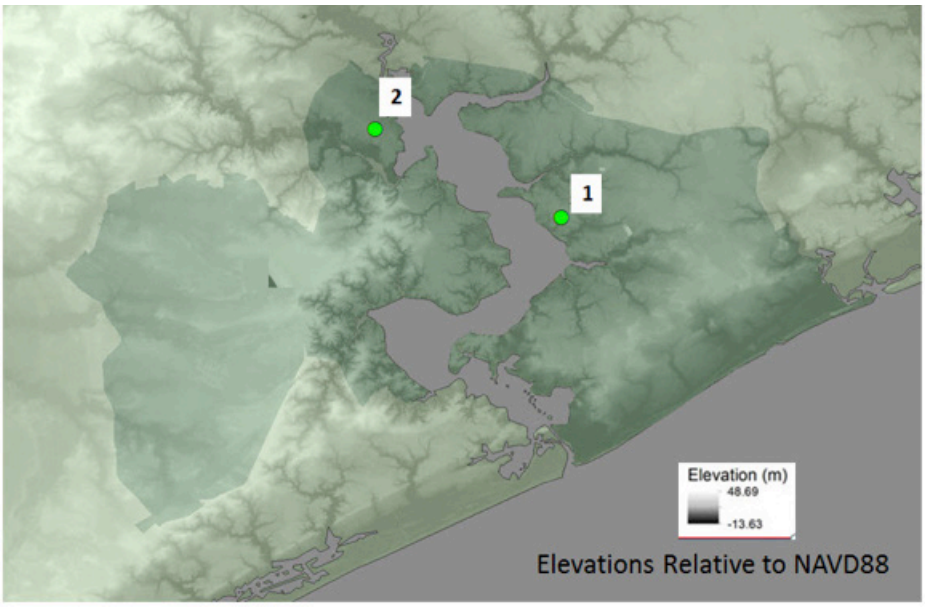

Figure 4.17 Marine Corp Base Camp Lejeune Installation Boundary and Site Point Locations in the Vicinity of or Within Camp Lejeune
Sites depicted correspond to sites in the RPAD and are assigned random numbers here for illustrative purposes.

Table 4.5 NAVD88 Elevations and Tidal Datum Relationships for Camp Lejeune, North Carolina (Elevations in meters)

Site Designation	Name	NAVD88 Elevation	LMSL-NAVD88	MHW-NAVD88	MHHW-NAVD88
1	MCB Camp Lejeune	7.45	-0.02	0.07	0.09
2	MCB Camp Lejeune West Site	6.49	-0.01	0.07	0.09

Because MCBCL has a barrier island associated with the Intracoastal Waterway, has extensive tidal marshes, and occurs along a shallow estuary with inlet and up-estuary constrictions, it exhibits significant variation in tidal amplitudes (i.e., differences in MHW and MHHW) along its shoreline as shown in Figure 4.18. The geodetic and tidal datum elevation relationships along the Atlantic Ocean shoreline differ significantly from those behind the barrier island and up inside the estuary. For the estuary in particular, this is because the range of tides is significantly reduced by the inlet constriction and shallow water proceeding up inside the estuary from the entrance to the open ocean. NAVD88 is 0.62 meters below MHHW along the ocean shore, whereas it is only 0.07 meters below MHHW at the head of the estuary at Jacksonville. Similarly, NAVD88 is 0.12 meters above MSL outside and only 0.02 meters above MSL at Jacksonville. VDatum coverage does not extend into the New River Estuary, so values cannot easily be interpolated based on tidal hydrodynamics. The various sites associated with MCBCL and the main installation itself can be "zoned" to a particular observation station in a manner that reflects use of the most appropriate value for the datum relationships, as indicated by the red dividing lines in Figure 4.18.

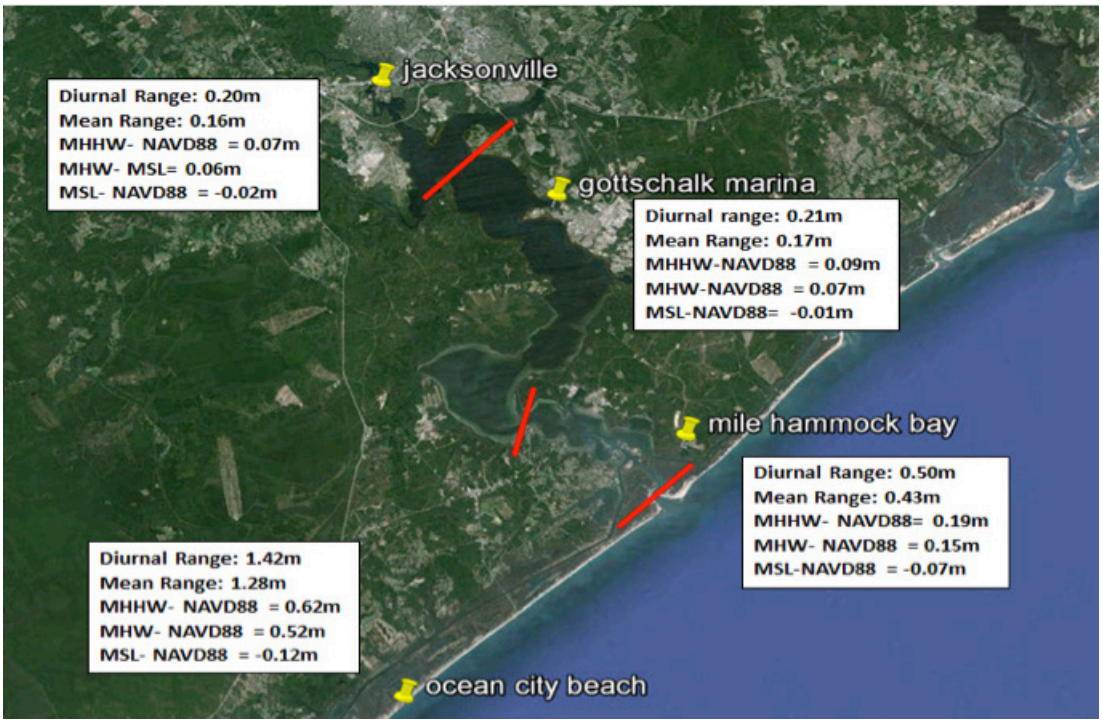

Figure 4.18 Tidal Variability Associated with Marine Corps Base Camp Lejeune
Legends show differences in MHHW, MHW, and MSL, relative to NADV88. Yellow pins are the locations of historical tide observations.

Figure 4.19 is a schematic of the basic geodetic and tidal datum elevation relationships using two of the installation locations. For sites that have a reference datum, combined scenario information (sea-level change plus extreme water level) can be determined relative to the reference datum. With a reference datum, topographic information, and MHHW level, any of the scenarios can be mapped across the spatial extent of an area of interest.

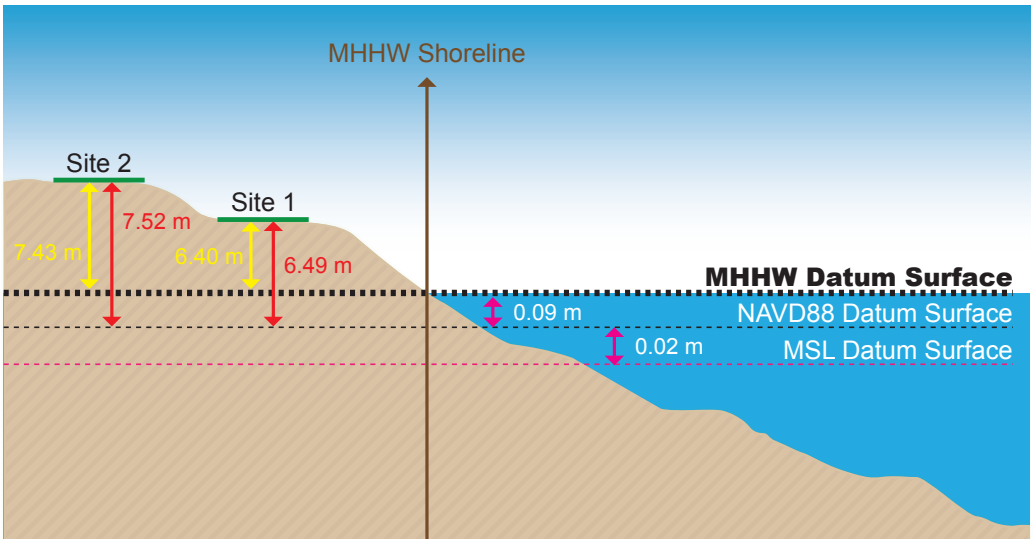

Figure 4.19 Schematic Diagram of Elevation Relationships for Marine Corps Base Camp Lejeune

4.5.3 Summary

The procedure for applying the SLC and EWL scenarios to those sites that represent a larger geographic footprint is to obtain a topographic DEM relative to NAVD88 (or other reference datum) and determine local MHHW and MSL elevation relationships. Vulnerability and impacts can be assessed by determining the elevation relationships for the locations with the lowest elevation topography and assessing assets that are in an exposed location relative to the chosen scenario. Once the total scenario adjustment values are determined, they can be contoured on a DEM to visually identify areas on a site that may be at risk.

For sites that exhibit significant variations in their near-shore tidal datums and for which an interpolation tool such as VDatum is not available, the procedure is somewhat more complex. Variations in tidal surface (expressed as differences in MHHW) need to be accounted for by "zoning" each portion of a site that uses a specific MHW value. The scenario database contains site-specific MHHW information associated with sites within or in close proximity to MCBCL that reflect the zones shown in Figure 4.18. For other sites that may have site-specific variation in MHHW, the same process as outlined above should be accomplished by site planners based on local knowledge.

Overall guidance for mapping impacts of sea-level rise and other types of inundation can be found in NOAA (2010a, 2012). These documents provide guidance on integrating topographic surfaces with geodetic datum surfaces and tidal datum surfaces and then using them to illustrate water level elevation impacts. NOAA (2012) in particular provides different options for creating a tidal surface map if an area will experience different values of MHW. These include using "local" tide gauges and interpolating between them and using VDatum either where it has already been modeled or where it has not by extending its water surface inland by one or more methods.

4.6 Uncertainty Characterization

Contributions to uncertainty in this study are numerous. Some uncertainties can be described quantitatively whereas others can be described only qualitatively. If only climate-related information were involved, we could invoke the conceptualization of Hawkins and Sutton (2009, 2011) with respect to the contributions of emissions scenario, structural (model), and internal (natural variability) to uncertainty; however, other sources are involved relevant to this study. Before describing these, however, it is important to note that uncertainty attributable to scenarios cannot be quantified because by definition scenarios are not assigned likelihoods—though as Hawkins and Sutton (2009, 2011) illustrate, scenario uncertainty tends to be less important unless longer timeframes are involved. The other two types of climate-related uncertainty affect the confidence that can be placed in the DSL and ice melt adjustments, but even here the climate models are only part of the uncertainty that must be considered. At the regional scale, ice melt fingerprints, for example, add additional uncertainty.

Beyond the preceding, the issues involved in regionally adjusting the global SLR scenarios, adding EWL estimates, and applying the combined results to determine potential inundation and flooding levels at a particular site add additional contributions to uncertainty. These differ from the climate-related modeling contributions and generally relate to measurement errors. These errors can relate

to mostly static measurements (i.e., topographic measurements or datums and their conversions, though over long timeframes datums can change) or rates and cyclical behavior whose effect on uncertainty may increase as either longer timeframes are considered (i.e., VLM) or the chance of occurrence involves rare events (e.g., 1% annual chance event estimates). Section 5.2.3 provides case studies that illustrate the effect of topographic errors on mapping scenario information. Finally, with respect to estimating future sea levels, other factors that may affect future EWLs currently cannot be easily quantified. These include the effects of waves, nonlinearity of storm surge, and responses of biological and physical systems to sea-level change. Table 4.6 summarizes, by component, the types of uncertainty considered and how they were addressed in this report.

Especially with respect to international or U.S. climate assessments (e.g., see Mastrandrea et al. 2010), guidance on treatment of uncertainties has been developed. In general two metrics are encouraged when communicating the uncertainty in key findings: (1) confidence in the validity of a finding and (2) quantified measures of uncertainty in a finding expressed probabilistically, which can include expert judgment. In Section 3 and in some cases Section 4, we describe how we addressed these metrics for the individual components that we considered in this study. To address the issue of confidence we indicate the degree to which our findings are comparable to similarly related findings in the literature (in some cases using this information to validate our findings); however, we do not attempt to add the calibrated language recommended by Mastrandrea et al. (2010) to describe our degree of confidence. Assessing multiple sources of information, such as for VLM information, also serves to increase the confidence in our findings.

To address measures of uncertainty, in the scenario database we include model-spread information to characterize the uncertainty in the DSL and ice melt adjustment estimates, though additional non-quantified uncertainty estimates may be associated with the spatial patterns themselves above and beyond the uncertainties due to temperature effects. In addition, to first generate the contributions of the various components of ice melt (i.e., glaciers, Greenland, and Antarctica) we ran Monte Carlo simulations to estimate the probability distributions of all contributions to global sea level needed to achieve the 1.5-meter and 2.0-meter scenarios (see Section 3.4.4 for details). For errors associated with observational records, we included standard estimates of error associated with the VLM and EWL estimates that were sensitive to the data source considered and its length of record. The use of Regional Frequency Analysis was in part related to overcoming the lack of a representative tide gauge at a site or an insufficient record length at sites where a gauge was present. In many cases, however, we found that an RFA also improved the statistical confidence intervals associated with rarer events. We note that we did not explicitly account for any possible inter-site correlation between annual-highest NTR within our regional set of tide gauges. Such event correlation would, in some instances, produce under-estimation in our RFA confidence intervals. Nonetheless, regional information helps to mitigate the influence of previously unobserved low probability and high magnitude events (e.g., Hurricane Sandy) on the overall statistical probability of extreme events or to compensate for the lack of tide-gauge observed rare events at some locations that otherwise are still prone to their occurrence. For example, some areas along the U.S. Southeast Coast have not experienced hurricanes captured by the tide gauges, but are located where such events are physically plausible (see Section 4.4.4).

Combining uncertainties presents additional challenges. Church et al. (2013c) provide a formulaic approach to combining uncertainties that affect regional sea-level projections in which correlated uncertainties (in this case to global air temperature) are added linearly and other uncertainty components are added in quadrature (these uncertainties could be dominated by the magnitude of climate change or by methodological uncertainty [see Church et al. 2013c]). The covariance structure associated with the ice melt components, in particular, has been difficult to quantify (see Grinsted et al. 2015 for an attempt to address covariance issues in part), which adds additional uncertainty. The addition of EWLs adds additional layers of complexity for characterizing overall uncertainty (see Kopp et al. 2014 and Tebaldi et al. 2012 for example attempts to combine SLR and flood risk uncertainty estimates involving storm surge). Combining uncertainties in any quantitative manner was considered beyond the scope of the present study given its focus on providing screening-level scenario information, the complexities involved, and the unresolved science issues.

Table 4.6 Sources of Uncertainty

Component	Types of Uncertainty	How Addressed in the Report
Global Scenarios	To the extent these are based on plausible future emissions trajectories that are dependent on human behaviors and policy choices, these legitimately cannot be assigned likelihoods. As a result, rather than assigning scenarios specific probabilities or creating a probability distribution around a central tendency, the objective is to capture the full range of potential futures within a risk management context. Instead of attempting to narrow uncertainty regarding particular futures, a scenario approach enables managing the uncertainty.	▪ Bounding scenarios are used based on observational information, process models, expert elicitation, and an understanding of physical limits. ▪ Although probabilities are not considered explicitly, taking a more expansive view of model spread information and confidence from the perspective of the decision-makers concern with the 1% chance outcome provides additional support for the upper scenarios. ▪ The range of plausible scenarios was obtained from Parris et al. (2012), who expressed greater than 90% confidence that global mean sea level would not fall outside 0.2 to 2.0 meters by 2100 (starting from 1992).
Dynamical Sea Level	For a given scenario, multiple types of uncertainty must be considered: ▪ Scale factor at a particular point, ▪ Global temperature that is a parameter of the pattern scaling, and ▪ Pattern scaling across models.	▪ Perrette et al. (2013) demonstrated the validity of using the pattern-scaling approach. ▪ For a given scenario, uncertainty in global temperature was estimated from the model spread provided by Perrette et al. (2013). ▪ The variability of pattern scaling across models was not considered but data provided by Perrette et al. (2013) has shown that the patterns across models are generally similar.
Ice-Melt Fingerprints	For a given scenario, multiple types of uncertainty must be considered: ▪ Fingerprint approach and its variability across models, ▪ Contributions of individual ice-melt components, and ▪ Geometry of melt.	▪ The fingerprint approach, commonly used in the literature, is considered to be the current practice and no effort was made to seek an alternative. Because no reliable estimates of this uncertainty exist, we did not address this uncertainty. ▪ The uncertainties of individual ice-melt contributions were determined from the Monte Carlo approach (see Table 3.8). ▪ We applied the geometry assumptions of Bamber and Riva (2010) as used by Perrette et al. (2013)

Section 5.0
Case Studies and Additional Considerations

How scenario information is applied can be just as important as the values themselves. As we stress repeatedly throughout this report, one answer to the question "What future scenario should I use to plan for sea-level change?" does not exist. In this section additional information (via case studies and other discussions) is intended to foster better understanding of the influence of physical setting (Section 5.1), data availability and quality (Section 5.2), and the nature of the decision type and decision-maker's tolerance for risk on the choice and application of the scenarios developed by this effort (Section 5.3). Section 5.3 concludes with a brief treatment regarding scenario application in the zero (i.e., 2015) to twenty-year timeframe. We do not offer the following as explicit guidance; rather we attempt to illustrate the use of scenarios acknowledging some confounding factors, data limitations and how they might be addressed, and specific application considerations. Other approaches, especially with regard to addressing data issues and concepts of application, may be appropriate.

5.1 Influence of Physical Setting

Two main and potentially exacerbating effects can result from physical setting; scenario users should consider these effects when applying sea-level change and extreme water level (EWL) scenarios. This section addresses nonlinear effects of storm surge (Section 5.1.1) and the influence of wave environments on extreme water levels (Section 5.1.2). These are both important considerations whose quantitative assessments were beyond the scope of the present effort. Moving forward, however, they are both important considerations that deserve further research attention in support of vulnerability and impact assessment and other uses in the coastal environment.

5.1.1 Nonlinear effects of storm surge

Storm surge is generally considered to be caused primarily by low atmospheric pressure and high wind speed. The air pressure linearly affects storm surge but this is not necessarily the case with the wind-driven component of surge, which is a function of wind speed, fetch length, and depth. Many studies, and some current public policy (USACE 2014), assume surge is independent from sea-level rise (SLR) and that total water level (for SLR scenarios) can be calculated by simply adding sea-level rise to storm surge magnitude. This approach, however, has been described as "simplistic" (Woodruff et al. 2013) and can result in a potentially significant underestimation of actual future water levels.

When modeling storm surge in open water with constant depth and constant bottom roughness, surge magnitude is proportional to:

$$surge \propto U^2 \frac{W}{h} \quad [5–1]$$

in which *U* is wind speed, *W* is the distance over which the wind blows in the same direction (uninterrupted), and *h* is the mean water depth over the region where the wind blows (Resio 2008).

This, in turn, makes surge magnitude inversely proportional to water depth:

$$surge \propto \frac{1}{h} \quad [5–2]$$

From this relationship, one would expect surge magnitude to decrease with increasing sea levels. This has been shown to be true in various open water numerical modeling studies; however, the effects of storm orientation, shoreline geometry, bottom roughness, and bathymetry combine to create strong nonlinear effects on storm surge magnitude in many areas, often resulting in a disproportionate amplification in surge magnitude not represented by this open water relationship. It is important to note that Equation 5–2 is applicable in open water settings only; the studies reviewed below illustrate conditions in which Equation 5–2 does not hold.

Multiple published studies over the past eight years have evaluated the nonlinear effects of SLR on storm surge (Bilskie et al. 2014, Irish et al. 2014, Nadal-Caraballo et al. 2015, Smith et al. 2008, 2010, Woodruff et al. 2013). These studies evaluated the potential effects of SLR on storm surge magnitude for historical storms such as Hurricanes Katrina and Sandy as well as for synthetic storms and focused on two primary areas: (1) the northern Gulf of Mexico (Alabama, Mississippi and Louisiana) and (2) the U.S. North Atlantic Coast between North Carolina and New Brunswick, Canada.

Smith et al. (2008, 2010) analyzed synthetic storms along coastal Louisiana and Mississippi. Their analyses considered six synthetic hurricanes in southeastern Louisiana with different tracks and orientations, which all generated water levels of approximately 1% annual exceedance probability or 100-year storms (see Figure 5.1). The effects of SLR on surge were somewhat consistent for all six storms with specific results provided for one storm to illustrate the effects. Those results showed that some areas experienced almost linear effects of SLR on total water level, a few areas showed decreases in surge magnitude, and several areas, where base surge magnitudes were in the moderate range (relative to the entire study area), showed surge magnitudes increasing by two to three times the amount of relative SLR over broad areas and increasing by as much as five times the relative sea SLR in some isolated areas. Common characteristics of the areas experiencing increased surge were that they were on the right side of the storm track (thus experiencing stronger side onshore winds) and that they were in shallow water where the magnitude of SLR was a significant percentage of the total water depth.

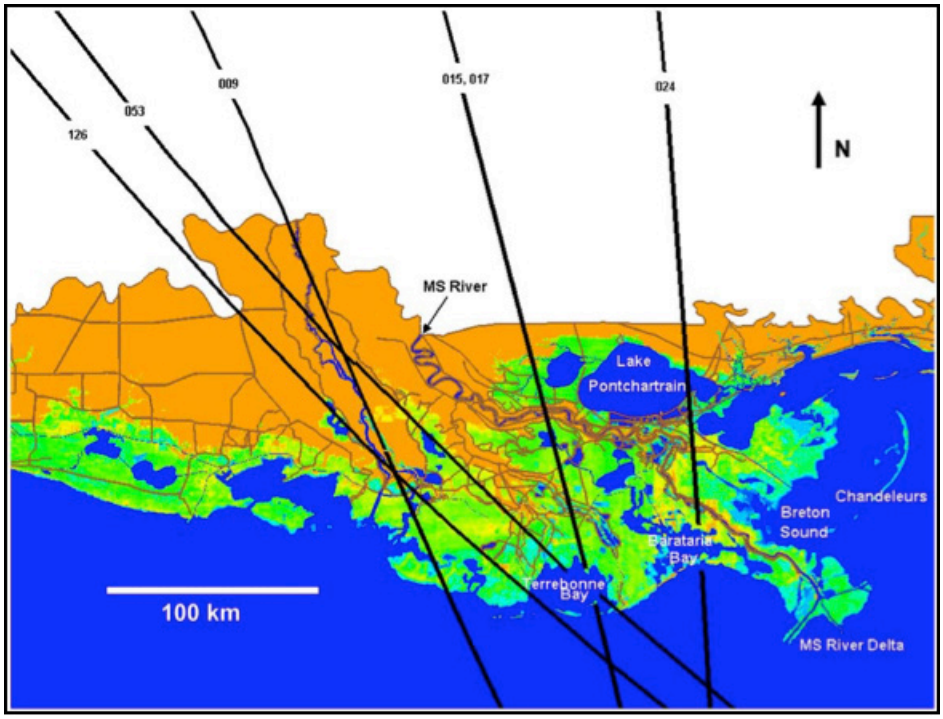

Figure 5.1 Synthetic Hurricane Tracks
(from Smith et al. 2010, with permission)

Irish et al. (2013) evaluated the effects of two sea-level rise scenarios (0.18 meters increase and 0.75 meters increase) on Hurricane Katrina along the Louisiana and Mississippi coasts. They considered the relative effects of hurricane intensification and SLR (both concerns associated with changing climate) and found the effects of SLR to be much more significant than hurricane intensification, depending on the bathymetric setting and the corresponding nonlinear effects of SLR on surge magnitude. They concluded that the increases in flood elevation for a given storm, depending on the setting, may greatly exceed the SLR for that region. The Irish et al. (2013) analysis showed differing effects of SLR on storm surge with total water surface increases relative to SLR varying from 50% to 169% in certain areas of interest (see Table 5.1).

Bilskie et al. (2014) investigated the nonlinear effects of SLR on storm surge by considering multiple influencing factors including: increased depth, topography, land use, and land cover. Their work demonstrated that regions experiencing a linear increase in total water level are primarily off the coast in deeper water, thus corroborating the findings of Smith et al. (2010) that the ratio of SLR to water depth has an effect on the nonlinear increase in surge magnitude. Bilskie et al.'s (2104) study of the Mississippi and Alabama coasts also found that maximum water level increased an additional 80% of the applied SLR in most areas (e.g., Mobile Bay and western Mississippi Sound). This resulted in amplification of storm surge greater than the amount of SLR.

Table 5.1 Sea-Level Rise Effects on Hurricane Katrina Near-Shore Surge Magnitude in Louisiana and Mississippi
(adapted from Irish et al. 2013, with permission)

Location	Increase in Surge Magnitude (SLR = 0.18 meters)	Increase in Surge Magnitude (SLR = 0.75 meters)
Lake Pontchartrain, LA	0.29 (161%)	0.98 (131%)
New Orleans, LA, 17th Street Canal (near levee breach)	0.22 (122%)	0.77 (103%)
New Orleans, LA, Lower 9th Ward (near IHNC levee breach)	0.09 (50%)	0.74 (99%)
Plaquemines Parish, LA, East Bank	0.11 (61%)	0.60 (80%)
Grand Isle, LA	0.09 (50%)	0.53 (71%)
Bay St. Louis, MS	0.32 (178%)	1.27 (169%)
Biloxi, MS	0.19 (106%)	0.80 (107%)

The studies cited above evaluated SLR on storm surge for areas of the northern Gulf of Mexico. More recent work by the U.S. Army Corps of Engineers (USACE), as part of the North Atlantic Coastal Comprehensive Study, evaluated the nonlinear effects of SLR on storm surge for the northeastern United States between North Carolina and New Brunswick. As part of this study, USACE performed a detailed numerical modeling evaluation of storm surge using both current values for mean sea level and a potential 1-meter rise in sea level. Similar to the conclusions by Smith et al. (2010) and Bilskie et al. (2014), USACE found that many deeper water and open coastline locations experience only small nonlinear effects of SLR. Other locations, with shallow water, fringing marshes, or irregular shoreline geometries experienced storm surge increases equal to approximately 180% of the SLR magnitude or almost double the effect of the SLR by itself. This value is identical to what Bilskie et al. (2014) found for the Alabama and Mississippi coasts (Cialone et al. 2014, Nadal-Caraballo et al. 2015). For these locations, a simple linear summation approach for calculating total water level from surge and a 1-meter rise in sea level would result in underestimating total water level by 0.8 meters (2.6 feet).

…many deeper water and open coastline locations experience only small nonlinear effects of SLR. Other locations, with shallow water, fringing marshes, or irregular shoreline geometries experienced storm surge increases equal to… almost double the effect of the SLR by itself.

In combination, the studies referenced in this section clearly demonstrate the importance of properly considering the nonlinear effects of SLR on storm surge magnitude and total water level. A linear summation of SLR and storm surge can overestimate total water level in some locations, which would result in unnecessarily conservative design considerations. On the other hand, it can significantly underestimate total water level in other locations, which would result in underestimating risk and therefore designing and implementing ineffective design alternatives.

5.1.2 Influence of wave environments on extreme total water level estimates

The physical setting of a location often will favor particular high water components. For instance, when extreme (still) water levels occur, certain locations around the world are much more tidally influenced than other locations (Merrifield et al. 2013). Sweet et al. (2014) provide a ratio for the U.S. coasts, identifying regions where tides (e.g., West Coast) or nontidal effects (e.g., Gulf Coast) tend to drive the extent and timing of high-water events. High-water components shown (Figure 5.2) for NOAA tide gauges at the Battery, New York, and San Francisco, California, show differing influences of cool-season storm surges (Battery) and solstice-enhanced tides (San Francisco) relative to a flood threshold level for minor (nuisance level) impacts.

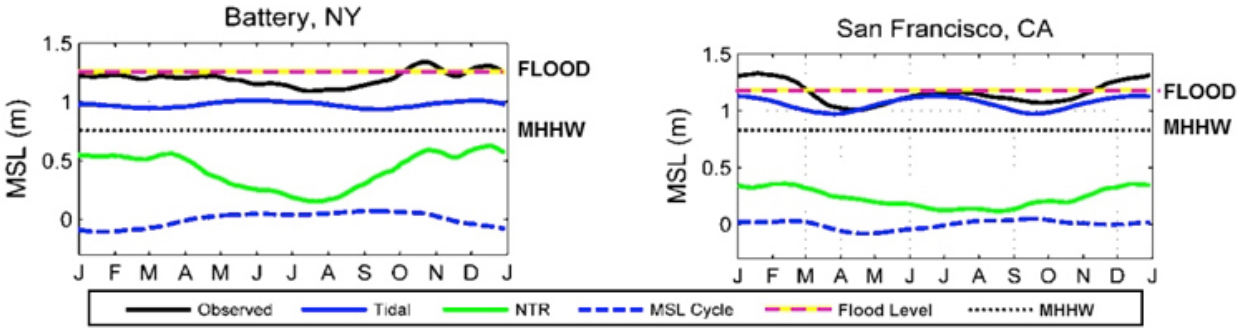

Figure 5.2 Maximum Observed Water Levels per Calendar Day over the 1980–2009 Period
Water levels (black lines) are shown relative to NOAA's mean sea level (MSL) tidal datum and local minor "nuisance" flood impact level (yellow-magenta dashed line) and MHHW datum elevation (black dotted line). The maximum water level series is decomposed into a low-frequency MSL cycle (blue dash), predicted tide (blue line: without the annual and semi-annual harmonic fits) and remaining nontidal residual (NTR: green) all smoothed by a 30-day running filter shown for the Battery, NY and San Francisco, CA. Note the components are not necessarily additive due to the smoothing process of each individual component. (from Sweet et al. 2014)

As seen in Figure 4.11, the probability for extreme nontidal residual (NTR) events differs spatially due to storm-generating characteristics and bathymetric constraints of water level set-up imparted by the width of the adjacent continental shelf. Often, greatest impacts (e.g., coastal erosion, island overwash) along an open coast are the result of wave effects (e.g., run-up) and characterized in terms of a total water level (TWL; Moritz et al. 2015, Ruggiero et al. 2010). See Figure 3.12 for an illustration of TWL components. This is especially true where historically storm surge (NTR) is relatively small and extreme wave patterns and their effects are relatively large (e.g., West Coast and islands generally). Figure 5.3 shows the history of maximum significant wave heights for the active month of January derived from multiple satellite altimeter records. The northern hemisphere and adjacent boundary regions are especially vulnerable to large wave impacts. For instance,

along dune-fronted coasts typical of much of the West Coast, K. Serafin (personal communication 2015) has indicated that the value exceeded by 2% of the run-up events ($R_{2\%}$; Stockdon et al. 2006) occurring during the 100-year TWL event ranges from about three to seven times higher in elevation than the NTR component. This ratio of $R_{2\%}$ to NTR is higher along the California Coast and decreases northward along coastal Washington State, where NTR probabilities become increasingly larger in magnitude (e.g., Figure 4.11).

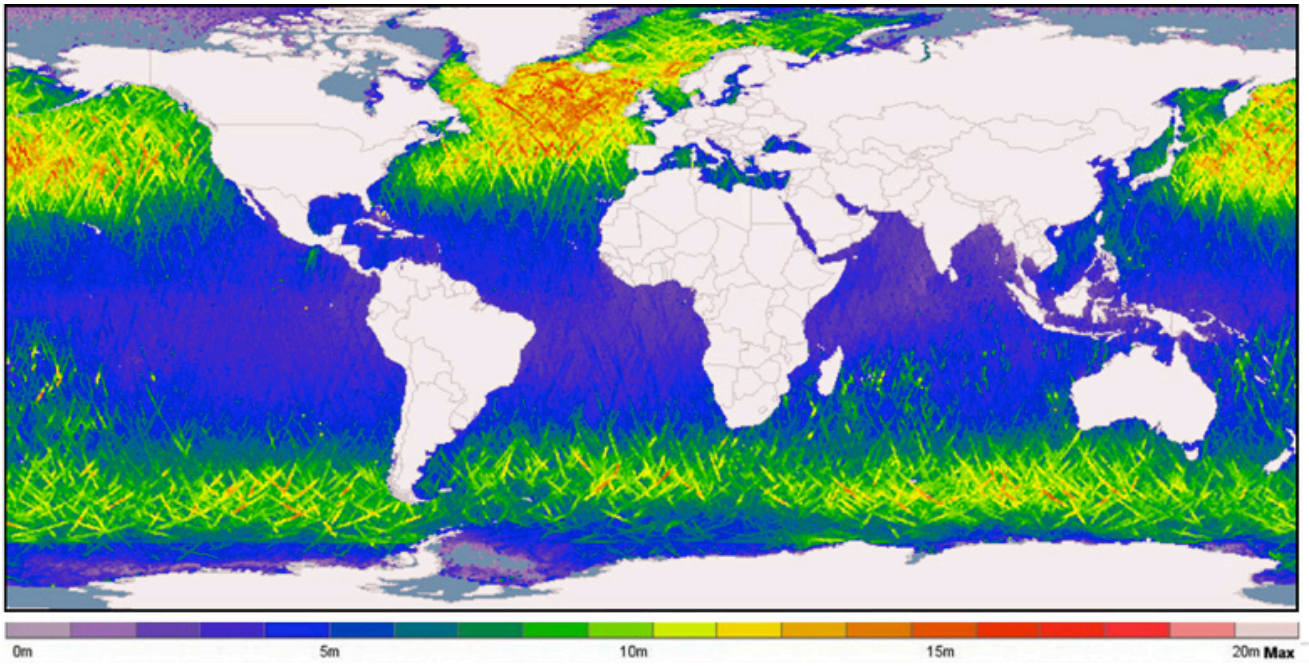

Figure 5.3 Multi-year Quarter-Degree Maximum Significant Wave Height Climatology for the Month of January
Data are derived from ENVISAT, ERS1, ERS2, GFO, Jason1, Jason2 and TOPEX Satellite Altimeter. Data are from the GlobWave project (http://globwave.ifremer.fr/) and are processed and plotted by the Australian Government's HM Branch METOC Geospatial service (http://www.metoc.gov.au/products/wms_globwave, accessed December 2015).

In terms of impacts to infrastructure along developed coastlines (e.g., overtopping of seawalls or damaging hydraulic conditions in harbors), Sweet et al. (2015) provide estimates of high-frequency wave-related effects present during hourly sampling at tide gauges utilizing the standard deviation (sigma) of the water level measurement. Tide gauges are usually located in protected harbors and not exposed to breaking-wave conditions. As a result, tide gauges generally do not experience wave runup (on a sloping beach), but they do experience a more dynamic range of water levels than the slow-changing "average" water levels that they are designed to report (i.e., SWL) and used within this study. Sweet et al. (2015) define this dynamic component to include incident and infragravity wave-band variability, which can be as large as or larger than the NTR water level component during an extreme event.

The magnitude of the dynamic range is defined by Sweet et al. (2015) as SWL + α*sigma with "α" an exceedance duration coefficient associated with the sampling period (e.g., α of 1.96 would

approximate the 95% of the typical Gaussian water level distribution). Figure 5.4 shows the ratio of the 99.5% of daily maxima NTR to sigma over 1996–2014, which approximates the largest event (NTR or sigma event, as they are typically not correlated) per year on average. When the ratio is less than two, 1.96*sigma has a magnitude on par with or larger than the NTR. This is more apparent progressively southward along the West Coast (similar to the pattern of K. Serafin, personal communication 2015) and islands exposed to the dominant wave regime (e.g., northern shore of Hawaii), where NTR storm surge is typically smaller in magnitude compared to the U.S. East and Gulf Coasts. It should be noted that dynamic components associated with the built environment or TWLs affecting sloping beaches are not explicitly accounted for in the study herein and should be considered when extreme water level events are typically the result of damaging waves (e.g., small value of NTR to sigma ratio in Figure 5.4) compared to extreme storm surges.

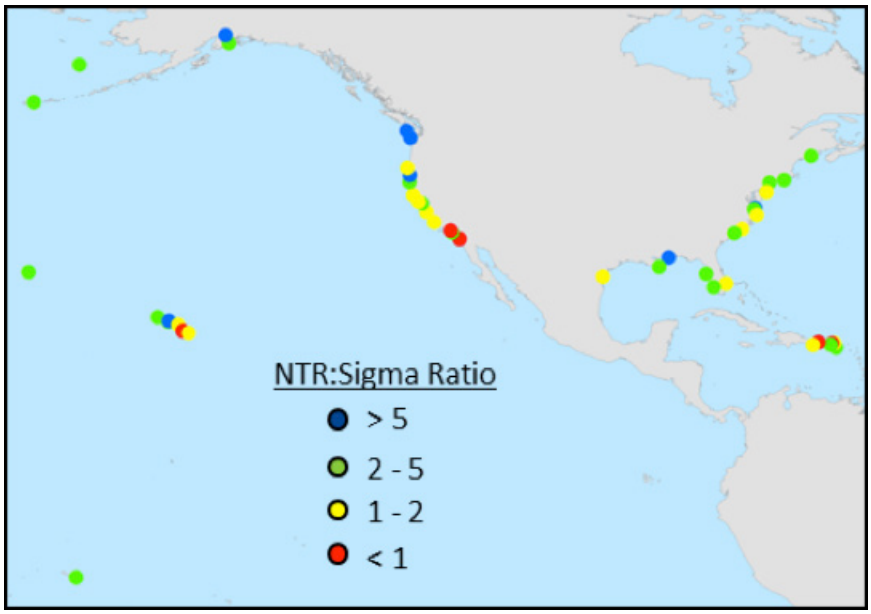

Figure 5.4 Ratio between the 99.5% of Daily Maxima of Hourly NTR and Standard Deviation (sigma) Computed during Water Level Sampling over 1996–2014
(adapted from Sweet et al. 2015: Fig. 4b)

5.2 Influence of Data Availability and Quality

Data availability and quality strongly affect the capability to develop and apply scenario information. Three types of data issues are addressed in this section. First, Section 5.2.1 provides a case study on the application of a regional frequency analysis (RFA; see Sections 3.5.4 and 4.4.1 for details). Tide gauges are a necessary component for deriving EWL statistics, yet close to half of the military coastal sites considered in this study lack a representative tide gauge of sufficient record length to calculate EWL values. An RFA (using tide gauges across a region of interest) provides an alternate approach. The case study below provides an illustration of the analysis and its implications for a particular site. Some sites, in particular international sites, lack tidal datums or geodetic datums or both. Datums are necessary for anchoring scenario information in the vertical dimension. Section 5.2.2 provides general guidance on how sites lacking these datums might

address these data gaps. Finally, Section 5.2.3 provides a case study that illustrates the critical importance of having high-resolution topographic information for mapping scenarios in a spatially explicit manner. The section also describes the importance of understanding any variation in the tidal surface at a site for mapping scenarios involving EWLs.

5.2.1 Regional frequency analysis versus a single tide gauge analysis

To estimate EWL probabilities at as many as possible of the 1,774 global Department of Defense (DoD) coastal sites, when only about half (52.6%, Table 3.10) have a co-located (defined herein as less than 50 kilometers [km] away from the site being considered) tide gauge of sufficient record length (defined herein as at least 30 years) to provide a direct statistical estimate, requires a regional approach. A robust approach is based on a regional frequency analysis or RFA using a network of tide gauges. The RFA approach enables an EWL probability estimate for locations not co-located with a tide gauge, helps reduce prediction error of low probability events, and minimizes record-length statistical biases even for sites with a co-located gauge (Hosking and Wallis 1997). In the usage followed herein, we construct a regional extreme distribution using Generalized Extreme Value (GEV) fits (Coles 2001) from time series of normalized nontidal residual annual maxima consisting of three to five regional tide gauges located less than 400 km distance away from the site of interest. This distance is less than the synoptic scale "footprint" of extratropical systems and maximum winds diameters of most tropical systems.

The precise number of gauges used is objectively chosen by a "heterogeneity" statistical measure. The regional distribution is localized by scaling by the mean annual NTR value, which is either from the co-located tide gauge (if less than 50 km away) or the group average if the closest tide gauge is greater than 50 km away. We utilize the NTR component instead of the "observed" water level because EWL events are dependent on both storm surge magnitude and tidal phase, the latter of which can be as large as or larger than the storm surge. To express the extreme NTR probabilities in terms of potential impacts, we express them relative to the mean higher high water (MHHW) tidal datum. Along most of the continental United States, a connection between MHHW and a land-based geodetic datum (e.g., map datum) is readily available from NOAA (http://vdatum.noaa.gov/).

Here, we provide an example of how a group of tide gauges through usage of the RFA method can provide actionable information for a screening-level vulnerability or impact assessment regarding EWLs for Tyndall Air Force Base (AFB) in Florida (Figure 5.5). Tyndall AFB is classified as a Category 1 site (Table 3.9) with a long-term (Panama City; greater than 30 years' record) tide gauge co-located (less than 50 km), whose NTR extreme probability is based on a set of five (homogeneous; H less than 1) tide gauge NTR series. The five tide gauges have record lengths that range from 12 to 88 years in record (Figure 5.5) and from about 20 to 250 km away in distance. Single-gauge GEV analysis and return-level interval curves (return curves) are shown in Figure 5.6 for the five tide gauges and reveal the propensity for extremely large storm surge events with positive return interval curves (upward-sloping shapes). It is also clear, however, that the uncertainty or spread of the 90th percentile confidence interval (dashed lines) becomes quite large

when stand-out (i.e., event that may be viewed as an outlier relative to the rest of the distribution) extreme occurrences occur and more so when over a relatively short record length (Dauphin Island, Alabama; Apalachicola, Florida). To account for this, the RFA process establishes a larger sample size of NTR annual extremes to assess return probabilities for events of various magnitudes.

After normalization, a regional curve is composed whose unique return level interval curve for Tyndall AFB (bottom right in Figure 5.6) is *localized* by scaling of the mean annual maxima NTR value from the co-located tide gauge in Panama City. The return curve for Tyndall AFB is similar in expected value to the individual analysis at Panama City, but has a narrower spread in the 90th percentile confidence interval. In Figure 5.7, we compare results obtained by filtering out all but the highest value across the region of the annual maximum NTR events recorded at each tide gauge location that happen to occur within a 5-day window. This process arbitrarily minimizes event dependencies during the RFA process but might in fact eliminate two independent NTR events from possible rapid succession of storms (i.e., clustering). The GEV results with the 5-day filter shown in Figure 5.7(a) are largely unchanged as compared to the results without usage of the spatial-temporal filter in Figure 5.7(b). The NTR probabilities are slightly less (about 5 centimeters [cm]) at the 5-, 20-, 50-, and 100-yr change event levels when the 5-day filter is applied and the spread of the 90th percentile confidence intervals are 20 cm larger at the 100-year level and 10 cm at the 20-year level. The RFA-based return curves, in general, are largely influenced at lower probabilities (longer return periods) by the regional storm surge response experienced during Hurricane Opal in 1995. As shown in Figure 4.11 the RFA-based estimates when applied to MHHW provide comparable results in hurricane prone regions to single gauge analyses, especially at the lesser magnitude probabilities (e.g., 20-year events). A more detailed analysis employing synthetic results from dynamical models (e.g., Haigh et al. 2014a, Nadal-Caraballo et al. 2015) may be warranted if impacts from rare events (e.g., 100-year event from a hurricane strike) are the major concern today or in the future.

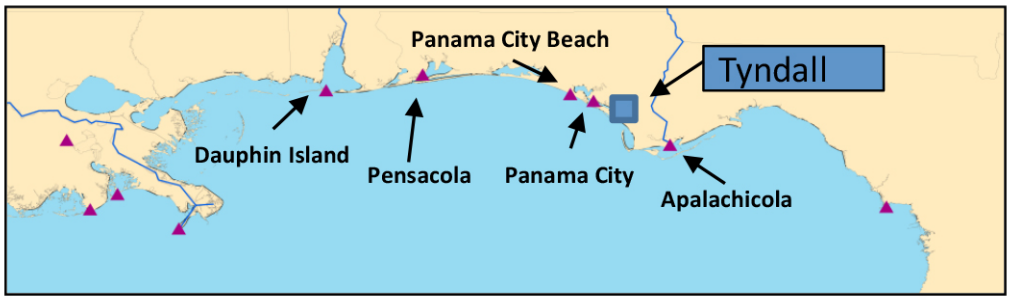

Figure 5.5 Location Diagram for Alabama and Florida Sites Depicted in Figure 5.6
Purple triangles indicate tide gauges.

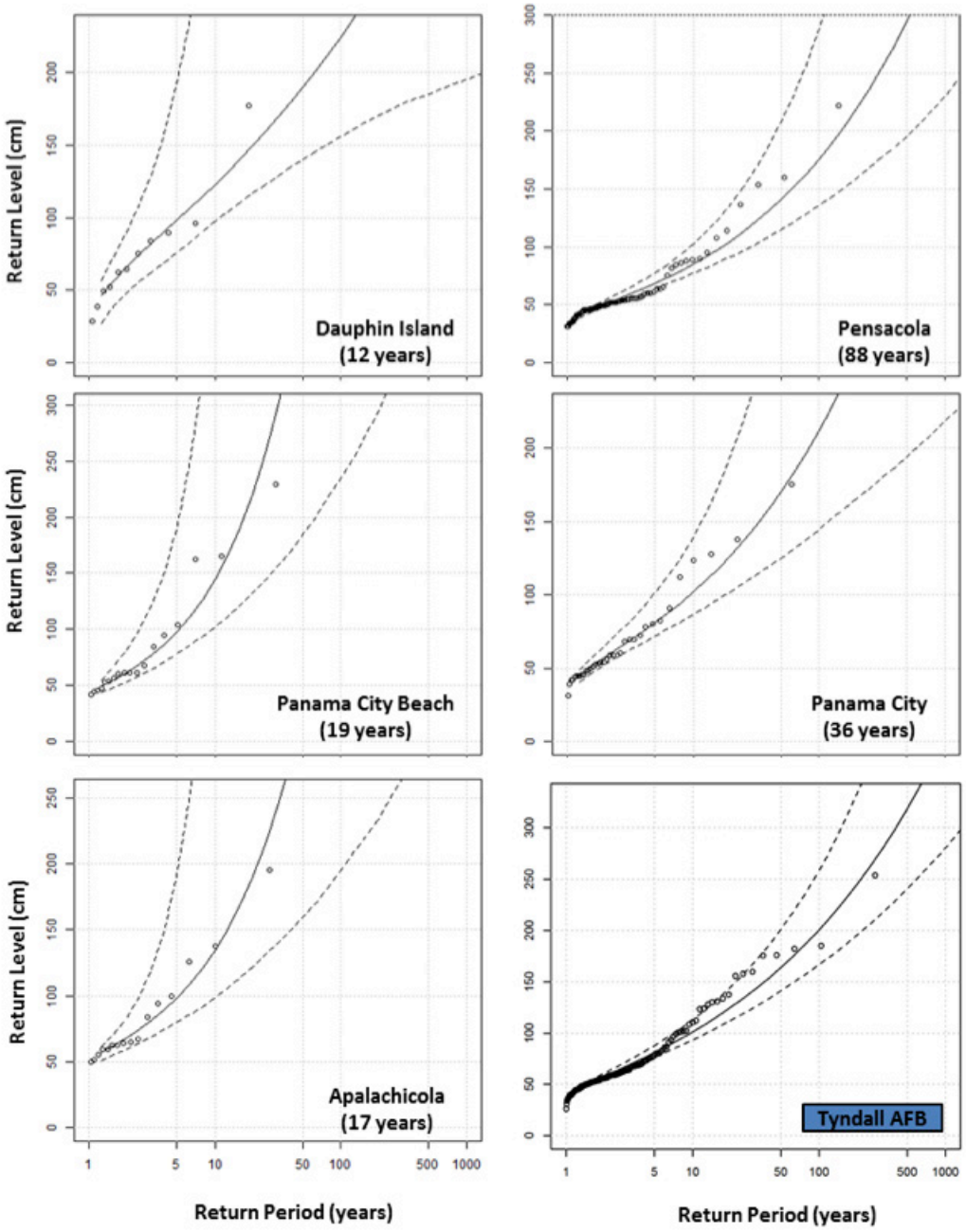

Figure 5.6 Examples of Return-Level Interval Curves for Annual NTR Maxima (circles) Based on Regional Frequency Analysis (RFA) for Tyndall Air Force Base

Fit by GEV based on five individual tide gauges (purple triangles) within the Northern Gulf of Mexico with GEV fits shown. The spread of the 90th percentile confidence interval (dashed) is larger at longer return periods for shorter record lengths and even more so with the occurrence of a stand-out extreme-event occurrence (larger shape parameter; Figure 3.19). The Cunnane plotting position (Coles 2001) is used to illustrate the annual NTR maxima data.

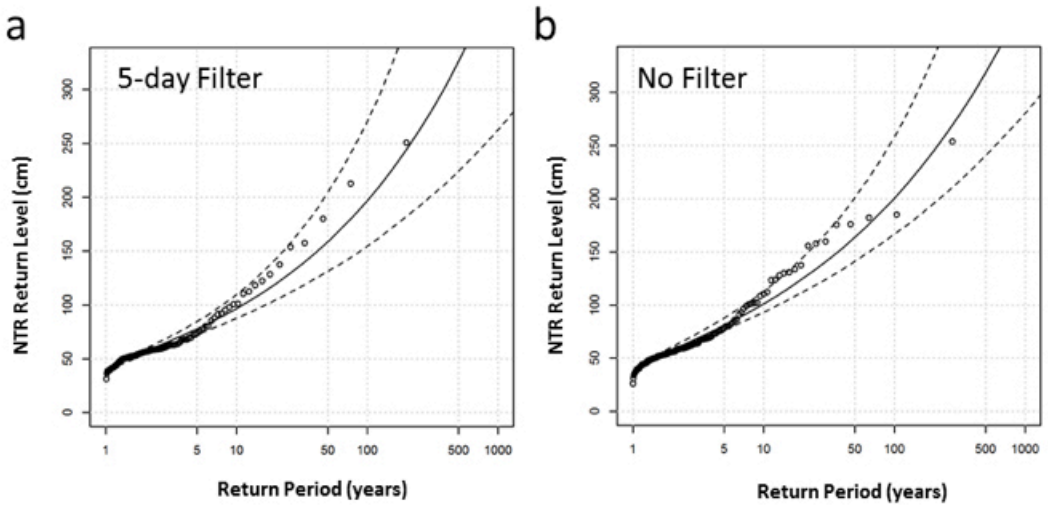

Figure 5.7 Return-Level Interval Curves (solid line) and the 5th and 95th Percentile Confidence Intervals (dashed lines) for Annual NTR Maxima (circles) based on Regional Frequency Analysis (RFA) for Tyndall Air Force Base

A 5-day spatial-temporal filter is applied in (a) to minimize event dependences within the region and in (b) no filter was applied (and shown in Figure 5.7, bottom right) prior to fitting the regional data set with the GEV distribution.

5.2.2 Installations without tidal datums and geodetic elevation references

Continental United States and Caribbean

For locations where tidal information is not available in the lower 48 states, Puerto Rico, and the U.S. Virgin Islands, the NOAA VDatum tool (NOAA 2012) can be used to obtain required elevation relationships among Mean Higher High Water (MHHW), Mean Sea Level (MSL), and NAVD88 or other appropriate geodetic datums such as PRVD02 in Puerto Rico or VIVD09 for the Virgin Islands. This means in most instances that a tide gauge will not be required for obtaining tidal datum elevations for areas covered by the VDatum model grids.

To actually apply the datum information, the local installation managers must translate local reference elevation drawings to the applicable geodetic datum. If a local reference mark exists with a published elevation in the NOAA National Geodetic Survey benchmark database (http://www.ngs.noaa.gov/datasheets/), then that benchmark(s) can be used for control. If no local reference benchmark exists, then a reference benchmark should be established and occupied with a static Global Positioning System (GPS) survey for a minimum of 3-hour to 24-hour successive observations sessions to obtain a reasonable geodetic datum vertical elevation accuracy. The GPS data must be processed through the NGS Online Positioning User Service (OPUS) system to obtain results (http://www.ngs.noaa.gov/OPUS/about.jsp, accessed December 2015). The OPUS solutions will provide elevation relationships to geodetic (NAVD88) and ellipsoidal datums. This GPS observation should be repeated once per year to monitor for vertical land movement.

Other Locations

For those global locations where little is known of the elevations of tidal and geodetic datums and the relationship of sea level to the local topographic elevations, a short-term tide gauge should be established and operated for a minimum of three months to provide estimates of local tidal datum elevations relative to local land. One year of continuous measurements is preferred so that seasonal variations, which are usually quite large, can be taken into account. The absolute minimum duration of observations is 30 days and applies to areas with strong tidal signals that dominate all other sources of water level variation. Uncertainty in datum elevations will be significantly reduced with longer measurement time periods.

The approach can be summarized as follows:

1. Install an off-the-shelf water-level sensor and self-recording data collection system along the shore closest to the site under consideration. Use existing infrastructure if possible to mount the sensor.
   a. The sensor type is not restricted and can be a pressure sensor, bubbler/pressure, microwave, acoustic, or even float-operated.
   b. The sensor should be installed at an elevation such that it collects the lowest and highest expected water levels.
   c. The sensor must be a version calibrated by the manufacturer to measure the expected range of water levels.

2. Survey the sensor into the vertical reference system used for the location. This enables water levels and datums to be determined relative to the land and the location infrastructure.
   a. The sensor "0" or measurement reference point must be surveyed-in (or steel-tape measured) to a fixed leveling point above the sensor. This fixed leveling point then can be connected to nearby reference benchmarks and critical vertical survey points via survey levels or via kinematic GPS surveys.
   b. The sensor "0" elevation must be held fixed during the deployment period. If the sensor is reinstalled for any reason, it should be placed back at the same vertical elevation. If not, then the data collected after re-installation will have to be corrected such that it is referenced to the same initial vertical "0" for processing and tabulation.
   c. Levels or surveys to the benchmarks should be performed upon installation and at the 3-month removal stage. If left in operation for longer time periods, annual levels are required.

3. The tides are tabulated from the time series of measurements.
   a. The water-level data should be collected at a minimum of 10-minute intervals; however, a 5- or 6-minute interval is preferred for locations with higher ranges of tide.
   b. Typically, two high tides and two low tides occur each tidal day (i.e., 24 hours, 50 minutes). The times and heights of each high and low tide are selected from the record. The higher of the two high waters and the lower of the two low waters each tidal day are annotated as part of the tabulation. Note that for some areas with diurnal tides, most tidal days will have only one high tide and one low tide.

c. Mean high water (MHW) is the numerical average of all the observed high tides. Mean higher high water (MHHW) is the numerical average of all of the high tides annotated as the higher high tide for each tidal day pair. Similar calculations are made for mean low water (MLW) and mean lower low water (MLLW).
d. Mean sea level (MSL) is calculated by averaging all of the observed values over the time period of deployment.
e. Mean values can be determined separately for each calendar month for longer records or simply over the time period of the data for shorter records.
f. The mean range of tide can be determined by subtracting MLW from MHW. The diurnal range of tide is determined by subtracting MLLW from MHHW.

4. Tides are typically referenced to 19-year time periods called tidal datum epochs. If an existing long-term tide station exists in the region and has the same tide-type, then an adjustment to obtain an equivalent 19-year value can be obtained by performing a simultaneous comparison of the tides and/or mean values following the guidelines found in NOAA (2003). Note that if a nearby comparison station does not exist for comparison, then a longer dataset should be obtained (minimum of one year) to minimize error.

5. Once datum values are determined from the observations, and because the sensors are surveyed-in, the water levels and tidal datums can be related to the reference benchmark elevations, which in turn relate the water level elevations to site topography and elevations of key infrastructure.

6. It is advisable that the reference benchmarks be surveyed using static GPS observations as well so that elevations can at least be determined relative to the GPS-derived ellipsoid and elevations can be compared to elevations from other nearby GPS measurements.

5.2.3 Effects of topographic data quality on inundation mapping

One important application of regional SLR and EWL scenarios involves exploring potential inundation areas for individual DoD sites by mapping scenarios in a spatially explicit manner. When assessing the potential horizontal extent of inland inundation, scenarios of global SLR, associated regional adjustments, and EWL estimates introduce only a portion of the overall uncertainty. In addressing uncertainty more broadly to inform decision-making, application of scenarios also must take into consideration the topographic and tidal surface information available at a given DoD site and the uncertainties associated with these respective datasets. This case study examines appropriate methods for addressing these uncertainties that take into account the availability and quality of spatial data with differing degrees of horizontal resolution and elevation measurement error.

Horizontal resolution of topographic data differs across datasets. Regardless of resolution, all topographic data have vertical measurement error associated with each reported elevation at discrete geographical coordinate points. This error introduces uncertainty when mapping the spatial extent of inundation from SLR or EWL scenarios. Measurement error specific to each individual coordinate point differs across a dataset; however, a calculated root mean square error

(RMSE) represents the standard deviation for the entire dataset. This RMSE provides the statistical basis for developing inundation maps for elevations that take into account vertical measurement error associated with the topographic dataset used (in addition to the scenario elevation itself). The mapping process can be carried out at one standard deviation of elevation measurement error (using the RMSE) or at specified levels of confidence by using multiples of this RMSE.

Examples provided below involve the development of inundation maps within ArcGIS that incorporate digital elevation model (DEM) elevation uncertainty through the conversion of RMSEs from differing DEMs into linear errors (LE)—multiples of the RMSE—at specified confidence levels. Taken together, these calculated LEs provide a suite of elevations that represent the inundation depth expected for a given scenario but at different confidence levels. Depending on the tolerance for risk in a particular situation, a decision-maker may choose the appropriate confidence level given the decision to be made. Comparative depictions illustrate how uncertainty in elevation measurements among available topographic datasets, as well as tolerance for risk, should play a role in decision-making processes that involve SLR or EWL scenario application.

Challenges of Initial Coarse Mapping Techniques for Incorporating Uncertainty

Under conditions with limited available spatial information, one may attempt to conduct an initial coarse visual assessment by depicting bands of uncertainty using an RMSE calculated from the entire national elevation dataset (NED; 1/3 arc-second DEM). This approach was used in the coarse elevation screening process discussed in Section 4.1.

Figure 5.8 illustrates an inundation map for Marine Corps Base Camp Lejeune (MCBCL) West Site using the 1.55-meter RMSE for the NED dataset (Gesch et al. 2014). The dark blue color represents the current NAVD88 datum surface. The lighter blue shows projected inundation impacts of a 1.0-meter SLR scenario (the mean, or inundation depth without any error associated with topographic data). The remaining color bands represent additional areas of inundation when applying estimates of LE at three levels of confidence: 80% (purple), 95% (orange), and 99% (green). Gesch et al. (2009), however, explain that the RMSE used in calculating LE should never exceed the inundation scenario itself in magnitude. This introductory example demonstrates an approach that would *not* be regarded as best practice in accounting for elevation uncertainty, because the RMSE value, 1.55 meters, is larger than the SLR scenario value, 1.0 meters.

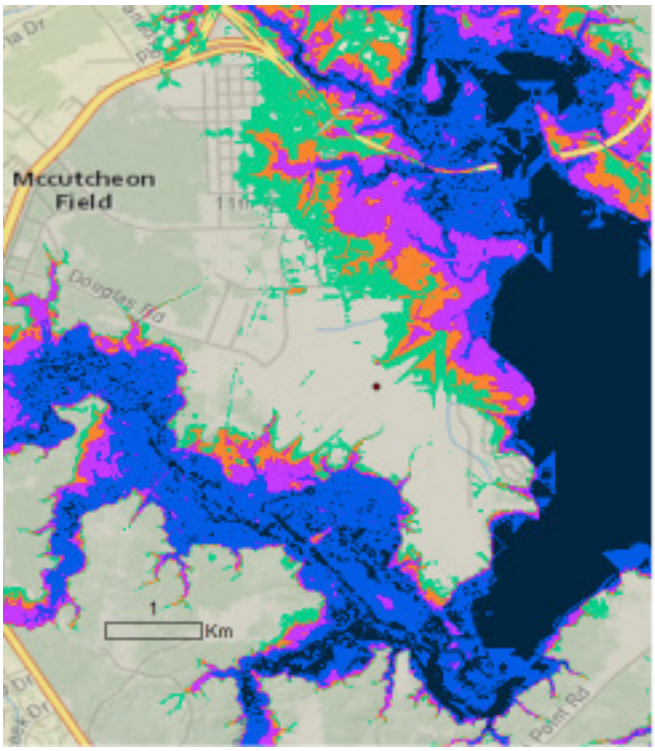

Figure 5.8 MCBCL West Site 1.0-Meter Inundation Map
(NED 1/3 arc-second DEM dataset)

Coarse LE estimation techniques, when the RMSE value is *less* than the scenario value, can provide utility. For example, an appropriate SLR or EWL mean scenario value in this case must be higher than 1.55 meters. Given a mean error equal to zero and normal statistical distribution of DEM measurement errors around the mean, the RMSE for the NED dataset would represent one standard deviation from the mean scenario value and allow for an accounting of LE at various confidence levels (Gesch 2012). Therefore, mapping inundation at 80% confidence requires increasing the projected inundation elevation from the mean scenario level by 1.282 standard deviations (i.e., an additional 1.55*1.282 meters). For 95% and 99% confidence, the inundation elevation is extended further from the mean by 1.960 and 2.576 standard deviations, respectively. This error causes projected horizontal extent of inundation to spread out in both directions from the mean, but the maps provided in this case study show uncertainty bands only in the inland direction. This enhances visual clarity and emphasizes potential inundation impacts.

The relatively large 1.55-meter RMSE of the NED dataset limits its utility in developing LE estimates and projecting inundation under many potential SLR and EWL scenarios of interest to DoD. In addition, even when properly applied to calculate LE and develop projections at different levels of confidence, the large uncertainty bands result in projected inundation that extends inland to widely differing horizontal extents. This large uncertainty can confound decision-making. Improving the accuracy of these assessments, as well as providing the capability to address lower SLR scenarios, requires elevation data of greater accuracy and an improved method for addressing topographic uncertainty. One such method involves reducing the RMSE used to calculate LE at each respective confidence level. Further discussion below outlines methods for carrying out this process in support of scenario mapping efforts.

Methods Available to Account for Uncertainty with Improved Accuracy

The process described above relied on the RMSE as calculated from the entire nationwide NED dataset. Even when applied appropriately, the coarse RMSE values provide results with significant uncertainty in the horizontal extent of inundation versus an analysis with higher resolution spatial information. To improve the accuracy of this type of coarse assessment approach, Gesch (2009) provides a method for refining the RMSE calculation by using an independent set of high-accuracy geodetic control points that can be compared against co-located points on DEMs of differing resolution. The author provides a detailed procedure outlining this process for mapping inundation at the 95% confidence level. Gesch (2012, 2013) and other authors have carried out similar analyses that incorporate other confidence levels for mapping inundation uncertainty, such as 80% (NOAA 2010b) and 99% (Priest et al. 2009). Although methodologies and source datasets used by each author differ, the methods applied by Gesch et al. (2009) do not preclude the ability to derive results for these other confidence intervals when instructive. Decision-makers can benefit from this wider range of available data and approaches, depending on the particular application, their associated risk tolerance, and need for accuracy and confidence in the results. This process can be carried out using multiple DEMs of differing spatial resolution and at multiple confidence levels to meet these various needs.

The following outlines the steps required to carry out this process per Gesch et al. (2009) (*exemplary items specific to the case study are in italics for the MCBCL West Site*). These steps address the same 1.0-meter SLR scenario discussed above in relation to the NED 1/3 arc-second dataset, but for the purpose of further illustration they also address calculations for a low elevation 0.5-meter regionally adjusted SLR scenario and a 3.4-meter combined SLR/EWL scenario. The 3.4-meter scenario is taken from the accompanying EWL database as the 2% annual chance event in 2065. The outline and subsequent discussion also addresses the availability of DEMs at more than one level of spatial resolution.

1. Access U.S. Geological Survey website and search for geospatial information system (GIS) data maps: http://viewer.nationalmap.gov/launch/
2. Download GIS data for the desired location at desired resolution:
   a. Under Elevation Products (3DEP) check availability for the area in question
   b. Available categories include 1/3 arc-second DEM and 1/9 arc-second DEM (Note that these have different spatial coverage extents; and other dataset resolutions are available, such as the 1-meter DEM, on Terrain Navigator Pro [TNP] at https://www.terrainnavigator.com/Product.)
3. For each desired DEM select "Find Products" and download the respective file(s) to ArcGIS (for finer spatial datasets, this process should be repeated for subsections to map the entire area)
4. Obtain spatial dataset containing location points and boundaries to make accessible from ArcGIS
5. Open ArcGIS and create new file, adding the following initial layers:
   a. National Geographic World map (base layer) (http://www.arcgis.com/home/webmap/viewer.html?webmap=d94dcdbe78e141c2b2d3a91d5ca8b9c9, accessed December 2015)
   b. Points and GIS boundary shapefiles (new group layer)
   c. Desired *1/3 and 1/9 arc-second* DEM layers (create histograms for each)
6. Append any higher resolution (*1/9 arc-second DEM*) layers to manipulate as one layer
7. Change symbology from default stretched to classified symbology; allowing manual breaks
8. Follow the vertical accuracy assessment method:
   a. Access an independent reference set of high-accuracy geodetic control points
      i. Add this layer *from the National Geodetic Survey (NGS) North Carolina file* to the ArcGIS file
      ii. Using spatial analyst tools, calculate the elevation of each point and add to properties
   b. Open the attribute tables for both the DEM site points and the reference points
      i. Find all points with matching lat/long coordinates between the two datasets
      ii. Using this data solve the root mean square error (RMSE) equation

      $RMSE = \text{sqrt}\ [\Sigma(z_{data1}-z_{check1})^2/n]$

      z_{data1} = point elevation from DEM

      z_{check1} = point elevation from reference

      n = number of points compared (4)

      iii. Using the RMSE, solve for linear error (LE) at desired confidence levels

      *LE(99%) = 2.576*RMSE; LE(95%) = 1.960*RMSE; LE(80%) = 1.282*RMSE*

9. Access the properties of each (*1/3 and 1/9 arc-second*) DEM layer and change the symbology to break at:
   a. NAVD88 Datum Surface (0 meters)
   b. Desired SLR or EWL scenario level(s) (*e.g., 0.5 meter, 1.0 meter, 3.4 meter*)
   c. Each applicable scenario inundation level plus LE for respective confidence level(s) [*e.g., LE(99%), LE(95%), LE(80%)*]
   d. Show all higher elevations above the inundation levels as clear
10. Zoom to show differences due to varying resolution(s) and confidence level(s)
11. Export images showing the chosen *1/3 arc-second and 1/9 arc-second* layers
12. Develop tables showing the results for chosen *1/3 arc-second and 1/9 arc-second DEM layers* at all calculated confidence levels.

After carrying out this process for each DEM and each confidence level, results are shown below in Table 5.2. This table shows how various combinations of scenario, resolution, and confidence level produce greatly differing results with respect to the inundation elevation expressed on the GIS contour maps. For example, using the 1/9 arc-second USGS DEM to map a 1.0-meter SLR scenario adds 0.90 meters of LE at 95% confidence. Therefore, for a 1.0-meter scenario, the projected inundation elevation at 95% confidence is 1.90 meters (see value in highlighted box of Table 5.2). Note that one should not map the 0.5-meter scenario using the 1/3 arc-second DEM because the 0.62-meter RMSE exceeds the 0.5-meter scenario value.

Table 5.2 Water Levels for Inundation Mapping under Various DEM Resolutions and Confidence Levels

1/9 arc-second USGS (RMSE=0.46 meters)					1/3 arc-second USGS (RMSE=0.62 meters)				
CL	LE (m)	Water level (meter [m]) for each Scenario			CL	LE (m)	Water level (meter [m]) for each Scenario		
		3.4-m	**1-m**	**0.5-m**			**3.4-m**	**1-m**	**0.5-m**
99%	1.19	4.59	2.19	1.69	99%	1.59	4.99	2.59	N/A
95%	0.90	4.30	1.90	1.40	95%	1.21	4.61	2.21	N/A
80%	0.59	3.99	1.59	1.09	80%	0.79	4.19	1.79	N/A

Also note that as the confidence level increases, so also does the LE. This has two effects: (1) it expands the width (horizontal extent) of the potential inundation zone (in both landward and shoreward directions) and (2) it may obscure the ability to visually depict the low-end scenarios. Higher resolution topographic data can reduce the effect of LE to a certain extent (compare the 1/9 arc-second information to the 1/3 arc-second information in Table 5.2), but it does not completely remove its influence. To view the effect of a low-end scenario, the user still may have to accept the application of a lower confidence level.

Proper Dataset Selection and Application for Scenario Inundation Mapping

Deciding on the proper combination to use in providing decision support depends heavily on the availability of the data, the circumstances of risk tolerance surrounding that decision, and other factors. The following three maps and accompanying discussion illustrate how these choices result in differing visualizations of inundation outcomes, each designed to support decision-making under different sets of conditions.

In this first case, conducting an initial screening-level vulnerability assessment on the impacts of a 0.5-meter SLR scenario requires the highest resolution dataset available—the 1/9 arc-second resolution DEM—to keep the RMSE below 0.5 meter. Furthermore, relaxing the confidence level prevents obscuring the potential impact of the scenario at its mean inundation level while still addressing uncertainty. Figure 5.9 shows that relaxing the confidence and displaying only the LE (80%) band enables a depiction of this low 0.5-meter scenario's potential impact. For a case in which the scenario's effect still cannot be viewed, it may make sense to further relax the confidence (e.g., to a 50% confidence level; not shown in table 5.2). Using a 50% confidence level, the uncertainty band would add only 0.31 meters of LE, further emphasizing potential impacts of the 0.5-meter scenario mean inundation level itself (albeit at a reduced level of confidence in the potential extent of inundation). Note that mapping a 0.2-meter SLR scenario would require a dataset with greater vertical accuracy than those available and possibly necessitate a detailed site-specific topographic study.

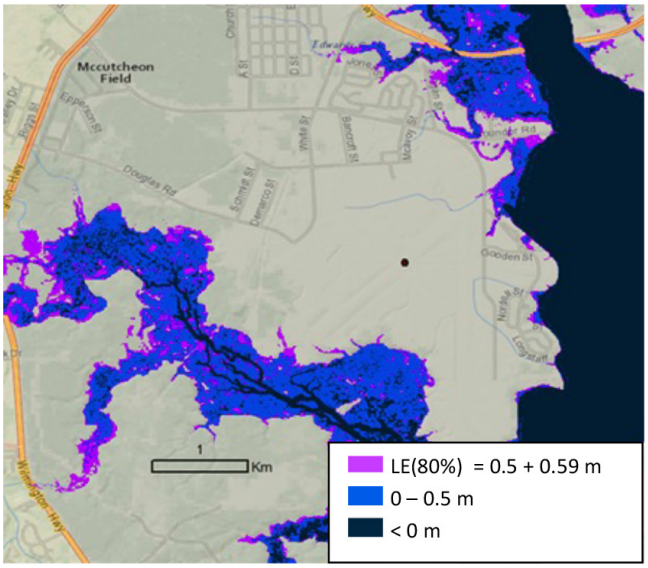

Figure 5.9 MCBCL West Site 0.5-Meter Inundation Map
(NED 1/9 arc-second DEM dataset)

Another situation may arise in which one needs to map, for example, the potential inundation for a 2% annual chance event in 2065. In this second case, showing the LE bands at 95% and 99% confidence will increase the horizontal extent of inundation further than at 80% confidence, but in comparison to the larger 3.4-meter EWL scenario, it will not prevent viewing the consequences of the scenario itself. It will enable, however, a decision-maker to assess the vulnerability of important assets to a much higher level of confidence. The availability of two DEMs with differing levels of resolution (USGS DEMs at 1/3 arc-second and 1/9 arc-second) also allows for a comparison of results between the two respective inundation maps.

Figure 5.10 shows that when modeling combined SLR and EWL scenarios, such as the 3.4-meter 2% annual chance event for 2065, the additional information provided by reviewing a much higher 99% confidence level contour for a higher elevation scenario could significantly alter the decision-making process as related to infrastructure or other assets. Applying the additional level of confidence also does not obscure the scenario itself, given the relative magnitude of the scenario's impacts.

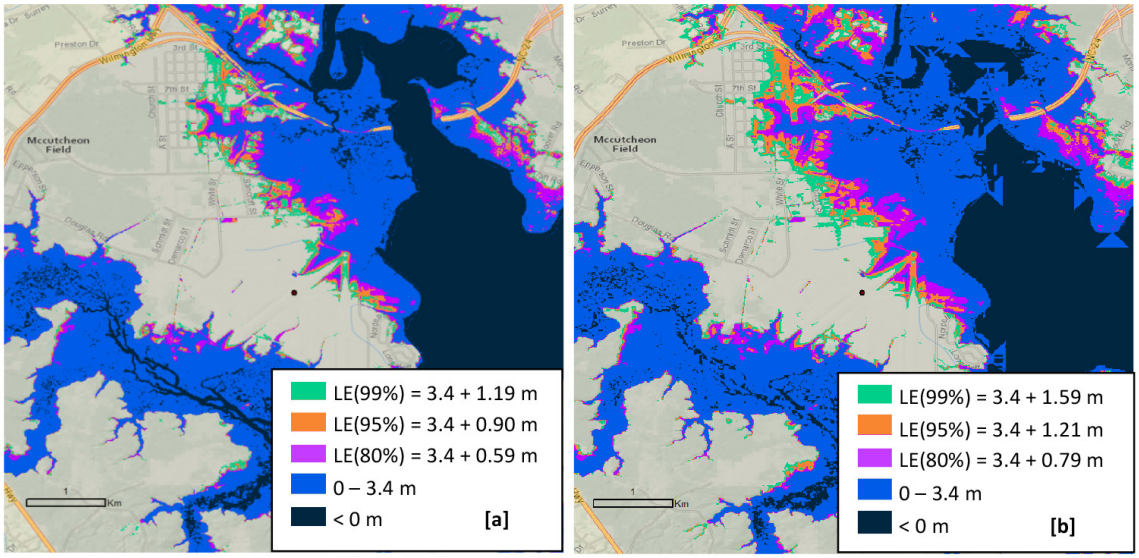

Figure 5.10 MCBCL West Site 3.4-Meter Inundation Map
([a] NED 1/9 arc-second DEM dataset; [b] NED 1/3 arc-second DEM dataset)

Side-by-side comparison of the 1/9 arc-second and 1/3 arc-second DEMs in Figure 5.10 facilitates a visual assessment of the difference in projected extent of inundation, but a decision-maker may want to supplement this with an understanding of total projected inundation area. To accomplish this, one can utilize *Project Raster* and the *Surface Volume* function within *ArcToolbox* (a detailed discussion of underlying methodologies falls beyond the scope of this case study). Although these area determinations involve complex three-dimensional topographies and introduce additional sources of uncertainty (Poulter and Halpin 2008), they can provide a rough quantitative comparison of results. In this case, with relative differences depending on confidence level, use of the 1/3 arc-second DEM can result in a projected inundation area over three times as extensive as the 1/9 arc-second DEM. This can also help decision-makers to further understand the advantages gained from using datasets with improved vertical accuracy to reduce LE.

Incorporating an Understanding of Differences in Tidal Surface Elevation

Overall error derived from SLR/EWL scenarios, regional adjustments, and topographic data potentially requires further adjustment to reflect uncertainty associated with tidal elevations, which also can play a role in mapping inundation with greater accuracy (NOAA 2010a). These differing tidal surfaces can introduce differences in tidal surface elevation errors (e.g., spatially explicit differences in mean higher high water [MHHW] due to shoreline configuration and bathymetry) not addressed in the analyses above. This can be especially important in achieving comprehensive SLR and EWL inundation projections for entire installations and other larger areas where one must consider the effect of differing MHHW offsets from MSL. In some instances, larger areas such as entire installations may require EWL inundation assessments of this nature. This process would need to account for differing offsets in each associated area and ensure that a given scenario and associated uncertainties are mapped properly in accordance with the selected EWL scenario, DEM, and confidence level.

In the case of MCBCL West Site, the nearby MCBCL main installation has a different MHHW offset (see Section 4.5 for a discussion of tidal surface variation in the vicinity of MCBCL; because of the New River Estuary and other physical features, MHHW varies across the installation). Accordingly, mapping these locations together under a single inundation scenario would require accounting for the variation associated with the tidal surfaces. In sites where MHHW differs across an area of assessment, VDatum can help to quantify this additional variation in key elevation surfaces per the discussion in NOAA (2010b). In areas where VDatum is not available, this variation cannot be quantified but can be explained in a qualitative manner.

This case study illustrates the critical importance of having high-accuracy, high-resolution topographic information for mapping differing SLR and combined SLR and EWL scenarios in a spatially explicit manner. The information available from this type of analysis, including inundation maps that incorporate LE at desired confidence levels, can provide a starting point for informed decision-making under uncertainty. In many cases, however, the visual data conveyed in an inundation map and accompanying inundation area calculations cannot on their own adequately inform a decision-maker. This is further complemented by taking a risk-based framing approach as discussed in the following section.

5.3 Scenario Application and Decision-Making under Uncertainty: A Risk-Based Framing Approach

In the two preceding sections the focus was to provide a richer understanding of how sea-level change and extreme water level scenario values, and their application, are influenced by both physical setting and the availability and quality of relevant datasets. In those two cases, location and knowledge about that location influence both relative (i.e., to the global mean) exposure to future sea-level conditions and the ability to even qualitatively assess potential vulnerability and impacts to such conditions. This section focuses more directly on applying the scenarios themselves to support decision-making while accounting for the uncertainty inherent within the global scenarios that are themselves contingent on myriad factors, including the vagaries of human choices. When additional uncertainties are involved, such as those resulting from the process models and observations on which the scenario values depend, decision-makers need additional tools to assist in understanding their scenario choices and in some cases effectively narrowing such choices.

We first briefly discuss some general background and principles associated with risk-based framing. This is followed by descriptions of several different approaches for scenario application under uncertainty. A concluding sub-section addresses the special case of near-term, sea-level rise scenarios: that is, over the timeframe from zero to 20 years (assuming a start date of 2015).

5.3.1 Bounding uncertainty and risk: general principles of risk-based framing

General Discussion

In its traditional usage risk is defined as the likelihood of occurrence of some condition or event multiplied by the consequence. In a more quantitative sense the risk associated with a particular set of conditions can be described by a probability distribution that then leads to potential future states of differing probability. Within this context, futures that can be described according to

a probability distribution lend themselves to a "predict-then-act" decision-analytic approach. This often comports to a decision-maker's desire to base decisions on a "most likely," essentially deterministic future.

Given the uncertainties inherent with climate change, however, such strictly probabilistic approaches are not feasible. The uncertainties associated with the natural variability of the climate system, climate model input and output differences, and different possible emissions futures effectively preclude assigning probabilities to possible resultant futures. Climate change therefore leads to a class of decisions characterized by deep uncertainty. Deep uncertainty is the presence of one or more of the following conditions: (1) multiple possible futures without known relative probabilities, (2) multiple worldviews that are divergent but equally valid, and (3) interrelated decisions that adapt over time in a dependent manner (Hallegatte et al. 2012). The national security community has prior experience with decision-making under uncertainty (Davis 2012), though not yet associated with climate change, and various approaches have been developed to support such decisions (Hallegatte et al. 2012). Importantly, Davis (2012) identifies the need for an adaptive approach to decision-making under uncertainty and avoidance of the "once-and-for-all" type of decision-making.

Herein, we take a broader view of risk that is not dependent on assigning likelihoods or probabilities and instead follow what we will refer to as a risk-based framing approach. Contrary to traditional definitions of risk, such an approach acknowledges that risk under conditions of deep uncertainty cannot be defined in a strictly probabilistic sense and instead is dependent on the type of decision involved, its intended longevity, and a decision-maker's tolerance for the adverse consequences of a wrong decision. As a result, within the context of a risk-based framing approach to decision-making, the objective is to assist decision-makers and practitioners in ***managing uncertainty*** or, when such uncertainty is largely irreducible, to ***reduce risk*** (Hinkel et al. 2015). The objective is ***not to reduce uncertainty*** with the intent of manufacturing a pseudo-deterministic approach centered on a "most likely" future. Rather, the overall goal here is to increase the robustness of decisions against a range of plausible future conditions. A risk-based framing approach also encourages decision-makers to avoid the "uncertainty fallacy" (Lemos and Rood 2010), in which systemic reductions in uncertainty presumably are required before available information can be used to support a decision. This false need for certainty often can lead to decision paralysis. Finally, climate-derived futures are not the only source of uncertainty that may affect decisions in the coastal environment. Moreover, rather than expecting "perfect forecasts," future plausible conditions of SLC and EWLs need to be integrated with other stressors and sources of information that may affect the decision (Lemos and Rood 2010).

The concept of robustness of decisions was mentioned in the preceding paragraph. To avoid settling on a definition of robust decision-making that is tied directly to a particular methodological framework, we take a more inclusive approach here and define robust decisions as those that meet the decision-maker's objectives across a range of plausible futures. Robust decision-making processes are iterative and adaptive by nature (Hallegatte et al. 2012) and can be effectively used to support a risk-based framing approach. They are potentially sensitive to "worst-case scenarios"; however, Hallegatte et al. (2012) argue that rather than this property being an artifact of the various

methodological approaches, it reflects more the reality of climate change and its associated deep uncertainty. Although their usage differs according to the methodology employed, scenarios often are used in robust approaches (Groves and Lempert 2006). In deciding how to best apply scenarios for decision-making, one also should consider whether particular circumstances might enable different strategies to be considered as options across one or more scenarios. For example, strategies can be: (1) "low regret[1]," in which actions taken today to reduce risk may have continued benefits under climate change, (2) reversible and flexible, in which future options to respond to increased water levels are preserved while keeping committed costs low, (3) related to a safety margin, in which the costs to reduce vulnerability or risk are reasonable, or (4) associated with reducing the decision-making time horizon, in which the timeframe over which a decision is intended to be operational is purposely reduced (Hallegatte et al. 2012). Each of these preceding strategies should be kept in mind as scenario application choices are made to support particular decisions.

…within the context of a risk-based framing approach to decision-making, the objective is to assist decision-makers and practitioners in managing uncertainty or, when such uncertainty is largely irreducible, to reduce risk (Hinkel et al. 2015). The objective is not to reduce uncertainty with the intent of manufacturing a pseudo-deterministic approach centered on a "most likely" future. Rather, the overall goal here is to increase the robustness of decisions against a range of plausible future conditions.

Risk-Based Framing in the Coastal Environs

The coastal environs are an active area of research and application with regard to risk management in the context of climate change. To some degree the ability to quantitatively determine at least the directionality of change in sea levels at a location simplifies the decision context; however, as demonstrated throughout this report through the development of the regionalized scenarios, significant uncertainties still remain about the magnitude of change and its timing. Moreover, the underlying global trend in SLR creates two types of risk. The first we are familiar with—the rare event. This risk will be exacerbated by SLR in the future independent of any non-stationary effect on storm statistics. The second, perhaps more subtle, risk that is forming in our collective conscience in an accelerated manner is the increase in frequency and duration of low magnitude (i.e., nuisance, minor, and even moderate) flooding events (Sweet and Park 2014). Prudent floodplain management compels us to assess the impacts of the *rare* 1% annual chance event and, as a result, helps to reduce risk when applied within a climate change context for the planning and construction of future infrastructure meant to last well into the latter half of the century. Potential changes in future *recurrent* flooding periodicities and durations, however, will affect extant infrastructure in ways for which we are not currently prepared. Even partial or temporary loss of

[1]Hallegatte et al. (2012) use the term "no regret"; however, we contend that no decision is completely without regret and that a more appropriate strategy is to minimize regret.

functionality can be problematic if the infrastructure has a critical mission role. The adaptive actions currently employed (e.g., temporary closure of gravity drainage systems, expedient flood-fighting methods) to reduce recurrent flood impacts or recover from such impacts may be acceptable when assumed to occur infrequently; however, they take on new significance when they become the new normal.

Two general approaches present themselves in conveying these two types of risk that are not necessarily unique to each risk but offer different perspectives on viewing and applying scenario information. In the first approach the focus is on changes in magnitude of the extremes in water levels relative to a current condition. This approach can be most effectively applied to assess the effect on either extant or future infrastructure or on sites in general in terms of a potential vulnerability or impact and is the manner in which scenario information is presented in the scenario database. In the latter approach the focus is on existing elevations of concern to infrastructure managers and either when or how more frequent in the future they may be exceeded. This "threshold" approach is especially helpful for assessing the consequences of recurrent low magnitude events to extant infrastructure. It enables the manager to assess the effect of changes in recurrence interval (i.e., non-stationarity) on the effectiveness and efficiency of adaptive actions over time and the acceptability of periodic reductions in mission functionality of the infrastructure or site. Although both approaches are complementary with regard to addressing the entire risk envelope, our ability to address the second approach was somewhat limited in this study. The time-slice dependent nature of the DSL and ice melt adjustments precluded the type of analysis to provide scenario-based changes in the return intervals of extreme water level events relative to a fixed elevation. For sites at which DSL and ice melt are not significant contributors to the regionalized SLR scenarios, it would be possible to develop indices of return intervals for critical elevations for different scenarios.

In summary we encourage decision-makers to consider not only the extremes when determining appropriate application of the combined sea-level change and extreme water level scenarios but also to consider in appropriate decision contexts how events such as the 5% and 20% annual chance events, when considered in the context of SLR, may affect their scenario choices and ultimate decisions. Moreover, when available to them, decision-makers and practitioners should take advantage of the complementary and meaningful ways of presenting risk-based scenario information. Another useful manner in which to convey return period and risk, from a design life perspective, is provided in the text box on the following two pages.

Concepts of Return Period and Risk under Non-stationarity

The traditional methods of determining return period and risk of extreme sea-level events and floods assume two key conditions:

(1) extreme events arise from a stationary probability distribution, and
(2) the occurrences of extreme events are independent.

Communicating the probabilities of extreme events using return period and their risks, however, is not particularly useful under conditions of non-stationarity. This is because the probability of exceedances above a particular elevation threshold (e.g., seawall height) will be increasing (or decreasing) with time due to changes in relative mean sea level and in some cases storminess. In coastal regions, such increases will result in the increased frequency of storm surge or tidal flooding, a phenomenon now dubbed as "nuisance flooding" or "recurrent flooding." Determination of future risks requires a new paradigm.

Since publication of the frequently cited paper by Milly et al. (2008), hydrologists have worked on developing new methods for determining risks and return periods under conditions of non-stationarity (Cooley 2013, Salas and Obeysekera 2014, Obeysekera and Salas 2016).The application of these techniques to scenario-based extreme sea levels was demonstrated by Salas and Obeysekera (2014). These new concepts are based on two fundamental metrics:

(1) Expected Waiting Time for the first exceedance above a threshold, and
(2) Expected Number of Events over the design life time of a facility.

The methods enable planners to determine the actual return period and risks due to non-stationarity. Such tools can be used for communicating risks to decision-makers effectively.

For instance, the first figure below shows what is known as the "non-stationary return period curve" that relates the actual return period as a function of the design return period to be used for determining the size of the facility at the beginning of its operation. As an example, for a facility planned to accommodate a 50-year return period, the actual return period is reduced to about 25 years due to rising sea levels. Because of non-stationarity, the risk of exceeding a threshold also would increase. Such an increase is shown in the second figure below. For each design return period, an assumption of SLR results in an increase in the risk of failure at any point in time across the project life.

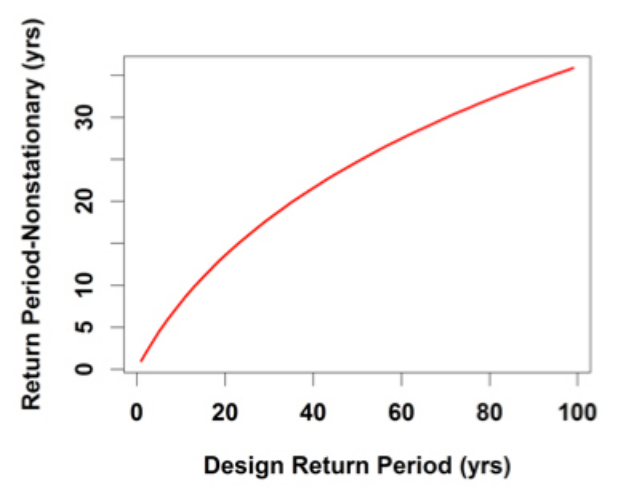

Return Period Curve Relating Non-Stationary Return Period as a Function of Design Return Period

This curve was developed using annual extreme values at the Sewells Point, Virginia, tide gauge and a global sea- level rise scenario of 1.0 meter. The extreme values were fitted using the Generalized Extreme Value (GEV) following the methods described in Salas and Obeysekera (2014) and Coles (2001).

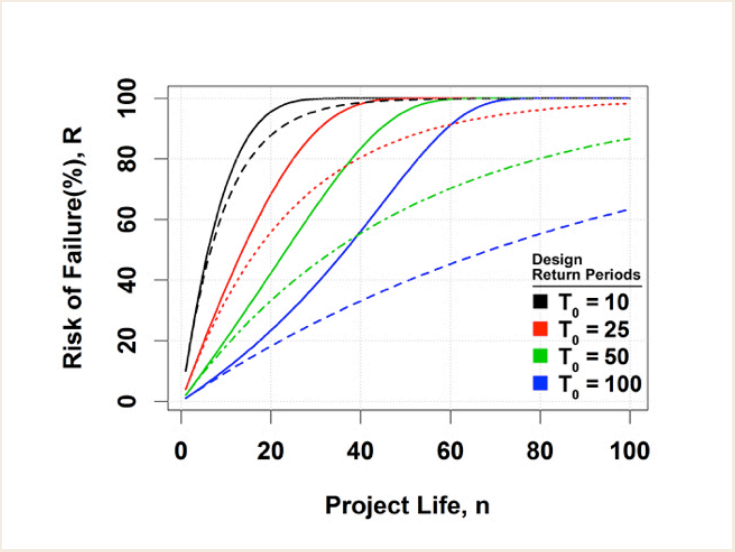

Risk Curves Relating Non-Stationary Return Risk as a Function of Project Life (years) and Various Design Return Periods as Denoted by T0 (years)

These curves were developed using annual extreme values at the Sewells Point, Virginia, tide gauge and a global sea-level rise scenario of 1.0 meters. T0 denotes the original design return period in which black equals 10 years, red equals 25 years, green equals 50 years, and blue equals 100 years. The dashed lines represent the risk of failure (i.e., exceeding a threshold such as sea wall height) over the design life, n. The solid curves represent the corresponding risk curve due to increasing sea levels. The extreme values were fitted as described above.

Although Hinkel et al. (2015) drew a clear distinction in the perspectives between "reducing uncertainty" and "reducing risk" with respect to the development, and more importantly in the context of this report the application, of SLR scenarios, they certainly were not the first in taking a risk-management perspective on the issue. In support of the Third National Climate Assessment for the United States, Parris et al. (2012) took such a view; however, given their focus on global scenarios they were able to provide only limited guidance on their regionalization and subsequent application. Still, they were able to place each scenario into an appropriate risk-tolerance context while retaining the call for the usage of multiple scenarios in the decision-making context.

Within the last few years additional studies have been taking a more holistic view of the application of scenarios and assessing the trade-offs involved in the economics of different response options, the SLR and EWLscenario assumed, and the associated uncertainties. Aerts et al. (2014) assessed the preceding for New York City and showed through their modeling that investment choices from a cost-effectiveness (cost-benefit analysis) perspective are sensitive to the climate-related scenarios considered, discount rate used, response strategy employed, and timing of investment. The authors argued for the importance of maintaining policy flexibility in response to new information on future scenarios becoming available given that uncertainties in future conditions significantly affected the results (Aerts et al. 2014).

A second study also investigated the effect of expectations about future SLR on investment decisions, this time in the context of large capital infrastructure upgrade decisions facing the Port of Los Angeles (Lempert et al. 2012). These authors used a robust decision-making analysis approach and contrasted it with a probabilistic analysis approach. Their robust decision approach identified scenarios in which a decision to invest in a near-term response to extremes of SLR passed a cost-benefit test, and then they assembled scientific evidence of different confidence levels to assist decision-makers in judging whether the scenarios were sufficiently likely to justify making such investments. Because they eventually evaluated scenarios in a probabilistic sense, which seems counterintuitive to the way scenarios are defined, it is not surprising that the purely probabilistic approach resulted in similar investment recommendations (Lempert et al. 2012). This latter application of a likelihood to a scenario, as a way to assist decision-makers in justifying a particular response strategy, is seemingly an attempt to address a debate that on one side argues that users require guidance incorporating likelihoods for the use of scenarios and on the other side argues that assigning probability estimates to scenarios leads to a misleading degree of certainty about the future and to conflict among users when agreement cannot be reached between users on the probabilities assigned (Groves and Lempert 2006).

We argue here that attempting to consider scenarios in a probabilistic sense is still mostly emerging science with no agreed-on approach within the scientific community, and that its application should be considered with caution by decision-makers and practitioners. This situation is complex, in that the global SLR scenarios are in part based on probabilistic information that was either associated with models or expert elicitation. For example, to arrive at the 1.5-meter and 2.0-meter scenarios required the view of experts on ice-sheet dynamics and their likelihood, particularly with regard to Antarctica, and sampling of associated probability distributions; however, it would be a mistake from a risk management perspective to assume that the scenarios in combination form a probability distribution with an inherent central tendency.

Finally, the U.S. Army Corps of Engineers has had considerable experience in applying risk management and cost-benefit approaches to coastal management decisions, as well as a long history of considering SLR in its decision-making. Their guidance (USACE 2014) with regard to procedures for evaluating sea-level change on USACE projects contains extensive information on incorporating sea-level change into the USACE decision-making process. Although its focus is from the perspective of USACE "projects," the framing concepts employed are generally applicable and will be referred to often in the sections below that outline different approaches to the use of the scenarios developed in this document and the accompanying scenario database. Most importantly, the USACE guidance emphasizes robust project (and overall system) performance that is both flexible and adaptable to a range of future conditions, time period analyses that consider an adaptation horizon (to 100 years) that accounts for a potential service life beyond design life, use of multiple scenarios, and a consideration of performance thresholds as a way to understand current and future vulnerabilities (USACE 2014).

5.3.2 Emissions scenario-based approach

Although we argue strongly against the use of scenarios in a probabilistic sense and encourage the use of multiple scenarios in all cases, we also recognize that some decision-makers may feel comfortable making certain assumptions about future conditions. One of these may be in association with emissions futures. They may assess current conditions and determine that current trends will continue into the future and that their tolerance for risk for a particular decision is low, or they may determine that emissions will decrease in the future and they can afford to increase their risk tolerance. They could assume, for example, that Representative Concentration Pathway (RCP 8.5) most closely reflects the global community's current emissions trajectory and assert either that: (1) the world will stay on this trajectory or (2) their decision's tolerance for risk requires a robust approach and they will assume the conservative (highest) emissions scenario regardless of whether they judge future emissions might decrease.

It is important to note that although we follow the Intergovernmental Panel on Climate Change's usage of RCPs in its Fifth Assessment Report, especially with regard to projections of global SLR (Church et al. 2013a), we do so as a means to create plausible storylines for the individual scenarios for those who desire to consider that association. As a result, a one-to-one correspondence does not exist between the Church et al. (2013a) SLR projections and the family of global SLR scenarios developed herein; however, the associations are nevertheless important given the use of RCP-driven, process-based models to generate the DSL and ice melt adjustments (see Table 3.3 and Sections 3.4.3 and 3.4.4). To continue the RCP 8.5 example in this context, a decision-maker could use the 1.0-meter global scenario as a lower bound scenario (note this usage would be at the higher end of the range for this emissions scenario in Church et al. 2013a) and then choose either the 1.5-meter or 2.0-meter scenario to bound the upper end of their risk tolerance. The upper-end choice in this example is driven by the degree to which dynamic ice loss in Antarctica occurs and is most important for decisions whose operational lifetime needs to extend towards the end of the century (the implications of the timing issue is addressed again in Section 5.3.4). Each global scenario choice in this example has a dependency on RCP 8.5 as an underlying emissions driver. (See 3.3.1 and 3.3.2 for discussion of upper and lower bounding for global SLR scenarios.)

Similarly, decision-makers may choose to use emissions scenarios that are associated with some degree of aggressive GHG mitigation (0.2-meter and 0.5-meter scenarios or RCP 2.6 and 4.5, respectively). These scenarios also may be applicable for high-risk tolerance decisions or short- to moderate-term effective timeframe decisions (i.e., within the next 20 years or so) that can be frequently revisited (see Section 5.3.3). Regardless of the low-end choice, at least two scenarios always should be considered to ensure a robust decision.

5.3.3 Accounting for decision type, operational timeframe, and tolerance for risk

The three aspects of decisions of relevance here—decision type, operational timeframe over which the decision needs to function in an effective manner, and the tolerance for risk associated with the decision—are closely related and thus not necessarily independent. Figure 5.10 attempts to capture the first two aspects pictorially, given that the third aspect—tolerance for risk—is a somewhat subjective choice, and illustrates the potential close relationship between decision type and operational timeframe. Despite the close linkages, it is helpful to consider the three aspects separately and their effect on the application of the combined SLC and EWL scenarios.

Decision Type

Decision type itself includes a number of considerations affecting scenario choice. First is whether the decision involves a maintenance action, a major rehabilitation of an existing infrastructure, or the design and construction of new infrastructure. Figure 5.11 reflects climate impacts that should be considered for decisions made now that are expected to be robust to future conditions. For example, maintenance actions would consider near-term climate conditions unless aspects of these actions could be expected to continue over the long term, in which case they should also consider how long-term effects would impact decisions made now. In some cases, major refurbishment requires consideration of conditions in the mid-term, while long-lived infrastructure decisions should always consider longer-term climate effects. In this context the decision-maker and practitioner need to consider two different but related risks: (1) whether a particular future will change a particular decision's overall useful life and (2) whether during that lifetime the decision's level of performance will decline below what is planned (USACE 2014). The choice of a more conservative future based on smaller increases in sea level to guide the decision may lead to unanticipated consequences. Moreover, a consideration of both aspects of risk may shift the focus of the assessment from that of the endpoint to the rate at which a particular future is reached (USACE 2014). Second, for DoD, although decisions are implemented at the installation level, the type of decision also depends on whether it has an effect on other levels of governance within DoD. In this context DoD is an enterprise system in which the effect on the entire system is considered as part of the decision context and the degree to which "missions" are redundant or easily transferable to other installations may come into play. Third, base realignment decisions are related to the preceding. In this case the focus is not necessarily on an isolated decision about a particular element of infrastructure, but a more strategic focus on the implications for an entire installation and again the effects on the aggregate system.

Figure 5.11 Two Aspects of the Decision Context Affecting Application of Sea-Level Change and Extreme Water Level Scenarios: Decision Type and Operational Timeframe
See text for further details and discussion of the third aspect: tolerance for risk.

Fourth, thresholds in infrastructure (or system when infrastructure is considered in a system context) performance affected by both climate means and extremes also should be considered. Limiting the upper bounding scenario to one that places infrastructure or a system close to a threshold value would reduce the robustness of a decision (USACE 2014). Finally, the reader is reminded that the primary decision context addressed by this report is vulnerability and impact assessment under climate change within a screening context. As a result, for other types of decisions—such as engineering design—the degree of granularity needed to be achieved in terms of characterizing thresholds and the cost effectiveness of a decision will differ and potentially affect scenario choice.

Operational Timeframe

The timeframe over which a decision is intended to be effective also affects scenario choice. The first consideration is whether the decision involves permanent or long-lived versus temporary infrastructure (Figure 5.11). Temporary infrastructure in most cases may have an operational life that is not affected by scenario choice. Second, for decisions that may not extend much beyond 2035, the choice of an upper bounding scenario is not as critical because little divergence occurs between scenario end points before mid-century. As the expected performance lifetime of infrastructure increases (to design life and potentially beyond), the divergence in scenarios past mid-century becomes more apparent and the decision becomes more sensitive to scenario choice. Thus, longer-term decisions may entail the need for a broader perspective on the plausible scenario futures to consider. Such decisions are of the type that may not be revisited for some time or once made may preclude or constrain future responses (USACE 2014). As discussed above, the rate at which a particular future is achieved also could affect the operational timeframe of a decision. Finally, purposefully reducing the decision-making time horizon over which a decision is expected to be effective (see Hallegatte et al. 2012) as a hedge against uncertainty also can affect scenario choice.

Tolerance for Risk

A decision-maker's tolerance for risk plays a primary role in scenario selection. In a general sense, a low tolerance for risk would imply the choice of a higher upper bound scenario and a high tolerance for risk would imply the opposite choice. Risk in this context also involves a qualitative or quantitative sense of the cost-benefit trade-off associated with the decision, but for a mission agency such as DoD this is not necessarily strictly so. Besides cost, a DoD decision-maker also should consider more readily quantified aspects of the decision, such as whether a decision represents an irreversible commitment of resources (e.g., the decision to build a new pier to a certain operational elevation is not necessarily a decision easily revisited once the pier is constructed), versus whether the decision is mission critical. In the latter case a decision-maker may adjust his or her tolerance for risk, and by association the choice of scenario, based on the critical nature of the infrastructure involved; however, they also may have other options to consider (such as moving the mission to a different location) that may affect this choice. Finally, whether the scenarios are being applied in a vulnerability screening context versus making a specific response decision that has to be resourced may affect how risk tolerance is viewed, though this does not a priori determine whether this expands or contracts the risk envelope to be considered. Response strategies also may come into play when scenarios are used to support a robust response; in such instances a low regret action or the need to apply a safety margin may affect the perception of risk tolerance (see Hallegatte et al. 2012).

Summary

The three aspects of a decision discussed above need to be considered in an integrated manner when choosing the range of scenarios to be considered. No matter the decision, multiple scenarios should be considered. In the most simplistic terms, a decision that involves enduring or permanent infrastructure meant to perform at least 50 years into the future (whether extant or planned new infrastructure), is mission critical with limited alternative options, and represents an irreversible commitment of resources, would dictate a consideration of the upper-end scenarios. This is in contrast to a decision involving temporary, non-mission critical infrastructure that has an anticipated operational lifetime of five years or less. For this situation a consideration of SLR scenarios likely is not even needed. See the text box below for a summary of tips on selecting scenarios to fit decision parameters.

A Quick Guide to the Use of the Five Global SLR Scenarios Developed in this Report

- *The two lower scenarios (0.2 and 0.5 meters) may be appropriate when a decision can tolerate a high degree of risk (e.g., projects with a short lifespan or planning areas with flexibility to make alternative choices within the near-term). These scenarios primarily address ocean warming.*
  - *Where local relative sea level (LRSL) is falling, the use of the lowest scenario (0.2 meters) may be appropriate.*
  - *Where LRSL is rising, the 0.5-meter scenario may be appropriate as the minimum scenario because it includes the effects of accelerated ocean warming, whereas the lowest scenario is simply an extrapolation of the existing sea-level trend into the future and assumes no acceleration.*
- *The higher scenarios (1.0, 1.5, and 2.0 meters) should be considered in situations when a decision has little tolerance for risk. These situations include projects or assets with a long lifespan, in which losses would be catastrophic and when limited flexibility is available to adapt in the near or long term, and those assets that serve critical military functions (e.g., ports and associated infrastructure). These scenarios address not only ocean warming, but also contributions from glaciers and ice sheets. They differ in the source that contributes to the mass loss with Antarctica dominating the contribution for the 2.0-meter scenario (see Table 3.8).*

5.3.4 Adaptive Risk Management

Climate change is a phenomenon that will play out over long time periods. Given its sensitivity to a variety of uncertainties, when the situation permits it is prudent to apply the combined SLC and EWL scenarios in an adaptive manner. This precaution derives from a number of factors. First, decision-makers and practitioners should not presume that the future will follow exactly any particular scenario. Even if the future happens to follow the general trend of a scenario when averaged over time, it is likely that at any particular point in time natural variability in the climate and physical/biological response systems will lead to noticeable deviations from the scenario trajectory. The challenge will be to account for natural variability

To preclude an over-commitment of resources, it is better when a decision involves either reversible aspects or an ability to phase in the needed responses. The overarching goal is to maintain future options to respond to changing conditions while retaining the robustness of the decision over time in a cost-effective manner.

while assessing whether changes in the trends (not just in the means but in the variance of extremes as well) warrant a change in a decision. Maintaining the ability to flexibly respond would be ideal. Second, some decisions may be quite expensive if implemented fully and based on a high-end scenario. To preclude an over-commitment of resources, it is better when a decision involves either reversible aspects or an ability to phase in the needed responses. The overarching goal is to maintain future options to respond to changing conditions while retaining the robustness of the decision over time in a cost-effective manner.

Based on the preceding considerations, the basic elements of an adaptive approach to coastal risk management can be outlined as follows: (1) apply scenarios and invest in measures to maintain infrastructure and mission functions in the near to moderate timeframes (less than 20 years to perhaps mid-century), (2) monitor trends in sea level and extreme water levels over time, and (3) periodically update the assessment of the upper bound scenarios for the longer timeframes (perhaps on the order of four to seven years, commensurate with the periodicity of U.S. and international climate assessments) and implement new measures accordingly. Such an approach is consistent with the recommendations of Hinkel et al. (2015) and USACE (2014), as well as Hallegatte et al.'s (2012) notion of a reversible and flexible strategy, in which future options to respond to increased water levels are preserved while keeping committed costs low (see Lowe et al. [2009] for an international example regarding the Thames River Barrier, in which an adaptive approach was followed that considered a range of SLR scenarios but then tracked rates of SLR over time to periodically evaluate appropriate response options and update them accordingly). For an irreversible decision, such as described above, that essentially must be front-loaded, an adaptive risk management approach may not be possible but more often than not it should be applicable to many decisions. It does require, however, recognition that the decision process is iterative and must be periodically revisited to test the validity of its assumptions over time. This in itself is a risk—that future planners, engineers, and policy-makers will fail to take the necessary adaptive steps—that will need to be considered (USACE 2014).

Figure 5.12 shows conceptually how an adaptive risk management approach to scenario usage may occur. Consider a decision to maintain resilience against flooding in which the future exposure levels to flooding are uncertain (note that future exposure uncertainties also could be dependent on non-climate related futures, such as land uses in a watershed). In Phase 1, current protections against flooding may be adequate and in the near-term (for illustrative purposes, the present time to 2035) may be insensitive to scenario choice on the upper end. The key decision in Phase 1 is to preserve future options to respond to an uncertain long-term flood risk. This could be as simple as ensuring that any land ownership or land-use restrictions needed to ensure future protections are in place; however, this also requires that the long-term objective(s) of the flood management decision are recognized early so that the appropriate set of options can be considered at a future time. In addition, in an adaptive response exposure levels must be periodically monitored and enable sufficient lead time to facilitate planning and implementing the next phase's response actions. Monitoring of local conditions and changes in the understanding of current and future global sea-level trends may accelerate or delay the next phase's decision point so the initial decision still needs to be sufficiently robust.

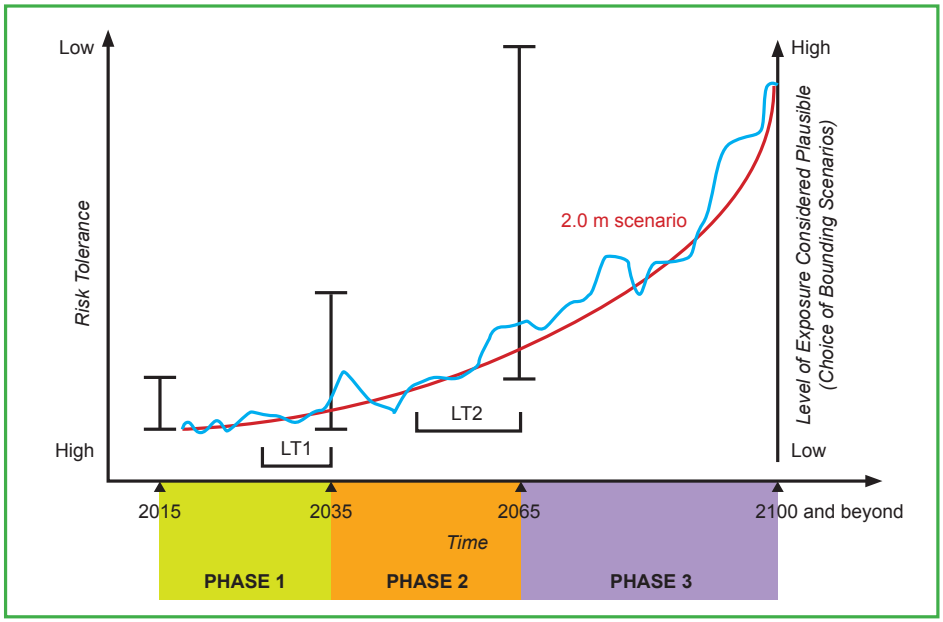

Figure 5.12 Conceptual Diagram of an Adaptive Use of Scenarios
The terms LT1 and LT2 refer to lead times 1 and 2, respectively. The red line represents a hypothetical illustration of how the actual mean sea-level trend may express itself over time in relation to scenario choices and risk tolerance. The phases are the different assessment and planning horizons over which different scenario choices and response decisions must be made. In actuality, natural variability in mean sea level, as illustrated by the blue line, will occur about the scenario curve, but not to the extent that it will impact the usage here as an example. See the text for additional details.

Based on the results of monitoring and improved understanding, adjusted scenarios for Phase 2 can be chosen. Again, for illustrative purposes and to maintain consistency with the time horizons chosen for study herein, we chose 2065 as an exemplar breakpoint between Phases 2 and 3. The key points for Phase 2 are that as we move past mid-century, scenario choices, especially the upper bound considered, take on more and more importance (uncertainty potentially increases). And the rate at which sea-level changes may dictate the need for more lead times in the decision process in regard to the response in Phase 3. The Phase 2 response actions may now include, besides continued monitoring, implementation of protective features determined prior to the end of Phase 1. It is still important that these actions be adaptive, maintain desired protection levels under certainty, and preserve future options for Phase 3. New bounding scenarios are assessed as part of the decision process informing Phase 3 that again may have to account for accelerations in sea-level rise. Uncertainties may or may not have increased depending on whether earlier societal choices have stabilized a particular emissions trajectory or new science has improved understanding of future plausible sea levels. In Phase 3, the decisions from Phase 2 are implemented and adjusted as appropriate through continued monitoring and improved scientific understanding of future conditions.

The above conceptualization is not meant to be prescriptive. Other types of decisions may lend themselves to a different number of phases, use different scenario assumptions, and consider different time horizons. The key points to remember regarding an adaptive risk management approach and use of bounding scenarios are that the decision process is iterative and each decision point, and thus choice of bounding scenarios, should be robust for the desired timeframe, not preclude future response options, and facilitate the appropriate timing of the next decision.

The key points to remember regarding an adaptive risk management approach and use of bounding scenarios are that the decision process is iterative and each decision point, and thus choice of bounding scenarios, should be robust for the desired timeframe, not preclude future response options, and facilitate the appropriate timing of the next decision.

5.3.5 Special case: the zero to twenty-year timeframe

Sea-level rise scenarios based on the RCPs generally show little divergence in their median values even through mid-century (Kopp et al. 2014). Even at the 99% probability level, the spread in the upper bound across RCP 2.6, RCP 4.5, and RCP 8.5 scenarios according to Kopp et al. (2014) is no more than 1 cm by 2030 and 6 cm by 2050, with a maximum value approximating 0.2 meters and 0.5 meters, respectively. It should be noted that Kopp et al. (2014) uses a 2000 baseline and the subsequent time horizons they considered differ than those considered herein. We note, however, that the maximum difference in scenario expression between 2030 and 2050, a twenty-year difference, is no more than 0.3 meters. This provides a reasonable but somewhat conservative basis for a maximum SLR scenario for the period 2015 (Year 0 for this report) to 2035, given we are addressing an earlier time period than Kopp et al. (2014).

As a result, for those decisions with consequences limited to less than 20 years, we can offer those decision-makers interested in more near-term SLR scenarios a simplified set of scenarios and adjustments. It is incumbent on the decision-maker, however, to decide under what circumstances the consequences of his orher decision do not extend past 20 years and when it is appropriate to apply the simplified approach. We recommend the use of two global mean SLR scenarios—the 0.2 meter and 2.0 meter scenarios as defined by their endpoints at 2100—but only following their expression for the period 2015 to 2035 (see Figure 5.13). The 2.0-meter upper-bound scenario adds approximately 0.3 meter above the low-end scenario at 2035 and so is comparable to the Kopp et al. (2014) analysis above; however, by retaining explicit use of the 2.0-meter scenario we retain the anchor to the 1992 tidal epoch and the form of the quadratic for this scenario through the period 2015 to 2035 as shown in Figure 5.13. The offset from the 0.2-meter scenario at 2015 is negligible and can be ignored for the present purpose.

For this application, local or regional systemic adjustments would involve only a consideration of local vertical land movement (VLM). As a result, we are making an additional simplifying assumption that to 2035, the regional deviations from the global mean attributable to DSL and ice-melt processes will be negligible. Adjustments for EWLs can be added as discussed in Section

3.5; however, one other consideration affects this timeframe and needs to be incorporated into the scenarios as an additional adjustment.

Coupled oceanic-atmospheric processes occur over different timescales, and depending on the period of interest and their effect on mean sea level, can be considered to represent either a systemic trend or a cyclical event. For DSL we considered only those changes related to ocean circulation and other phenomena that would express themselves as a trend through the end of this century. For interannual and decadal cycles, such as the El Niño Southern Oscillation (ENSO) and Pacific Decadal Oscillation (PDO), respectively, we considered their effects to average out over long timeframes (i.e., beyond 20 years) and, as a result, not to represent any long-term trend. For the moderate timeframe of zero to 20 years, however, their cyclical nature and the resultant short-term effect on mean sea level may be important to consider.

The magnitude of the effect is location-specific but in extreme situations the variance in the mean sea-level trend caused by these decadal cycles could approach the spread in the recommended SLR scenarios themselves during this time period. Figure 5.13 illustrates this effect as a modest amount of interannual variability (IAV) that—given we assume its range at a particular location does not change over time (stationarity assumptions)—will dominate the SLR trend in the near term and will become less important over longer time horizons.

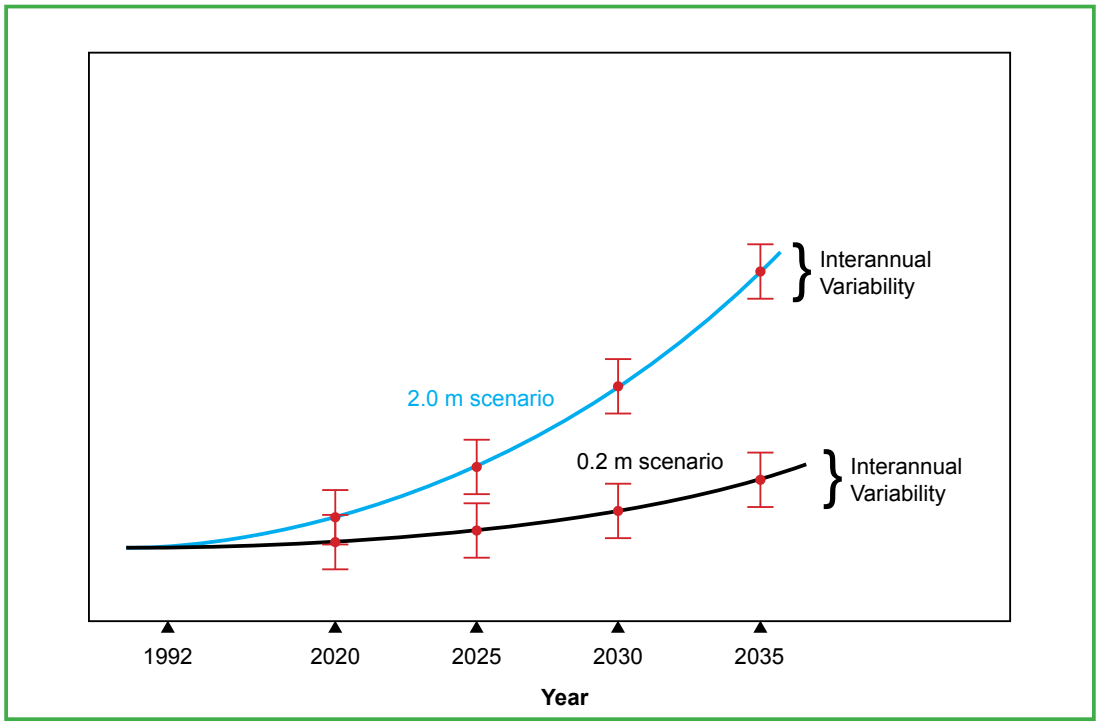

Figure 5.13 Conceptual Diagram to Illustrate Application of SLR Scenarios in the Zero to 20-Year Timeframe
The depiction of interannual variability is illustrative and not to scale with the rest of the figure.

Figure 5.14 provides an illustrative example of a time series of annual mean sea level for two sites that exhibit IAV: San Diego, California, and Norfolk, Virginia. To quantify the variability, the figure shows for each site two standard deviations of the detrended annual MSL residuals. We regard this as a conservative estimate of the variability that should be considered as the adjustment to the SLR scenarios.

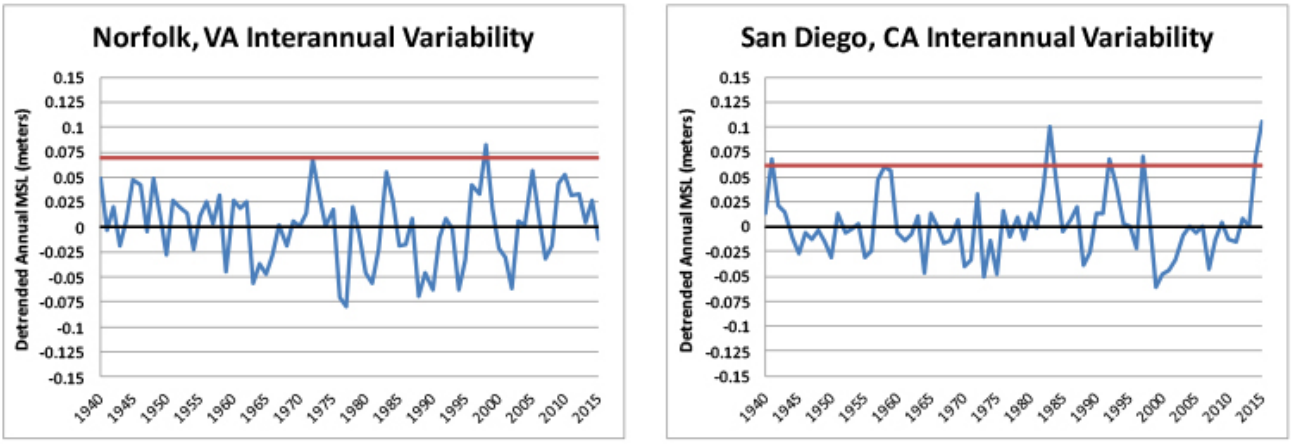

Figure 5.14 Interannual Variability in the Detrended Tide Gauge Records for Norfolk, Virginia, (left) and San Diego, California (right)
Red line identifies the upper two standard deviation annual MSL in meters.

Sites possessing a representative tide gauge (located within 50 km of the site and with at least 30 years of record) can similarly determine an appropriate value for IAV. For sites lacking a representative tide gauge, see section 5.2.2 for a possible approach to installing a tide gauge and acquiring the requisite information.

To summarize the preceding in terms of developing and applying SLR scenarios for the zero to twenty-year timeframe, consider the following steps:

1. Calculate relevant scenario information below in 5-year time steps: 2020 to 2035. Round all values to 0.1 meter.
2. Determine local mean sea level (MSL) in terms of the local geodetic datum (e.g., NAVD88) and 1992 tidal epoch. If you do not have a value for MSL tied to the 1992 tidal epoch, refer to Section 5.2.2 for guidance on installations without tidal datums and geodetic elevation references.
3. For each of the two global SLR curves (0.2 meters and 2.0 meters), calculate its value for each 5-year increment, relative to the 1992 value determined in Step 2.
4. Calculate the contribution of the site-specific VLM for each 5-year increment. Add this to values calculated in Step 3.

5. Calculate the contribution of IAV in the tide gauge record, specific to the site. To be conservative, compute two standard deviations of the residuals in the detrended annual MSL. Assume this number stays the same for each 5-year increment (i.e., assume stationarity). Add this value to the values calculated in Step 4.
6. Prepare a table of values for each 5-year increment for each curve that is the sum of local MSL, the global SLR scenario value at 2020, 2025, 2030, and 2035, VLM, and IAV. For each global SLR scenario, the value will be the total scenario value in MSL. Sums in the table will reveal the offset value between the two curves for each 5-year increment beyond 2015, which should equal 0.3 meters at 2035.
7. If the user desires, values can be added to account for different annual chance probabilities of EWL.

Table 5.3 on the following page provides an illustrative example of applying these steps for the tide gauges at Norfolk, Virginia, and San Diego, California. The values in the table for the global scenarios at the different five-year increments apply for all sites. Values for VLM, IAV, and annual chance event (ACE) are site-specific. The table illustrates converting the information to the local reference datum for Norfolk and San Diego. Although the values for VLM at these two sites do not appear to change over the 20-year period, this is due to rounding associated with our choice of 0.1 meter as being the threshold for significance. The values do in fact change slightly with time. Although the IAV values are the same for both sites and, by our assumption of stationarity do not change with time, this again also is influenced by rounding. In addition, whereas the spread between the calculated low and high scenarios should increase with time, at time 2025 the apparent decrease in the spread compared to 2020 can be attributed to rounding of the scenario values. Finally, note for these two sites that within the zero to 20-year timeframe, the annual chance event (ACE) plays the dominant role in the total scenario values.

Table 5.3 Illustrative Table of Zero to 20-Year Sea-Level Rise Scenario Values for (a) Norfolk, Virginia, and (b) San Diego, California

Blue rows indicate data common to all DoD sites.

A) Norfolk

Scenario	2020 (change since 1992, with respect to NAVD88	2025	2030	2035
Lowest - 0.2-meter	0.0	0.1	0.1	0.1
MSL at Norfolk, relative to NAVD88	-0.1	-0.1	-0.1	-0.1
VLM	0.1	0.1	0.1	0.1
IAV	0.1	0.1	0.1	0.1
ACE (20% value calculated for illustrative purposes)	1.1	1.1	1.1	1.1
TOTAL LOW VALUE	**1.2**	**1.3**	**1.3**	**1.3**
Highest - 2.0-meter	0.2	0.2	0.3	0.4
MSL at Norfolk, relative to NAVD88	-0.1	-0.1	-0.1	-0.1
VLM	0.1	0.1	0.1	0.1
IAV	0.1	0.1	0.1	0.1
ACE (20% value calculated for illustrative purposes)	1.1	1.1	1.1	1.1
TOTAL HIGH VALUE	**1.4**	**1.4**	**1.5**	**1.6**

B) San Diego

Scenario	2020 (change since 1992, with respect to NAVD88	2025	2030	2035
Lowest - 0.2-meter	0.0	0.1	0.1	0.1
MSL at Norfolk, relative to NAVD88	0.1	0.1	0.1	0.1
VLM	0.0	0.0	0.0	0.0
IAV	0.1	0.1	0.1	0.1
ACE (20% value calculated for illustrative purposes)	0.4	0.4	0.4	0.4
TOTAL LOW VALUE	**0.6**	**0.7**	**0.7**	**0.7**
Highest - 2.0-meter	0.2	0.2	0.3	0.4
MSL at Norfolk, relative to NAVD88	0.1	0.1	0.1	0.1
VLM	0.0	0.0	0.0	0.0
IAV	0.1	0.1	0.1	0.1
ACE (20% value calculated for illustrative purposes)	0.4	0.4	0.4	0.4
TOTAL HIGH VALUE	**0.8**	**0.8**	**0.9**	**1.0**

Epilogue

This epilogue contains four parts. Part 1 briefly addresses the addition of sites to the scenario database subsequent to the analyses conducted as part of this report. Part 2 highlights the significant agency and peer review comments on the draft report and how they were addressed in the final version. Part 3, itself a response to review comments, summarizes our view of key research gaps that should be addressed to further advance the development and use of sea-level rise (SLR) and extreme water level (EWL) scenarios to support coastal risk management. Part 4 provides major conclusions and lessons learned discovered through the over 2-year process to produce this report and associated database.

Part 1 - Sites added to the scenario database

The Department of Defense's (DoD) Real Property Assets Database (RPAD) is dynamic. Updates made in 2015 to RPAD, along with an additional quality assurance review of all potential sites within the 20-kilometer (km) buffer and otherwise tidally influenced sites (spurred in part by Military Service beta test review of the scenario database), added an additional 39 sites (for a new total of 1,813 sites) to the scenario database. These additional sites were identified after the aggregate site analyses that contributed to this report were completed. These additional sites were assigned the full complement of scenario-related information, including regional frequency analysis-derived EWL values, as applicable, as for the original 1,774 sites.

Part 2 - Significant agency and peer review comments

Although each agency or peer reviewer supported the need for this effort and general approach toward providing sea level and EWL scenario information, each of the reviewers also provided substantive comments that significantly improved the report and the interpretation of its findings. In some cases, reviewers requested additional justification for our methodological approach and in limited instances expressed some disagreement. For each of the significant comments that identified a disagreement or need for additional justification (summarized in bolded font below), a short narrative is provided describing our response to the comment.

The choice of the upper scenarios (1.5 meters and 2.0 meters) falls outside the range provided by the Intergovernmental Panel on Climate Change (IPCC; Church et al. 2013a). Reviewers differed on whether they considered our use of and justification for upper bound scenarios as appropriate. This report, similar to the manner of Parris et al. (2012), U.S. Army Corps of Engineers (USACE; 2014), and Hinkel et al. (2015), took a risk management approach to defining

a plausible upper set of scenarios to bound future risks. In such an approach, risk managers are concerned with high consequence events that lie within the plausible range of potential futures. Our approach does not assign likelihoods to any specific scenario, but rather in a manner similar to Parris et al. (2012) expresses confidence that we have captured the plausible range of potential future global sea levels. We assert that this is an appropriate approach given the purposes of this report and that some of the uncertainties involved cannot be assigned probabilities in any objective sense. Part of the disagreement on the upper scenarios relates to consideration of the collapse of the West Antarctic ice sheet and its associated magnitude of mass loss, as well as the "calibrated uncertainty language" (Hinkel et al. 2015) used by the IPCC to estimate the upper end of the Representative Concentration Pathway (RCP) 8.5 scenario. Recent expert elicitation approaches to estimating ice-sheet mass losses and their application in more expansive probabilistic approaches provide support for the use of the upper scenarios in a risk management context (e.g., see Kopp et al. 2014); however, other investigators contend that these estimates should be more constrained (see Clark et al. 2015, Ritz et al. 2015). We recognize the significance and scientific value of these recent findings and viewpoints, but still argue that a risk-based framing approach needs to account for future SLR that the scientific community is not yet prepared to quantify with confidence.

Moreover, 2100 is becoming more and more an arbitrary and less useful cut-off point for assigning SLR scenario endpoints. Several reviewers wanted us to further emphasize the consequences of post-2100 SLR. The available data limit us in doing this in any explicit quantitative sense; however, for those concerned that the upper bounding scenarios are more tenuous because of their reliance on expert elicitation, their use may provide some degree of additional protection as we begin to plan for time periods in the twenty-second century and await refined information that extends beyond 2100.

Justify the assumption of stationarity in nontidal residuals for estimating EWLs versus applying scenarios that incorporate non-stationarity.

We analyzed the annual-highest nontidal response measured at a global set of tide gauges to estimate contemporary EWL probabilities across the globe. An underlying assumption is that the only factor that will cause EWL probabilities to change in the future is increases in local mean sea level (MSL). This assumption is supported through historical tide gauge observations, which show that magnitude changes in EWLs are predominantly attributed to similar magnitude changes in MSL (Menéndez and Woodworth 2010). We note that important time-varying EWL patterns occur in the historical record. For instance, El Niño Southern Oscillation (ENSO) causes interannual variability in regional MSL, which manifests locally as prolonged nontidal changes in water levels relative to long-term trends. The ENSO also affects storm tracks and regional storm surge frequencies. Increases in both prolonged and punctuated nontidal responses can lead to annual clustering of high-water events, such as occurs during the El Niño phase of ENSO when the annual chance of less extreme "nuisance" tidal floods increases along the U.S. East and West Coasts (Sweet and Park, 2014). Future prognosis of EWL probabilities dependent on climate variability (e.g., ENSO) is beyond the scope of this report and an active topic of research. We note, however, that we do apply historical estimates of interannual variability in MSL in a special case of projecting SLR scenarios between 2015 and 2035.

It was recommended that we consider future changes in tropical storm strength (surge magnitudes) in a warmer climate, which is a topic of active research. The challenge for this assessment and others is to provide a contemporary assessment (let alone future estimates) of the low-probability event, such as from direct landfall of tropical storms (hurricanes) for a *particular* location through direct measurements. Because of the rarity of such storms from the perspective of a direct strike over a specific geographic location, individual tide gauges generally lack a sufficient sample size to make a robust estimate in a probabilistic sense. We partially overcame this limitation through our use of a regional network of tide gauges to estimate a site's extreme event probabilities (additional details provided immediately below).

The regional frequency analysis (RFA) uncertainty bounds require some caution in interpretation due to the possibility that information from tide gauges within a region may be highly correlated, which may lead to overconfidence in the uncertainty bounds. (i.e., confidence bounds are unduly tightened due to correlated events)

We employed a regional approach to estimate a location's extreme nontidal event probabilities. This approach combines annual-highest nontidal water level information from multiple tide gauges exposed to similar synoptic phenomena (e.g., tropical storms, nor'easters, etc.). The regional probability distribution is rescaled to a site's characteristic (average of annual-highest values of record) surge response (e.g., attenuation or amplification from local bathymetry) when a local representative tide gauge was available or by the average from the regional set of tide gauges when a local tide gauge was not available. The local extreme nontidal probabilities were then linked to local mean higher high water tidal datums (when available) to provide impact elevations needed for planning purposes.

The advantages of a regional approach include the ability to: (1) provide extreme probabilities for locations without a tide gauge and (2) increase the sample size of rare-event measurements (e.g., landfall of tropical cyclones) that are typically too sparse to be captured within an individual tide gauge's record to make robust probabilistic estimates. The effect of an overall larger pool of regional measurements is a refined estimate of rare (and less rare) event probabilities with narrower confidence intervals. The RFA spatial method assumes all data are independent samples. On occasion, however, the annual-highest events across a region may be in response to the same storm, with the result that some lesser magnitude events would be removed from consideration in the probability distribution. We did not attempt to distinguish such overlap because of difficulties in discerning particular storm "footprints" across our extremely large number of regions (i.e., those delineated by a set radius of 400 km around our DoD sites). As a result, we acknowledge that some correlation may exist within a region's data and lead to an underestimate in our reported probability confidence bounds (e.g., the upper-end confidence level is statistically lower than it might be otherwise). If risk managers are focused on rare-event probabilities, they should be aware of this fact and consider using simulated results from dynamical models to gain a fuller spectrum of possibilities.

The report needs to better characterize the sources of uncertainty in a clear, conceptual framework that allows the reader to better judge their contributions to and impacts on the use of scenario information.

Uncertainties in individual components contributing to regional sea level at a particular point can be large and together they may result in significant uncertainty bounds. The work reported in this study made an attempt to quantify some of the uncertainties associated with individual components and the approaches used to do this are summarized in the report; however, concerns regarding the difficulties in accounting for cross-correlation among various components led to the decision not to aggregate uncertainties. The authors were fully aware of such attempts in the literature but such efforts were not rigorous in terms of accounting for the cross-correlation among various components. For instance, Church et al (2013b, supplementary material, Eq. 13.SM.1) simply added the individual variances to provide an estimate of regional error. Grinsted et al. (2015), however, went further and used an estimate of covariance matrix to account for such cross-correlation but its determination included many assumptions and was only accomplished relative to the RCP 8.5 scenario. Moreover, our study added additional component uncertainties, such as estimates for vertical land movement (VLM) rates that included measurement error and unquantified uncertainties that related to the proximity of the data source to the site of interest. Because the objective of this study was primarily for screening-level assessment of potential vulnerabilities or impacts at individual sites, the uncertainty estimation in terms of aggregated and quantified values, although desirable, was not deemed critical. The authors recognized that uncertainty quantification is an important task that should be the subject of active research (see below). To summarize the types of uncertainty and how we addressed them in the report, we added a new table to Section 4.6 (Table 4.6) to capture more succinctly the various contributions.

Two sources of uncertainty or assumptions related to adjustments to the global SLR scenarios require further explanation: (1) process model differences in the spatial patterns produced, whether from ice-melt fingerprinting or dynamical sea-level pattern scaling and (2) assumptions about the spatial distribution of ice mass loss at the source.

Although the use of ice-melt fingerprints scaled by mass loss has been reported in the literature by many (e.g., Grinsted et al. 2015), the pattern scaling adopted for the dynamical sea-level (DSL) adjustments used in this report (primarily based on Perrette et al. 2013) has received less attention. Our use of pattern scaling was based on the median values derived from multiple (20) process models (Perrette et al. 2013). Although Perrette et al. (2013) recognized that the pattern scaling is global climate model-specific, the spatial patterns of the scale factors generally appeared similar across most models, except at extreme high latitudes (Figures S2 and S4 in Perrette et al. 2013). Consequently, the median pattern scaling was used for each scenario without any consideration for model spread. Our validation of the spatial pattern, based on its similarity to Yin (2012), is our only measure of the robustness of this pattern besides the validation efforts for the overall pattern-scaling approach reported by Perrette et al. (2013). Future work may need to include the uncertainty in scale factors due to model spread.

As noted in Section 3.4.4, Grinsted et al. (2015) incorporated the uncertainty in the ice-melt fingerprints by using alternative configurations presented by Bamber and Riva (2010) and Kopp et al. (2014); however, their projection was for one scenario, namely RCP 8.5. We considered the

upper and lower bounds of the fingerprints provided by Perrette et al. (2013) but they yielded unrealistic results for bounding uncertainty and were not considered further. In view of the lack of uncertainty estimates for fingerprints in the current body of literature, particularly for all the scenarios considered in the current study, it was assumed that the median fingerprints provided by Perrette et al. (2013) are reasonably robust and meet the needs of a screening level analysis of regional projections.

Another factor that may cause uncertainty in fingerprints is the incomplete knowledge of the geometry of melt. The model used by Perrette et al. (2013), attributed to Bamber and Riva (2010), assumed the present-day distribution of mass loss though the distribution is likely to change in the future. The exact distribution of mass loss region, however, is important only in the near-field of an ice sheet (less than 1000 km) (Perrette et al. 2013). As a result, the geometry of melt may not play a significant role for most of the sites analyzed in the report.

Address how current natural variability in sea level may present a significant risk even in the near term.
Reviewers correctly pointed out that near-term SLR can pose significant risks to coastal areas. Haigh et al. (2014b) noted that significant variations in interannual to multi-decadal sea-level variations occur in MSL. Although they were concerned with evaluating methods associated with the capability to detect significant accelerations in SLR, these variations are important for another reason. Because the recent rise in MSL is generally the dominant cause of the observed increase in the frequency of extreme events (Hunter 2012, Hunter et al. 2013), in the moderate timeframe considered in this report (i.e., out to 2035) cyclical variations in MSL that otherwise will average out over longer timescales are important to consider when assessing risk from extreme and lesser events. We address this important concern in two ways: (1) for EWL statistics, we do not focus solely on the rare events (i.e., 1% and 2% annual chance events) but also provide information on the lesser but more frequent events (i.e., 5% and 20% annual chance events) and (2) for the zero to 20-year timeframe, we acknowledge the importance of interannual variation in MSL within this timeframe and include it as an adjustment (see Section 5.3.5). Additional suggestions were made about approaches for accounting for this additional risk (i.e., Hunter 2012, Hunter et al. 2013). We acknowledge that users may want to consider such methods (as well as potentially others, some of which we illustrate as examples); however, we are careful in this report to assist in the interpretation and use of scenarios without implying we are offering explicit guidance as to how users should proceed. We considered providing guidance that might be viewed as prescriptive to be beyond the scope of the current effort, but recognize that it may be valuable to consider this in an appropriate context as a next step.

Acknowledge the role of "event footprint" and "storm clustering" as a component of risk.
Two additional components of risk management in the coastal environment were raised associated with storm events: (1) multiple sites or installations could be impacted by the same storm event (the concept of an event footprint) and (2) storm events could "cluster," such that two relatively small events occurring close in time could result in more damage than a single larger event. As noted by the reviewer, these considerations were outside the scope of the present study, but we note them here as they are important considerations that military planners and managers at

different organization levels may want to account for as they make risk-based decisions in the coastal environment.

Clarify how adaptive risk management is more efficient than a predict-then-act approach.
The adaptive use of scenarios, highlighted pictorially in Figure 5.11, is an iterative approach in which decision-makers must assess their risk on an ongoing basis, implement a response that is adaptive to climate change in the near term but also maintains appropriate future options for adaptation in the long term (i.e., early actions do not preclude later options), and tracks changing environmental conditions, the response action's effectiveness, and emerging understanding of the climate system and how it may behave in the future. As a result, the decision-maker must maintain both a near-term and long-term perspective regarding the consequences of their actions and update them iteratively over time as new information becomes available. This approach is different from a predict-then-act approach in that no assumption is made of a most likely future at any point in the decision process that would dictate a singular response action to an assumed future climate. The adaptive use of scenarios helps to avoid inefficiencies associated with either under- or over-protective responses.

Describe the process for vetting the scenarios and their development and the degree to which end users were part of the discussion on application of the scenarios.
The working group for this effort included technical experts from the National Oceanic and Atmospheric Administration, Strategic Environmental Research and Development Program (SERDP), Office of the Oceanographer of the Navy, USACE, and South Florida Water Management District. Each of these individuals is involved in the translation of scientific information for use by end users and, in particular, is extensively involved in providing actionable science in the coastal environment. The working group also engaged outside experts during the process of method development to obtain relevant datasets and validate methodological approaches.

Periodic briefings were made to a broad range of user communities that informed these entities of the scenario development process and scenario application issues. The primary audiences for these briefings were the DoD Climate Change Adaptation Working Group and DoD Assessment Guidance Sub-Working Group. Various other groups that showed interest in the process were briefed, including individuals associated with updating DoD Unified Facilities Criteria, DoD Joint Land Use Study program managers, the Interagency Forum on Climate Change Impacts and Adaptations, South Florida Water Management District, U.S. Global Change Research Program (USGCRP), USGCRP-National Oceans Council SLR-Flood Risk Task Force, U.S. Coast Guard, Union of Concerned Scientists, academic staff of the U.S. Naval Academy, agency science leadership, and the Northern Gulf of Mexico Sentinel Site Cooperative. In each of these presentations, individuals provided feedback on scenario development and their possible application. Finally, a focus group of representatives from all of the Military Services and the Office of the Secretary of Defense (OSD) conducted Beta testing of the scenario database and its associated Graphical User Interface (GUI), which provided the interim "results" of our effort. Beta testers were asked to comment on the usefulness of the database for decision-making purposes by OSD and the Military Services. We anticipate that our target users will access the database of scenario values through the GUI more than they will consult the report, which serves primarily to document the purpose and methodology behind the SLR and EWL scenario development.

Part 3 - Key information or research gaps

Potential non-stationarity of future storm statistics.
As we noted above, time-varying patterns occur that affect the frequency of storms and their storm tracks, which can lead to clustering of storm surges and impacts in both time and space. These prolonged and punctuated event responses do not typically represent a persistent long-term "trend" and future prognosis of their time-specific states—at a point location or in a spatial sense—is an active area of research. In addition, although climate scientists in some cases have begun to project qualitative increases in storminess, no consensus currently exists around an approach to provide quantitative projections for future storminess. Given our tide gauge-based approach to estimating EWL statistics, adjusting these values to account for potential future non-stationarity also presents additional methodological challenges.

Nonlinearities of storm surge associated with sea-level rise.
We did not account for potential changes in storm surge magnitudes likely to occur in dynamical responses to rising ocean levels, at least in specific but also widespread locales. This is an active research question that is sensitive to a number of locally relevant factors, such as shoreline geometry and bathymetry, identified in Section 5.1.1. To the extent that a nonlinear response can be significant in some areas, finer degrees of vulnerability and impact assessment and adaptive responses should explicitly incorporate their considerations. Coarse screening-level assessments also could be aided by simple rules that enable incorporating a "safety" factor that accounts for the nonlinearity of storm surge response with SLR in areas anticipated to be conducive to such effects. Sea-level rise also could lead to changes in tidal amplitudes, but such changes may be small overall or confined to specific locations (Hunter et al. 2013). Similarly, in wave-dominated areas around Pacific Basin coral atolls, wave heights will be affected by changes in sea level if bathymetric characteristics change as well. This also is an active area of research.

Coastal response.
The SLR and EWL scenarios developed in this report treated the response of the coastal environment (regardless of whether its physical, biological, and/or human-built aspects are considered) as passive; as a result, water levels based on the scenarios would rise as if in a bathtub. In reality, natural coastal features will respond dynamically and current or future human actions will occur that could significantly alter the pattern of local land inundation and flood risk due to SLR. The spatial extent of natural responses could be significant and in general may act to reduce risk (Lentz et al. 2016). Different from the non-stationarity and nonlinear response issues discussed above, coastal response represents a conservative assumption in the use of the scenarios developed in this report. Still, continued research in this area is warranted to better understand how the natural and built systems will respond and how their responses may affect vulnerability and impact assessment and the tools and methods available to facilitate an adaptive response.

Gridded vertical land movement information.
The VLM data acquired and processed for this report supported a site-based approach. We followed this approach given the global nature of the DoD enterprise and because the RPAD provided a convenient and standard information framework on top of which to assign scenario values for widely distributed assets. We used three types of information, only one of which—glacial

isostatic adjustment data—was available as a gridded product. The other two sources—tide gauges and global positioning system—are point data. The distance away a site was located in relation to the three sources was a major contributor to uncertainty in the VLM rate estimates. Instead of a site-based approach, some stakeholders may desire that VLM information be made available in a continuous manner or at least perhaps via a gridded product at a useful spatial scale. Either way, this presents several challenges given the nature of the VLM source data and how confidence in their representativeness decreases with distance from the source. Factors such as surficial geology and human activities (e.g., groundwater and hydrocarbon fluid withdrawal), and the spatial scales at which they change, will affect the ability to provide gridded VLM data and characterize its associated uncertainties. A simple gridded interpolation model would not work well in areas where discontinuities occur in VLM rates, such as on opposite sides of fault lines or "bull's eye" effects of localized anomalies in VLM due to point source fluid withdrawal. Integration of repeat GPS surveys and continuous GPS data combined with Interferometric Synthetic Aperture Radar remote sensing data have been used successfully to obtain estimates of VLM with high spatial resolution (see Sneed et al. 2001).

Temporally continuous dynamical sea-level pattern scaling and ice-melt fingerprints.
The use of pattern scaling for DSL and fingerprints for ice melt as fixed over time and across global scenarios requires further validation. Although it is challenging to simulate the patterns across all global climate models and RCPs for different time epochs, further validation of the normalization used in this report may be warranted. A particularly difficult aspect of this research is the specification of global scenario and the need to determine the spatial pattern corresponding to those prescribed scenarios. Although it is possible to define exact RCPs corresponding to the prescribed global scenarios and time epochs used in this study, such an effort can be extensive and require significant resources. This is an area of necessary research, particularly if more accurate site-specific adjustments for DSL and ice melt aspects are needed.

In addition, the available process model data sets were based on time slices that precluded us in applying DSL and ice melt adjustments as continuous functions in time. This limited us as well in how we could apply the EWL scenarios atop the SLR scenarios. Users desire information in a temporally continuous manner, which also would enable more user-friendly means of conveying the risk aspects. Despite this need, future advancements also should account for the other sources of natural variability that come into play when conveying risk in a continuous temporal fashion.

Finally, another area of needed research is the incorporation of pattern scaling and fingerprint variability across GCMs in the uncertainty estimation. Fingerprint variability also may need to account for different melt geometries to the extent that certain sites are affected by the assumptions inherent in different melt patterns.

Uncertainty Characterization.
Several reviewers commented on uncertainty characterization, with a focus on quantification when feasible. We recognize this as a major research challenge. The uncertainty in projecting global MSL (hence a broad range in projections) is partly addressed by the particular scenario approach used here that attempts to bound the range of plausible futures versus predict any particular future.

Assigning probabilities to various scenarios may be desirable, but it is not feasible in part because of the lack of accepted practice for a probabilistic framework but also due to the nature of the scenarios themselves (i.e., their dependency on uncertain human behaviors). This clearly is an area of needed research.

Notwithstanding the non-probabilistic nature of the global scenarios, once a scenario is chosen, any attempt to produce quantitative estimates of uncertainty in projected sea level at a location requires knowledge of the uncertainty associated with individual component contributions. In addition one must know how the component contributions are expressed differentially (both regionally and locally) before they are then aggregated to compute the overall sea level. Moreover, different *v* of uncertainty are involved, such as measurement error related to VLM or model spread for the process model-based information. Combining these types and magnitudes of uncertainties is challenging. The VLM uncertainty also included proximity issues, given the site-based approach used in this report. We did not quantify the uncertainties associated with distance from the source measurement; instead, we presented them in a qualitative fashion. In addition, the estimation of uncertainty in individual components is difficult in a scenario-based approach in which a global MSL is specified upfront if the available process model information does not match exactly the assumptions associated with the scenario. Finally, such an effort becomes even more complicated because of potential cross-correlations among the individual components and the difficulties in estimating them. The preceding challenges also should be an active area of research in the future.

Scenario application in a risk management context.
Our attempt in this report was not only to provide specific scenario values in a global context, but also to provide some context for understanding what was behind the numbers and how they could be applied. Realistically, we may have only scratched the surface for what is needed here. Efforts such as this one and that of USACE (2014) are attempts to "operationalize" the use of scenario information, though we explicitly avoid in this report offering our discussion of scenario application as guidance. Given the human dimensions of the decision-making process, we contend that the use of scenarios in a risk management context transcends traditional predict-then-act approaches and sees the importance of assisting decision-makers with managing risk under a non-stationary and an uncertain future as a key area for future applied research.

Part 4 – Major conclusions and lessons learned

Coastal risk management is an iterative enterprise, especially under the non-stationary conditions of climate change.
Through this exercise, we tried to provide bounding information for coastal risk management under climate change, but at the same time we also identified needs for future research. Coastal risk management under climate change poses new challenges. Although coastal communities have experience in understanding and managing risk in the coastal environment, that experience has largely been drawn from a stationary, and often linear, deterministic world. With climate change, conditions of non-stationarity and nonlinear responses must be taken into account. Moreover, the importance of observational data, their spatial distribution, quality, and uncertainty are enhanced when the effects of SLR and associated EWLs are now distributed across entire coastlines.
Our observational networks were not set up in response to concerns about SLR. It has only been

relatively recently that SLR scenarios have caught the attention of risk managers and the public.

The global scenarios of Parris et al. (2012) prepared in support of the Third National Climate Assessment were the first attempt to develop a national set of global SLR scenarios. These authors, however, recognized that for effective decision-making, these scenarios would need to be localized. This report, as well as other concurrent activities recognizing this need, takes the next step in regionalizing the global SLR scenarios to account for the three major adjustments related to the non-uniform distribution of sea-level change around the globe. Yet given that the adjustments are fairly coarse and the underlying scenarios are non-probabilistic, the scenario values developed are still best used in a screening context or in a relative risk evaluation context, whether that be at a global, national, Military Service, or installation level. For example, the DoD may want to assess the relative vulnerability of all of its coastal sites, whereas an installation manager may want to assess the relative vulnerability of particular assets within an installation.

Through the process of developing scenarios for regionalized SLR and EWL in a global context, the working group recognized that we are also on a pathway of discovery regarding the development and application of scenarios. In other words, we: (1) had to be open to the use of approaches such as RFA that enabled us to extend the applicability of our approach to sites that under traditional approaches would not be addressed, (2) identified the limitations of our current understanding, data, and methods, (3) understood the ultimate necessity of conveying the uncertainties involved, even if qualitatively, to those audiences that may have use of these scenarios, and (4) identified new areas of inquiry that are needed to enhance the use of scenarios for coastal risk management purposes. We were able to provide site-specific data to help planners and managers at different organizational levels, but recognize that this advancement is merely one step in the iterative process to improve methodologies for risk management decisions.

From the standpoint of flood risks, this report addresses regional adjustments to sea level and extremes associated with still (not total) water levels.
Risk managers may need to further take account of, as part of their vulnerability and impact assessments, other factors such as the effects of waves when assessing consequences of total water level extremes. Our report uses information for tide gauges that are usually located in harbors and other protected environments and whose engineered structures and sample schemes are intended to filter out wave effects. The effects of waves may be important to consider especially in wave-dominated locations versus storm-surge locations.

Constraints of current scientific understanding.
Through the development process, we identified a number of areas of inquiry that were ultimately beyond the scope of this current effort but nevertheless are important considerations for future research and for better conveying the scenario information for coastal risk management. These include a more holistic and comprehensive treatment of uncertainty, recognizing that the sources and methods of characterization of these uncertainties are quite diverse, let alone being able to combine them in any realistic (meaningful) manner. Moreover, the preceding includes placing these uncertainties into an appropriate context that allows appropriate and effective decision-making. In addition, we are limited by either our current understanding of how physical coastal processes

may behave under rising sea levels or perhaps, more likely, not by a lack of understanding, but by a lack of adequate data, methodological tools, and resources to adequately investigate these phenomena on a site-specific basis. For example, we understand that wave processes may be important at some locations, but we do not have the data, methodologies, or resources to be able to quantify wave contributions at all sites. Notwithstanding the preceding, depending on the decision to be made and the risk tolerance of that decision, exact understanding of these processes may not be needed. In other words, some locations and decisions may not be sensitive to uncertainties in these physical processes; thus, additional resources to further quantify uncertainties may not be warranted. Proper uncertainty quantification is deemed challenging, though this is not critical for the screening-level exercise that was the subject of this study.

Significant findings.

- The three regional or local adjustments to global mean sea level considered herein—VLM, DSL pattern scaling, and ice-melt fingerprinting—are not necessarily consistent in their directionality (i.e., increases or decreases in sea level) and magnitude at a particular site. In some cases, positive and negative adjustments to sea level may cancel each other. In some regions, the VLM rate can exceed that of regional SLR from the combination of DSL and ice-melt effects by an order of magnitude in either direction.
- VLM rates are independent of climate factors. Given the scenario independence and assumed linearity of VLM rates, geographic location plays the critical role in a broad assessment of relative SLR contributions from VLM compared with other components of regionalized adjustments.
- DSL adjustments generally tend to increase sea level at DoD sites in the northern hemisphere and decrease sea level in the southern hemisphere.
- The more prominent influence of near-field effects (i.e., sea levels fall [negative adjustment] near the area of ice-mass loss) further amplifies late century impacts for DoD sites in close proximity to one of the three contributing sources of ice melt. The sites that will experience the greatest positive SLR adjustments from ice mass loss from Antarctica are located in the Pacific Ocean.
- By employing the RFA method, we were able to expand the number of the original 1,774 sites for which EWL values could be provided from 53% to almost 86% of the sites.
- With regard to EWL, we did not de-emphasize importance of the 1% event, but rather equally emphasized the importance of considering higher frequency events that result in recurrent flooding in coastal risk management decisions.
- Location with respect to physical setting (e.g., shoreline configuration and local and regional bathymetry) plays a significant role in determining whether storm surge is a key component of EWLs at a particular site and how these levels may change under SLR.

THIS PAGE LEFT INTENTIONALLY BLANK

Literature Cited

Aerts, J.C.J.H., W.J. Wouter Botzen, K. Emmanuel, N. Ling, H. de Moel, and E.O. Michel-Kerjan. 2014. Evaluating Flood Resilience Strategies for Coastal Megacities. *Science* 344:473–475.

Arns, A., T. Wahl, S. Dangendorf, and J. Jensen. 2014. The Impact of Sea Level Rise on Storm Surge Levels in the Northern Part of the German Bight. *Coastal Engineering* 96:118–131.

Arns, A., T. Wahl, I. Haigh, and J. Jensen. 2015. Determining Return Intervals at Ungauged Coastal Sites: A Case Study for Northern Germany. *Ocean Dynamics* 65:539–554.

Bamber, J. and R. Riva. 2010. The Sea Level Fingerprint of Recent Ice Mass Fluxes. *The Cryosphere* 4:621–627.

Bamber, J.L. and W.P. Aspinall. 2013. An Expert Judgment Assessment of Future Sea Level Rise from the Ice Sheets. *Nature Climate Change* 3:424–427.

Bardet, L., C.M. Duluc, V. Rebour, and J. L'Her. 2011. Regional Frequency Analysis of Extreme Storm Surges along the French Coast. *Natural Hazards and Earth System Sciences* 11:1627–1639.

Batstone, C., M. Lawless, K. Horburgh, D. Blackman, and J.A. Tawn. 2009. Calculating Extreme Sea Level Probabilities around Complex Coastlines: A Best Practice Approach. In *Proceedings – Irish National Hydrology Conference 2009 (Tullamore, Ireland)*, 24–32.

Bernardara, P., M. Andreewsky, and M. Benoit. 2011. Application of Regional Frequency Analysis to the Estimation of Extreme Storm Surges. *Journal of Geophysical Research: Oceans* 116:C02008. doi:10.1029/2010JC006229.

Bilbao, R.A.F., J.M. Gregory, and N. Bouttes. 2015. Analysis of the Regional Pattern of Sea Level Change Due to Ocean Dynamics and Density Change for 1993–2099 in Observations and CMIP5 AOGCMs. *Climate Dynamics* 45:2647–2666. doi:10.1007/s00382-015-2499-z.

Bilskie, M.V., S.C. Hagen, S.C. Medeiros, and D.L. Passeri. 2014. Dynamics of Sea Level Rise and Coastal Flooding on a Changing Landscape. *Geophysical Research Letters* 41:927–934.

Bindoff, N.L. et al. 2007. Observations: Oceanic Climate Change and Sea Level. In *Climate Change 2007: The Physical Science Basis*. Contribution of Working Group I to the Fourth Assessment Report of the Intergovernmental Panel on Climate Change, edited by S. Solomon, D. Qin, M. Manning, Z. Chen, M. Marquis, K.B. Averyt, M. Tignor, and H.L. Miller, 385–432. Cambridge, United Kingdom and New York, New York: Cambridge University Press.

Boesch, D.F. et al. 2013. *Updating Maryland's Sea-Level Rise Projections. Special Report of the Scientific and Technical Working Group to the Maryland Climate Change Commission*. Cambridge, Maryland: University of Maryland Center for Environmental Science.

Bromirski, P.D., A.J. Miller, R.E. Flick, and G. Auad. 2011. Dynamical Suppression of Sea Level Rise along the Pacific Coast of North America: Indications for Imminent Acceleration. *Journal of Geophysical Research*: *Oceans* 116:C07005. doi:10.1029/2010JC006759.

Carignan, K.S., L.A. Taylor, B.W. Eakins, R.J. Caldwell, D.Z. Friday, P.R. Grothe, and E. Lim. 2011. *Digital Elevation Models of Central California and San Francisco Bay: Procedures, Data Sources and Analysis*. National Oceanic and Atmospheric Administration (NOAA) Technical Memorandum NESDIS NGDC-52. Boulder, Colorado: NOAA, National Geophysical Data Center, Marine Geology and Geophysics Division.

Church, J.A., N.J. White, R. Coleman, K. Lambeck, and J.X. Mitrovica. 2004. Estimates of the Regional Distribution of Sea Level Rise over the 1950–2000. *Journal of Climate* 17:2609–2625.

Church, J.A., J.R. Hunter, K. McInnes, and N.J. White. 2006. Sea-level Rise Around the Australian Coastline and the Changing Frequency of Extreme Events. *Australian Meteorological Magazine* 55: 253-260.

Church, J.A. and N.J. White. 2011. Sea-Level Rise from the Late 19th to the Early 21st Century. *Surveys in Geophysics* 32:585–602.

Church, J.A. et al. 2013a. Sea Level Change. In Climate Change 2013: *The Physical Science Basis. Contribution of Working Group I to the Fifth Assessment Report of the Intergovernmental Panel on Climate Change*, edited by T.F. Stocker, D. Qin, G.-K. Plattner, M. Tignor, S.K. Allen, J. Boschung, A. Nauels, Y. Xia, V. Bex, and P.M. Midgley, 1137–1216. Cambridge, United Kingdom: Cambridge University Press.

Church, J.A. et al. 2013b. Sea Level Change Supplementary Material. In *Climate Change 2013: The Physical Science Basis. Contribution of Working Group I to the Fifth Assessment Report of the Intergovernmental Panel on Climate Change*, edited by T.F. Stocker, D. Qin, G.-K. Plattner, M. Tignor, S.K. Allen, J. Boschung, A. Nauels, Y. Xia, V. Bex, and P.M. Midgley, 13SM-1–13SM-8. Cambridge, United Kingdom: Cambridge University Press.

Church, J.S. et al. 2013c. Sea-Level Rise by 2100. *Science* 342:1445.

Cialone, M.A. et al. 2015. *North Atlantic Coast Comprehensive Study (NACCS) Coastal Storm Model Simulations: Waves and Water Levels*. ERDC/CHL TR-15-14. Vicksburg, Mississippi: U.S. Army Corps of Engineers (USACE), Engineer Research and Development Center, Coastal and Hydraulics Laboratory.

Clark, P.U., J.A. Church, J.M. Gregory, and A.J. Payne. 2015. Recent Progress in Understanding and Projecting Regional and Global Mean Sea Level Change. *Current Climate Change Reports* 1:224–246, doi:10.1007/s40641-015-0024-4.

Coles, S. 2001. *An Introduction to Statistical Modeling of Extreme Values*. London, United Kingdom: Springer-Verlag.

Cooley, D. 2013. Return Periods and Return Levels under Climate Change. In *Extremes in a Changing Climate: Detection, Analysis and Uncertainty*, edited by A. AghaKouchak, D. Easterling, K. Hsu, S. Schubert, and S. Sorooshian, 97–114. Netherlands: Springer Netherlands.

Dalrymple, T. 1960. *Flood Frequency Analysis*. U.S. Geological Survey Water-Supply Paper 1543-A. Washington, D.C.: U.S. Government Printing Office.

Davis, P.K. 2012. *Lessons from RAND's Work on Planning under Uncertainty for National Security*. Technical Report prepared for the Office of the Secretary of Defense. Arlington, Virginia: RAND National Defense Research Institute.

Department of Defense (DoD). 2014. *2014 Climate Change Adaptation Roadmap*. Alexandria, Virginia: U.S. DoD, Office of the Deputy Under Secretary of Defense for Installations and Environment.

Donnelly, J.P., A.D. Hawkes, P. Lane, D. MacDonald, B.N. Shuman, M.R. Toomey, P.J. van Hengstum, and J.D. Woodruff. 2015. Climate Forcing of Unprecedented Intense-Hurricane Activity in the Last 2000 Years. *Earth's Future* 3:49–65. doi:10.1002/2014EF000274.

Ezer, T. 2013. Sea Level Rise, Spatially Uneven and Temporally Unsteady: Why the U.S. East Coast, the Global Tide Gauge Record, and the Global Altimeter Data Show Different Trends. *Geophysical Research Letters* 40:5439–5444. doi:10.1002/2013GL057952.

Ezer, T., L.P. Atkinson, W.B. Corlett, and J.L. Blanco. 2013. Gulf Stream's Induced Sea Level Rise and Variability along the U.S. Mid-Atlantic Coast. *Journal of Geophysical Research: Oceans* 118:685–697. doi:10.1002/jgrc.20091.

Ezer, T. and L.P. Atkinson. 2014. Accelerated Flooding along the U.S. East Coast: On the Impact of Sea Level Rise, Tides, Storms, the Gulf Stream and NAO. *Earth's Future* 2:362–382. doi:10.1002/2014EF000252.

Ezer, T. 2015. Detecting Changes in the Transport of the Gulf Stream and the Atlantic Overturning Circulation from Coastal Sea Level Data: The Extreme Decline in 2009–2010 and Estimated Variations for 1935–2012. *Global and Planetary Change* 129:23–36.

Farrell, W.E. and J.A. Clark. 1976. On Postglacial Sea Level. *Geophysical Journal of the Royal Astronomical Society* 46:647–667.

Federal Emergency Management Agency (FEMA). 2013. *Standards for Flood Risk Analysis and Mapping*. Federal Insurance and Mitigation Administration Policy FP 204-078-1. Washington, D.C.: FEMA.

FEMA. 2015. *Guidelines for Implementing Executive Order 11988, Floodplain Management, and Executive Order 13690, Establishing a Federal Flood Risk Management Standard and a Process for Further Soliciting and Considering Stakeholder Input*. Washington, D.C.: FEMA.

Flick, R., K. Knuuti, and S. Gill. 2012. Matching Mean Sea Level Rise Projections to Local Elevation Datums. *Journal of Waterway, Port, Coastal, and Ocean Engineering* 139:142–146.

Galloway, D.L., D.R. Jones, and S.E. Ingebritsen. 2000. *Measuring Land Subsidence from Space*. U.S. Geological Survey Fact Sheet-051-00. Sacramento, California: U.S. Geological Survey.

Gesch, D., M. Oimoen, S. Greenlee, C. Nelson, M. Steuck, and D. Tyler. 2002. The National Elevation Dataset. *Journal of the American Society for Photogrammetry and Remote Sensing* 61:5–11.

Gesch, D.B. 2009. Analysis of Lidar Elevation Data for Improved Identification and Delineation of Lands Vulnerable to Sea-Level Rise. *Journal of Coastal Research SI* 53:49–58. doi:10.2112/SI53-006.1.

Gesch, D.B., B.T. Gutierrez, and S.K. Gill. 2009. Coastal Elevations. In *Coastal Sensitivity to Sea-Level Rise: A Focus on the Mid-Atlantic Region*. A report by the U.S. Climate Change Science Program and the Subcommittee on Global Change Research. J.G. Titus (coordinating lead author), K.E. Anderson, D.R. Cahoon, D.B. Gesch, S.K. Gill, B.T. Gutierrez, E.R. Thieler, and S.J. Williams (lead authors), 25-42. Washington, D.C.: U.S. Environmental Protection Agency.

Gesch, D.B. 2012. Elevation Uncertainty in Coastal Inundation Hazard Assessments. In *Natural Disasters*, edited by S. Cheval, 121-140. Rijeka, Croatia: InTech. doi:10.5772/31972.

Gesch, D.B. 2013. Consideration of Vertical Uncertainty in Elevation-Based Sea-Level Rise Assessments: Mobile Bay, Alabama Case Study. *Journal of Coastal Research SI* 63:197-210. doi:10.2112/SI63-016.1.

Gesch, D.B., M.J. Oimoen, and G.A. Evans. 2014. Accuracy Assessment of the U.S. Geological Survey National Elevation Dataset, and Comparison with Other Large-Area Elevation Datasets—SRTM and ASTER. *U.S. Geological Survey Open-File Report 2014–1008*. Reston, Virginia: U.S. Geological Survey, 10p. doi:10.3133/ofr20141008.

Grinsted, A., J. C. Moore, and S. Jevrejeva. 2012. Homogeneous Record of Atlantic Hurricane Surge. In *Proceedings of the National Academies of Science,* 109(48):19,513–19,514. doi:10.1073/pnas.1216735109.

Grinsted, A., S. Jevrejeva, R.E.M. Riva, and D. Dahl-Jensen. 2015. Sea Level Rise Projections for Northern Europe under RCP 8.5. *Climate Research* 64:15–23.

Groves, D.G. and R.J. Lempert. 2006. A New Analytic Method for Finding Policy-Relevant Scenarios. *Global Environmental Change* 17:73–85.

Haigh, I.D., R. Nicholls, and N. Wells. 2010. A Comparison of the Main Methods for Estimating Probabilities of Extreme Still Water Levels. *Coastal Engineering* 57:838–849.

Haigh, I.D., M. Eliot, and C. Pattiaratchi. 2011. Modeling Global Influences of the 18.6-Year Nodal Cycle and Quasi-4.4 Year Cycle on High Tidal Levels. *Journal of Geophysical Research-Oceans* 116:C06025. doi:10.1029/2010JC006645.

Haigh, I.D., L.R. MacPherson, M.S. Mason, E.M.S. Wijeratne, C.B. Pattiaratchi, R.P. Crompton, and S. George. 2014a. Estimating Present Day Extreme Water Level Exceedance Probabilities around the Coastline of Australia: Tropical Cyclone-Induced Storm Surges. *Climate Dynamics* 42:139–157. doi:10.1007/s00382-012-1653-0.

Haigh, I.D. , T. Wahl, E.J. Rohling, R.M. Price, C.B. Pattiaratchi, F.M. Calafat, and S. Dangendorf. 2014b. Timescales for Detecting a Significant Acceleration in Sea Level Rise. *Nature Communications* 5:3635. doi:10.1038/ncomms4635.

Haigh, I.D., E.M.S. Wijeratne, L.R. MacPherson, C.B. Pattiaratchi, M.S. Mason, R.P. Crompton, and S. George. 2014c. Estimating Present Day Extreme Water Level Exceedance Probabilities around the Coastline of Australia: Tides, Extra-Tropical Storm Surges and Mean Sea Level. *Climate Dynamics* 42:121–138. doi:10.1007/s00382-012-1652-1.

Hallegatte, S., A. Shah, R. Lempert, C. Brown, and S. Gill. 2012. *Investment Decision Making under Deep Uncertainty—Application to Climate Change*. Policy Research Working Paper 6193. Washington, D.C.: The World Bank, Sustainable Development Network, Office of the Chief Economist.

Hawkins, E. and R. Sutton. 2009. The Potential to Narrow Uncertainty in Regional Climate Predictions. *Bulletin of the American Meteorological Society* 90:1095–1107.

Hawkins, E. and R. Sutton. 2011. The Potential to Narrow Uncertainty in Projections of Regional Precipitation Change. *Climate Dynamics* 37:407–418.

Hay, C.C., E. Morrow, R.E. Kopp, and J.X. Mitrovica. 2013. Estimating the Sources of Global Sea Level Rise with Data Assimilation Techniques. In *Proceedings of the National Academy of Sciences* 110:3692–3699.

Hay, C.C., J.X. Mitrovica, N. Gomez, J.R. Crevling, J. Austermann, and R.E. Kopp. 2014. The Sea Level Fingerprints of Ice-Sheet Collapse during Interglacial Periods. *Quaternary Science Reviews* 87:60–69.

Hay, C.C., E. Morrow, R.E. Kopp, and J.X. Mitrovica. 2015. Probabilistic Reanalysis of Twentieth-Century Sea-Level Rise. *Nature* 517:481–484. doi:10.1038/nature14093.

Hinkel, J., C. Jaeger, R.J. Nicholls, J. Lowe, O. Renn, and S. Peijun. 2015. Sea-Level Rise Scenarios and Coastal Risk Management. *Nature Climate Change* 5:188–190.

Hoeke, R.K., K.L. McInnes, J. Kruger, R. McNaught, J. Hunter, and S. Smithers. 2013. Widespread Inundation of Pacific Islands by Distant-Source Wind-Waves. *Global and Planetary Change* 108:128–138. doi:10.1016/j.gloplacha.2013.06.006.

Horsburgh, K.J. and C. Wilson. 2007. Tide-Surge Interaction and Its Role in the Distribution of Surge Residuals in the North Sea. *Journal of Geophysical Research* 112:C08003. doi:10.1029/2006JC004033.

Horton, B.P., S. Rahmstorf, S.E. Engelhart, and A.C. Kemp. 2014. Expert Assessment of Sea-Level Rise by AD 2100 and AD 2300. *Quaternary Science Reviews* 84:1–6.

Hosking, J.R.M. 2012. Towards Statistical Modeling of Tsunami Occurrence with Regional Frequency Analysis. *Journal of Math-for-Industry* 4A:41–48.

Hosking, J.R.M. and J.R. Wallis.1988. The Effect of Intersite Dependence on Regional Flood Frequency Analysis. *Water Resources Research* 24:588–600.

Hosking, J.R.M. and J.R. Wallis. 1997. *Regional Frequency Analysis – An Approach Based on L-Moments*. Cambridge, United Kingdom and New York, New York: Cambridge University Press.

Hunter, J. 2010. Estimating Sea-Level Extremes under Conditions of Uncertain Sea-Level Rise. *Climatic Change* 99:331–350. doi:10.1007/s10584-009-9671-6.

Hunter, J. 2012. A Simple Technique for Estimating an Allowance for Uncertain Sea-Level Rise. *Climatic Change* 113:239–252.

Hunter, J., J.A. Church, N.J. White, and X. Zhang. 2013. Towards a Globally Regionally Varying Allowance for Sea-Level Rise. *Ocean Engineering* 71:17–27.

Intergovernmental Panel on Climate Change (IPCC). 2001. *Climate Change 2001: Synthesis Report. A Contribution of Working Groups I, II, and III to the Third Assessment Report of the Intergovernmental Panel on Climate Change*, edited by the Core Writing Team and T.R. Watson. Cambridge, United Kingdom and New York, New York: Cambridge University Press.

Irish, J.L., A. Sleath, M.A. Cialone, T.R. Knutson, and R.E. Jensen. 2013. Simulations of Hurricane Katrina (2005) under Sea Level and Climate Conditions for 1900. *Climatic Change* 122:635–649.

Jet Propulsion Laboratory (JPL) of the California Institute of Technology. 2013. Introduction to JPL's GPS Time Series. Pasadena, California: National Aeronautics and Space Administration. Accessed October 2015: http://sideshow.jpl.nasa.gov/post/tables/GPS_Time_Series.pdf.

Jevrejeva, S., A. Grinsted, and J.C. Moore. 2014. Upper Limit for Sea Level Projections by 2100. *Environmental Research Letters* 9:1–9.

Klein Tank, A., J. Beersma, J. Bessembinder, B. van den Hurk, and G. Lenderink. 2015. *KNMI'14 Climate Scenarios for the Netherlands*. A Guide for Professionals in Climate Adaptation. De Bilt, The Netherlands: KNMI.

Knutson T.R., J.L. McBride, J. Chan, K. Emanuel, G. Holland, C. Landsea, I. Held, J.P. Kossin, A. K. Srivastava,, and M. Sugi. 2010. Tropical Cyclones and Climate Change. *Nature Geoscience* 3:157–163.

Kopp, R.E., R.M. Horton, C.M. Little, J.X. Mitrovica, M. Oppenheimer, D.J. Rasmussen, B.H. Strauss, and C. Tebaldi. 2014. Probabilistic 21st and 22nd Century Sea-Level Projections at a Global Network of Tide-Gauge Sites. *Earth's Future* 2:1–24.

Kopp, R.E., B.P. Horton, A.C. Kemp, and C. Tebaldi. 2015. Past and Future Sea-Level Rise along the Coast of North Carolina, USA. *Climatic Change* 132:693–707.

Lemos, M.C. and R.B. Rood. 2010. Climate Projections and Their Impact on Policy and Practice. *Wiley Interdisciplinary Reviews - Climate Change* 1:670–682.

Lempert, R.R., R.L. Sriver, and K. Keller (RAND). 2012. *Characterizing Uncertain Sea Level Projections to Support Investment Decisions*. A White Paper from the California Energy Commission's California Climate Change Center. CEC-500-2012-056. Sacramento, California: California Energy Commission.

Lentz, E.E., E.R. Thieler, N.G. Plant, S.R. Stippa, R.M. Horton, and D.B. Gesch. 2016. Evaluation of Dynamic Coastal Response to Sea-Level Rise Modifies Inundation Likelihood. *Nature Climate Change*. doi:10.1038/NCLIMATE2957.

Lin, N., P. Lane, K.A. Emanuel, R.M. Sullivan, and J.P. Donnelly. 2014. Heightened Hurricane Surge Risk in Northwest Florida Revealed from Climatological-Hydrodynamic Modeling and Paleorecord Reconstruction. *Journal of Geophysical Research: Atmospheres* 119:8606–8623.

Little, C.M., R.M. Horton, R.E. Kopp, M. Oppenheimer, G.A. Vecchi, and G. Villarini. 2015a. Joint Projections of U.S. East Coast Sea Level and Storm Surge. *Nature Climate Change* 5:1114–1120.

Little, C.M., R.M. Horton, R.E. Kopp, M. Oppenheimer, and S. Yip. 2015b. Uncertainty in Twenty-First Century CMIP5 Sea Level Projections. *Journal of Climate* 28:838–852.

Lowe, J.A., C.P. Howard, A. Pardaens, J. Tinker, J. Holt, S. Wakelin, G. Milne, J. Leake, J. Wolf, K. Horsburgh, T. Reeder, G. Jenkins, J. Ridley, S. Dye, and S. Bradley. 2009. *UK Climate Projections Science Report: Marine and Coastal Projections*. Exeter, United Kingdom:Met Office Hadley Centre.

Mailier, P. J., D. B. Stephenson, C. A. T. Ferro, and K. I. Hodges. 2006. Serial Clustering of Extratropical Cyclones. *Monthly Weather Review* 134:2224–2240.

Massachusetts Office of Coastal Zone Management (CZM). 2013. *Sea Level Rise: Understanding and Applying Trends and Future Scenarios for Analysis and Planning*. Boston, Massachusetts: Massachusetts Office of Coastal Zone Management.

Marbaix, P. and R.J. Nicholls. 2007. Accurately Determining the Risks of Rising Sea Level. *Eos, Transactions of the American Geophysical Union* 88:441–442.

Marcos, M., F. M. Calafat, A. Berihuete, and S. Dangendorf. 2015. Long-Term Variations in Global Sea Level Extremes. *Journal of Geophysical Research: Oceans* 120:8115–8134. doi:10.1002/2015JC011173.

Marcy, D., W. Brooks, K. Draganov, B. Hadley, C. Haynes, N. Herold, J. McCombs, M. Pendleton, S. Ryan, K. Schmid, M. Sutherland, and K. Waters. 2011. New Mapping Tool and Techniques for Visualizing Sea Level Rise and Coastal Flooding Impacts. In *Proceedings of the 2011 Solutions to Coastal Disasters Conference, Anchorage, Alaska, June 26–29, 2011*, edited by L.A. Wallendorf, C. Jones, L. Ewing, and B. Battalio, 474–490. Reston, Virginia: American Society of Civil Engineers.

Mastrandrea, M.D., C.B. Field, T.F. Stocker, O. Edenhofer, K.L. Ebi, D. Frame, H. Held, E. Kriegler, K. Mach, P. Matschoss, G.-K. Plattner, G.W. Yohe, and F.W. Zwiers. 2010. *Guidance Note for Lead Authors of the IPCC Fifth Assessment Report on Consistent Treatment of Uncertainties*. Geneva, Switzerland: Intergovernmental Panel on Climate Change.

Mawdsley, R.J., I.D. Haigh, and N.C. Wells. 2015. Global Secular Changes in Different Tidal High Water, Low Water and Range Levels. *Earth's Future* 3:66–81. doi:10.1002/2014EF000282.

Mawdsley, R. and I.D. Haigh. In Press. Spatial and Temporal Variability and Long-Term Trends in Skew Surges Globally. *Frontiers in Marine Science*. doi:10.3389/fmars.2016.00029

McInnes, K.L., I. Macadam, G.D. Hubbert, and J.G. O'Grady. 2009. A Modelling Approach for Estimating the Frequency of Sea Level Extremes and the Impact of Climate Change in Southeast Australia. *Natural Hazards* 51:115–137.

Meehl, G.A., A. Hu, C. Tebaldi, J.M. Arblaster, W.M. Washington, H. Teng, B.M. Sanderson, T. Ault, W.G. Strand, and J.B. White III. 2012. Relative Outcomes of Climate Change Mitigation Related to Global Temperatures versus Sea-Level Rise. *Nature Climate Change* 2:576–580.

Melillo, J.M., T.C. Richmond, and G.W. Yohe, eds. 2014. *Climate Change Impacts in the United States*: *The Third National Climate Assessment*. U.S. Global Change Research Program. Washington, D.C.: U.S. Government Printing Office. doi:10.7930/J0Z31WJ2.

Menéndez, M. and P.L. Woodworth. 2010. Changes in Extreme High Water Levels Based on a Quasi-Global Tide-Gauge Data Set. *Journal of Geophysical Research: Oceans* 115:C10011. doi:10.1029/2009JC005997.

Merrifield, M.A., P.R. Thompson, and M. Lander. 2012. Multidecadal Sea Level Anomalies and Trends in the Western Tropical Pacific. *Geophysical Research Letters* 39:L13602. doi:10.1029/2012GL052032.

Merrifield, M.A., A.S. Genz, C.P. Kontoes, and J.J. Marra. 2013. Annual Maximum Water Levels from Tide Gauges: Contributing Factors and Geographic Patterns. *Journal of Geophysical Research: Oceans* 118:2535–2546. doi:10.1002/jgrc.20173.

Merrifield, M.A., P. Thompson, E. Leuliette, G.T. Mitchum, D.P. Chambers, S. Jevrejeva, R.S. Nerem, M. Menéndez, W. Sweet, B. Hamlington, and J.J. Marra. 2015. Sea Level Variability and Change. In *State of the Climate in 2014. Special Supplement to the Bulletin of the American Meteorological Society* 96:S82–S85. Boston, Massachusetts: American Meteorological Society.

Miller, K.G., R.E. Kopp, B.P. Horton, J.V. Browning, and A.C. Kemp. 2013. A Geologic Perspective on Sea-Level Rise and Its Impacts along the U.S. Mid-Atlantic Coast. *Earth's Future* 1:3–18.

Milly, P.C.D., J. Betancourt, M. Falkenmark, R.M. Hirsch, W.Z. Kundzewicz, D.P. Lettenmaier, and R.J. Stouffer. 2008. Stationarity Is Dead: Whither Water Management? *Science* 319:573–574.

Mitrovica, J.X., M.E. Tamisiea, J.L. Davis, and G.A. Milne. 2001. Recent Mass Balance of Polar Ice Sheets Inferred from Patterns of Global Sea-Level Change. *Nature* 409:1026–1029.

Mitrovica, J.X., N. Gomez, and P.U. Clark. 2009. The Sea-Level Fingerprint of West Antarctic Collapse. *Science* 323:753. doi:10.1126/science.1166510.

Mitrovica, J.X., N. Gomez, E. Morrow, C. Hay, K. Laychev, and M.E. Tamisea. 2011. On the Robustness of Predictions of Sea Level Fingerprints. *Geophysical Journal International* 187:729–742.

Moritz, H.P., K. White, B. Gouldby, W. Sweet, P. Ruggiero, P. O'Brien, H.R. Moritz, T. Wahl, N.C. Nadal-Carabello, and W. Veatch. 2015. USACE Adaptation Approach for Future Coastal Climate Conditions. In *Proceedings of the Institution of Civil Engineers - Maritime Engineering* 168:111–117.

Moss, R.M. et al. 2008. *Towards New Scenarios for Analysis of Emissions, Climate Change, Impacts, and Response Strategies*. Technical Summary. IPCC Expert Meeting Report. Geneva, Switzerland: Intergovernmental Panel on Climate Change.

Moss, R.M. et al. 2010. The Next Generation of Scenarios for Climate Change Research and Assessment. *Nature* 463:747–756.

Moss, R.H. and G. Yohe. 2011. *Assessing and Communicating Confidence Levels and Uncertainties in the Main Conclusions of the NCA 2013 Report: Guidance for Authors and Contributors.* Washington, D.C.: National Climate Assessment Development and Advisory Committee.

Nadal-Caraballo, N.C. and J.A. Melby. 2014. *North Atlantic Coast Comprehensive Study Phase 1: Statistical Analysis of Historical Extreme Water Levels with Sea Level Change*. Report ERCD/CHL TR-14-7. Vicksburg, Mississippi: USACE, Engineer Research and Development Center.

Nadal-Caraballo, N.C., J.A. Melby, V.M. Gonzalez, and A.T. Cox. 2015. *North Atlantic Coast Comprehensive Study: Coastal Storm Hazards from Virginia to Maine*. Report ERCD/CHL TR-15-5. Vicksburg, Mississippi: USACE, Engineer Research and Development Center.

Nakicenovic, N. et al. 2000. *IPCC Special Report on Emissions Scenarios: Summary for Policymakers*. A Special Report of IPCC Working Group III. Geneva, Switzerland: Intergovernmental Panel on Climate Change.

National Research Council. 2011. *National Security Implications of Climate Change for U.S. Naval Forces*. Committee on National Security Implications of Climate Change for U.S. Naval Forces, Naval Studies Board, Division on Engineering and Physical Sciences. Washington, D.C.: The National Academies Press.

National Research Council. 2012. *Sea-Level Rise for the Coasts of California, Oregon, and Washington: Past, Present, and Future*. Committee on Sea Level Rise in California, Oregon, Washington; Board on Earth Sciences and Resources and Ocean Studies Board; Division on Earth and Life Studies. National Research Council of the National Academies. Washington, D.C.: The National Academies Press.

New York City Panel on Climate Change. 2013. *Climate Risk Information 2013: Observations, Climate Change Projections, and Maps*, edited by C. Rosenzweig and W. Solecki, NPCC2. New York, New York: The City of New York.

NOAA. 2001. *Tidal Datums and Their Applications*. NOAA Special Publication NOS CO-OPS 1. Silver Spring, Maryland: NOAA, National Ocean Service, Center for Operational Oceanographic Products and Services.

NOAA. 2003. *Computational Techniques for Tidal Datums Handbook*. NOAA Special Publication NOS CO-OPS 2. Silver Spring, Maryland: U.S. Department of Commerce, NOAA, National Ocean Service, Center for Operational Oceanographic Products and Services.

NOAA. 2010a. *Technical Considerations for Use of Geospatial Data in Sea Level Change Mapping and Assessment*. NOAA Technical Report NOS 2010-01. Washington, D.C.: U.S. Department of Commerce, NOAA, National Ocean Service.

NOAA.2010b. *Mapping Inundation Uncertainty*. Charleston, South Carolina: NOAA, Coastal Services Center.

NOAA. 2012. *VDatum Manual for Development and Support of NOAA's Vertical Datum Transformation Tool, VDATUM*, Version 1.01. Washington, D.C.: U.S. Department of Commerce, NOAA, National Ocean Service, Office of Coast Survey, National Geodetic Survey, Center for Operational Oceanographic Products and Services.

Obeysekera, J. and J. Park. 2013. Scenario-Based Projection of Extreme Sea Levels. *Journal of Coastal Research* 29:1–7. doi:10.2112/JCOASTRES-D-12-00127.1.

Obeysekera, J. and J. Salas. 2016. Frequency of Recurrent Extremes under Nonstationarity. *Journal of Hydrologic Engineering*. doi:10.1061/(ASCE)HE.1943-5584.0001339, 04016005.

Park, J. and W. Sweet. 2015. Accelerated Sea Level Rise and Florida Current Transport. *Ocean Science* 11:607--615. doi:10.5194/0s-11-607-2015.

Parris, A.P., P. Bromirski, V. Burkett, D. Cayan, M. Culver, J. Hall, R. Horton, K. Knuuti, R. Moss, J. Obeysekera, A. Sallenger, and J. Weiss. 2012. *Global Sea Level Rise Scenarios for the United States National Climate Assessment*. NOAA Technical Report OAR CPO-1. Silver Spring, Maryland: NOAA.

Pawlowicz, R., B. Beardsley, and S. Lentz. 2002. Classical Tidal Harmonic Analysis Including Error Estimates in MATLAB Using T_TIDE. *Computers and Geosciences* 28:929–937.

Peltier, W.R. 1998. Postglacial Variations in the Level of the Sea: Implications for Climate Dynamics and Solid-Earth Geophysics. *Reviews of Geophysics* 36:603–689. doi:10.1029/98RG02638.

Peltier, W.R. 2004. Global Glacial Isostasy and the Surface of the Ice-Age Earth: The ICE-5G (VM2) Model and GRACE. *Annual Review of Earth and Planetary Sciences* 32:111–149. doi:10.1146/annurev.earth.32.082503.144359.

Perrette, M., F. Landerer, R. Riva, K. Frieler, and M. Meinshausen. 2013. A Scaling Approach to Project Regional Sea Level Rise and Its Uncertainties. *Earth System Dynamics* 4:11–29.

Pfeffer, W.T., J.T. Harper, and S. O'Neel. 2008. Kinematic Constraints on Glacier Contributions to 21st-Century Sea-Level Rise. *Science* 321:1340–1343.

Plag, H.P. and H.U. Juttner. 2001. Inversion of Global Tide Gauge Data for Present-Day Ice Load Changes. *Memoirs of National Institute of Polar Research* 54:301–317.

Poulter, B. and P.N. Halpin. 2008. Raster Modelling of Coastal Flooding from Sea-Level Rise. *International Journal of Geographical Information Science* 22:167–182. doi:10.1080/13658810701371858.

Priest, G.R., C. Goldfinger, K. Wang, R.C. Witter, Y. Zhang, and A.M. Baptista. 2009. Confidence Levels for Tsumani-Inundation Limits in Northern Oregon Inferred from a 10,000-Year History of Great Earthquakes at the Cascadia Subduction Zone. *Natural Hazards* 54:27–73. doi:10.1007/s1 1069-009-9453-5.

Pugh, D.T. and J.M. Vassie. 1980. Applications of the Joint Probability Method for Extreme Sea Level Computations. *Proceedings of the Institution of Civil Engineers* 69:959–975.

Rahmstorf, S. 2007. A Semi-Empirical Approach to Projecting Future Sea-Level Rise. *Science* 315:368–370.

Reager, J.T., A.S. Gardner, J.S. Famiglietti, D.N. Wiese, A. Eicker, and M.-H. Lo. 2016. A Decade of Sea Level Rise Slowed by Climate-Driven Hydrology. *Science* 351:699–702.

Resio, D.T. and J.J. Westerink. 2008. Modeling the Physics of Storm Surges. *Physics Today* 61:33–38.

Richter, K., R.E.M. Riva, and H. Drange. 2013. Impact of Self-Attraction and Loading Effects Induced by Shelf Mass Loading on Projected Sea Level Rise. *Geophysical Research Letters* 40:1144–1148.

Ritz, C., T.L. Edwards, G. Durand, A.J. Payne, V. Peyaud, and R.C.A. Hindmarsh. 2015. Potential Sea-Level Rise from the Antarctic Ice-Sheet Instability Constrained by Observations. *Nature* 528:115–118. doi:10.1038/nature16147.

Rohling, E.J., I.D. Haigh, G.L. Foster, A.P. Roberts, and K.M. Grant. 2013. A Geological Perspective on Potential Future Sea-Level Rise. *Scientific Reports* 3:3461. doi:10.1038/srep03461.

Ruggiero, P., P.D. Komar, and J.C. Allan. 2010. Increasing Wave Heights and Extreme Value Projections: The Wave Climate of the U.S. Pacific Northwest. *Coastal Engineering* 57:539–552.

Russo, E.J. and J.A. Hall. 2012. Section 4.5 Implications for Coastal Military Installations and Readiness. In Coastal Impacts, Adaptation, and Vulnerabilities: *A Technical Input to the 2013 National Climate Assessment*, edited by V. Burkett and M. Davidson, 92–97. Washington, D.C.: NOAA and Island Press.

Salas, J.D. and J. Obeysekera. 2014. Revisiting the Concepts of Return Period and Risk for Nonstationary Hydrologic Extreme Events. *Journal of Hydrologic Engineering* 19:554–568. doi:10.1061/(ASCE)HE.1943-5584.0000820.

Scafetta, N. 2014. Multi-Scale Dynamical Analysis (MSDA) of Sea Level Records Versus PDO, AMO, and NAO Indexes. *Climate Dynamics* 43:175–192.

Scileppi, E. and J.P. Donnelly. 2007. Sedimentary Evidence of Hurricane Strikes in Western Long Island, New York. *Geochemistry, Geophysics, Geosystems* 8:Q06011. doi:10.1029/2006GC001463.

Serafin, K.A. and P. Ruggiero. 2014. Simulating Extreme Total Water Levels Using a Time-Dependent, Extreme Value Approach. *Journal of Geophysical Research: Oceans* 119:6305–6329. doi:10.1002/2014JC010093.

Slangen, A.B.A., C.A. Katsman, R.S.W. van de Wal, L.L.A. Vermeersen, and R.E.M. Riva. 2012. Towards Regional Projections of Twenty-First Century Sea-Level Change based on IPCC Scenarios. *Climate Dynamics* 38:1191–1209.

Smith, J.M., M.A. Cialone, T.V. Wamsley, and T.O. McAlpin. 2010. Potential Impact of Sea Level Rise on Coastal Surges in Southeast Louisiana. *Ocean Engineering* 37:37–47.

Smith, J.M., T.V. Wamsley, M.A. Cialone, and J. Atkinson. 2008. Potential Impacts of Sea Level Rise on Storm Surge and Waves in Southeast Louisiana. In *Proceedings of the 31st International Conference on Coastal Engineering*, 1060–1071. Singapore: World Scientific.

Snay, R., M. Cline, W. Dillinger, R. Foote, S. Hilla, W. Kass, J. Ray, J. Rohde, G. Sella, and T. Soler. 2007. Using Global Positioning System-Derived Crustal Velocities to Estimate Rates of Absolute Sea Level Change from North American Tide Gauge Records. *Journal of Geophysical Research* 112:B04409. doi:10.1029/2006JB004606.

Sneed, M., M.E. Ikehara, D.L. Galloway, and F. Amelung, 2001. Detection and Measurement of Land Subsidence Using Global Positioning System and Interferometric Synthetic Aperture Radar, Cochella Valley, California 1996-98. U.S. Geological Survey Water-Resources Investigation Report 01-4193. Sacramento, California: U.S Geological Survey.

Southeast Florida Regional Climate Change Compact Sea Level Rise Work Group (Compact). 2015. *Unified Sea Level Rise Projection for Southeast Florida*. A document prepared for the Southeast Florida Regional Climate Change Compact Steering Committee.

Spada, G., J.L. Bamber, and R.T.W.L. Hurkmans. 2013. The Gravitationally Consistent Sea-Level Fingerprint of Future Terrestrial Ice Loss. *Geophysical Research Letters* 40:482–486.

Sriver, R.L., N.M. Urban, R. Olson, and K. Keller. 2012. Toward a Physically Plausible Upper Bound of Sea-Level Rise Projections. *Climatic Change* 115:893–902.

Stockdon, H.F., R.A. Holman, P.A. Howd, and A.H. Sallenger. 2006. Empirical Parameterization of Setup, Swash, and Runup. *Coastal Engineering* 53:573–588.

Strategic Environmental Research and Development Program (SERDP). 2013. *Assessing Impacts of Climate Change on Coastal Military Installations: Policy Implications*. Alexandria, Virginia: U.S. DoD.

Sweet, W.V. and C. Zervas. 2011. Cool-Season Sea Level Anomalies and Storm Surges along the U.S. East Coast: Climatology and Comparison with the 2009/10 El Niño. *Monthly Weather Review* 139:2290–2299. doi:10.1175/MWR-D-10-05043.1.

Sweet, W.V., C. Zervas, S. Gill, and J. Park. 2013. Hurricane Sandy Inundation Probabilities Today and Tomorrow. In Explaining Extreme Events of 2012 from a Climate Perspective. *Bulletin of the American Meteorological Society* 94(9):S17–S20.

Sweet, W.V., J. Park, J.J. Marra, C. Zervas, and S. Gill. 2014. *Sea Level Rise and Nuisance Flood Frequency Changes around the United States*. NOAA Technical Report NOS CO-OPS 73. Silver Spring, Maryland: U.S. Department of Commerce, NOAA, National Ocean Service, Center for Operational Oceanographic Products and Services.

Sweet, W.V. and J. Park. 2014. From the Extreme to the Mean: Acceleration and Tipping Points of Coastal Inundation from Sea Level Rise. *Earth's Future* 2:579–600. doi:10.1002/2014EF000272.

Sweet, W.V., J. Park, S. Gill, and J. Marra. 2015. New Ways to Measure Waves and Their Effects at NOAA Tide Gauges: A Hawaiian-Network Perspective. *Geophysical Research Letters* 42:9355–9361. doi:10.1002/2015GL066030.

Talke, S.A., P. Orton, and D.A. Jay. 2014. Increasing Storm Tides in New York Harbor, 1844–2013. *Geophysical Research Letters* 41:3149–3155. doi:10.1002/2014GL059574.

Tamisiea, M.E., E.M. Hill, R.M. Ponte, J.L. Davis, I. Velicogna, and N.T. Vinogradova. 2010. Impact of Self-Attraction and Loading on the Annual Cycle in Sea Level. *Journal of Geophysical Research: Oceans* 115:C07004.

Tamisiea, M.E. 2011. Ongoing Glacial Isostatic Contributions to Observations of Sea Level Change. *Geophysical Journal International* 186:1036--1044. doi:10.1111/j.1365-246X.2011.05116.x

Tawn, J.A. and J.M. Vassie. 1989. Extreme Sea Levels: The Joint Probabilities Method Revisited and Revised. *Proceedings of the Institution of Civil Engineers* 87:429–442.

Tawn, J.A. 1992. Estimating Probabilities of Extreme Sea-Levels. *Journal of the Royal Statistical Society: Series C: Applied Statistics* 41:77–93.

Tebaldi, C., B.H. Strauss, and C.E. Zervas. 2012. Modeling Sea Level Rise Impacts on Storm Surges along U.S. Coasts. *Environmental Research Letters* 7:1–11. doi:10.1088/1748-9326/7/1/014032.

Thompson, K.R., N.B. Bernier, and P. Chan. 2009. Extreme Sea Levels, Coastal Flooding and Climate Change with a Focus on Atlantic Canada. *Natural Hazards* 51:139–150.

Thompson, P.R., G.T. Mitchum, C. Vonesch, and J. Li. 2013. Variability of Winter Storminess in the Eastern United States during the Twentieth Century from Tide Gauges. *Journal of Climate* 26:9713–9726.

USACE. 2009. *Water Resources Policies and Authorities Incorporating Sea-Level Change Considerations in Civil Works Programs*. EC 1165-2-211. Washington, D.C.: USACE.

USACE. 2011. *Sea-Level Change Considerations for Civil Works Programs*. EC 1165-2-212. Washington, D.C.: USACE.

USACE. 2013. *Incorporating Sea Level Change in Civil Works Programs*. ER 1100-2-8162. Washington, D.C.: USACE.

USACE. 2014. *Procedures to Evaluate Sea Level Change: Impacts, Responses, and Adaptation*. Engineer Technical Letter 1100-2-1. Washington, D.C.: USACE.

Vecchi, G.A. and T. R. Knutson. 2008. On Estimates of Historical North Atlantic Tropical Cyclone Activity. *Journal of Climate* 21:3580–3600.

Vinogradova, N.T., R.M. Ponte, M.E. Tamisiea, K.J. Quinn, E.M. Hill, and J.L. Davis. 2011. Self-Attraction and Loading Effects on Ocean Mass Redistribution at Monthly and Longer Time Scales. *Journal of Geophysical Research* 116:C08041.

Wahl, T. and D.P. Chambers. 2015. Evidence for Multidecadal Variability in U.S. Extreme Sea Level Records. *Journal of Geophysical Research: Oceans* 120:1527–1544. doi:10.1002/2014JC010443.

Watson, C.S., N.J. White, J.A. Church, M.A. King, R.J. Burgette, and B. Legresy. 2015. Unabated Global Mean Sea-Level Rise over the Satellite Altimeter Era. *Nature Climate Change* 5:565–568.

Weaver, C.P., R.J. Lempert, C. Brown, J.A. Hall, D. Revell, and D. Sarewitz. 2013. Improving the Contribution of Climate Model Information to Decision Making: The Value and Demands of Robust Decision Frameworks. *Wiley Interdisciplinary Reviews - Climate Change* 4:39–60.

Weinkle, J., R. Maue, R. Pielke, Jr. 2012. Historical Global Tropical Cyclone Landfalls. Journal of Climate 25:4729--4735.

Weiss, J., P. Bernardara, and M. Benoit. 2014. Formation of Homogeneous Regions for Regional Frequency Analysis of Extreme Significant Wave Heights. *Journal of Geophysical Research: Oceans* 119:2906–2922. doi:10.1002/2013JC009668.

Weyant, J., C. Azar, M. Kainuma, J. Kejun, N. Nakicenovic, P.R. Shukla, E. La Rovere, and G. Yohe. 2009. *Report of 2.6 Versus 2.9 Watts/m^2 RCPP Evaluation Panel*. Geneva, Switzerland: Intergovernmental Panel on Climate Change.

White, S. 2007. Utilization of LiDAR and NOAA's Vertical Datum Transformation Tool (VDatum) for Shoreline Delineation. In *Proceedings of the Marine Technology Society / IEEE Oceans Conference*, 1–6. Vancouver, British Columbia: IEEE.

Woodruff, J.D., J.L. Irish, and S.J. Camargo. 2013. Coastal Flooding by Tropical Cyclones and Sea-Level Rise. *Nature* 504:44–52.

Woodward, R.S. 1888. On the Form and Position of Mean Sea Level. *Bulletin of the United States Geological Survey* 48:87–170.

Woodworth, P.L. and M. Menéndez. 2015. Changes in the Mesoscale Variability and in Extreme Sea Levels over Two Decades as Observed by Satellite Altimetry. *Journal of Geophysical Research: Oceans* 120:64–77. doi:10.1002/2014JC010363.

Yin, J.J., M.E. Schlesinger, and R.J. Stouffer. 2009. Model Projections of Rapid Sea-Level Rise on the Northeast Coast of the United States. *Nature Geoscience* 2:262–266.

Yin, J.J., S.M. Griffies, and R.J. Stouffer. 2010. Spatial Variability of Sea Level Rise in Twenty-First Century Projections. *Journal of Climate* 23:4585–4607.

Yin, J.J. 2012. Century to Multi-Century Sea Level Projections from CMIP5 Models. *Geophysical Research Letters* 39:L17709. doi:10.1029/2012GL052947.

Zervas, C. 2009. *Sea Level Variations of the United States 1854–2006*. NOAA Technical Report NOS CO-OPS 053. Silver Spring, Maryland: U.S. Department of Commerce, NOAA, National Ocean Service, Center for Operational Oceanographic Products and Services.

Zervas, C. 2013. *Extreme Water Levels of the United States 1893–2010*. NOAA Technical Report NOS CO-OPS 67. Silver Spring, Maryland: U.S. Department of Commerce, NOAA, National Ocean Service, Center for Operational Oceanographic Products and Services.

Zervas, C., S. Gill, and W. Sweet. 2013. *Estimating Vertical Land Motion from Long-Term Tide Gauge Records*. Technical Report NOS CO-OPS 065. Silver Spring, Maryland: U.S. Department of Commerce, NOAA, National Ocean Service, Center for Operational Oceanographic Products and Services.

Zhang, K., B. C. Douglas, and S. P. Leatherman, 2000: Twentieth Century Storm Activity along the U.S. East Coast. *Journal of Climate* 13:1748–1760.

Zhong, L., L. Ming, and M.G.G. Foreman. 2008. Resonance and Sea Level Variability in Chesapeake Bay. *Continental Shelf Research* 28:2565−2573.

Appendix A
Glossary

Actionable science — Science that provides data, analyses, scenarios, projections, or tools that can support decisions related to managing the risks and impacts associated with climate change. It is ideally co-produced by scientists, practitioners/users, and decision-makers and creates relevant, reliable, understandable, rigorous, and accessible products to meet the needs of stakeholders (adapted from the Advisory Committee on Climate Change and Natural Resource Science, United States Geological Survey website, accessed January 2016).

Adaptation — Action that can be implemented as a response to changes in the climate to harness and leverage its beneficial opportunities (e.g., expand polar shipping routes) or ameliorate its negative effects (e.g., protect installations from sea-level rise) (National Research Council [NRC] 2010).

Adaptive capacity — Ability of a system to adjust to climate change (including climate variability and extremes) to moderate potential damages, take advantage of opportunities, or cope with consequences (Parry et al. 2007).

Annual chance event — For purposes of this report, an annual chance event is the designation of a storm using statistical analyses to estimate the probability of occurrence for an event of prescribed magnitude within an annual timeframe. It refers to a particular magnitude of storm that, based on historic data, has a measured and ascribed chance of occurring in a 1-year period.

Barystatic — Global mean sea-level change resulting from change in the mass of the ocean. Barystatic and steric sea-level changes do not include the effect of changes in the shape of ocean basins induced by the change in the ocean mass and its distribution.

Built infrastructure Basic equipment, utilities, productive enterprises, installations, and services essential for the development, operation, and growth of an organization, city, or nation (based on Parry et al. [2007] definition of infrastructure). This includes all building and permanent installations necessary for the support, deployment, redeployment, and military forces operations (e.g., barracks, headquarters, airfields, communications, facilities, stores, port installations, and maintenance stations (based on JP1-02 [2001] definition of infrastructure).

Climate Mean and variability of relevant quantities of the climate system over a period of at least a month. These quantities are most often surface variables such as temperature, precipitation, and wind. Climate in a wider sense is the state of the climate system, often characterized through statistics that may include the mean, standard deviation, and statistics of extremes, etc. A typical period of time over which to characterize the state of the climate system is 30 years, as defined by the World Meteorological Organization (Parry et al. 2007).

Climate change scenario Plausible and often simplified representation of the future climate, based on an internally consistent set of climatological relationships and assumptions of radiative forcing, typically constructed for explicit use as input to climate change impact models. A "climate change scenario" is the difference between a future climate scenario and the current climate (Parry et al. 2007).

Climate change Any change in climate over time, whether due to natural variability or as a result of human activity. Anthropogenic climate change, as defined by the United Nations Framework Convention on Climate Change, refers to a change in climate that is attributed directly or indirectly to human activity that alters the composition of the global atmosphere and that is in addition to natural climate variability observed over comparable time periods (based on Parry et al. 2007).

Climate system System defined by the dynamics and interactions of five major components: atmosphere, hydrosphere, cryosphere, land surface, and biosphere. Climate system dynamics are driven by both internal and external forcing, such as volcanic eruptions, solar variations, or human-induced modifications to the planetary radiative balance, for instance via anthropogenic emissions of greenhouse gases and/or land-use changes (Parry et al. 2007).

Climate variability	Variations of climate on all temporal and spatial scales beyond that of individual weather events. Variability may be due to natural internal processes within the climate system, or due to variations in natural or anthropogenic external forcing (Parry et al. 2007).
Digital elevation model	A computerized representation of cartographic/geographic information in a raster form, providing a sampled array of elevations for a number of ground positions at regularly spaced intervals. Datasets provide elevations in xyz coordinates at differing levels of spatial resolution (e.g., 15 minute, 2 arc-second, or 1 degree) (USGS website, accessed January 2016).
Downscaling	Method that derives local- to regional-scale (typically 10 to 100 kilometers) information from larger-scale models or data analyses (Parry et al. 2007). For climate information, downscaling can be accomplished by either statistical or dynamical (regional climate model) means.
Dynamical sea level	Regional variations of global sea level caused by long-term changes in winds, air pressure, air-sea heat and freshwater fluxes, and ocean currents due to climate change (adapted from Perrette et al. 2013).
El Niño Southern Oscillation	The large-scale ocean-atmosphere climate phenomenon linked to a periodic warming in sea-surface temperatures across the central and east-central equatorial Pacific (between approximately the date line and 120°W). El Niño represents the warm phase of the El Niño Southern Oscillation (ENSO) cycle, and it is sometimes referred to as a Pacific warm episode. National Oceanic and Atmospheric Administration's (NOAA's) Climate Prediction Center, which is part of the National Weather Service, declares the onset of an El Niño episode when the 3-month average sea-surface temperature departure exceeds 0.5°C in the east-central equatorial Pacific (between 5°N-5°S and 170°W-120°W) (NOAA website, accessed January 2016).
Exposure	Extent to which something is in contact with or subject to climate variations or changes, including derivative effects such as sea-level rise (adapted from Strategic Environmental Research and Development Program (SERDP) 2013).
Extreme event	Event that is rare within its statistical reference distribution at a particular place. Definitions of "rare" differ, but an extreme weather event would normally be as rare as or rarer than the 10th or 90th percentile. By definition, the characteristics of what is called "extreme weather" may differ from place to place. Extreme weather events may typically include floods and droughts (Parry et al. 2007).

Extreme value analysis Application of statistical techniques to establish a probability distribution when sufficient data records exist to describe historic flooding (usually associated with rare and often destructive events) by characterizing the upper tail of a location's water level distribution (adapted from Coles 2001).

Extreme water level Elevation of the sea surface defined with an exceedance probability curve as a function of the return period, which is the average length of time between exceedances of a given elevation. These are presented as mean distributions, as well as at specified confidence levels (NOAA website, accessed January 2016).

Fingerprint The rapid melting of the Earth's ice reservoirs that will produce geographically distinct patterns of sea-level change. This spatially variable pattern of sea-level change follows mass changes in a specific ice sheet or glacier that produce a distinct geometry of sea-level change (Mitrovica et al. 2011).

Flooding Although "flooding" and "inundation" often have been used interchangeably, some authors (Flick et al. 2012b) suggest that "flooding" better describes normally dry areas that become wet, but then eventually dry again. Moreover, Flick et al. (2012b) suggest that "flooding" should be reserved for water elevations above MLLW (mean lower low water), including periodic tidal flooding between MLLW and MHW (mean high water) and episodic flooding above MHW.

Forcing The influence a factor has in altering the balance of incoming and outgoing energy in the Earth-atmosphere system, and thereby its importance as a potential climate change mechanism (adapted from Solomon et al. 2007a). Examples of forcing factors include changes in the atmospheric concentrations of greenhouse gases such as carbon dioxide and methane, changes in the atmospheric concentration of tiny airborne particulate matter, changes in the reflectivity of the land surface, and changes in output from the sun.

Generalized extreme value	A family of continuous probability distributions developed within extreme value theory. Extreme value theory provides the statistical framework to make inferences about the probability of very rare or extreme events. The Generalized Extreme Value (GEV) distribution unites the Gumbel, Fréchet, and Weibull distributions into a single family to allow a continuous range of possible shapes. The GEV distribution is parameterized with a shape parameter, location parameter, and scale parameter. Based on the extreme value theorem the GEV distribution is the limit distribution of properly normalized maxima of a sequence of independent and identically distributed random variables. Thus, the GEV distribution is used as an approximation to model the maxima of long (finite) sequences of random variables (adapted from Coles 2001).
Glacial isostatic adjustment	Rebound of the Earth's crust causing changes in relative sea level, caused by a change in the local radius of the solid Earth (Peltier 1998).
Global sea level	The average height of all the Earth's oceans (NOAA website, accessed January 2016).
Global sea-level rise	The increase currently observed in the average Global Sea-Level Trend, which is primarily attributed to changes in ocean volume due to two factors: mass addition through ice melt and thermal expansion (NOAA website, accessed January 2016).
Impact	The positive or negative effect on the natural or built environment caused by climate variability or change. Climate variability and change can have multiple impacts on people and communities, infrastructure and the services it provides, and ecosystems and natural resources (SERDP 2013).
Impact assessment	Practice of identifying and evaluating, in monetary and/or non-monetary terms, the effects of climate variability or change on natural and human systems (Parry et al. 2007). It is often a quantitative assessment, in which some degree of specificity is provided for the associated climate, environmental (biophysical) process, and impact models. An evaluation of the uncertainties involved is a necessary and integral contribution to reported outcomes. It may require high-resolution data. Impact assessment may lead to identification of adaptation strategies that can reduce system vulnerabilities.
Inundation	Although "flooding" and "inundation" often have been used interchangeably, some authors (e.g., Flick et al. 2012b) suggest that "inundation" better describes the condition of formerly dry areas becoming permanently submerged, such as when the annual average elevation of MLLW rises relative to land.

Likelihood Likelihood of an occurrence, outcome, or result, when this can be estimated probabilistically (Parry et al. 2007).

Mean higher high water datum The average of the higher high water height of each tidal day observed over the National Tidal Datum Epoch. For stations with shorter series, comparison of simultaneous observations with a control tide station is made to derive the equivalent datum of the National Tidal Datum Epoch. Some locations have diurnal tides: one high tide and one low tide per day. At most locations, semidiurnal tides occur: the tide cycles through a high and low twice each day, with one of the two high tides being higher than the other and one of the two low tides being lower than the other (NOAA website, accessed January 2016).

Mean high water datum The average of all the high water heights observed over the National Tidal Datum Epoch. For stations with shorter series, comparison of simultaneous observations with a control tide station is made in order to derive the equivalent datum of the National Tidal Datum Epoch (NOAA website, accessed January 2016).

Mean low water The average of all the low water heights observed over the National Tidal Datum Epoch. For stations with shorter series, comparison of simultaneous observations with a control tide station is made in order to derive the equivalent datum of the National Tidal Datum Epoch (NOAA website, accessed January 2016).

Mean lower low water The average of the lower low water height of each tidal day observed over the National Tidal Datum Epoch. For stations with shorter series, comparison of simultaneous observations with a control tide station is made to derive the equivalent datum of the National Tidal Datum Epoch. Mean lower low water is the reference chart datum for NOAA nautical charts and tide tables. (NOAA website, accessed January 2016).

Mean sea level Mean sea level as a tidal datum is computed as a mean of hourly water level heights observed over 19 years (NOAA website, accessed January 2016). Mean sea level also can be defined as an average sea level over a specified time, such as annual or monthly mean sea level.

Mitigation	Intervention to reduce the causes of changes in climate, such as through reducing emissions of greenhouse gases to the atmosphere and enhancing greenhouse gas sinks (NRC 2010, Solomon et al. 2007b). A human intervention to reduce the sources or enhance the sinks of greenhouse gases. This definition differs substantively from, and should not be confused with, the definition provided in the Terminology and Index section of the Code of Federal Regulations, Protection of Environment, Council on Environmental Quality (40 CFR 1508.20), which considers a hierarchical approach and includes the concepts of avoiding environmental impacts, minimizing impacts, rectifying the impact, reducing or eliminating the impact over time, and compensating for the impact.
National Climate Assessment	A report that collects, integrates, and assesses climate-related observations and research from around the United States, helping to understand changes in climate and what they mean. The report includes analyses of impacts on sectors and regions of the U.S.
National Tidal Datum Epoch	The specific 19-year period adopted by the National Ocean Service as the official time segment over which tide observations are taken and reduced to obtain mean values (e.g., mean lower low water, etc.) for tidal datums. It is necessary for standardization because of periodic and apparent secular trends in sea level. The present National Tidal Datum Epoch is 1983 through 2001 and is actively considered for revision every 20 to 25 years. Tidal datums in certain regions with anomalous sea-level changes (e.g., Alaska, Gulf of Mexico) are calculated on a modified 5-year epoch (NOAA website, accessed January 2016).
Natural (green) Infrastructure	Features of the land and water environments, including their biota and associated ecological processes that directly or indirectly support society. In a Department of Defense context, this support may serve military readiness or provide protective functions for built infrastructure during extreme weather events. In the first case, natural ecological systems often provide needed training landscapes and training realism. These can range from permafrost-controlled ecological systems of Alaska to barrier islands off the coasts of several military installations. In the second case, coastal wetlands and barrier islands serve to protect mainland areas from the effects of storms. Natural infrastructure often implies interconnected ecosystems and other natural features that support characteristics of the water, vegetation, and soil that are essential to sustaining life (SERDP 2013).

Nontidal residual

Water level components forming in response to ocean and atmospheric forcing (not associated with the astronomical tide). These components exhibit significant seasonal variability and differ between geographical areas (Sweet et al. 2014).

North American Vertical Datum

For North America, the surface of zero elevation to which heights of various points are referred in order that those heights be in a consistent system. More broadly, a vertical datum is the entire system of the zero elevation surface and methods of determining heights relative to that surface. The North American Vertical Datum of 1988 (NAVD88) is the vertical control datum established in 1991 by the minimum-constraint adjustment of the Canadian-Mexican-United States leveling observations. It held fixed the height of the primary tidal bench mark, referenced to the new International Great Lakes Datum of 1985 local mean sea-level height value, at Father Point/Rimouski, Quebec, Canada. This allows for relationships between past and current geodetic vertical datums, as well as various water level/tidal datums (e.g., Mean High Water) (NOAA National Geodetic Survey website, accessed January 2016).

Pacific Decadal Oscillation

The Pacific Decadal Oscillation (PDO) is a climate index based upon patterns of variation in sea surface temperature of the North Pacific from 1900 to the present (Mantua et al. 1997). The PDO is often described as a long-lived El Niño-like pattern of Pacific climate variability (Zhang et al. 1997). As seen with the better-known El Niño Southern Oscillation (ENSO), extremes in the PDO pattern are marked by widespread variations in the Pacific Basin and the North American climate. In parallel with the ENSO phenomenon, the extreme phases of the PDO have been classified as being either warm or cool, as defined by ocean temperature anomalies in the northeast and tropical Pacific Ocean. When sea surface temperatures (SST) are anomalously cool in the interior North Pacific and warm along the Pacific Coast, and when sea-level pressures are below average over the North Pacific, the PDO has a positive value. When the climate anomaly patterns are reversed, with warm SST anomalies in the interior and cool SST anomalies along the North American coast, or above average sea-level pressures over the North Pacific, the PDO has a negative value (all references in paragraph courtesy of Mantua 1999, NOAA website, accessed January 2016).

Pattern scaling

In general, a way of determining regionally differentiated projections of future climate change under further scenarios, when simulations with fully coupled climate models are not available (Tebaldi and Arblaster 2014). For purposes of this report, and to distinguish it from ice-melt fingerprinting, it is defined as the non-uniform distribution of changes in global mean sea level attributable to dynamic changes in ocean circulation, meteorology, and changes in salinity. In short, it refers to the spatial pattern exhibited by dynamical sea level.

Prediction[2]

The result of an attempt to produce an estimate of the actual evolution of a quantity or set of quantities in the future. Because the climate system may be highly sensitive to initial conditions and is nonlinear and chaotic, and our understanding of its behavior is imperfect, "predicting" future climate is inherently limited (adapted from Solomon et al. 2007b).

Projection[3]

Potential future evolution of a quantity or set of quantities, often computed with the aid of a model. Projections are distinguished from predictions to emphasize that projections involve assumptions or scenarios concerning, for example, future socioeconomic and technological developments that may or may not be realized and are therefore subject to substantial uncertainty (adapted from Solomon et al. 2007b).

Regional frequency analysis

Procedures for statistical frequency analysis of a single set of data are well established. It is often the case, however, that many related samples of data are available for analysis. These may, for example, be meteorological or environmental observations of the same variable at different monitoring sites. If event frequencies are similar for the different observed quantities, then more accurate conclusions can be reached by analyzing all of the data samples together than by using only a single sample. In environmental applications, this approach is known as *regional frequency analysis*, because the data samples analyzed are typically observations of the same variable at a number of measuring sites within a suitably defined "region" (Hosking and Wallis 1997).

Representative Concentration Pathway

Specific emission scenarios derived from peer-reviewed literature and defined as plausible pathways towards reaching corresponding radiative forcing trajectories (climate models require data on the time-evolving emissions or concentrations of radiatively active constituents). The word "representative" signifies that each Representative Concentration Pathway provides only one of many possible scenarios that would lead to the specific radiative forcing characteristics. The term "pathway" emphasizes that not only the long-term concentration levels are of interest, but also the trajectory taken over time to reach that outcome (adapted from Moss et al. 2010).

Resilience

Capability to anticipate, prepare for, respond to, and recover from significant multi-hazard threats with minimum damage to social well-being, the economy, and the environment (NRC 2010). Ability of a social or ecological system to absorb disturbances while retaining the same basic structure and ways of functioning, capacity for self-organization, and capacity to adapt to stress and change (Parry et al. 2007).

[1]Some authors (see Weaver et al. 2013) suggest that semantic confusion surrounds the use of prediction, projection, and scenario and that in some applications, the terms are used as shorthand for describing a continuum of decreasingly confident statements about the future, from prediction through projection to scenario. Weaver et al. (2013) favor adopting functional definitions that describe the relation of the conceptualization captured by a term to decision-making; although this approach may better distinguish the usage of prediction and scenario, it may reduce the utility of projection in terms of adding functional clarity.

[2]See Footnote 1.

Risk

Combination of the magnitude of the potential consequence(s) of climate change impact(s) and the likelihood that the consequence(s) will occur (NRC 2010).

Risk-based framing

For the purposes of this report, a broader view of risk is taken that is not dependent on assigning likelihoods or probabilities. The approach acknowledges that risk under conditions of deep uncertainty cannot be defined in a strictly probabilistic sense and instead is dependent on the type of decision involved, its intended longevity, and a decision-maker's tolerance for the adverse consequences of a wrong decision.

Robust decision-making

For purposes of this report and to avoid settling on a definition of robust decision-making that is tied directly to a particular methodological framework, this report takes a more inclusive approach and defines robust decisions as those that meet the decision-maker's objectives across a range of plausible futures. Robust decision-making processes are iterative and adaptive by nature (Hallegatte et al. 2012) and can be effectively used to support a risk-based framing approach.

Scenario[4]

Description of potential future conditions produced to inform decision-making under uncertainty. Scenarios can help inform specific decisions, or they can provide inputs to assessments, models, or other decision-support activities when these activities need specification of potential future conditions. They also can provide various forms of indirect decision support, such as clarifying an issue's importance, framing a decision agenda, altering habitual thinking, stimulating creativity, clarifying points of agreement and disagreement, identifying and engaging needed participants, or providing structure for analysis of potential future decisions (Parson et al. 2007).

Most importantly, scenario as used in this report refers to a plausible and scientifically credible view of the future that can assist decision-makers in managing uncertainty. In this context a scenario is not assigned a likelihood.

Sensitivity

Degree to which a system may be affected, either adversely or beneficially, by climate variability or change (Parry et al. 2007).

Steric sea-level change

Sea-level changes induced by changes in water density are called steric. Density changes induced by temperature changes only are called thermosteric and density changes induced by salinity changes are called halosteric (Solomon et al. 2007b).

[4]See Footnote 1.

Still water level Elevation of the water surface in the absence of waves and wave effects. Primary components are the astronomical tide, interannual variability such as forcings from El Niño, and surge (adapted from Moritz et al. 2015).

Total water level Water level resulting from complex interactions between multiple oceanographic, hydrologic, geologic, and meteorological forcings that act over a wide range of scales. Important components include astronomical tide, wave set-up, wind set-up, large-scale storm surge, precipitation, fluvial discharges, monthly mean sea-level anomalies, and land subsidence or uplift (Moritz et al. 2015).

Vertical land movement Measured trends in vertical land motion due to a variety of factors, including response of the earth's surface to the last ice age (modeled by Glacial Isostatic Adjustment models), local uplift from isostatic rebound in glacial fjords, post-earthquake deformations, volcanism, and slow tectonic movement. Locally, land subsidence also can be due to withdrawal of hydrocarbons (oil and gas) and groundwater and local sediment compaction (Zervas 2013).

Vulnerability Degree to which a system is susceptible to, or unable to cope with, the adverse effects of climate change, including climate variability and extremes (NRC 2010).

Vulnerability assessment Practice of identifying and evaluating the effects of climate change and climate variability on natural and human systems to understand system vulnerability (adapted from SERDP 2013).

In this report, we interpret this definition to imply a form of qualitative assessment or an assessment that is less quantitatively rigorous than an impact assessment. The degree of specificity in the climate, environmental process, and impact models is not as stringent as for an impact assessment, even when accompanied by an evaluation of the uncertainties involved. Moreover, from this perspective, data requirements, including their spatial granularity, can be more relaxed than what is required for an impact assessment. Vulnerability assessments, when defined this way, may best be tied to an initial screening process that may lead to the more detailed impact assessments for those locales and systems identified as most vulnerable or mission-critical.

References

Coles, S. 2001. *An Introduction to Statistical Modeling of Extreme Values*. London, United Kingdom: Springer-Verlag.

Flick, R.E., D.B. Chadwick, J. Briscoe, and K.C. Harper. 2012b. "Flooding" versus "Inundation." *Eos, Transactions of the American Geophysical Union* 93:365–366.

Hallegatte, S., A. Shah, R. Lempert, C. Brown, and S. Gill. 2012. *Investment Decision Making under Deep Uncertainty—Application to Climate Change*. Policy Research Working Paper 6193. Washington, D.C.: The World Bank, Sustainable Development Network, Office of the Chief Economist.

Hosking, J.R.M. and J.R. Wallis. 1997. Regional Frequency Analysis – An Approach Based on L-Moments. Cambridge, United Kingdom and New York, New York: Cambridge University Press.

Joint Publication 1-02 (JP1-02). 2001. Department of Defense Dictionary of Military and Associated Terms.

Mitrovica, J.X., N. Gomez, E. Morrow, C. Hay, K. Laychev, and M.E. Tamisea. 2011. On the Robustness of Predictions of Sea Level Fingerprints. *Geophysical Journal International* 187:729–742.

Moritz, H.P., K. White, B. Gouldby, W. Sweet, P. Ruggiero, P. O'Brien, H.R. Moritz, T. Wahl, N.C. Nadal-Carabello, and W. Veatch. 2015. USACE Adaptation Approach for Future Coastal Climate Conditions. *Proceedings of the Institution of Civil Engineers - Maritime Engineering* 168:111–117.

Moss, R.M. et al. 2010. The Next Generation of Scenarios for Climate Change Research and Assessment. *Nature* 463:747–756.

National Research Council (NRC). 2010. *Adapting to the Impacts of Climate Change, America's Climate Choices: Panel on Adapting to the Impacts of Climate Change*. Washington, D.C.: The National Academies Press.

Parry, M.L., O.F. Canziani, J.P. Palutikof, P.J. van der Linden, and C.E. Hanson, eds. 2007. Appendix I: Glossary. In *Climate Change 2007: Impacts, Adaptation and Vulnerability. Contribution of Working Group II to the Fourth Assessment Report of the Intergovernmental Panel on Climate Change*, 869–883. Cambridge, United Kingdom and New York, New York: Cambridge University Press.

Parson, E., V. Burkett, K. Fisher-Vanden, D. Keith, L. Mearns, H. Pitcher, C. Rosenzweig, and M. Webster. 2007. *Global Change Scenarios: Their Development and Use*. Sub-Report 2.1B of Synthesis and Assessment Product 2.1 by the U.S. Climate Change Science Program and the Subcommittee on Global Change Research. Washington, D.C.: U.S. Department of Energy, Office of Biological and Environmental Research.

Peltier, W.R. 1998. Postglacial Variations in the Level of the Sea: Implications for Climate Dynamics and Solid-Earth Geophysics. *Reviews of Geophysics* 36:603–689. doi: 10.1029/98RG02638.

Perrette, M., F. Landerer, R. Riva, K. Frieler, and M. Meinshausen. 2013. A Scaling Approach to Project Regional Sea Level Rise and Its Uncertainties. *Earth System Dynamics* 4:11–29.

Solomon, S., D. Qin, M. Manning, Z. Chen, M. Marquis, K.B. Averyt, M. Tignor and H.L. Miller (eds.). 2007a. Summary for Policymakers. Contribution of Working Group I [Physical Science] to the Fourth Assessment Report of the Intergovernmental Panel on Climate Change. Cambridge, United Kingdom and New York, New York: Cambridge University Press.

Solomon, S., D. Qin, M. Manning, M. Marquis, K. Averyt, M.M.B. Tignor, H.L. Miller, Jr., Z. Chen (eds.), 2007b. Annex 1, Glossary. Contribution of Working Group I [Physical Science] to the Fourth Assessment Report of the Intergovernmental Panel on Climate Change. Cambridge, United Kingdom and New York, New York: Cambridge University Press.

Strategic Environmental Research and Development Program (SERDP). 2013. *Assessing Impacts of Climate Change on Coastal Military Installations: Policy Implications*. Alexandria, Virginia: U.S. Department of Defense.

Sweet, W.V., J. Park, J.J. Marra, C. Zervas, and S. Gill. 2014. *Sea Level Rise and Nuisance Flood Frequency Changes around the United States*. NOAA Technical Report NOS CO-OPS 73. Silver Spring, Maryland: U.S. Department of Commerce, NOAA, National Ocean Service, Center for Operational Oceanographic Products and Services.

Tebaldi, C. and J.M. Arblaster. 2014. Pattern Scaling: Its Strengths and Limitations, and an Update on the Latest Model Simulations. *Climatic Change* 122:459–471.

Zervas, C., S. Gill, and W. Sweet. 2013. *Estimating Vertical Land Motion from Long-Term Tide Gauge Records*. Technical Report NOS CO-OPS 065. Silver Spring, Maryland: U.S. Department of Commerce, NOAA, National Ocean Service, Center for Operational Oceanographic Products and Services.

THIS PAGE LEFT INTENTIONALLY BLANK

Appendix B

Review of Select Federal Tools Relating to Sea-Level Change Depiction and Potential Impacts

The following pages provide descriptions of four tools developed by Federal agencies for use in calculating or visualizing sea-level change or coastal storms, and the impacts of these phenomena. For each tool, the description includes a discussion of the tool's primary purpose, the intended audience, geographic scope, implications for future use, relationship to the information provided in the main report on sea-level rise and extreme water level scenarios, and a list of references.

The following tools are described:

Sea Level Rise and Coastal Flooding Impacts Viewer
(National Oceanic and Atmospheric Administration)

Sea Level Change Calculator Tool
(U.S. Army Corps of Engineers)

Coastal Storm Modeling System (CoSMoS)
(U.S. Geological Survey)

Coastal Vulnerability Index
(U.S. Geological Survey)

SEA LEVEL RISE AND COASTAL FLOODING IMPACTS VIEWER

National Oceanic and Atmospheric Administration (NOAA)

Purpose:

The purpose of this data viewer is to provide coastal managers and scientists with a preliminary look at sea-level rise (SLR) and coastal flooding impacts. The viewer is a screening-level tool that uses nationally consistent datasets and analyses. Data and map services can be accessed and used at several spatial scales to help assess vulnerabilities and develop adaptation for a range of scenarios. This tool has the capability to show potential impacts from a range of inundation scenarios from 0 to 6 feet above current Mean Higher High Water (MHHW), which captures many global and local SLR scenarios such as those developed by Parris et al. (2012), the National Research Council (NRC 2012), and the New York City Panel on Climate Change (NPCC 2013). The tool also provides a geospatial representation of mapping confidence (Schmid et al. 2014), nuisance flooding, and impacts of SLR on flood frequency (Sweet et al. 2014, Sweet and Park 2014).

Brief tool description/overview:

Mapping sea-level changes in a geographic information system (GIS) gives users the ability to overlay potentially impacted areas with other data, such as critical infrastructure, roads, ecologically sensitive areas, demographics, and economics. Providing maps on the web via Internet mapping technologies enables the user to have an interactive experience that truly brings out the "visual" part of the map definition.

Culver et al. (2010) listed several data and tool needs that were lacking at the time this tool was developed. The purpose of the tool was to address many of the following needs and build on previous interagency efforts:

- Communication of uncertainty
- Societal and economic impacts
- Natural resource impacts, scenario approaches
- Mapping on the best available topographic data
- Mapping using latest techniques in datum transformation
- Accounting for error.

Being able to visualize potential impacts from SLR is a powerful teaching and planning tool, and the SLR and Coastal Flooding Impacts Viewer brings this capability to coastal communities.

Features of the tool include the following:

- Displays potential future sea levels
- Provides simulations of SLR at local landmarks
- Communicates the spatial uncertainty of mapped sea levels
- Models potential marsh migration due to SLR
- Overlays social and economic data onto potential SLR
- Examines how tidal flooding will become more frequent with SLR

The data and maps in this tool illustrate the scale of potential flooding, not the exact location, and do not account for erosion, subsidence, or future construction. Water levels are shown as they would appear during the highest high tides (excludes wind driven tides or storm surge). The data, maps, and information provided should be used only as a screening-level tool for management decisions. As with all remotely sensed data, all features should be verified with a site visit. The data and maps in this tool are provided "as is," without warranty to their performance, merchantable state, or fitness for any particular purpose. The entire risk associated with the results and performance of these data is assumed by the user. This tool should be used strictly as a planning reference tool and not for navigation, permitting, or other legal purposes.

Mapping methods are provided on the tool website https://coast.noaa.gov/digitalcoast/tools/slr and are discussed in Marcy et al. 2011.

Audience:
This tool is directed primarily at coastal resource managers, floodplain managers, and local planners and decision-makers, but it also can be used by the general public to communicate the impacts of SLR and coastal flooding.

Geographic scope:
The tool, data, and map services are available for all U.S Ocean Coastal States (excluding Alaska) and territories (including Puerto Rico, U.S. Virgin Islands, Guam, Saipan, and American Samoa). Maps are not currently available for Alaska because of the inaccuracy of existing elevation data and gaps in vertical datum transformation.

Implications for the future:
This tool enables users to specify inundation scenarios ranging from 0 to 6 feet above current MHHW to visualize potential impacts. No indication of plausibility is provided with any given future scenario. Inundation impacts from SLR or from event-driven coastal flooding can be evaluated. The tool does not have a time component, so the user can determine a future scenario and use the tool to visualize the results or download the data. A disclaimer is provided with the tool to express its limitations. Inundation scenarios are mapped in 1-foot elevation increments, which the user can select.

Relationship to the *Regional Sea Level Scenarios for Coastal Risk Management* report

- This tool does not explicitly use global or relative SLR scenarios. It is up to the user to select different levels of inundation; therefore, it can be used to visualize and determine impacts to any global or relative scenario (within a 1-foot mapping unit, based on limits of the vertical accuracy of the underlying elevation data).
- Maps provided in this tool are based on best-available elevation data and MHHW surface from the NOAA VDATUM model (http://vdatum.noaa.gov/), when such information is available.
- This tool can be used to visualize any new global, regional, or local relative SLR scenarios that are developed, assuming the upper range is not greater than 6 feet.

References

Culver, M.E., J.R. Schubel, M.A. Davidson, J. Haines, and K.C. Texeira, eds. 2010. *Proceedings from the Sea Level Rise and Inundation Community Workshop*, Lansdowne, Virginia, December 3 to 5, 2009. Charleston, South Carolina: National Oceanic and Atmospheric Administration and U.S. Geological Survey.

Marcy, D., W. Brooks, K. Draganov, B. Hadley, C. Haynes, N. Herold, J. McCombs, M. Pendleton, S. Ryan, K. Schmid, M. Sutherland, and K. Waters. 2011. New Mapping Tool and Techniques for Visualizing Sea Level Rise and Coastal Flooding Impacts. In *Proceedings of the 2011 Solutions to Coastal Disasters Conference, Anchorage, Alaska, June 26 to June 29, 2011*, edited by L.A. Wallendorf, C. Jones, L. Ewing, and B. Battalio, 474–490. Reston, Virginia: American Society of Civil Engineers.

National Research Council (NRC). 2012. *Sea-Level Rise for the Coasts of California, Oregon, and Washington: Past, Present, and Future*. Washington, D.C.: The National Academies Press. http://www.nap.edu/openbook.php?record_id=13389.

New York City Panel on Climate Change (NPCC). 2013. *New York City Panel on Climate Change*. New York, New York: New York City Mayor's Office of Sustainability. http://www.nyc.gov/html/planyc2030/downloads/pdf/NPCC_Climate%20Projections_2013.pdf.

Parris, A., P. Bromirski, V. Burkett, D. Cayan, M. Culver, J. Hall, R. Horton, K. Knuuti, R. Moss, J. Obeysekera, A. Sallenger, and J. Weiss. 2012. *Global Sea Level Rise Scenarios for the United States National Climate Assessment*. NOAA Technical Report OAR CPO-1. Silver Spring, Maryland: U.S. Department of Commerce, National Oceanic and Atmospheric Administration, Climate Program Office. http://cpo.noaa.gov/sites/cpo/Reports/2012/NOAA_SLR_r3.pdf.

Schmid, K., B. Hadley, and K. Waters. 2014. Mapping and Portraying Inundation Uncertainty of Bathtub-Type Models. *Journal of Coastal Research* 30:548–561.

Sweet, W.V., J. Park, J.J. Marra, C. Zervas, and S. Gill. 2014. *Sea Level Rise and Nuisance Flood Frequency Changes around the United States*. NOAA Technical Report NOS CO-OPS 73. Silver Spring, Maryland: U.S. Department of Commerce, National Oceanic and Atmospheric Administration, National Ocean Service, Center for Operational Oceanographic Products and Services.

Sweet, W.V. and J. Park. 2014. From the Extreme to the Mean: Acceleration and Tipping Points of Coastal Inundation from Sea Level Rise. *Earth's Future* 2:579–600. doi:10.1002/2014EF000272.

USACE SEA LEVEL CHANGE CALCULATOR

U.S. Army Corps of Engineers (USACE)

Purpose:
The need to incorporate projected changes to local mean sea level into the design of USACE Civil Works projects required the development of a simple, web-based tool to provide repeatable analytical results. The purpose of this tool is to support coastal managers, planners, and scientists in calculating the USACE sea-level change (SLC) scenarios based on coastal tide gauge data in the United States, including the effects of vertical land movement. This tool has the capability to compare the USACE scenarios with additional scenarios such as those developed by a National Oceanic and Atmospheric Administration (NOAA)-led working group in support of the National Climate Assessment (Parris et al. 2012), the National Research Council (NRC 2012), and the New York City Panel on Climate Change (NPCC 2013).

Brief tool description/overview:
The USACE Sea Level Change Curve Calculator uses the methodology described in Engineer Regulation (ER) 1100-2-8162, Incorporating Sea Level Changes in Civil Works Programs (USACE 2013), to estimate SLC for the three USACE scenarios. These low, intermediate, and high scenarios are based on different assumptions about physical processes and causes, and no one scenario is considered more likely than another. The results of the tool are intended for relatively simple studies, screening-level vulnerability assessments, and similar studies as described in Engineer Technical Letter (ETL) 1100-2-1 (USACE 2014). The results of this tool alone are not appropriate for detailed engineering design where consequences are high.

The USACE Sea Level Change Curve Calculator consists of a web-based tool that produces a table and graph of the projected SLCs based on a user-selected long-term tide gauge, project start date, and project life span, as well as other user-provided information such as critical elevation thresholds. The tool enables the user to estimate extreme still water levels for these scenarios using linear superposition based on the generalized extreme value statistical function (NOAA 2013) applied to recorded historic monthly extreme water level values. The tool also enables the user to estimate extreme values using a percentile statistical function. Both methods use data recorded and validated by NOAA at their tide gauges. It is important to note that the extreme values at the tide gauges can be significantly different than those that may occur at a project site, in part determined by distance from the project site and whether the underlying surficial geologies are similar. The level of confidence in the exceedance probability increases with longer return periods.

Audience:
This publicly available tool was developed for use by USACE staff in preliminary studies and screening-level risk assessments. The tool also has utility for local or state planners and decision-makers, as well as members of the general public who would like to explore potential future impacts from changing sea levels.

Geographic scope:
This tool is designed to work in United States (U.S.) coastal areas in all 50 states and territories where long-term (greater than 40 years of records) tidal stations exist. ETL 1100-2-1 (USACE 2014) describes geographical factors that should be considered when evaluating the appropriateness of a particular tide gauge, with respect to the specific plan or site under consideration.

Implications for the future:
- This tool produces low, intermediate, and high scenarios based on user input in accordance with USACE guidance (USACE 2013, 2014).
- The tool uses USACE SLC scenarios described in ER 1100-2-8162 and ETL 1100-2-1 (USACE 2013, 2014), both of which address plausibility and basis for the tool. The basis for these scenarios is provided in the first major national study addressing rising sea levels, conducted by the NRC (1987). This report, *Responding to Changes in Sea Level: Engineering Implications*, suggested that due to the uncertainty in future conditions, the use of three plausible scenarios of future conditions would best support policy and engineering design decision-making.
- The tool uses a continuous time function to display the USACE and NOAA SLC scenarios, and provides bar graphs for the NRC and NPCC scenarios at their respective discrete time periods.

Relationship to the *Regional Sea Level Scenarios for Coastal Risk Management* report:
USACE updated its guidance on considerations for SLC in Civil Works programs beginning in 2009 to ensure sustainable performance in the future in response to post-Katrina recommendations around land subsidence, tidal fluctuations, and SLC. These USACE efforts and the resulting policy and guidance included in ER 1100-2-8162 (USACE 2013) and ETL 1100-2-1 (USACE 2014) predate the present study and should be considered aligned with, though slightly different from, the study results reported herein for locations near long-term tide gauges in the United States. The USACE guidance does not prohibit the use of other scenarios, and although the USACE tool does not include dynamic sea level and regional ice-melt effects it does allow for the consideration of regional effects, so the present study's results could be used in conjunction with the USACE Sea Level Change Curve Calculator in the U.S., and can supplement the tool outside the U.S. The Sea Level Change Curve Calculator provides a graph and table showing the relationship of the various gauge datums.

References
National Oceanic and Atmospheric Administration (NOAA). 2013. *Extreme Water Levels of the United States 1893–2010*. NOAA Technical Report NOS CO-OPS 067. Silver Spring, Maryland: U.S. Department of Commerce, National Oceanic and Atmospheric Administration, National Ocean Service, Center for Operational Oceanographic Products and Services. http://tidesandcurrents.noaa.gov/publications/NOAA_Technical_Report_NOS_COOPS_067a.pdf.

National Research Council (NRC). 1987. *Responding to Changes in Sea Level: Engineering Implications*. Washington, D.C.: The National Academies Press. http://www.nap.edu/catalog.php?record_id=1006.

National Research Council (NRC). 2012. *Sea-Level Rise for the Coasts of California, Oregon, and Washington: Past, Present, and Future*. Washington, D.C.: The National Academies Press. http://www.nap.edu/openbook.php?record_id=13389.

New York City Panel on Climate Change (NPCC). 2013. *New York City Panel on Climate Change*. New York, New York: New York City Mayor's Office of Sustainability. http://www.nyc.gov/html/planyc2030/downloads/pdf/NPCC_Climate%20Projections_2013.pdf.

Parris, A., P. Bromirski, V. Burkett, D. Cayan, M. Culver, J. Hall, R. Horton, K. Knuuti, R. Moss, J. Obeysekera, A. Sallenger, and J. Weiss. 2012. *Global Sea Level Rise Scenarios for the United States National Climate Assessment*. NOAA Technical Report OAR CPO-1. Silver Spring, Maryland: U.S. Department of Commerce, National Oceanic and Atmospheric Administration, Climate Program Office. http://cpo.noaa.gov/sites/cpo/Reports/2012/NOAA_SLR_r3.pdf.

U.S. Army Corps of Engineers (USACE). 2013. *Incorporating Sea-Level Change in Civil Works Programs*. ER 1100-2-8162. Washington, D.C.: U.S. Army Corps of Engineers. http://www.publications.usace.army.mil/Portals/76/Publications/EngineerRegulations/ER_1100-2-8162.pdf.

USACE. 2014. *Procedures to Evaluate Sea Level Change*: Impacts, Responses, and Adaptation. ETL 1100-2-1. Washington, D.C.: U.S. Army Corps of Engineers. http://www.publications.usace.army.mil/Portals/76/Publications/EngineerTechnicalLetters/ETL_1100-2-1.pdf.

USGS: COASTAL STORM MODELING SYSTEM (CoSMoS)

U.S. Geological Survey (USGS)

Purpose:

The Coastal Storm Modeling System (CoSMoS), available at http://walrus.wr.usgs.gov/coastal_processes/cosmos/index.html, was developed for hindcast studies, operational applications and future climate scenarios (sea-level rise [SLR] and storms) to provide emergency responders and coastal planners with critical storm-hazard information that can be used to increase public safety, mitigate physical damages, and more effectively manage and allocate resources within complex coastal settings (Barnard et al. 2009). To provide this information, key storm hazards such as flood extent, duration of flooding, wave height, and currents are explicitly modeled within CoSMoS, accounting for all pertinent physics and variation in storm conditions. In addition to select modeled historical events, future climate-based flood-hazard projections provide local decision-makers with actionable and easily applied data to develop strategies ensuring healthy and viable coastal ecosystems and communities in the 21st century. Because coastal stakeholders' assessments of future vulnerability can differ widely in geographic scope, analysis horizon, and definitions of acceptable risk, CoSMoS delivers a broad ensemble of modeled projections to support diverse planning needs, supplied in adaptable data formats for customized analysis. Individual simulations represent more than 40 scenarios covering a range of potential SLR (0 meters to 2 meters, plus an extreme 5-meter case) and storm conditions (average daily, 1-year, 20-year, and 100-year storm conditions), yielding a robust dataset that provides critical information for wide-ranging risk assessments and analysis techniques.

Brief tool description/overview:

CoSMoS framework and outputs:

CoSMoS primarily addresses dynamic coastal flooding associated with storms, which can contribute up to 5 meters or more of elevated water levels in certain locations. Without accounting for this component of flooding, a significant aspect of vulnerability is missed. CoSMoS uses explicit, deterministic models to include all the relevant physics (e.g., tides, swell, wind waves, and surge) of a coastal storm. The system is driven by the global WAVEWATCH III (WWIII) wave model, the TOPEX/Poseidon satellite altimetry-based global tide model, and atmospheric forcing data to determine regional wave and water-level boundary conditions, which are dynamically downscaled to the local level using a series of nested Delft3D wave (SWAN) and tide (FLOW) models. Different sources of atmospheric data are used depending on the mode in which CoSMoS is run: historical, operational, or future climate. The SWAN and FLOW model data are ultimately linked at the coast to tightly spaced eXtreme Beach (XBeach) cross-shore profile models and a Bayesian probabilistic cliff failure model. Model results are projected onto high-resolution Digital Elevation Models (DEMs) to create flood-hazard projections with coincident flood depths and extents, currents, wave heights, and shoreline change at the local scale. This is performed for each scenario. Scenarios are defined by a storm event, derived from atmospheric and wave input conditions, in combination with possible changes in sea level.

All CoSMoS results are presented in shapefiles and are able to be used in Geographic Information System (GIS) platforms for customized statistical analysis or inclusion with physical resource and social data. Results also have been collated by frequency of inundation and by SLR value to create total-ensemble and SLR-suite flood risk statistics, respectively.

CoSMoS in future climate mode:

To address future climate conditions, CoSMoS employs atmospheric forcing from global climate models and dynamically downscaled WWIII data. Storm events in the 21st century are identified and extracted from the atmospheric models and derived wave data at return periods of 1, 20, and 100 years. Additional conditions include average daily conditions and a king tide event, or extreme high tide, and all storm conditions are paired with different values of SLR for an event scenario. Modeled event scenarios feature the full spectrum of anticipated global SLR (0 to 2 meters at 0.25-meter increments, and an extreme 5-meter case; Intergovernmental Panel on Climate Change 2007, National Research Council 2012, Vermeer and Rahmstorf 2009) and storm conditions to meet multiple planning needs. Scenarios with a SLR of 0 meters (no sea-level rise) are included in this broad ensemble of modeled conditions as they provide calibration for the model system as well as a baseline for comparing other event projections. Where data are available, long-term terrain changes, including vertical land movement (VLM) and marsh accretion estimates, are included in the DEM projections and in calculations of uncertainty. These data are produced and available from experts in external studies and organizations.

CoSMoS simulations for Central California and San Francisco Bay are available in an online decision support tool as part of the Our Coast, Our Future (OCOF) collaborative at http://data.prbo.org/apps/ocof/. Within the online tool, users can select from and easily shift between all 21st century SLR and storm scenarios to visualize flood extent, depth, and model uncertainty. Respective wave height, currents, and event-based shoreline change for each scenario are also available, and can be displayed over GIS databases of ecology, land use, and infrastructure.

CoSMoS does not address the validity or probability of specific SLR projections, but accounts for the plausible range of SLR values to meet different management or planning horizons and degrees of risk tolerance. Additionally, storms used in the modeling system are identified and taken from GCMs rather than from historical tide gauge records and meteorological observations, as the past few decades may not be indicative of future climate. Numerous studies (Barnard et al. 2014, Erikson et al. 2015) have shown that future storm wave and wind conditions are likely to evolve in a nonlinear fashion unlike past conditions and are dependent on complex atmosphere-ocean interactions that the GCMs simulate. For example, GCM data and studies suggest that storms affecting the western U.S. coast may change in intensity during the 21st century, but may also transit along different trajectories toward the coast (Neelin et al. 2013). WWIII data (Erikson et al. 2015) for the mid and end of the 21st century suggest that incident storm-related wave directions will shift, thus potentially shifting vulnerable regions of exposed coast.

Because a user can select data from individual simulations of a range of SLR values and storm conditions, or statistics from the entire ensemble or a select subset, the combined dataset is very flexible and able to support risk assessments spanning multiple geographic and time scales. For

example, inspecting the total ensemble can show "tipping points" of risk with regard to SLR for both large and localized areas, and inspecting subsets of the ensemble can show risks for particular storm intensities. In this way, CoSMoS can aid in screening for regional vulnerabilities requiring more in-depth study, as well as determining local hazards.

The current CoSMoS version runs simulations for individual storm events, so it does not address long-term or multi-decadal shoreline evolution. However, the projection capability using an evolving DEM accounting for long-term coastal change is in development for future implementation. The models also do not account for any alterations to present flood control structures unless customized changes are made within the model system to simulate specific modifications to levees, dikes, and seawalls.

CoSMoS in historical mode:
To support hindcast studies, select historical cases with historical or synthetically-created forcing data are modeled for southern California. These storm events are also coupled with a range of SLR for a suite of hazard projections, available on line at http://walrus.wr.usgs.gov/coastal_processes/cosmos/socal1.0/index.html.

CoSMoS in operational mode:
CoSMoS is currently in development for operational use with National Weather Service to produce near real-time and multi-day coastal flooding forecasts. The goal of this research is to align CoSMoS' ocean-based flooding projection with current numerical weather prediction models and watershed flooding models for comprehensive coastal flood forecasts. The initial development and testing for this merged flood model is focused on sites in San Francisco Bay.

Audience:
The online tool and model development was primarily directed at the range of community decision-makers, resource managers, and planners invested in the coastal zone, as the suite of results can be used to determine regional thresholds of risk as well as flood inundation hazards at multiple planning horizons. The online tool, however, can be used by and is also available to the general public.

Geographic scope:
Although the modeling system was initially developed for use in the high wave-energy environment of the U.S. West Coast, CoSMoS methodology is not site-specific and can be utilized on sandy coasts, cliff-backed coasts, and estuaries throughout the world given sufficient topographic, bathymetric, and model calibration data. At the present time, CoSMoS results are available for central and southern California, including San Francisco Bay. Expansions along the U.S West Coast and into the Pacific islands are under discussion.

Implications for the future:
CoSMoS data does not use a time slice or depiction of a specific time period, but rather shows flood potential, areas of vulnerability, and highlights locations and regions where more specialized analysis may be needed. As previously noted, the individual scenarios within CoSMoS

depict potential flood hazards from a range of plausible SLR and projected storm conditions. Thus, a specific time in the 21st century can be investigated by using particular SLR scenarios corresponding to an area's anticipated SLR rate. To assist California users in identifying SLR values for particular studies, OCOF's online tool shows published and expected SLR values (COCAT 2010, 2013, IPCC 2007, NRC 2012, Vermeer and Rahmstorf, 2009) throughout the 21st century as well as times by which certain SLR thresholds are calculated to occur. Conversely, investigating a collection or entire suite of scenarios can depict areas of significant vulnerability and highlight areas of concern. Total-ensemble and SLR-suite flood risk statistics provide additional data to help identify and understand future vulnerabilities.

Relationship to the *Regional Sea Level Scenarios for Coastal Risk Management* report:
As CoSMoS does not specifically address SLR probability, but instead depicts hazards from potential SLR values with future storm conditions, CoSMoS projections would be an excellent complement to this report's SLR fingerprint and VLM data that are used to adjust the global SLR scenarios. Additionally, should this report's VLM data be included in CoSMoS processes, results would yield more robust hazard projections.

Depending on how the complete suite or subset of data is examined, resulting information can be both policy-relevant and educational, enhancing conclusions drawn from this report. To reduce uncertainty for specific long-term planning, it is ideal to have separate case studies or data constraining probable SLR values for an area of interest. Again, given this report's SLR fingerprint investigation, those data and the CoSMoS tool would be complementary.

In some locations, this report's historically-based extreme water level calculations from tide gauge data may not directly correspond to modeled future storm conditions. Without consideration of wave information, especially changes in direction or height along the area of interest, certain locations may indicate potentially conflicting information. Such areas, however, should only reinforce the need for more observation and investigation in those locations, to determine important drivers of local hazards and accurately gauge future risk.

References:
Barnard, P.L., B. O'Reilly, M. van Ormondt, E. Elias, P. Ruggiero, L.H. Erikson, C. Hapke, B.D. Collins, R.T. Guza, P.N. Adams, and J. Thomas. 2009. *The Framework of a Coastal Hazards Model: A Tool for Predicting the Impact of Severe Storms*. U.S. Geological Survey Open-File Report 2009-1073. Reston, Virginia: U.S. Department of the Interior, U.S. Geological Survey. http://pubs.usgs.gov/of/2009/1073/.

Barnard, P.L., M. van Ormondt, L.H. Erikson, J. Eshleman, C. Hapke, P. Ruggiero, P.N. Adams, and A.C. Foxgrover. 2014. Development of the Coastal Storm Modeling System (CoSMoS) for Predicting the Impact of Storms on High-Energy, Active-Margin Coasts. *Natural Hazards* 74:1095–1125. doi: 10.1007/s11069-014-1236-y.

Coastal and Ocean Working Group of the California Climate Action Team (CO-CAT). 2010. *State of California Sea-Level Rise Interim Guidance Document*. Sacramento, California: State of California. http://www.opc.ca.gov/webmaster/ftp/pdf/agenda_items/20100911/14.%20SLR/1011_COPC_SLR_Interim_Guidance.pdf.

CO-CAT. 2013. *State of California Sea-Level Rise Guidance Document. Sacramento, California: State of California*. http://www.opc.ca.gov/webmaster/ftp/pdf/docs/2013_SLR_Guidance_Update_FINAL1.pdf.

Erikson, L.H., C.A. Hegermiller, P.L. Barnard, P. Ruggiero, M. van Ormondt. 2015. Projected Wave Conditions in the Eastern North Pacific under the Influence of Two CMIP5 Climate Scenarios. *Ocean Modelling* 96:171–185.

Intergovernmental Panel on Climate Change (IPCC). 2007. *Climate Change 2007: Synthesis Report. Contribution of Working Groups I, II and III to the Fourth Assessment Report of the Intergovernmental Panel on Climate Change*, edited by The Core Writing Team, R.K. Pachauri, and A. Reisinger. Geneva, Switzerland: IPCC.

National Research Council (NRC). 2012. *Sea-Level Rise for the Coasts of California, Oregon, and Washington: Past, Present, and Future. Washington, D.C.*: The National Academies Press.

Neelin, J.D., B. Langenbrunner, J.E. Meyerson, A. Hall, and N. Berg. 2013. California Winter Precipitation Change under Global Warming in the Coupled Model Intercomparison Project 5 Ensemble. *Journal of Climate* 26:6238–6256. doi:10.1175/JCLI-D-12-00514.1.

Vermeer, M. and S. Rahmstorf. 2009. Global Sea Level Linked to Global Temperature. In *Proceedings of the National Academy of Sciences of the United States of America* 106:21527–21532. doi: 10.1073/pnas.0907765106.

COASTAL VULNERABILITY INDEX

U.S. Geological Survey (USGS)

Purpose:
The coastal zone is a highly dynamic environment that changes in response to a variety of physical, biological, and social factors at short and long timescales. These include landscape and habitat changes, as well as societal actions to manage or adapt. But the range of physical and biological responses in coastal environments associated with climate change and sea-level rise (SLR) is poorly understood at some of the critical time and space scales required for decision making. Building on previous work by Gornitz et al. (1994), the USGS's Coastal Vulnerability Index (CVI) provides a broad assessment of the coastal vulnerability to SLR for the United States (Thieler and Hammar-Klose 1999, 2000a, 2000b). The CVI approach has been applied by the USGS and other investigators at locations worldwide and has formed the basis for further quantitative assessments.

Brief tool description/overview:
Index-based assessments quantify the likelihood that physical changes may occur based on analysis of the following variables: tidal range, ice cover, wave height, coastal slope, historical shoreline change rate, geomorphology, and historical rate of relative sea- or lake-level change. This approach seeks to combine a coastal system's susceptibility to change with its natural ability to adapt to changing environmental conditions, and it provides a measure of the system's potential vulnerability to the effects of sea- or lake-level change (Pendleton et al. 2010).

The USGS CVI uses the methodology described by Thieler and Hammar-Klose (1999) to calculate a single vulnerability metric from characterizations of the variables above. This yields an objective, quantitative measure of coastal vulnerability to SLR. The results are intended for relatively simple studies, screening-level vulnerability assessments, and similar studies. The results of this assessment method alone are not appropriate for detailed engineering design. Subsequent work (e.g., Gutierrez et al. 2011, 2014) has used CVI data to develop Bayesian networks that produce probabilistic assessments of shoreline change.

Audience:
This publicly-available dataset was developed for use by the USGS in preliminary studies and screening-level vulnerability assessments. This approach also has utility for regional (e.g., federal, non-governmental organization) or state-level land managers, planners, and decision-makers, as well as members of the general public who would like to explore potential future impacts from changing sea level. CVI and related data are available through the USGS Coastal Change Hazards portal at http://marine.usgs.gov/coastalchangehazardsportal/.

Geographic scope:
The original USGS CVI provided preliminary assessments for the contiguous 48 states. Subsequent work applied this approach to 22 national park units worldwide (see http://woodshole.er.usgs.gov/project-pages/nps-cvi/, accessed January 2016). More recently, as a contribution to the 2014 National Climate Assessment, Gutierrez et al. (2014) used CVI and other data to develop a probabilistic assessment of shoreline-change vulnerability to SLR for coastal areas in all 50 states.

Implications for the future:
- This assessment method produces objective, quantitative, and reproducible results that can be updated as new information becomes available. The underlying data are drawn from published, peer-reviewed sources.
- This assessment method can be adapted to a variety of regional and larger scales.
- The underlying data used in this assessment method can be repurposed for a variety of basic and applied scientific and management applications.

Relationship to the *Regional Sea Level Scenarios for Coastal Risk Management* report:
The USGS CVI provides complementary information for USACE studies that address policy and guidance included in ER 1100-2-8162 and ETL 1100-2-1 (USACE 2013, 2014). Similarly, the USGS CVI can be used in association with the present study's results. It also can be used for locations outside the U.S. as a screening tool. This assessment method could be used in conjunction with the USACE Sea Level Change Curve Calculator and the scenario database accompanying this report (and other tools that can provide input data for the CVI method) in the United States.

References:
Gornitz, V.M., R.C. Daniels, T.W. White, and K.R. Birdwell. 1994. The Development of a Coastal Vulnerability Assessment Database: Vulnerability to Sea-Level Rise in the U.S. Southeast. *Journal of Coastal Research*, 327–338. http://www.jstor.org/stable/25735608.

Gutierrez, B.T., N.G. Plant, and E.R. Thieler. 2011. A Bayesian Network to Predict Coastal Vulnerability to Sea-Level Rise. *Journal of Geophysical Research: Earth Surface* 116:F02009. doi:10.1029/2010JF001891.

Gutierrez, B.T., N.G. Plant, E.A. Pendleton, and E.R. Thieler. 2014. *Using a Bayesian Network to Predict Shoreline Change Vulnerability to Sea-Level Rise for the Coasts of the United States*. Open-File Report 2014-1083. Reston, Virginia: U.S. Geological Survey. doi:10.3133/ofr20141083.

Pendleton, E.A., E.R. Thieler, and S.J. Williams. 2010. Importance of Coastal Change Variables in Determining Vulnerability to Sea- and Lake-Level Change. *Journal of Coastal Research* 26:176–183. doi:10.2112/08-1102.1.

Thieler, E.R. and E.S. Hammar-Klose. 1999. *National Assessment of Coastal Vulnerability to Sea-Level Rise: Preliminary Results for the U.S. Atlantic Coast*. Open-File Report 99-593. Woods Hole, Massachusetts: U.S. Geological Survey. http://pubs.usgs.gov/of/of99-593/.

Thieler, E.R. and E.S. Hammar-Klose. 2000a. *National Assessment of Coastal Vulnerability to Sea-Level Rise: Preliminary Results for the U.S. Pacific Coast*. Open-File Report 00-178. Woods Hole, Massachusetts: U.S. Geological Survey. http://pubs.usgs.gov/of/of00-178/.

Thieler, E.R. and E.S. Hammar-Klose. 2000b. *National Assessment of Coastal Vulnerability to Sea-Level Rise: Preliminary Results for the U.S. Gulf of Mexico Coast*. Open-File Report 00-179. Woods Hole, Massachusetts: U.S. Geological Survey. http://pubs.usgs.gov/of/of00-179/.

U.S. Army Corps of Engineers (USACE). 2013. *Incorporating Sea-Level Change in Civil Works Programs*. ER 1100-2-8162. Washington, D.C.: U.S. Army Corps of Engineers. http://www.publications.usace.army.mil/Portals/76/Publications/EngineerRegulations/ER_1100-2-8162.pdf.

USACE. 2014. *Procedures to Evaluate Sea Level Change: Impacts, Responses, and Adaptation*. ETL 1100-2-1. Washington, D.C.: U.S. Army Corps of Engineers. http://www.publications.usace.army.mil/Portals/76/Publications/EngineerTechnicalLetters/ETL_1100-2-1.pdf.

THIS PAGE LEFT INTENTIONALLY BLANK

Appendix C
Adjustment Component Tables

This Appendix provides a tabular breakdown by each adjustment component to enable better visualization of contributions to overall sea-level rise adjustments under each combination of scenario and timeframe. These tables provide the underlying data used to generate Table 4.1. The first three tables under each scenario provide the minimum and maximum values for the three individual adjustment components (i.e., Vertical Land Movement, Dynamic Sea Level, and Ice Melt) occurring within each timeframe across all Department of Defense sites evaluated. The last table under each scenario provides the minimum and maximum Total Adjustment when all three individual components are added at a particular site (for example, the maximum total adjustment that occurred across all 1,774 sites for the 0.2-meter scenario at 2100 was 1.2 meters). As a result, because minimum and maximum component values do not necessarily occur at the same site, the values in the Total Adjustment tables are not a direct summation of the values in the three component tables.

All values are provided in meters (m)

Scenario: 0.2-meter

Vertical Land Movement

Timeframe	2035	2065	2100
Min =	-0.9	-1.6	-2.3
Max =	0.5	0.8	1.2

Dynamic Sea Level

Timeframe	2035	2065	2100
Min =	0	0	0
Max =	0.1	0.1	0.1

Ice Melt

Timeframe	2035	2065	2100
Min =	-0.1	-0.1	-0.2
Max =	0	0	0

Total Adjustment (Individual Site)

Timeframe	2035	2065	2100
Min =	-0.9	-1.6	-2.3
Max =	0.5	0.8	1.2

Scenario: 0.5-meter

Vertical Land Movement

Timeframe	2035	2065	2100
Min =	-0.9	-1.6	-2.3
Max =	0.5	0.8	1.2

Dynamic Sea Level

Timeframe	2035	2065	2100
Min =	0	0	0
Max =	0.1	0.1	0.1

Ice Melt

Timeframe	2035	2065	2100
Min =	-0.1	-0.1	-0.3
Max =	0	0	0

Total Adjustment (Individual Site)

Timeframe	2035	2065	2100
Min =	-0.9	-1.6	-2.3
Max =	0.5	0.8	1.2

Scenario: 1.0-meter

Vertical Land Movement

Timeframe	2035	2065	2100
Min =	-0.9	-1.6	-2.3
Max =	0.5	0.8	1.2

Dynamic Sea Level

Timeframe	2035	2065	2100
Min =	0	0	-0.1
Max =	0.1	0.2	0.3

Ice Melt

Timeframe	2035	2065	2100
Min =	-0.1	-0.3	-0.9
Max =	0	0.1	0.1

Total Adjustment (Individual Site)

Timeframe	2035	2065	2100
Min =	-0.9	-1.6	-2.3
Max =	0.5	0.8	1.2

Scenario: 1.5-meter

Vertical Land Movement

Timeframe	2035	2065	2100
Min =	-0.9	-1.6	-2.3
Max =	0.5	0.8	1.2

Dynamic Sea Level

Timeframe	2035	2065	2100
Min =	0	-0.1	-0.1
Max =	0.1	0.2	0.4

Ice Melt

Timeframe	2035	2065	2100
Min =	-0.1	-0.4	-1.5
Max =	0	0.1	0.2

Total Adjustment (Individual Site)

Timeframe	2035	2065	2100
Min =	-0.9	-1.6	-2.3
Max =	0.5	0.8	1.3

Scenario: 2.0-meter

Vertical Land Movement

Timeframe	2035	2065	2100
Min =	-0.9	-1.6	-2.3
Max =	0.5	0.8	1.2

Dynamic Sea Level

Timeframe	2035	2065	2100
Min =	0	-0.1	-0.1
Max =	0.1	0.3	0.5

Ice Melt

Timeframe	2035	2065	2100
Min =	-0.1	-0.3	-1.5
Max =	0.1	0.2	0.4

Total Adjustment (Individual Site)

Timeframe	2035	2065	2100
Min =	-0.9	-1.5	-2.2
Max =	0.5	0.9	1.5